Comparative Proteomic Profiling and Biomarker Discovery in Complex Biological Samples by Mass Spectrometry

By

Di Ma

A dissertation submitted in partial fulfillment of

the requirements for the degree of

Doctor of Philosophy

(Pharmaceutical Sciences)

at the

UNIVERSITY OF WISCONSIN-MADISON

2012

Date of final oral examination: 11/19/12
The dissertation is approved by the following members of the Final Oral Committee:
Lingjun Li, Professor, Pharmaceutical Sciences
Albee Messing, Professor, Comparative Biosciences
Manish Patankar, Associate Professor, Obstetrics and Gynecology
Joel Pedersen, Professor, Soil Science
Richard Peterson, Professor, Pharmaceutical Sciences

Acknowledgement

I would first like to thank my advisor Professor Lingjun Li for her guidance and support throughout my thesis research. Lingjun's enthusiasm for science, interest to explore new technologies combined with her broad knowledge from years of experience made a profound impact on me and motivated me to be a much better researcher than what I was content to be. I thank Lingjun for the opportunity to work in her lab and for guidance into "all things" analytical chemistry.

I thank my thesis committee that includes Professors Albee Messing, Manish Patankar, Joel Pedersen and Dick Peterson. I appreciate their support, advice and instruction during my thesis work.

I have been fortunate to participate in several collaborations with groups on and off campus. I thank Professor Manish Patankar, Drs. Arvinder Kapur and Weifeng Cao for the work we did together for proteomic analysis of NK cells. I thank Professor Judd Aiken, Drs. Allen Herbst and Xin Wei for the work we did together to identify prion disease biomarker. I thank Dr. Xudong (Daniel) Shi and Chenxi Yang for the work we did together for the secretome research. I am thankful for the experiences that I had working with so many excellent scientists.

I thank my coworkers in the Li lab for all of their support. In particular, I thank former member Dr. Xin Wei for his mentorship after I joined lab. Without his support I could not have adapted to the lab in the quick manner as I did to begin my independent research. In addition, I would especially like to thank Dr. Rob Sturm, Dr. Robby Cunningham, Dr. Weifeng Cao, Dr. Chenxi Jia, Claire Schmerberg and Chris Lietz for their technical support whenever I ran into

problems. I also enjoyed working with Chenxi Yang in the past few months. The discussions with her added more insights and inspiration into my research.

I thank the Analytical Instrument Center at School of Pharmacy, in particular, Dr. Cameron Scarlett for access to the Bruker amaZon ion trap mass spectrometer. I thank Linda Frei, Ken Niemeyer, Joni Mitchell, Jenny Hergenrother and Tom O'Connor for administrative assistance.

Last but not least, I thank my father Wu Ma and my mother Wei Jin for their undying love and support. My parents' dedication to hard work inspired me to fulfill my dreams to make a positive impact to society. I thank my awesome husband Kong Xiong for his infinite love and support especially during setbacks throughout graduate school when nothing seemed reassuring but his words of encouragement. I could not have made through graduate school without him. I dedicate this thesis to my family and to the reunion with my "Big Cheeks".

Table of Contents

		Page
Acknowledgements		i
Table of Contents		iii
Abstract		iv
Chapter 1:	Introduction: Background and Research Summary	1
Chapter 2:	Mass Spectrometry-Based Proteomics and Peptidomics for Systems Biology and Biomarker Discovery	9
Chapter 3:	Differential Expression of Proteins in Naïve and IL-2 Stimulated Primary Human NK Cells Identified by Global Proteomics	67
Chapter 4:	Comparative Secretome Analysis of Vascular Smooth Muscle Cells in Response to Smad3-Dpendent TGF-β Signaling	104
Chapter 5:	Searching for Reliable Pre-mortem Protein Biomarkers for Prion Diseases – Progress and Challenges to Date	130
Chapter 6:	Identification and Validation of a Potential Protein Biomarker for Prion Diseases by Mass Spectrometry-Based Quantitative Glycoproteomics	169
Chapter 7:	Conclusions and Future Directions	207
Appendix 1:	Selected Protocols for Comparative Proteomic Profiling and Biomarker Discovery in Complex Biological Samples by Mass	217
Appendix 2:	List of IL-2 Regulated Proteins in Human Primary NK Cells Identified From All Three Donors (Chapter 3)	229
Appendix 4:	List of Publications and Presentations	248

Comparative Proteomic Profiling and Biomarker Discovery in Complex Biological Samples by Mass Spectrometry

Di Ma

Under the supervision of Professor Lingjun Li

at the University of Wisconsin-Madison

Abstract

Advances in mass spectrometry (MS) technology have made MS-based proteomics a promising tool for protein profiling and biomarker discovery in various types of biological samples such as cell cultures, tissues, and biological fluids. MS-based proteomics has been widely applied to molecular and cellular biology to elucidate biological and pathophysiological processes. However, MS analyses of biological samples are often challenging due to the vast complexity and large dynamic range. Because disease identifying biomarkers are more likely to be low abundance proteins, it is imperative to remove the highly abundant proteins or apply enrichment techniques during sample preparation to allow detection and improve coverage of the low abundance proteins for MS analysis. In addition, the complexity of the digested biological samples can be reduced by applying multiple orthogonal separations prior to LC-MS/MS such as multidimensional protein identification technology (MudPIT). In this dissertation, the major objectives include the following: (1) method development of sample preparation and chromatographic separation for MS-based quantitative proteomics, and (2) their applications in large-scale protein characterization in complex biological samples for differential expression analysis and biomarker discovery will be discussed. First, a method of MudPIT combined with ESI-MS/MS was optimized and performed for global proteome profiling in naïve and

interleukin-2 (IL-2)-activated natural killer cells. In order to identify IL-2 regulated proteins that may lead to the discovery of new molecular pathways involved in IL-2 signaling, spectral counting, which is a label-free quantification strategy for comparative proteomic analysis was utilized due to the simplicity and sensitivity of this approach. A similar sample preparation and quantification strategy was also applied to the comparative secretome analysis in rat vascular smooth muscle cells (VSMCs) stimulated by transforming growth factor-β (TGF-β), which led to the identification of secreted proteins that may be associated with TGF-β signaling in VSMCs. Although multi-dimensional separation proved to be essential and effective to reduce sample complexity, it is sometimes insufficient for proteome profiling in biofluids such as plasma where only a few high abundance proteins comprise majority of the serum proteome. To improve the identifications of low abundance proteins in MS analysis, it is imperative to remove the highly abundant proteins or apply enrichment techniques prior to MS analysis. To tackle this problem, lectin affinity chromatography (LAC) was utilized in sample preparation of mouse plasma affected by prion disease to specifically enrich glycoproteins that may prove to be important biomarkers for prion diseases. The combination of LAC and MudPIT significantly reduced sample complexity and led to the discovery of a panel of potential biomarkers including the validation of serum amyloid P-component (SAP). Furthermore, PNGase F digestion analysis confirmed that the glycosylated form of SAP could be used as a potential diagnostic biomarker for prion diseases and that glycosylated SAP plays an important role in the progression of prion disease. Collectively, the work included in this thesis extends the capability of mass spectrometry as a powerful analytical tool for large-scale proteomic analysis in complex biological samples to identify disease biomarkers or biomolecules involved in critical cellular processes.

Chapter 1

Introduction: Background and Research Summary

1.1 Introduction

The main objective of this dissertation focuses on the utilization of mass spectrometry (MS) for large-scale proteomic profiling in complex biological samples and application of this technology to discover biomarkers or protein factors that are associated with human diseases. For this purpose, the research included in this dissertation includes topics ranging from analytical method development for improved protein characterization and quantification, to biological validation of potential protein biomarkers identified by MS analysis. In this dissertation MS-based proteomics techniques were applied to vastly different collaborative projects where analyses were challenged by sample complexity. This chapter outlines the overall structure of this dissertation with a background overview of MS-based proteomics and general introductions to each research project.

1.2 Background Overview

Advances in MS have made MS-based proteomics and peptidomics a method of choice for large scale protein characterization and biomarker discovery. Coupled with different sample preparation and separation techniques, MS-based proteomics and peptidomics can be utilized to study peptide and protein identification, structures, modifications and interactions in various types of samples including cultured cells, animal tissue, biological fluids, etc[1-3]. Such applications have significantly promoted the research in molecular and cellular biology and provided insights into identification of novel target proteins that are involved in critical biological and pathophysiological processes that include deciphering their roles related to the development of diseases [3].

Chapter 2 provides a comprehensive introduction to MS-based proteomics and peptidomics including its applications in different biologic materials. A detailed workflow of MS-based proteomics and peptidomics which covers common strategies and techniques used in sample preparation, sample separation, peptide fragmentation, post-translational modifications, quantification, bioinformatics, and validation are reviewed. The background reviewed in Chapter 2 is closely related to the studies discussed in Chapters 3, 4 and 6.

1.3 Differential Expression of Proteins in Naïve and IL-2 Stimulated Primary Human NK Cells Identified by Mass Spectrometry-Based Proteomic analysis (Chapter 3)

Natural Killer (NK) cells efficiently cytolyse tumors and virulent cells[4]. The development and functional activity of NK cells are regulated by a host of cytokines, including interleukin 2 (IL-2) which stimulates the proliferation of NK cells and increases NK cell activity[5]. Although how IL-2 mediates its effects has been investigated, little is known about the alterations in the global NK cell proteome following IL-2 activation. With the development of NK cell-based immunotherapy relying on activation via IL-2, it is important to conduct a comprehensive proteomic analysis of the NK cell to delineate molecular pathways that may impinge or accentuate the immune responses. Therefore, we characterized the proteome of naïve and IL-2 activated primary NK cells by MS-based quantitative proteomics. The research presented in Chapter 3 aims to characterize the proteome of naïve and IL-2-activated primary NK cells and identify IL-2 proteins that may lead to the discovery of new molecular pathways involved in IL-2 signaling. Comparative analysis of naïve and IL-2-activated NK cells isolated from healthy donors was performed using 2D LC ESI-MS/MS followed by label-free quantification. In total, more than 2000 proteins were identified from naïve and IL-2-activated

cells and 382 proteins in NK cells were found to be differentially expressed following IL-2 activation. Functional annotation and pathway analysis was also performed to identify novel pathways not previously known to be involved in IL-2 signaling. The identification of IL-2 regulated proteins provides new insights into NK cell biology and provides preliminary information to elucidate the mechanism(s) of IL-2 signaling in NK cells.

1.4 Comparative Secretome Analysis of Vascular Smooth Muscle Cells in Response to TGF-β (Chapter 4)

Secretome, in a less strict definition, includes the proteins of extracellular matrix (ECM) as well as proteins shed from the surface of living cells[6]. Proteins of the secretome often play a key role in cell signaling, communication and migration[7]. In the formation and development of intimal hyperplasia, which is a complex process associated with abnormal behavior of vascular smooth muscle cells (VSMCs) following surgical intervention of atherosclerosis, it is believed that transforming growth factor β (TGF-β) is one of the critical factors that triggers VSMCs transform from a quiescent, differentiated state to a proliferative and synthetic phenotype[8, 9]. However, the molecular mechanisms by which TGF-β triggers VSMC proliferation after vascular injury remain unclear. We proposed that one of the mechanisms through which TGF-β enhances intimal hyperplasia is the induction of secreted proteins that contribute to the proliferative and synthetic features of VSMCs. In Chapter 4 we characterize the proteins secreted from cultured VSMCs and assess temporal changes in the secretome in response to TGF-β. We performed LC ESI-MS/MS for protein identification and subsequently examined our dataset in bioinformatics resources to filter out intracellular contaminants. The use of one-dimensional LC-MS/MS resulted in identifications of 264 proteins from conditioned media of

control and TGF-β stimulated VSMCs, 165 of which were putative secreted proteins. The quantitative analysis by spectral counting revealed 32 secreted proteins that were significantly up or down-regulated in response to TGF-β. The characterization of secretome of VSMCs and the TGF-β induced factors identified from comparative analysis may provide novel targets for the investigations of the role of TGF-β in atherosclerotic process.

1.5 Identification and Validation of a Potential Protein Biomarker for Prion Diseases by Mass Spectrometry-Based Proteomics (Chapters 5 & 6)

Prion diseases are a family of fatal neurodegenerative diseases affecting the central nervous system of human and other animals. Current diagnostic tests have focused on detection of the causal agent of the disease, the abnormal prion protein, or other individual proteins that correlate with the prion diseases[10, 11]. These tests are inadequate because they are post-mortem, low throughput and not sufficiently sensitive to detect infection early in the pre-clinical period. Clearly, there is an urgent need for the development of a reliable, sensitive, and specific ante-mortem diagnostic test for the pre-clinical identification of prion-infected animals or individuals. However, the identification of potential protein biomarkers from biofluid samples is challenging due to sample complexity and limited dynamic range of detection[12, 13]. In Chapter 5 we reviewed the use of the latest proteomic technologies for the identification of promising prion disease biomarkers, the challenges that exist in biomarker development pipeline and the new directions of utilizing proteomics for future biomarker discovery in the context of prion disease diagnostics. The background reviewed in this chapter is closely related to the research conducted and described in Chapter 6.

In the past few years our lab have collaborated with Dr. Judd Aiken's lab at the University of Alberta in the development of an integrated MS-based platform to identify and characterize potential biomarkers in mice plasma infected with prion disease. In Chapter 6, a quantitative glycoproteomic approach was employed to reduce sample complexity. Lectin affinity chromatography (LAC) and multi-dimensional separations was utilized to detect low abundance glycoproteins. Protein identifications were performed by LC-MS/MS analysis, and relative quantification of proteins in control or prion infected samples were obtained by isotopic labeling approach using formaldehyde. Overall 708 proteins were identified, 111 of which showed more than 2-fold increase or decrease in concentration. Among the up-regulated proteins, serum amyloid component-P (SAP) in prion infected samples was validated by Western blotting. Furthermore, PNGase F digestion and Western blotting analysis revealed that only the glycosylated form of SAP was significantly elevated in mice with early prion infection. Our findings suggested glycosylated that SAP could be potentially used as a diagnostic biomarker for prion diseases.

1.6 Conclusions

Collectively, all the research projects included in this thesis focused on the method development and applications of MS-based proteomic analysis in complex biological samples. The work included in this thesis covered the methods for quantitative proteomic analysis in different types of samples including cell lysates, cell culture media and plasma. However, the general workflows and optimized methods for sample preparation and separation can be applied to the analysis of other complex biological samples. The results and methods from the present work will provide valuable references for future MS-based proteomic analysis in our lab.

Moreover, utilizing MS-based proteomics, we were able to identify key protein factors and biomarkers that may be associated with human diseases. These findings will serve as a starting point for further investigations into the molecular mechanisms of disease development.

References

1. Wei, X.; Li, L., Mass spectrometry-based proteomics and peptidomics for biomarker discovery in neurodegenerative diseases. *Int J Clin Exp Pathol* **2009,** 2, (2), 132-48.
2. Yates, J. R.; Ruse, C. I.; Nakorchevsky, A., Proteomics by mass spectrometry: approaches, advances, and applications. *Annu Rev Biomed Eng* **2009,** 11, 49-79.
3. Walther, T. C.; Mann, M., Mass spectrometry-based proteomics in cell biology. *J Cell Biol* **2010,** 190, (4), 491-500.
4. Trinchieri, G., Biology of natural killer cells. *Adv Immunol* **1989,** 47, 187-376.
5. Henney, C. S.; Kuribayashi, K.; Kern, D. E.; Gillis, S., Interleukin-2 augments natural killer cell activity. *Nature* **1981,** 291, (5813), 335-8.
6. Makridakis, M.; Vlahou, A., Secretome proteomics for discovery of cancer biomarkers. *J Proteomics* **2010,** 73, (12), 2291-305.
7. Frantz, C.; Stewart, K. M.; Weaver, V. M., The extracellular matrix at a glance. *J Cell Sci* **2010,** 123, (Pt 24), 4195-200.
8. McCaffrey, T. A.; Consigli, S.; Du, B.; Falcone, D. J.; Sanborn, T. A.; Spokojny, A. M.; Bush, H. L., Jr., Decreased type II/type I TGF-beta receptor ratio in cells derived from human atherosclerotic lesions. Conversion from an antiproliferative to profibrotic response to TGF-beta1. *J Clin Invest* **1995,** 96, (6), 2667-75.
9. Mii, S.; Ware, J. A.; Kent, K. C., Transforming growth factor-beta inhibits human vascular smooth muscle cell growth and migration. *Surgery* **1993,** 114, (2), 464-70.
10. Schaller, O.; Fatzer, R.; Stack, M.; Clark, J.; Cooley, W.; Biffiger, K.; Egli, S.; Doherr, M.; Vandevelde, M.; Heim, D.; Oesch, B.; Moser, M., Validation of a western immunoblotting procedure for bovine PrP(Sc) detection and its use as a rapid surveillance method for the diagnosis of bovine spongiform encephalopathy (BSE). *Acta Neuropathol* **1999,** 98, (5), 437-43.
11. Oesch, B.; Doherr, M.; Heim, D.; Fischer, K.; Egli, S.; Bolliger, S.; Biffiger, K.; Schaller, O.; Vandevelde, M.; Moser, M., Application of Prionics Western blotting procedure to screen for BSE in cattle regularly slaughtered at Swiss abattoirs. *Arch Virol Suppl* **2000**, (16), 189-95.
12. Anderson, N. L.; Anderson, N. G., The human plasma proteome: history, character, and diagnostic prospects. *Mol Cell Proteomics* **2002,** 1, (11), 845-67.
13. Maccarrone, G.; Milfay, D.; Birg, I.; Rosenhagen, M.; Holsboer, F.; Grimm, R.; Bailey, J.; Zolotarjova, N.; Turck, C. W., Mining the human cerebrospinal fluid proteome by immunodepletion and shotgun mass spectrometry. *Electrophoresis* **2004,** 25, (14), 2402-12.

Chapter 2

Mass Spectrometry-based Proteomics and Peptidomics for Systems Biology and Biomarker Discovery

Adapted from: "Mass spectrometry-Based Proteomics and Peptidomics for Systems Biology and Biomarker Discovery." Cunningham R, Ma D, Li, L. *Frontiers in Biology*. 2012; 7(4): 313-35.

Abstract

The scientific community has shown great interest in the field of mass spectrometry-based proteomics and peptidomics for its applications in biology. Proteomics technologies have evolved to produce large datasets of proteins or peptides involved in various biological and disease progression processes producing testable hypothesis for complex biological questions. This review provides an introduction and insight to relevant topics in proteomics and peptidomics including biological material selection, sample preparation, separation techniques, peptide fragmentation, post-translation modifications, quantification, bioinformatics, and biomarker discovery and validation. In addition, current literature and remaining challenges and emerging technologies for proteomics and peptidomics are presented.

Introduction

The field of proteomics has seen a huge expansion in the last two decades. Multiple factors have contributed to the rapid expansion of this field including the ever evolving mass spectrometry instrumentation, new sample preparation methods, genomic sequencing of numerous model organisms allowing database searching of proteomes, improved quantitation capabilities, and availability of bioinformatic tools. The ability to investigate the proteomes of numerous biological samples, and the ability to generate future hypothesis driven experiments makes proteomics and biomarker studies exceedingly popular in biological studies today. In addition, the advances in post-translational modification (PTM) analysis and quantification ability further enhance the utility of mass spectrometry (MS)-based proteomics. A subset of proteomics research is devoted to profiling and quantifying neurologically related proteins and endogenous peptides, which has progressed rapidly in the past decade. This review provides a general overview, as outlined in Figure 1, of proteomics technology including methodological and conceptual improvements with a focus on recent studies and neurological biomarker studies.

Biological Material Selection

The choice of biological matrix is an important first step in any proteomics analysis. The ease of sample collection (e.g., urine, plasma, or saliva) versus usefulness or localization of sample (e.g., specific tissue or proximity fluid) needs to be evaluated early on in a study design.

Plasma, derived by centrifugation of blood to remove whole cells, is a very popular choice in proteomics due to the high protein content (~65 mg /ml^{1}) and the ubiquitous nature of blood in the body and the ability to obtain large sample amounts or various time points without the need to sacrifice the animal or to perform invasive techniques. Plasma is centrifuged

immediately after sample collection unlike serum where coagulation needs to occur first. To obtain plasma, blood is collected in a tube with an anticoagulant added (EDTA, heparin, or citrate) and centrifuged, but previous reports have shown variable results when heparin has been used as an anticoagulant.[2] Human Proteome Organization (HUPO) specifically recommends the anticoagulants EDTA or citrate to treat plasma.[3, 4] One of the primary concerns with plasma is degradation of the protein content via endogenous proteases found in the sample[5]. One way to address this problem is the use of protease inhibitors. In addition, freeze/thaw cycles need to be minimized to prevent protein degradation and variability.[6, 7] Plasma proteomics has seen extensive coordinated efforts to start assessing the diagnostic needs using plasma.[8] HUPO also has established a public human database for plasma and serum proteomics from 35 collaborating labratories.[9] Large dynamic range studies have been performed on plasma with a starting sample amount of 2625 µl (157.5 mg), resulting in 3654 proteins identified with a sub 5% false discovery rate.[10]

The large dynamic range spanning across eleven orders of magnitude as visualized in Figure 2 is one of the biggest obstacles in plasma proteomics. Figure 2 also shows that as lower abundance proteins are investigated, the origins of those identified proteins are more diverse than the most abundant proteins. Recent mining of the plasma proteome showed an ability to search for disease biomarker applications across seven orders of magnitude. In addition, the tissue of origin for the identified plasma proteins were identified and its origin was more diverse as the protein concentration decreased.[11] Plasma has been used as a source for biomarker studies such as colorectal cancer,[12, 13] cardiovascular disease,[14] and abdominal aortic aneurysm.[15] Even though the blood brain barrier prevents direct blood to brain interaction, neurological disorders, such as Alzheimer's disease (AD), have had their proteomes studied using plasma.[16]

An alternative sample derived from blood is serum which is plasma allowed to coagulate instead of adding anti-coagulates. The time for coagulation is usually 30 minutes and during that time significant and random degradation from endogenous proteases can occur. The additional variability caused from the coagulation process can change the concentration of multiple, potentially valuable, biomarkers. As biodiversity between samples or organisms is a challenging endeavor, additional sample variability due to serum generation may be undesirable, but serum is still currently being used for biomarker disease studies.[17] Serum has been used to compare the proteome differences in neurological diseases such as AD, Parkinson's disease, and amyotrophic lateral sclerosis and a review can be found elsewhere discussing the subject.[18]

Cerebrospinal fluid (CSF) has a long history as a surrogate biopsy of brain or spinal cord in evaluating diseases of the central nervous system and has been used for studies in neurological disorders due to being a rich source of neuro-related proteins and peptides.[19] The protein composition of the most abundant proteins in CSF is well defined, and numerous studies exist to broaden the proteins identified.[20-22] CSF has an exceedingly low protein content (~0.4 μg/μL) which is ~100 times lower than serum or plasma, and over 60% of the total protein content in CSF consists of a single protein, albumin.[23-25] In addition, the variable concentrations of proteins span up to twelve orders of magnitude further complicating analysis and masking biologically relevant proteins to any given study.[26] One of the highest number of identified proteins is from Schutzer et. al with 2630 non-redundant proteins from 14 mL of pooled human CSF. This study involved the removal of highly abundant proteins by performing IgY-14 immunodepletion followed by two dimensional (2D) liquid chromatography (LC) separation.[27] Studies have also been performed to characterize individual biomarkers or complex patterns of biomarkers in various diseases in the CSF.[28, 29] One potential pitfall of CSF proteomic analysis is

contamination from blood, which can be identified by counting red blood cells present or examining surrogate markers from blood contamination other than hemoglobin such as peroxiredoxin, catalase, and carbonic anhydrase.[30] A proof of principle CSF peptidomics study identified numerous endogenous peptides associated with the central nervous system, which can be used as a bank for neurological disorder studies.[31] Numerous recent reports highlighted the utility of CSF analysis for biomarker studies in AD,[32, 33] medulloblastoma,[34] both post-mortem and ante-mortem.[35]

Cellular lysates offer the distinct advantage to work with a cell line, yeast, or bacteria with large amounts of proteins available for analysis,[36, 37] with *Saccharomyces cerevisiae* being the most common cell lysate.[38, 39] Other cell lines are also used including HeLa[40] and *E. coli*.[41] The ability to obtain milligrams of proteins easily to scale up experiments without animal sacrifice offers a clear advantage in biological sample selection. Current literature supports cellular lysate as a valued and sought after source of proteins for large scale proteomics experiments because of the ability to assess treatments, conditions, and testable hypothesis.[42-44] Cellular lysate from rat B104 neuroblastoma cell line was used as an *in vitro* model for cerebral ischemia and showed abundance changes in multiple proteins involved in various neurological disorders.[45]

Other Sources of Biological Samples

Urine

The urine proteome appears to be another attractive reservoir for biomarker discovery due to the relatively low complexity compared with the plasma proteome and the noninvasive collection of urine. Urine is often considered as an ideal source to identify biomarkers for renal

diseases due to the fact that in healthy adults approximately 70% of the urine proteome originate from the kidney and the urinary tract [46], thus, the use of urine to identify neurological disorders is neglected. However, strong evidence have shown that proteins that are associated with neurodegenerative diseases can be excreted in the urine[47-49], indicating the application of urine proteomics could be a useful approach to the discovery of biomarkers and development of diagnostic assays for neurodegenerative diseases. However, the current view of urine proteome is still limited by factors such as sample preparation techniques and sensitivity of the mass spectrometers. There has been a tremendous drive to increase the coverage of urine proteome. In a recent study, Court *et al*. compared and evaluated several different sample preparation methods with the objective of developing a standardized, robust, and scalable protocol that could be used in biomarkers development by shotgun proteomics [50]. In another study, Marimuthu *et al.* reported the largest catalog of proteins in urine identified in a single study to date. The proteomic analysis of urine samples pooled from healthy individuals was conducted by using high-resolution Fourier transform mass spectrometry. A total of 1823 proteins were identified, of which 671 proteins have not been previously reported in urine [51].

Saliva

For diagnosis purposes, saliva collection has the advantage of being an easy and non-invasive technique. The recent studies on saliva proteins that are critically involved in AD and Parkinson's diseases suggested that saliva could be a potentially important sample source to identify biomarkers for neurodegenerative diseases. Bermejo-Pareja *et al*. reported the level of salivary Aβ42 in patients with mild AD was noticeably increased compared to a group of controls [52]. In another study, Devic *et al*. identified two of the most important Parkinson's

disease related proteins— α-synuclein (α-Syn) and DJ-1 in human saliva [53]. They observed that salivary α-Syn levels tended to decrease while DJ-1 levels tended to increase in Parkinson's disease. The published results from this study also suggest that α-Syn might correlate with the severity of motor symptoms in Parkinson's disease. Due in part to recent advancements in MS-based proteomics has provided promising results in utilizing saliva to explore biomarkers for both local and systemic diseases [54, 55], the further profiling of saliva proteome will provide valuable biomarker discovery source for neurodegenerative diseases.

Tissue

Compared to body fluids such as plasma, serum and urine where the proteomic analysis is complicated by the wide dynamic range of protein concentration, the analysis of tissue homogenates using the well-established and conventional proteomic analysis techniques has the advantage of reduced dynamic range. However, the homogenization and extraction process may suffer from the caveat that spatial information is lost, which would be inadequate for the detection of biomarkers whose localization and distribution play important roles in disease development and progression. Matrix-assisted laser desorption/ionization (MALDI) imaging mass spectrometry (IMS) is a method that allows the investigation of a wide range of molecules including proteins, peptides, lipids, drugs and metabolites, directly in thin slices of tissue [56-59]. Because this technology allows for identification and simultaneous localization of biomolecules of interests in tissue sections, linking the spatial expression of molecules to histopathology, MALDI-IMS has been utilized as a powerful tool for the discovery of new cancer biomarker candidates as well as other clinical applications [60, 61]. The utilization of MALDI-IMS for human or animal brain tissue to identify or map the distribution of molecules related to neurodegenerative diseases were also recently reported [62, 63].

Secretome

There has been an increasing interest in the study of proteins secreted by various cells (the secretomes) from tissue-proximal fluids or conditioned media as a potential source of biomarkers. Cell secretomes mainly comprise proteins that are secreted or are shed from the cell surface, and these proteins can play important role in both physiological processes (e.g. cell signaling, communication, and migration) and pathological processes including tumor angiogenesis, differentiation, invasion, and metastasis. In particular, the study of cancer cell secretomes by MS based proteomics has offered new opportunities for cancer biomarker discovery as tumor proteins may be secreted or shed into the bloodstream and could be used as noninvasive biomarkers. The latest advances and challenges of sample preparation, sample concentration, and separation techniques used specifically for secretome analysis, and its clinical applications in the discovery of disease specific biomarkers have been comprehensively reviewed [64, 65]. Here, we only highlight the proteomic profiling of neural cells secretome that has been applied to neurosciences for a better understanding of the roles secreted proteins play in response to brain injury and neurological diseases. The LC-MS shotgun identification of proteins released by astrocytes has been recently reported [66-68]. In these studies the changes observed in the astrocyte secretomes induced by inflammatory cytokines or cholinergic stimulation were investigated.[66,67] Alternatively, our group performed 2D-LC separation and included cytoplasmic protein extract from astrocytes as a control to identify cytoplasmic protein contaminants which are not actively secreted from cells.[68]

Sample Preparation

Proteomic analysis and biomarker discovery research in biological samples such as body fluids, tissues, and cells are often hampered by the vast complexity and large dynamic range of the proteins. Because disease identifying biomarkers are more likely to be low-abundance proteins, it is imperative to remove the high-abundance proteins or apply enrichment techniques to allow detection and better coverage of the low-abundance proteins for MS analysis. Several strategies including depletion and protein equalizer approach have been used during sample preparation to reduce sample complexity [69, 70], and the latest advances of these methods have been reviewed by Selvaraju *et al.* [71]. Alternatively, the complexity of biological samples can be reduced by capturing a specific subproteome that may have the biological information of interest. The latter strategy is especially useful in the biomarker discovery where the changes in the proteome are not solely reflected through the concentration level of specific proteins but also through changes in the post-translational modifications (PTMs). Here, we will mainly discuss the enrichment of phosphoprotein/peptides, glycoprotein/peptides and sample preparation for peptidomics and membrane proteins.

Phosphoproteomics

Phosphorylation can act as a molecular switch on a protein by turning it on or off within the cell. It is thought that up to 30% of the proteins can be phosphorylated[72] and it plays significant roles in such biological processes as the cell cycle and signal transduction[73]. Currently, tens of thousands of phosphorylation sites can be proposed using analytical methods available today.[74, 75] The amino acids that are targeted for phosphorylation studies are serine, threonine, and tyrosine with the abundance of detection decreasing typically in that order. Other

amino acids have been reported to be phosphorylated, but traditional phosphoproteomics experiments ignore these rare events.[76]

In a typical large-scale phosphoproteomics experiment the sample size is usually in milligram amounts to account for the low stoichiometry of phosphorylated proteins. The large amount of protein is then digested, typically with trypsin, but, alternatively, experiments have been performed with Lys-C digestion to produce large enzymatic peptides. The larger peptides produced from Lys-C render higher charged peptides during electrospray ionization (ESI) and allow improved electron-based fragmentation to determine specific sites of phosphorylation.[77] From the pool of peptides, phosphopeptides must be enriched otherwise they will be masked by the vast number and higher ionization efficiency of non-phosphorylated peptides. The two most common enrichment techniques are immobilized metal ion affinity chromatography (IMAC) and metal oxide affinity chromatography (MOAC), TiO_2 being the most common oxide used for this purpose. A recent study reported that phosphorylation of neuronal intermediate filament proteins in neurofibrillary tangles are involved in Alzheimer's disease.[78]

Glycoproteomics

Protein glycosylation is one of the most common and complicated forms of PTM. Types of protein glycosylation in eukaryotes are categorized as either N-linked, where glycans are attached to asparagine residues in a consensus sequence N-X-S/T (X can be any amino acid except proline) via an N-acetylglucosamine (N-GlcNAc) residue, or the O-glycosylation, where the glycans are attached to serine or threonine. Glycosylation plays a fundamental role in numerous biological processes, and aberrant alterations in protein glycosylation are associated with neurodegenerative disease states, such as Creutzfeld-Jakob Disease (CJD) and AD [79, 80].

Due to the low abundance of glycosylated forms of proteins compared to non-glycosylated proteins, it is essential to enrich glycoproteins or glycopeptides in complex biological samples prior to MS analysis. Two of the most common enrichment methods used in glycoproteomics are lectin affinity chromatography (LAC) and hydrazide chemistry. The detailed methodologies of LAC, hydrazide chemistry and other enrichment methods in glycoproteomics have been extensively reviewed in the past [81, 82]. In particular, LAC is of great interest in studies of glycosylation alterations as markers of AD and other neurodegenerative diseases due to its recent applications in brain glycoproteomics [83]. Our group has utilized multi-lectin affinity chromatography containing concanavalin A (ConA) and wheat germ agglutinin (WGA) to enrich N-linked glycoproteins in control and prion-infected mouse plasma [84]. This method enabled us to identify a low-abundance glycoprotein serum amyloid P-component (SAP). PNGase F digestion and Western blotting validation confirmed that the glycosylated form of SAP was significantly elevated in mice with early prion infection, and it could be potentially used as a diagnostic biomarker for prion diseases.

Membrane proteins

Membrane proteins play an indispensable role in maintaining cellular integrity of their structure and perform many important functions, including signaling transduction, intercellular communication, vesicle trafficking, ion transport, and protein translocation/integration[85]. However, due to being relatively insoluble in water and low abundance, it is challenging to analyze membrane proteins by traditional MS-based proteomics approaches. Numerous efforts have been made to improve the solubility and enrichment of membrane proteins during sample preparation. Several comprehensive studies recently covered the commonly used technologies in

membrane proteomics and different strategies that circumvent technical issues specific to the membrane [86-90]. Recently, Sun *et al*. reported using 1-butyl-3-methyl imidazolium tetrafluoroborate (BMIM BF4), an ionic liquid (IL), as a sample preparation buffer for the analysis of integral membrane proteins (IMPs) by microcolumn reversed phase liquid chromatography (μRPLC)-electrospray ionization tandem mass spectrometry (ESI-MS/MS). The authors compared BMIM BF4 to the other commonly used solvents, such as sodium dodecyl sulfate, methanol, Rapigest, and urea, but they found that the number of identified IMPs from rat brain extracted by ILs was significantly increased. The improved identifications could be due to the fact that BMIM BF4 has higher thermal stability and thus offered higher solubilizing ability for IMPs which provided better compatibility for tryptic digestion than traditionally used solvent systems [38]. In addition to characterization of membrane proteome, the investigation of PTMs on membrane proteins is equally important for characterization of disease markers and drug treatment targets. Phosphorylations and glycosylations are the two most important PTMs for membrane proteins. In many membrane protein receptors, the cytoplasmic domains can be phosphorylated reversibly and function as signal transducers, whereas the receptor activities of the extracellular domains are mediated via *N*-linked glycosylation. Wiśniewski *et al*. provides an informative summary on recent advances in proteomic technology for the identification and characterization of these modifications [91]. Our group has pioneered the development of detergent assisted lectin affinity chromatography (DALAC) for the enrichment of hydrophobic glycoproteins using mouse brain extract [92]. We compared the binding efficiency of lectin affinity chromatography in the presence of four commonly used detergents and determined that under certain concentrations, detergents can minimize the nonspecific bindings and facilitate the elution of hydrophobic glycoproteins. In summary, NP-40 was suggested as the most suitable

detergent for DALAC due to the higher membrane protein recovery, glycoprotein recovery and membranous glycoprotein identifications compared to other detergents tested. In a different study on mouse brain membrane proteome, Zhang *et al*. reported an optimized protocol using electrostatic repulsion hydrophilic interaction chromatography (ERLIC) for the simultaneous enrichment of glyco- and phosphopeptides from mouse brain membrane protein preparation [93]. Using this protocol, they successfully identified 544 unique glycoproteins and 922 glycosylation sites, which were significantly higher than those using the hydrazide chemistry method. Additionally, a total of 383 phosphoproteins and 915 phosphorylation sites were identified, suggesting that the ERLIC separation has the potential for simultaneous analysis of both glyco- and phosphoproteomes.

Peptidomics

Peptidomics can be loosely defined as the study of the low molecular weight fraction of proteins encompassing biologically active endogenous peptides, protein fragments from endogenous protein degradation products, or other small proteins such as cytokines and signaling peptides. Studies can involve endogenous peptides,[94] peptidomic profiling,[33] and *de novo* sequencing of peptides.[95, 96] Neuropeptidomics focuses on biologically active short segments of peptides and have been investigated in numerous species including *Rattus,*[97, 98] *Mus musculus,*[99, 100] *Bovine taurus,* [101] Japanese quail diencephalon,[102] and invertebrates.[103-106] The isolation of peptides is typically performed through molecular weight cut-offs from either biofluids such as CSF, plasma or tissue extracts. If the protein and peptide content is high such as for tissue or cell lysates protein precipitation can be done via high organic solvents and the resulting supernatant can be analyzed for extracted peptides, where extraction solvent and conditions could have a

significant effect on what endogenous peptides are extracted from tissue.[107] A comparative peptidomic study of human cell lines highlights the utility of finding peptide signatures as potential biomarkers.[108] A thorough review of endogenous peptides and neuropeptides is beyond the scope of this review and an excellent review on this topic is available elsewhere.[109]

Fractionation and Separation

The mass spectrometer has a limited duty cycle and data dependent analysis can only scan a limited number of *m/z* peaks at any given time. In addition, significant ion suppression can occur if there is a difference in concentration between co-eluting peptides, or if too many peptides co-elute. Therefore, one of the biggest challenges in biomarker discovery is the complexity of the sample and the presence of high-abundance proteins in body fluids such as CSF, serum, and plasma. In addition to the removal of the most abundant proteins by immunodepletion, the reduction of the complexity of the sample by further fractionation is indispensable to facilitate the characterization of unidentified biomarkers from the low abundance proteins. Traditionally used techniques for complex protein analysis include: gel based fractionation methods such as two-dimensional gel electrophoresis (2D-GE) and its variation two-dimensional differential gel electrophoresis (2D-DIGE), or non-gel based, such as one- or multidimensional liquid chromatography (LC), and microscale separation techniques such as capillary electrophoresis (CE).

2D-GE MS has been widely used as a powerful tool to separate proteins and identify differentially expressed proteins ever since 2D gels were coupled to mass spectrometry. In 2D-GE MS thousands of proteins can be separated on a single gel according to p*I* and molecular weight. Individual protein spots that show differences in abundance between different samples

can then be excised from the gel, digested into peptides and analyzed by MALDI MS or by liquid chromatography tandem mass spectrometry (LC-MS/MS) for protein identification. The introduction of 2D-DIGE adds a quantitative strategy to gel electrophoresis by enabling multiple protein extracts to be separated on the same 2D gel, thus providing comparative analysis of proteomes in complex samples. In 2D-DIGE, protein extracts from two different conditions, and an internal standard can be labeled with fluorescent dyes, for example Cy3, Cy5 and Cy2 respectively prior to two-dimensional gel electrophoresis. Compared to traditional 2D-GE, 2D-DIGE provides the clear advantage of overcoming the inter-gel variation problem [110]. Proteomic profiling of CSF by 2D-GE and 2D-DIGE has led to the identification of putative biomarkers in multiple neurological disorders. For example, Brechlin *et al.* reported an optimized 2-DIGE protocol profiled CSF from 36 CJD patients. The applicability of their approach was proven by the detection of known CJD biomarkers such as 14-3-3 protein, neuron-specific enolase, lactate, dehydrogenase, and other proteins that are potentially relevant to CJD [111]. In another study to identify novel CSF biomarkers for multiple sclerosis, CSF from 112 multiple sclerosis patients and control individuals were analyzed by 2D-GE MS for comparative proteomics. Ten potential multiple sclerosis biomarkers were selected for validation by immunoassay [112]. These methodologies, sample preparation techniques, and applications of 2D-DIGE in neuroproteomics were reviewed by Diez *et al.*[113]. Although 2D gel provides excellent resolving power and capability to visualize abundance changes, there are some limitations to the method. For example, gel based separation is not suitable for low abundance proteins, extremely basic or acidic proteins, very small or large proteins, and hydrophobic proteins [114, 115].

Complementary to gel-based approaches, shotgun proteomics coupled to LC have become increasingly popular in proteomic research because they are reproducible, highly

automated, and capable of detecting low abundance proteins. Furthermore, another advantage of LC-MS shotgun proteomics is the suitability for isotope labeling for protein quantification which is reviewed in a later section. In shotgun proteomics, a protein mixture is digested and resulting peptides are separated by LC prior to tandem MS fragmentation, to identify different proteins by peptide sequencing. The most common separation for shotgun proteomics, peptidomics, or top-down proteomics experiments use low-pH reversed phase (RP) C18, C8, or C4 columns. RPLC is well established which provides high resolution, desalts the sample which can interfere with ionization, and the mobile phase is compatible with ESI. Nanoscale C18 columns allow for separation and introduction of sub microgram samples. If larger amounts of sample are available, two dimensional separations are usually preferred to greatly enhance the coverage of the investigated proteome, which will be discussed in depth later. It is preferable to have an orthogonal separation method and since RP separates via hydrophobicity, strong cation exchange (SCX) was the original choice due to its separation by charge. MudPIT (multidimensional protein identification technology) usually refers to the use of SCX as the first phase of separation and is a well-established platform.[116] SCX has the advantage over RP separation technologies to effectively remove interfering detergents from the sample. SCX separation is not based solely off charge and hydrophobicity contributes to elution, therefore a small amount of organic modifier, usually 10-15%, is added to lessen the hydrophobicity effects.[117] The addition of organic modifiers needs to be minimized otherwise binding to the C18 trap cartridge or C18 column will be reduced if performed on-line. SCX can be used for PTMs and offers specific applications for proteomic studies and an excellent, current review is offered on this subject elsewhere[118]. An alternative MudPIT separation scheme employing high pH RPLC as the first phase of separation and low pH RPLC in the second dimension (RP-RP) has been successfully

applied to the proteomic analysis of complex biological samples[119, 120]. The advantage of using RP as the first dimension is the higher resolution for separation and better compatibility with down-stream MS detection by eliminating salt. Song *et al*. reported a phosphoproteome analysis based on this 2D RP-RP coupling scheme[121].

Hydrophilic interaction chromatography (HILIC) employs distinct separation modality where the retention of peptides is increased with increasing polarity.[122] The loading of sample is done by high organic and eluted by increasing the percentage of the aqueous phase, or polarity of the mobile phase, opposite from RPLC, thus establishing orthogonality of the two separation modes [123]. HILIC has quickly become a very useful method and is actively used for proteomic experiments[124] for increased sensitivity,[125] phosphoproteomics,[126] glycoproteins,[127] and quantification studies.[128] An alternative and modification to HILIC is ERLIC, which adds an additional mode of separation by electrostatic attraction. An earlier study using ERLIC demonstrated the ability to separate phosphopeptides from non-phosphorylated peptides at pH=2.[129] A recent study looking into changes in the phosphoproteome of Marek's Disease applied ERLIC to chicken embryonic fibroblast lysate identifying only 1.3% phosphopeptides out of all the identified peptides. Due to the lack of isolation of phosphopeptides from ERLIC the investigators performed immobilized metal affinity chromatography (IMAC) enrichment on the fractions increasing identification of phosphopeptides over 50 fold.[130] A comparative study of ERLIC to HILIC and SCX following TiO_2 phospho-enrichment reported that SCX>ERLIC>HILIC for phosphopeptide identifications.[126]

Recent developments in instrumentation to combine LC with ion mobility spectrometry (IMS) and MS (LC-IMS-MS), offered more advantages than conventional LC due to the rapid, high-resolution separations of analytes based on their charge, mass and shape as reflected by

mobility in a given buffer gas. The mobility of an ion in a buffer gas is determined by the ion's charge and its collision cross-section with the buffer gas. The methodologies of IMS separations and the application of LC-IMS-MS for the proteomics analysis of complex systems, including human plasma have been reviewed by Clemmer's group [131-133]. They proposed a method that employs intrinsic amino acid size parameters to obtain ion mobility predictions which can be used to rank candidate peptide ion assignments and significantly improve peptide identification. [134]

Although 2D gel and LC are routinely used as separation techniques in MS-based proteomics, capillary electrophoresis (CE) has received increasing attention as a promising alternative due to the fast and high-resolution separation it offers. CE has a wide variety of operation modes, among which capillary zone electrophoresis (CZE) and capillary isoelectric focusing (CIEF) have the greatest potential applications in MS-based proteomics, thus will be highlighted here. CZE separates analytes by their charge-to-size ratios in buffers under a high electrical field and is often used as the final dimension prior to MS analysis, while the separation feature of CIEF is based on isoelectric point, and this technique is more suitable to be used as the first dimension separation. Detailed description of different CE–MS interfaces, sample preconcentration and capillary coating to minimize analyte adsorption could be found in several reviews [135-141]. CE technique is complementary to conventional LC in that it is suitable for the analysis of polar and chargeable compounds. Dovichi's group conducted proteomic analysis of the secreted protein fraction of *Mycobacterium marinum* which has intermediate protein complexity [142]. The tryptic digests were either analyzed by UPLC-ESI-MS/MS in triplicates or prefactionated by RPLC followed by CZE-ESI-MS/MS. It was demonstrated that the two methods identified similar numbers of peptides and proteins within similar analysis times.

However, CZE-ESI-MS/MS analysis of the prefractionated sample tended to identify more peptides that are basic and have lower *m/z* values than those identified by UPLC-ESI-MS/MS. This analysis also presented the largest number of protein identifications by using CE-MS/MS, suggesting the effectiveness of prefractionation of complex samples by LC method prior to CZE-ESI-MS/MS. The use of CIEF as the first dimension of separation provides both sample concentration and excellent resolving power. The combination of CIEF and RPLC separation has been applied to the proteomic analyses where the amount of protein sample is limited and cannot meet the requirement of minimal load amount for 2D LC-MS/MS [143, 144]. So far CE-MS has been widely applied to the proteomic analysis of various biological samples such as urine [145, 146], CSF [147], blood [148], frozen tissues [149], and the formalin-fixed and paraffin-embedded (FFPE) tissue samples [150]. The recent CE–MS applications to clinical proteomics have been summarized in several reviews [135, 151, 152].

Protein Quantification

In 2D gel electrophoresis, the quantitative analysis of protein mixtures is performed on the gel by comparing the intensity of the protein stain. The development of 2D-DIGE eliminated the gel-to-gel variation and greatly improved the quantitative capability and reliability of 2D gel methodology.[110] However, the accuracy of 2D gel based protein quantification suffers from the limitations that a seemingly single gel spot often contains multiple proteins and the difficulty of detecting proteins with extreme molecular weights and p*I* values as well as highly hydrophobic proteins such as membrane proteins. Therefore, non-gel based shotgun proteomics technology is more suitable for accurate and large-scale protein identification and quantification in complex samples. Briefly, the quantification in non-gel based shotgun proteomics can be categorized into

two major approaches: stable isotope labeling-based and label-free methods. The common strategies for quantitative proteomic analysis are reviewed and summarized in Table 1.

Isotope labeling methods

Because stable isotope-labeled peptides have the same chemical properties as their unlabeled counterparts, the two peptides within a mixture should exhibit identical behaviors in MS ionization. The mass difference introduced by isotope labeling enables the detection of a pair of two distinct peptide masses by MS within the mixture and allowing for the measurement of the relative abundance differences between two peptides. Depending on how isotopes are incorporated into the protein or peptide, these labeling methods can be divided into two groups: *In vitro* chemical derivatization techniques, which incorporate a label or tag into the peptide or protein during sample preparation; metabolic labeling techniques, which introduce the isotope label directly into the organism via isotope-enriched nutrients from food or media.

1. *In vitro* derivatization techniques

There are multiple methods to introduce heavy isotopes into proteins or peptides *in vitro*. The commonly used strategies include $^{18}O/\ ^{16}O$ enzymatic labeling, Isotope-Coded Affinity Tag (ICAT), Tandem Mass Tags (TMTs), and Isobaric Tags for Relative and Absolute Quantification (iTRAQ). The ^{18}O labeling method enzymatically cleaves the peptide bond with trypsin in the presence of ^{18}O-enriched H_2O and introduces 4-Da mass shift in the tryptic peptides [153]. The advantages of this method include: ^{18}O-enriched water is extremely stable; tryptic peptides will be labeled with the same mass shift; secondary reactions inherent to other chemical labeling can be avoided. Conversely, widespread use of ^{18}O-labeling has been hindered due to the difficulty of attaining complete ^{18}O incorporation and the lack of robustness [154, 155]. Currently, ICAT,

TMTs and iTRAQ methods are extensively used in quantitative proteomics. In ICAT, cysteine residues are specifically derivatized with a reagent containing either zero or eight deuterium atoms as well as a biotin group for affinity purification of cysteine-containing peptides [156, 157]. The advantage of ICAT is that the affinity purification via biotin moiety can facilitate the detection of low-abundance cysteine-containing peptides. In addition, the mass difference introduced by labeling increases mass spectral complexity, with quantification from the different precursor masses done by MS and peptide identification being achieved through tandem MS (MS/MS). This added complexity from different peptide masses was addressed by using isobaric labeling methods such as TMTs and iTRAQ [158, 159] where the same peptides in different samples are isobaric after tagging and appear as single *m/z* in MS scans, thus enhancing the peptide limit of detection and reducing the MS scan complexity. Isobaric labeling reagents are composed of a primary amine reactive group and an isotopic reporter group linked by an isotopic balancer group for the normalization of the total mass of the tags. The reporter group serves for quantification purpose since it is cleaved during collision-induced dissociation (CID) to yield a characteristic isotope-encoded fragment. Moreover, isobaric labeling methods allow the comparison of multiple samples within a single experiment. Recently, a 6-plex version of TMTs was reported [160], and iTRAQ enables up to eight samples to be labeled and relatively quantified in a single experiment [161]. 8-plex iTRAQ reagents have been used for the comparison of complicated biological samples such as CSF in the studies of neurodegenerative diseases [162]. Recently, our group developed a novel N, N-dimethyl leucine (DiLeu) 4-plex isobaric tandem mass (MS^2) tagging reagents with high quantitation efficacy. DiLeu has the advantage of synthetic simplicity and greatly reduced synthesis cost compared to TMTs and iTRAQ [163]. Xiang *et al*. demonstrated, that DiLeu produced comparable iTRAQ ability for protein sequence coverage

(~43%) and quantitation accuracy (<15%) for tryptically digested proteins. More importantly, DiLeu reagents could promote enhanced fragmentation of labeled peptides, thus allowing more confident peptide and protein identifications.

2. *In Vivo* Metabolic Labeling

Metabolic processes can also be employed for the incorporation of stable-isotope labels into the proteins or organisms by enriching culture media or food with light or heavy versions of isotope labels (^{2}H, ^{13}C, ^{15}N). The advantage of *in vivo* labeling is that metabolic labeling does not suffer from incomplete labeling which is an inherent drawback for *in vitro* derivatization techniques. In addition, metabolic labeling occurs from the start of the experiment, and proteins with light or heavy labels are simultaneously extracted, thus reducing the error and variability of quantification introduced during sample preparation. The most widely used strategy for metabolic labeling is known as stable-isotope labeling of amino acids in cell culture (SILAC) which was introduced by Mann and co-workers [164, 165]. In SILAC, one cell population is grown in normal, or light, media, while the other is grown in heavy media enriched with a heavy isotope-encoded (typically ^{13}C or ^{15}N) amino acid, such as arginine or leucine. Cells from the two populations are then combined; proteins are extracted, digested, and analyzed by MS. The relative protein expression differences are then determined from the extracted ion chromatograms from both the light and heavy peptide forms. SILAC has been shown to be a powerful tool for the study of intracellular signal transduction. In addition, this technique has recently been applied to the quantitative analysis of phosphotyrosine (pTyr) proteomes to characterize pTyr-dependent signaling pathways [166, 167].

Labe-free quantification

Although various isotope labeling methods have provided powerful tools for quantitative proteomics, several limitations of these approaches are noted. Labeling increases the cost and complexity of sample preparation, introduces potential errors during the labeling reaction. It also requires a higher sample concentration and complicates data processing and interpretation. In addition, so far only TMTs and iTRAQ allow the comparison of multiple (up to eight) samples simultaneously. The comparison of more than eight samples in a single experiment cannot be achieved by isotope labeling. In order to address these concerns, there has been significant interest in the development of label-free quantitative approaches. Current label-free quantification methods for MS-based proteomics were developed based on the observation that the chromatographic peak area of a peptide [168, 169] or frequency of MS/MS spectra [170] correlating to the protein or peptide concentration. Therefore, the two most common label-free quantification approaches are conducted by comparing: (i) area under the curve (AUC) of any given peptides [171, 172] or (ii) by frequency measurements of MS/MS spectra assigned to a protein, commonly referred to as spectral counting [173]. Several recent reviews provided detailed and comprehensive knowledge comparing label-free methods with labeling methods, data processing and commercially available software for label-free quantitative proteomics [174-177].

Dissociation Techniques

The vast majority of proteomic experiments have proteins or peptides being identified by two critical pieces of data obtained from the mass spectrometer. The first is the precursor ion identified by its *m/z*, which is informative to the mass of the peptide being analyzed. The second is the use of tandem mass spectrometry to fragment or dissociate the precursor ion and record the

generated fragment ion pattern to discern the amino acid sequence. The three most popular dissociation or fragmentation techniques for peptides are CID, electron-transfer dissociation (ETD), and high-energy collision dissociation (HCD). A recent study on the human plasma proteome demonstrated that combined fragmentation techniques enhance coverage by providing complementary information for identifications. CID enabled the greatest number of protein identifications, while HCD identified an additional 25% proteins and ETD contributed an additional 13% protein identifications.[178]

ETD/ECD

Electron capture dissociation (ECD) [179] preceded ETD, but ECD was developed for use in a Penning trap for Fourier transform ion cyclotron resonance (FTICR) mass spectrometers. ECD requires the ion of interest to be in contact with near-thermal electrons and for the electron capture event to occur on the millisecond time scale, but the time scale is inadequate for electron trapping in Paul traps or quadrupoles in the majority of mass spectrometers.[180] ETD involves a radical anion, like fluoranthene, with low electron affinity to be transferred to peptide cation, which results in more uniform cleavage along the peptide backbone. The cation accepts an electron and the newly formed odd-electron protonated peptide undergoes fragmentation by cleavage of the N-Cα bond which results in fragmentation ions consisting of c- and z•-type product ions. The uniformed cleavage results in reduced sequence discrimination to labile bonds such as PTMs and also provides improved sequencing for larger peptides compared to CID.[181] The realization that larger peptides produced better MS/MS quality spectra compared to CID led to a decision tree analysis strategy where peptide charge states and size determined whether the precursor peptide would be fragmented with CID or ETD.[182] One of the main benefits of

ETD/ECD is the ability to sequence peptides with labile PTMs such as phosphorylation[77, 183], sulfation[184], glycosylation[185], ubiquitination[186], and histone modifications.[187] ETD also has the benefit of providing better sequence information on larger neuropeptides when compared to CID[188]. However, a thorough analysis suggested that CID still yielded more peptide/protein identifications than ETD in large scale proteoimcs.[189]

HCD

High energy collision dissociation (HCD)[190] is an emerging fragmentation technique that offers improved detection of small reporter ions from iTRAQ-based studies.[191, 192] HCD is performed at a higher energy in a collision cell instead of an ion trap like CID, thus HCD does not suffer from the low-mass cutoff limitation. Furthermore, HCD offers enhanced fragmentation efficiency, assisting in MS/MS spectra interpretation and protein identification.[193] A major drawback for HCD is that the spectral acquisition times are up to two-fold longer due to increased ion requirement for Fourier transform detection in the orbitrap.[194] HCD has been reported to increase phosphopeptide identifications over CID,[74] but in a different study CID was reported to offer more phosphopeptide identifications over HCD.[194] Work has also been done to transfer the decision tree analysis for HCD which basically switches CID with HCD claiming better quality data determined by higher Mascot scores with more peptide identifications.[195]

MS^E

Data dependent acquisition (DDA) is the most commonly used ion selection process in mass spectrometers for proteomic experiments. An alternative process which does not have ion selection nor switch between MS and MS/MS modes is termed MS^E. MS^E is a data independent

mode and does not require precursor ions of a significant intensity to be selected for MS/MS analysis.[196] A data independent mode decouples the mass spectrometer choosing which precursor ions to fragment and when the ions are fragmented. MS^E works by a low or high energy scan and no ion isolation is occurring. The low energy scan is where the precursor ion is not fragmented, and the high energy scan allows fragmentation. The resulting mix of precursor and fragmentation ions is then detected simultaneously.[197] The data will then need to be deconvoluted using a proprietary, time-aligned algorithm that is discussed elsewhere.[198] The continuous data independent acquisition allows multiple MS/MS spectra to be collected during the natural analyte peak broadening observed in chromatography, which provides more data points for AUC label-free quantification. In addition, lower abundance peptides can be sequenced, as more MS/MS spectra are collected throughout the elution of an LC peak, allowing better signal averaging for smaller analyte peak of interest during coelution and reducing sampling bias in typical DDA experiments where only more abundant peaks can be selected for fragmentation.

A comparison of spiked internal protein standards into a complex protein digest provided evidence that MS^E was comparable to DDA analysis in LC-MS.[199] MS^E has been used for label free proteomics of immunodepleted serum in large scale proteomics samples.[200] In addition, MS^E was performed for the characterization of human cerebellum and primary visual cortex proteomes. Hundreds of proteins were identified, including many previously reported in neurological disorders.[201] MS^E is quickly becoming a versatile data acquisition method, recently used in such studies as cancer cells,[202] schizophrenia,[203] and pituitary proteome discovery.[204] The usefulness of MS^E as an unbiased data acquisition method is being assimilated into multiple proteomics studies including studies involving neurological disorders.

Data Analysis

One of the major bottlenecks in non-targeted proteomic experiments is how to handle the enormous amount of data obtained. Database searches, biostatistical analysis, *de novo* sequencing, PTM validation all have their place and multiple available platforms are available.

If the organism being studied has had its genome sequenced databases can be created with a list of proteins in the FASTA format to be used in database searching. There are numerous database searching algorithms for sequence identification of MS/MS data including Mascot[205], Sequest[206], Xtandem[207], OMSSA[208], and PEAKS.[209] These searching algorithms are performed by matching MS/MS spectra and precursor mass to sequences found within proteins. How well the actual spectra match the theoretical spectra determines a score, which is unique to the searching algorithm and usually can be extrapolated to the probability of a random hit. Recently, a database has been developed for PTM analysis by the use of the program SIMS.[210] Specifically for phosphopeptides, Ascore's algorithm scans the MS/MS data to determine the likelihood of correct phosphosite identification from the presence of site identifying product ions.[211] If the organism that is being analyzed has not had its genome sequenced and no (or very limited) FASTA database is available, a homology search can be performed using SPIDER[212] available with PEAKS software. Alternatively, individual MS/MS spectrum can be *de novo* sequenced, but software is available to perform automated *de novo* sequencing of numerous spectra (PEAKS,[208] DeNovoX, and PepSeq).

For large-scale protein identifications, the false discovery rate (FDR) must be established by the searching algorithm, and that is accomplished by re-searching the data with a false database created by reversing or scrambling the amino acid sequence of the original database

used for the protein search. Any hits from the false database will contribute to the FDR and this value can be adjusted, usually around 1%. An additional layer of confidence in the obtained data can be achieved in shotgun proteomics experiments by removing all the proteins that are identified by only one peptide.

Once a set of confident proteins or peptides have been generated from database searching, bioinformatic analysis or biostatistical analysis is needed. Numerous software packages are available for different purposes. FLEXIQuant is an example for absolute quantitation of isotopically labeled protein or peptides of interest.[213] FDR analysis of phosphopeptides or other specific PTMs can be adjusted with such software as Scaffold, providing data consisting only of a specific modification.[214] Bioinformatic tools, such as Scaffold or ProteoIQ, also include gene ontology (GO) analysis, which can classify identified proteins by three categories: cellular component, molecular function, or biological process. Custom bioinformatics programs can also be developed and are often useful in various proteomic studies, including biomarker discovery in neurological diseases.[215] More detailed review of bioinformatics in peptidomics[216] and proteomics[217] can be found elsewhere.

Validation of Biomarkers by Targeted Proteomics

The validation of putative biomarkers identified by MS-based proteomic analysis is often required to provide orthogonal analysis to rule out a false positive by MS and providing additional evidence for the biomarker candidate(s) from the study for future potential clinical assays. At present, antibody-based assays such as Western blotting, ELISA and immunochemistry are the most widely used methods for biomarker validation. Although accurate and well established, these methods rely on protein specific antibodies for the measurement of

the putative biomarker and could be difficult for large-scale validation of all or even a subset of a long list of putative protein biomarkers typically obtained by MS-based comparative proteomic analysis. Large scale validation is impractical due to the cost for each antibody, the labor to develop a publishable Western blot or ELISA, and the antibody availability for certain proteins. As an alternative strategy, quantitative assays based on multiple-reaction monitoring (MRM) MS using a triple quadrupole mass spectrometer have been employed in biomarker verification.

MRM is the most common use of MS/MS for absolute quantitation. It is a hypothesis driven experiment where the peptide of interest and its subsequent fragmentation pattern must be known prior to the quantitative MRM experiments. MRM involves selecting a specific *m/z* (first quadrupole) to be isolated for fragmentation (second quadrupole), followed by one or more of the most intense fragment ions (third quadrupole) being monitored. The ability to quantitate and thus validate the proteins or peptides as potential biomarkers is achieved by performing MRM on isotopically labeled reference peptide for targeted peptide/protein of interest. The main obstacle for quantification of peptides is interference and ion suppression effects from co-eluting substances. Since the isotopically labeled and native peptide will co-elute, the same interference and ion suppression will occur for both peptides, and thus correcting these interfering effects.

Peptides need to be systematically chosen for a highly sensitive and reproducible MRM experiment to ensure proper validation of putative biomarkers. Peptides require certain intrinsic properties which include an *m/z* within the practical mass detection range for the instrument and high ionization efficiency. If the desired peptide to be quantified is derived from a digestion, then peptides that have detectable incomplete digestion or missed cleavage site can be a major source of variability. Peptides with a methionine and to a lesser extent tryptophan are traditionally removed from consideration from MRM quantitative experiments due to the

variable nature of the oxidation that can occur. In addition, if chromatographic separation is performed the retention behavior of the peptide must be well behaved with little tailing effects, eluting late causing broadening of the peak, and even irreversible binding to the column. As an example, hydrophilic peptides being eluted off a C18 column may exhibit the previously described concerns and a different chromatographic separation will need to be explored for improved limits of detection, quantitation, and validation. To determine consistent peptide detection or usefulness of certain peptides databases such as Proteomics Database[218], PRIDE[219], PeptideAtlas[220] have been developed to compile proteomic data repositories from initial discovery experiments.

After the peptide is selected for analysis the proper MRM transitions need to be selected to optimize the sensitivity and selectivity of the experiment. It is common for investigators to select two or three of the most intense transitions for the proposed experiment. It is imperative that the same instrument is used for the determination of transition ions as different mass spectrometers may have a bias towards different fragment ions.

MRM experiments are still highly popular experiments for hypothesis directed experiments,[221] biomarker analysis,[222] and validation.[223] Validation of putative biomarkers is increasingly becoming a necessary step when performing large scale non-hypothesis driven proteomics experiments. The traditional validation techniques of ELISA, Western blotting, and immunohistochemistry are still used, but MRM experiments are becoming an attractive alternative for validation of putative biomarkers due to its enhanced throughput and specificity. Current work is still being performed to both expand the linear dynamic range[224] and sensitivity[225] of MRM. A recent endeavor to increase the sensitivity for MRM experiments was accomplished by “Pulsed MRM” via the use of an ion funnel trap to enhance confinement and

accumulation of ions. The authors claimed an increase by 5-fold for peak amplitude and a 2-3 fold reduction in chemical background.[225]

Remaining Challenges and Emerging Technologies

Large sample numbers for mass spectrometry analysis

Multiple conventional studies in proteomics have been performed on a single or a few biological samples. As bio-variability can be exceedingly high, the need for larger sample sizes is currently being investigated. Prentice *et al.* used a starting point of 3,200 patient samples from the Women's Health Institute (WHI) to probe the plasma proteome using MS for biomarkers. The study did not test the 3,200 patient samples by MS because even a simple one hour one dimensional RP analysis on a mass spectrometer would take months of instrument time for uninterrupted analysis. Instead, the authors pooled 100 samples together to bring the total number of pooled samples to 32. To provide relevant plasma biomarkers the samples were then subjected to immunodepletion, 2-D protein separation (96 fractions total), and then 1-D RPLC of tryptic peptide separation on-line interface to a mass spectrometer. The large sample cohorts help address bio-variability that can be a concern from small sample size proteomic experiments and provide ample sample amounts to investigate the low abundance proteins.[226]

Hemoglobin-derived neuropeptides and non-classical neuropeptides

Neuropeptides, such as neuropeptide Y and enkephalin, are short chains of amino acids that are secreted from a range of neuronal cells that signal nearby cells. In contrast, non-classical neuropeptides are termed as neuropeptides or "microproteins" which are derived from intracellular protein fragments and synthesized from the cytosol.[227] MS was recently used to

determine that hemopressins, which are hemoglobin-derived peptides, are upregulated in $Cpe^{fat/fat}$ mice brains. Gelman *et. al.* designed an MS experiment to compare hemoglobin-derived peptides, comparing the brain, blood, and heart peptidome in mice. The authors provided data that specific hemoglobin peptides were produced in the brain and were not produced in the blood. Certain alpha and beta hemoglobin peptides were also up regulated in the brain for $Cpe^{fat/fat}$ mice and bind to CB1 cannabinoid receptors.[228] As discussed earlier in the review, peptidomics and specifically neuropeptidomics are popular fields of study utilizing MS and non-classical neuropeptides is an exciting, emerging area of research that could further expand the diversity of cell-cell signaling molecules.

Ultrasensitive mass spectrometry for single cell analysis

In addition to large scale analysis, MS-based proteomics and peptidomics are making progress into ultrasensitive single cell analysis. The most successful MS-based techniques for single cell analysis was performed with MALDI, and studies that have been performed on relatively large neurons are reviewed elsewhere.[229] The ultrasensitive MS analysis is currently directed towards single cell analysis of smaller cells including cancer cells. The first challenge in single cell analysis is the isolation and further sample preparation to yield relevant data. Collection and isolation of a cell type can be accomplished using antibodies for fluorescence activated cell sorting (FACS) and immune magnetic separation. FACS works by flow cytometry sorting cells by a laser that excites a fluorescent tag that is attached to an antibody. Immune magnetic separation allows separation by antibodies with magnetic properties such as Dynabeads.[230] One exciting study combining FACS and MS termed mass cytometry. This technology works by infusing a droplet into an inductively coupled plasma mass spectrometer

(ICP-MS) containing a single cell bound to antibodies chelated to transition elements allowing a quantifying response between single cells.[231] Clearly, the future of single cell analysis for biomarker analysis and proteomics is encouraging and has the potential to be an emerging field in MS-based proteomics and peptidomics.

Laserspray ionization (LSI)

Laserspray ionization (LSI) is an exciting new method to produce multiply charged mass spectra from MALDI that is nearly identical to ESI.[232-234] Recently, it has been reported that LSI can be performed in lieu of matrix to produce a total solvent-free analysis.[234] The benefits of being able to generate multiply charged peptides without any solvent may offer advantages including MS analysis of insoluble membrane proteins or hydrophobic peptides, avoidance of chemical reactions while in solvents, a reduction of sample loss due to liquid sample preparation, and ability to avoid diffusion effects from tissue imaging studies.[234]

The multiply charged peptide and protein ions produced by LSI expand the mass range for tissue imaging analysis. More importantly, the multiply-charged peptide ions are amenable for electron-based fragmentation methods such as ETD or ECD, which can be employed in conjunction with tissue imaging experiments to yield *in situ* sequencing and identification of peptides of interest.[235]

Paper spray ionization

Paper spray (PS) is an ambient ionization method which was first reported using chromatography paper allowing detection of metabolites from dried blood spots. The original method used a cut out piece of paper with a voltage clipped on the back while applying 10 µL of

methanol/H_2O.[236] Improvements have been made to this technology to enhance analysis efficiency with a new solvent 9:1 dichloromethane/isopropanol (v/v) and the use of silica paper over chromatography paper.[237] Interesting applications or modifications have been made to PS including direct analysis of biological tissue[238] and leaf spray for direct analysis of plant materials[239], but both detect metabolites instead of proteins or peptides. Paper spray ionization was previously shown to enable detection of cytochrome c and bradykinin [2-9] standards, in a proof of principle study[240]. Clearly, the utility of PS analysis in proteomics and peptidomics is yet to be explored.

niECD

New fragmentation techniques have been investigated for their utility in proteomics and peptidomics, including a recently reported negative-ion electron capture dissociation (niECD). Acidic peptides which usually contain PTMs such as phosphorylation or sulfonation are often difficult to be detected as multiply charged peptides in the positive ion mode. As discussed earlier multiply charged peptides are required for ECD/ETD fragmentation. The fragmentation of niECD is accomplished by a multiply negatively charged peptide adding an electron. The resulting fragmentation of multiply sulfated and phosphorylated peptide and protein standards showed no sulfate loss and preserved phosphorylation site. The resulting fragmentation pattern from niECD was also improved in the peptide anions and provides a new strategy for *de novo* sequencing with PTM localization.[241]

Conclusions and Perspectives

Proteomics methodologies have produced large datasets of proteins involved in various biological and disease progression processes. Numerous mass spectrometry-based proteomics and peptidomics tools have been developed and are continuously being improved, in both chromatographic or electrophoretic separation and MS hardware and software. However, several important issues that remain to be addressed rely on further technical advances in proteomics analysis. When large proteomes consisting of thousands of proteins are analyzed and quantified, dynamic range is still limited with more abundant proteins being preferentially detected. Development and optimization of chemical tagging reagents that target specific protein classes maybe necessary to help enrich important signaling proteins and assess cellular and molecular heterogeneity of the proteome and peptidome. Furthermore, a significant bottleneck in usefulness of proteomics research is the ability to validate the results and provide clear significant biological relevance to the results. The idea of P4 medicine[242, 243] is an attractive concept where the four P's stand for predictive, preventive, personalized, and participatory. Proteomics is one of the critical "omics" fields and has led to the development of enabling innovative strategies to P4 medicine.[244] A goal of P4 medicine is to assess both early disease detection and disease progression in a person. A simplified example of how proteomics fits into P4 medicine is that certain brain-specific proteins could be used for diagnosis with presymptomatic prion disease.[244] The concept of proteomic experiments providing an individual biomarker is becoming more obsolete, with the revised vision being a biomolecular barcode that, could potentially be "scanned" or be a fingerprint for a specific disease or early onset to that disease being closer to reality. An excellent review on what biomarker analysis can do for true patients is available.[245]

Proteomics can also generate new hypothesis that can be tested by classical biochemical approaches. If a disease has an unknown pathogenesis, proteomics is a good starting point to try to assemble putative markers that can lead to further hypothesis for evaluation. If a particular protein or PTM is associated with a disease state either qualitatively or quantitatively, potential treatments could target that protein of interest, or investigators could monitor that protein or PTM during potential treatments of the disease. Proteomics has expanded greatly over the last few decades, with the goal of providing revealing insights to some of the most complex biological problems currently facing the scientific community.

Acknowledgements

Preparation of this manuscript was supported in part by the University of Wisconsin Graduate School, Wisconsin Alzheimer's Disease Research Center Pilot Grant, and a Department of Defense Pilot Award. L.L. acknowledges an H. I. Romnes Faculty Fellowship.

Figure 1. A summary of general workflows of biomarker discovery pipeline by MS-based proteomic approaches.

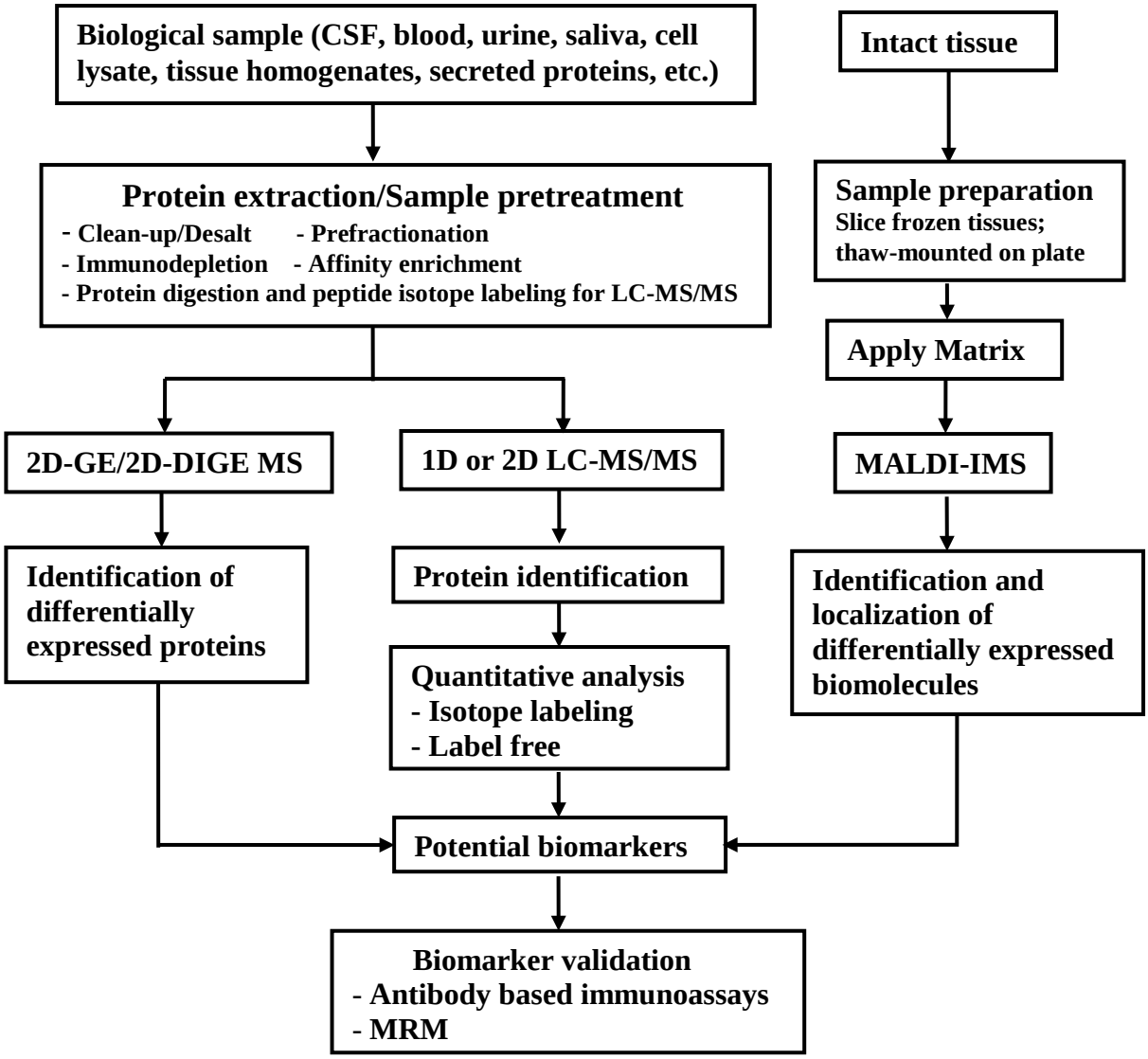

Figure 2. Tissue expression and dynamic range of the human plasma proteome**.** A pie chart representing the tissue of origin for the high abundance proteins shows that the majority of proteins come from the liver (A). Conversely, the lower abundance plasma proteins have a much more diverse tissue of origin (B and C). The large dynamic range of plasma proteins is presented and the proteins can be grouped into three categories (classical plasma proteins, tissue leakage products, interleukins/cytokines) (D). Adapted from Zhang et al[11] and Schiess et al.[246] with permission.

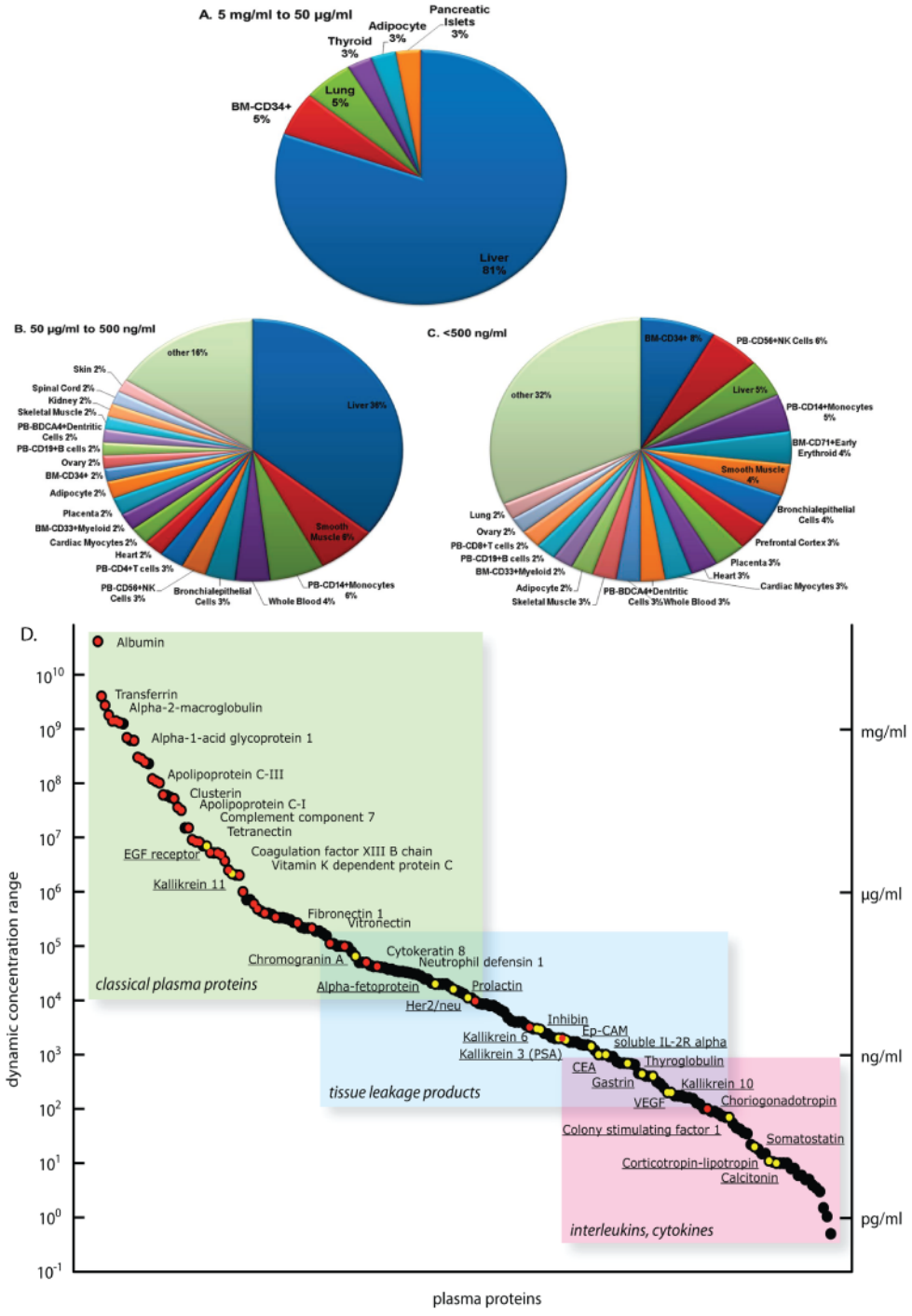
A. 5 mg/ml to 50 µg/ml
Pancreatic Islets 3%
Adipocyte 3%
Thyroid 3%
Lung 5%
BM-CD34+ 5%
Liver 81%
B. 50 µg/ml to 500 ng/ml
other 16%
Skin 2%
Spinal Cord 2%
Kidney 2%
Skeletal Muscle 2%
PB-BDCA4+Dentritic Cells 2%
PB-CD19+B cells 2%
Ovary 2%
BM-CD34+ 2%
Adipocyte 2%
Placenta 2%
BM-CD33+Myeloid 2%
Cardiac Myocytes 2%
Heart 2%
PB-CD4+T cells 3%
PB-CD56+NK Cells 3%
Bronchialepithelial Cells 3%
Whole Blood 4%
PB-CD14+Monocytes 6%
Smooth Muscle 6%
Liver 36%
C. <500 ng/ml
other 32%
BM-CD34+ 8%
PB-CD56+NK Cells 6%
Liver 5%
PB-CD14+Monocytes 5%
BM-CD71+Early Erythroid 4%
Smooth Muscle 4%
Bronchialepithelial Cells 4%
Prefrontal Cortex 3%
Placenta 3%
Heart 3%
Cardiac Myocytes 3%
Whole Blood 3%
PB-BDCA4+Dentritic Cells 3%
Skeletal Muscle 3%
Adipocyte 2%
BM-CD33+Myeloid 2%
PB-CD19+B cells 2%
PB-CD8+T cells 2%
Ovary 2%
Lung 2%
D.
Albumin
Transferrin
Alpha-2-macroglobulin
Alpha-1-acid glycoprotein 1
Apolipoprotein C-III
Clusterin
Apolipoprotein C-I
Complement component 7
Tetranectin
EGF receptor
Coagulation factor XIII B chain
Vitamin K dependent protein C
Kallikrein 11
Fibronectin 1
Vitronectin
Chromogranin A
Cytokeratin 8
Neutrophil defensin 1
classical plasma proteins
Alpha-fetoprotein
Prolactin
Her2/neu
Inhibin
Ep-CAM
Kallikrein 6
soluble IL-2R alpha
Kallikrein 3 (PSA)
Thyroglobulin
CEA
Gastrin
Kallikrein 10
tissue leakage products
VEGF
Choriogonadotropin
Colony stimulating factor 1
Somatostatin
Corticotropin-lipotropin
Calcitonin
interleukins, cytokines
dynamic concentration range
plasma proteins
mg/ml
µg/ml
ng/ml
pg/ml

Table 1. A summary of the common strategies applied to MS-based quantitative proteomic analysis

Gel based	**Stable isotope labeling**	**Label free**
2D-GE 2D-DIGE [110]	***In vitro* derivatization** $^{18}O/^{16}O$ [153] ICAT [156] TMT [159] iTRAQ [158] Formaldehyde [247] ICPL [248] ***In vivo* metabolic labeling** $^{14}N/^{15}N$ [249] SILAC [164]	AUC measurement [169, 172] Spectral counting [173]

AUC: Area Under Curve, ICAT: Isotope-Coded Affinity Tag, TMT: Tandem Mass Tags, iTRAQ: Isobaric Tags for Relative and Absolute Quantification , ICPL: Isotope Coded Protein Labeling, SILAC: Stable Isotope Labeling by Amino Acids in Cell Culture: Isobaric Tags for Relative and Absolute Quantification (iTRAQ)

References

1. Liu, T.; Qian, W. J.; Mottaz, H. M.; Gritsenko, M. A.; Norbeck, A. D.; Moore, R. J.; Purvine, S. O.; Camp, D. G., 2nd; Smith, R. D., Evaluation of multiprotein immunoaffinity subtraction for plasma proteomics and candidate biomarker discovery using mass spectrometry. *Mol Cell Proteomics* **2006,** 5, (11), 2167-74.
2. Holten-Andersen, M. N.; Murphy, G.; Nielsen, H. J.; Pedersen, A. N.; Christensen, I. J.; Hoyer-Hansen, G.; Brunner, N.; Stephens, R. W., Quantitation of TIMP-1 in plasma of healthy blood donors and patients with advanced cancer. *Br J Cancer* **1999,** 80, (3-4), 495-503.
3. Tammen, H.; Schulte, I.; Hess, R.; Menzel, C.; Kellmann, M.; Mohring, T.; Schulz-Knappe, P., Peptidomic analysis of human blood specimens: comparison between plasma specimens and serum by differential peptide display. *Proteomics* **2005,** 5, (13), 3414-22.
4. Rai, A. J.; Gelfand, C. A.; Haywood, B. C.; Warunek, D. J.; Yi, J.; Schuchard, M. D.; Mehigh, R. J.; Cockrill, S. L.; Scott, G. B.; Tammen, H.; Schulz-Knappe, P.; Speicher, D. W.; Vitzthum, F.; Haab, B. B.; Siest, G.; Chan, D. W., HUPO Plasma Proteome Project specimen collection and handling: towards the standardization of parameters for plasma proteome samples. *Proteomics* **2005,** 5, (13), 3262-77.
5. Lippi, G.; Guidi, G. C.; Mattiuzzi, C.; Plebani, M., Preanalytical variability: the dark side of the moon in laboratory testing. *Clin Chem Lab Med* **2006,** 44, (4), 358-65.
6. Holten-Andersen, M. N.; Schrohl, A. S.; Brunner, N.; Nielsen, H. J.; Hogdall, C. K.; Hogdall, E. V., Evaluation of sample handling in relation to levels of tissue inhibitor of metalloproteinases-1 measured in blood by immunoassay. *Int J Biol Markers* **2003,** 18, (3), 170-6.
7. Ytting, H.; Christensen, I. J.; Thiel, S.; Jensenius, J. C.; Svendsen, M. N.; Nielsen, L.; Lottenburger, T.; Nielsen, H. J., Biological variation in circulating levels of mannan-binding lectin (MBL) and MBL-associated serine protease-2 and the influence of age, gender and physical exercise. *Scand J Immunol* **2007,** 66, (4), 458-64.
8. Hanash, S., Building a foundation for the human proteome: the role of the Human Proteome Organization. *J Proteome Res* **2004,** 3, (2), 197-9.
9. Omenn, G. S.; States, D. J.; Adamski, M.; Blackwell, T. W.; Menon, R.; Hermjakob, H.; Apweiler, R.; Haab, B. B.; Simpson, R. J.; Eddes, J. S.; Kapp, E. A.; Moritz, R. L.; Chan, D. W.; Rai, A. J.; Admon, A.; Aebersold, R.; Eng, J.; Hancock, W. S.; Hefta, S. A.; Meyer, H.; Paik, Y. K.; Yoo, J. S.; Ping, P.; Pounds, J.; Adkins, J.; Qian, X.; Wang, R.; Wasinger, V.; Wu, C. Y.; Zhao, X.; Zeng, R.; Archakov, A.; Tsugita, A.; Beer, I.; Pandey, A.; Pisano, M.; Andrews, P.; Tammen, H.; Speicher, D. W.; Hanash, S. M., Overview of the HUPO Plasma Proteome Project: results from the pilot phase with 35 collaborating laboratories and multiple analytical groups, generating a core dataset of 3020 proteins and a publicly-available database. *Proteomics* **2005,** 5, (13), 3226-45.
10. Liu, T.; Qian, W. J.; Gritsenko, M. A.; Xiao, W.; Moldawer, L. L.; Kaushal, A.; Monroe, M. E.; Varnum, S. M.; Moore, R. J.; Purvine, S. O.; Maier, R. V.; Davis, R. W.; Tompkins, R. G.; Camp, D. G., 2nd; Smith, R. D., High dynamic range characterization of the trauma patient plasma proteome. *Mol Cell Proteomics* **2006,** 5, (10), 1899-913.
11. Zhang, Q.; Faca, V.; Hanash, S., Mining the plasma proteome for disease applications across seven logs of protein abundance. *J Proteome Res* **2011,** 10, (1), 46-50.
12. Matsubara, J.; Honda, K.; Ono, M.; Sekine, S.; Tanaka, Y.; Kobayashi, M.; Jung, G.; Sakuma, T.; Nakamori, S.; Sata, N.; Nagai, H.; Ioka, T.; Okusaka, T.; Kosuge, T.; Tsuchida, A.;

Shimahara, M.; Yasunami, Y.; Chiba, T.; Yamada, T., Identification of adipophilin as a potential plasma biomarker for colorectal cancer using label-free quantitative mass spectrometry and protein microarray. *Cancer Epidemiol Biomarkers Prev* **2011,** 20, (10), 2195-203.

13. Murakoshi, Y.; Honda, K.; Sasazuki, S.; Ono, M.; Negishi, A.; Matsubara, J.; Sakuma, T.; Kuwabara, H.; Nakamori, S.; Sata, N.; Nagai, H.; Ioka, T.; Okusaka, T.; Kosuge, T.; Shimahara, M.; Yasunami, Y.; Ino, Y.; Tsuchida, A.; Aoki, T.; Tsugane, S.; Yamada, T., Plasma biomarker discovery and validation for colorectal cancer by quantitative shotgun mass spectrometry and protein microarray. *Cancer Sci* **2011,** 102, (3), 630-8.

14. Addona, T. A.; Shi, X.; Keshishian, H.; Mani, D. R.; Burgess, M.; Gillette, M. A.; Clauser, K. R.; Shen, D.; Lewis, G. D.; Farrell, L. A.; Fifer, M. A.; Sabatine, M. S.; Gerszten, R. E.; Carr, S. A., A pipeline that integrates the discovery and verification of plasma protein biomarkers reveals candidate markers for cardiovascular disease. *Nat Biotechnol* **2011,** 29, (7), 635-43.

15. Acosta-Martin, A. E.; Panchaud, A.; Chwastyniak, M.; Dupont, A.; Juthier, F.; Gautier, C.; Jude, B.; Amouyel, P.; Goodlett, D. R.; Pinet, F., Quantitative mass spectrometry analysis using PAcIFIC for the identification of plasma diagnostic biomarkers for abdominal aortic aneurysm. *PLoS One* **2011,** 6, (12), e28698.

16. Ray, S.; Britschgi, M.; Herbert, C.; Takeda-Uchimura, Y.; Boxer, A.; Blennow, K.; Friedman, L. F.; Galasko, D. R.; Jutel, M.; Karydas, A.; Kaye, J. A.; Leszek, J.; Miller, B. L.; Minthon, L.; Quinn, J. F.; Rabinovici, G. D.; Robinson, W. H.; Sabbagh, M. N.; So, Y. T.; Sparks, D. L.; Tabaton, M.; Tinklenberg, J.; Yesavage, J. A.; Tibshirani, R.; Wyss-Coray, T., Classification and prediction of clinical Alzheimer's diagnosis based on plasma signaling proteins. *Nat Med* **2007,** 13, (11), 1359-62.

17. Lopez, M. F.; Kuppusamy, R.; Sarracino, D. A.; Prakash, A.; Athanas, M.; Krastins, B.; Rezai, T.; Sutton, J. N.; Peterman, S.; Nicolaides, K., Mass spectrometric discovery and selective reaction monitoring (SRM) of putative protein biomarker candidates in first trimester Trisomy 21 maternal serum. *J Proteome Res* **2011,** 10, (1), 133-42.

18. Sheta, E. A.; Appel, S. H.; Goldknopf, I. L., 2D gel blood serum biomarkers reveal differential clinical proteomics of the neurodegenerative diseases. *Expert Rev Proteomics* **2006,** 3, (1), 45-62.

19. Zhang, J.; Goodlett, D. R.; Montine, T. J., Proteomic biomarker discovery in cerebrospinal fluid for neurodegenerative diseases. *J Alzheimers Dis* **2005,** 8, (4), 377-86.

20. Yuan, X.; Desiderio, D. M., Proteomics analysis of prefractionated human lumbar cerebrospinal fluid. *Proteomics* **2005,** 5, (2), 541-50.

21. Wenner, B. R.; Lovell, M. A.; Lynn, B. C., Proteomic analysis of human ventricular cerebrospinal fluid from neurologically normal, elderly subjects using two-dimensional LC-MS/MS. *J Proteome Res* **2004,** 3, (1), 97-103.

22. Maccarrone, G.; Milfay, D.; Birg, I.; Rosenhagen, M.; Holsboer, F.; Grimm, R.; Bailey, J.; Zolotarjova, N.; Turck, C. W., Mining the human cerebrospinal fluid proteome by immunodepletion and shotgun mass spectrometry. *Electrophoresis* **2004,** 25, (14), 2402-12.

23. Yuan, X.; Desiderio, D. M., Proteomics analysis of human cerebrospinal fluid. *J Chromatogr B Analyt Technol Biomed Life Sci* **2005,** 815, (1-2), 179-89.

24. Wong, M.; Schlaggar, B. L.; Buller, R. S.; Storch, G. A.; Landt, M., Cerebrospinal fluid protein concentration in pediatric patients: defining clinically relevant reference values. *Arch Pediatr Adolesc Med* **2000,** 154, (8), 827-31.

25. Roche, S.; Gabelle, A.; Lehmann, S., Clinical proteomics of the cerebrospinal fluid: Towards the discovery of new biomarkers. *Proteomics Clin Appl* **2008,** 2, (3), 428-36.
26. Rozek, W.; Ricardo-Dukelow, M.; Holloway, S.; Gendelman, H. E.; Wojna, V.; Melendez, L. M.; Ciborowski, P., Cerebrospinal fluid proteomic profiling of HIV-1-infected patients with cognitive impairment. *J Proteome Res* **2007,** 6, (11), 4189-99.
27. Schutzer, S. E.; Liu, T.; Natelson, B. H.; Angel, T. E.; Schepmoes, A. A.; Purvine, S. O.; Hixson, K. K.; Lipton, M. S.; Camp, D. G.; Coyle, P. K.; Smith, R. D.; Bergquist, J., Establishing the proteome of normal human cerebrospinal fluid. *PLoS One* **2010,** 5, (6), e10980.
28. Zougman, A.; Pilch, B.; Podtelejnikov, A.; Kiehntopf, M.; Schnabel, C.; Kumar, C.; Mann, M., Integrated analysis of the cerebrospinal fluid peptidome and proteome. *J Proteome Res* **2008,** 7, (1), 386-99.
29. Sjodin, M. O.; Bergquist, J.; Wetterhall, M., Mining ventricular cerebrospinal fluid from patients with traumatic brain injury using hexapeptide ligand libraries to search for trauma biomarkers. *J Chromatogr B Analyt Technol Biomed Life Sci* **2010,** 878, (22), 2003-12.
30. You, J. S.; Gelfanova, V.; Knierman, M. D.; Witzmann, F. A.; Wang, M.; Hale, J. E., The impact of blood contamination on the proteome of cerebrospinal fluid. *Proteomics* **2005,** 5, (1), 290-6.
31. Yuan, X.; Desiderio, D. M., Human cerebrospinal fluid peptidomics. *J Mass Spectrom* **2005,** 40, (2), 176-81.
32. Ringman, J. M.; Schulman, H.; Becker, C.; Jones, T.; Bai, Y.; Immermann, F.; Cole, G.; Sokolow, S.; Gylys, K.; Geschwind, D. H.; Cummings, J. L.; Wan, H. I., Proteomic changes in cerebrospinal fluid of presymptomatic and affected persons carrying familial Alzheimer disease mutations. *Arch Neurol* **2012,** 69, (1), 96-104.
33. Jahn, H.; Wittke, S.; Zurbig, P.; Raedler, T. J.; Arlt, S.; Kellmann, M.; Mullen, W.; Eichenlaub, M.; Mischak, H.; Wiedemann, K., Peptide fingerprinting of Alzheimer's disease in cerebrospinal fluid: identification and prospective evaluation of new synaptic biomarkers. *PLoS One* **2011,** 6, (10), e26540.
34. Rajagopal, M. U.; Hathout, Y.; MacDonald, T. J.; Kieran, M. W.; Gururangan, S.; Blaney, S. M.; Phillips, P.; Packer, R.; Gordish-Dressman, H.; Rood, B. R., Proteomic profiling of cerebrospinal fluid identifies prostaglandin D2 synthase as a putative biomarker for pediatric medulloblastoma: A pediatric brain tumor consortium study. *Proteomics* **2011,** 11, (5), 935-43.
35. Giron, P.; Dayon, L.; Turck, N.; Hoogland, C.; Sanchez, J. C., Quantitative analysis of human cerebrospinal fluid proteins using a combination of cysteine tagging and amine-reactive isobaric labeling. *J Proteome Res* **2011,** 10, (1), 249-58.
36. Ting, L.; Rad, R.; Gygi, S. P.; Haas, W., MS3 eliminates ratio distortion in isobaric multiplexed quantitative proteomics. *Nat Methods* **2011,** 8, (11), 937-40.
37. Michalski, A.; Damoc, E.; Hauschild, J. P.; Lange, O.; Wieghaus, A.; Makarov, A.; Nagaraj, N.; Cox, J.; Mann, M.; Horning, S., Mass spectrometry-based proteomics using Q Exactive, a high-performance benchtop quadrupole Orbitrap mass spectrometer. *Mol Cell Proteomics* **2011,** 10, (9), M111 011015.
38. Spirin, V.; Shpunt, A.; Seebacher, J.; Gentzel, M.; Shevchenko, A.; Gygi, S.; Sunyaev, S., Assigning spectrum-specific P-values to protein identifications by mass spectrometry. *Bioinformatics* **2011,** 27, (8), 1128-34.
39. Kellie, J. F.; Catherman, A. D.; Durbin, K. R.; Tran, J. C.; Tipton, J. D.; Norris, J. L.; Witkowski, C. E.; Thomas, P. M.; Kelleher, N. L., Robust Analysis of the Yeast Proteome under

50 kDa by Molecular-Mass-Based Fractionation and Top-Down Mass Spectrometry. *Anal Chem* **2012,** 84, (1), 209-15.
40. Wilhelm, M.; Kirchner, M.; Steen, J. A.; Steen, H., mz5: Space- and Time-efficient Storage of Mass Spectrometry Data Sets. *Mol Cell Proteomics* **2012,** 11, (1), O111 011379.
41. Zhou, F.; Sikorski, T. W.; Ficarro, S. B.; Webber, J. T.; Marto, J. A., Online nanoflow reversed phase-strong anion exchange-reversed phase liquid chromatography-tandem mass spectrometry platform for efficient and in-depth proteome sequence analysis of complex organisms. *Anal Chem* **2011,** 83, (18), 6996-7005.
42. Winter, D.; Steen, H., Optimization of cell lysis and protein digestion protocols for the analysis of HeLa S3 cells by LC-MS/MS. *Proteomics* **2011,** 11, (24), 4726-30.
43. Shteynberg, D.; Deutsch, E. W.; Lam, H.; Eng, J. K.; Sun, Z.; Tasman, N.; Mendoza, L.; Moritz, R. L.; Aebersold, R.; Nesvizhskii, A. I., iProphet: multi-level integrative analysis of shotgun proteomic data improves peptide and protein identification rates and error estimates. *Mol Cell Proteomics* **2011,** 10, (12), M111 007690.
44. Kellie, J. F.; Catherman, A. D.; Durbin, K. R.; Tran, J. C.; Tipton, J. D.; Norris, J. L.; Witkowski, C. E.; Thomas, P. M.; Kelleher, N. L., Robust Analysis of the Yeast Proteome under 50 kDa by Molecular-Mass-Based Fractionation and Top-Down Mass Spectrometry. *Anal Chem* 84, (1), 209-15.
45. Datta, A.; Park, J. E.; Li, X.; Zhang, H.; Ho, Z. S.; Heese, K.; Lim, S. K.; Tam, J. P.; Sze, S. K., Phenotyping of an in vitro model of ischemic penumbra by iTRAQ-based shotgun quantitative proteomics. *J Proteome Res* 9, (1), 472-84.
46. Decramer, S.; Gonzalez de Peredo, A.; Breuil, B.; Mischak, H.; Monsarrat, B.; Bascands, J. L.; Schanstra, J. P., Urine in clinical proteomics. *Mol Cell Proteomics* **2008,** 7, (10), 1850-62.
47. De La Monte, S. M.; Wands, J. R., The AD7c-NTP neuronal thread protein biomarker for detecting Alzheimer's disease. *J Alzheimers Dis* **2001,** 3, (3), 345-353.
48. Van Dorsselaer, A.; Carapito, C.; Delalande, F.; Schaeffer-Reiss, C.; Thierse, D.; Diemer, H.; McNair, D. S.; Krewski, D.; Cashman, N. R., Detection of prion protein in urine-derived injectable fertility products by a targeted proteomic approach. *PLoS One* **2011,** 6, (3), e17815.
49. Kuwabara, Y.; Mine, K.; Katayama, A.; Inagawa, T.; Akira, S.; Takeshita, T., Proteomic analyses of recombinant human follicle-stimulating hormone and urinary-derived gonadotropin preparations. *J Reprod Med* **2009,** 54, (8), 459-66.
50. Court, M.; Selevsek, N.; Matondo, M.; Allory, Y.; Garin, J.; Masselon, C. D.; Domon, B., Toward a standardized urine proteome analysis methodology. *Proteomics* **2011,** 11, (6), 1160-71.
51. Marimuthu, A.; O'Meally, R. N.; Chaerkady, R.; Subbannayya, Y.; Nanjappa, V.; Kumar, P.; Kelkar, D. S.; Pinto, S. M.; Sharma, R.; Renuse, S.; Goel, R.; Christopher, R.; Delanghe, B.; Cole, R. N.; Harsha, H. C.; Pandey, A., A comprehensive map of the human urinary proteome. *J Proteome Res* **2011,** 10, (6), 2734-43.
52. Bermejo-Pareja, F.; Antequera, D.; Vargas, T.; Molina, J. A.; Carro, E., Saliva levels of Abeta1-42 as potential biomarker of Alzheimer's disease: a pilot study. *BMC Neurol* **2010,** 10, 108.
53. Devic, I.; Hwang, H.; Edgar, J. S.; Izutsu, K.; Presland, R.; Pan, C.; Goodlett, D. R.; Wang, Y.; Armaly, J.; Tumas, V.; Zabetian, C. P.; Leverenz, J. B.; Shi, M.; Zhang, J., Salivary alpha-synuclein and DJ-1: potential biomarkers for Parkinson's disease. *Brain* **2011,** 134, (Pt 7), e178.

54. Al-Tarawneh, S. K.; Border, M. B.; Dibble, C. F.; Bencharit, S., Defining salivary biomarkers using mass spectrometry-based proteomics: a systematic review. *OMICS* **2011,** 15, (6), 353-61.
55. Castagnola, M.; Cabras, T.; Vitali, A.; Sanna, M. T.; Messana, I., Biotechnological implications of the salivary proteome. *Trends Biotechnol* **2011,** 29, (8), 409-18.
56. Caprioli, R. M.; Farmer, T. B.; Gile, J., Molecular imaging of biological samples: localization of peptides and proteins using MALDI-TOF MS. *Anal Chem* **1997,** 69, (23), 4751-60.
57. Stoeckli, M.; Chaurand, P.; Hallahan, D. E.; Caprioli, R. M., Imaging mass spectrometry: a new technology for the analysis of protein expression in mammalian tissues. *Nat Med* **2001,** 7, (4), 493-6.
58. Chaurand, P.; Schwartz, S. A.; Caprioli, R. M., Imaging mass spectrometry: a new tool to investigate the spatial organization of peptides and proteins in mammalian tissue sections. *Curr Opin Chem Biol* **2002,** 6, (5), 676-81.
59. Chaurand, P.; Stoeckli, M.; Caprioli, R. M., Direct profiling of proteins in biological tissue sections by MALDI mass spectrometry. *Anal Chem* **1999,** 71, (23), 5263-70.
60. Seeley, E. H.; Caprioli, R. M., MALDI imaging mass spectrometry of human tissue: method challenges and clinical perspectives. *Trends Biotechnol* **2011,** 29, (3), 136-43.
61. Cazares, L. H.; Troyer, D. A.; Wang, B.; Drake, R. R.; Semmes, O. J., MALDI tissue imaging: from biomarker discovery to clinical applications. *Anal Bioanal Chem* **2011,** 401, (1), 17-27.
62. Stauber, J.; Lemaire, R.; Franck, J.; Bonnel, D.; Croix, D.; Day, R.; Wisztorski, M.; Fournier, I.; Salzet, M., MALDI imaging of formalin-fixed paraffin-embedded tissues: application to model animals of Parkinson disease for biomarker hunting. *J Proteome Res* **2008,** 7, (3), 969-78.
63. Yuki, D.; Sugiura, Y.; Zaima, N.; Akatsu, H.; Hashizume, Y.; Yamamoto, T.; Fujiwara, M.; Sugiyama, K.; Setou, M., Hydroxylated and non-hydroxylated sulfatide are distinctly distributed in the human cerebral cortex. *Neuroscience* **2011,** 193, 44-53.
64. Makridakis, M.; Vlahou, A., Secretome proteomics for discovery of cancer biomarkers. *J Proteomics* **2010,** 73, (12), 2291-305.
65. Dowling, P.; Clynes, M., Conditioned media from cell lines: a complementary model to clinical specimens for the discovery of disease-specific biomarkers. *Proteomics* **2011,** 11, (4), 794-804.
66. Moore, N. H.; Costa, L. G.; Shaffer, S. A.; Goodlett, D. R.; Guizzetti, M., Shotgun proteomics implicates extracellular matrix proteins and protease systems in neuronal development induced by astrocyte cholinergic stimulation. *J Neurochem* **2009,** 108, (4), 891-908.
67. Keene, S. D.; Greco, T. M.; Parastatidis, I.; Lee, S. H.; Hughes, E. G.; Balice-Gordon, R. J.; Speicher, D. W.; Ischiropoulos, H., Mass spectrometric and computational analysis of cytokine-induced alterations in the astrocyte secretome. *Proteomics* **2009,** 9, (3), 768-82.
68. Dowell, J. A.; Johnson, J. A.; Li, L., Identification of astrocyte secreted proteins with a combination of shotgun proteomics and bioinformatics. *J Proteome Res* **2009,** 8, (8), 4135-43.
69. Ahmed, F. E., Sample preparation and fractionation for proteome analysis and cancer biomarker discovery by mass spectrometry. *J Sep Sci* **2009,** 32, (5-6), 771-98.
70. Righetti, P. G.; Fasoli, E.; Boschetti, E., Combinatorial peptide ligand libraries: the conquest of the 'hidden proteome' advances at great strides. *Electrophoresis* **2011,** 32, (9), 960-6.

71. Selvaraju, S.; El Rassi, Z., Liquid-phase-based separation systems for depletion, prefractionation and enrichment of proteins in biological fluids and matrices for in-depth proteomics analysis - An update covering the period 2008-2011. *Electrophoresis* **2011,** 33, (1), 74-88.
72. Kalume, D. E.; Molina, H.; Pandey, A., Tackling the phosphoproteome: tools and strategies. *Curr Opin Chem Biol* **2003,** 7, (1), 64-9.
73. Cohen, P., The regulation of protein function by multisite phosphorylation--a 25 year update. *Trends Biochem Sci* **2000,** 25, (12), 596-601.
74. Nagaraj, N.; D'Souza, R. C.; Cox, J.; Olsen, J. V.; Mann, M., Feasibility of large-scale phosphoproteomics with higher energy collisional dissociation fragmentation. *J Proteome Res* **2010,** 9, (12), 6786-94.
75. Olsen, J. V.; Vermeulen, M.; Santamaria, A.; Kumar, C.; Miller, M. L.; Jensen, L. J.; Gnad, F.; Cox, J.; Jensen, T. S.; Nigg, E. A.; Brunak, S.; Mann, M., Quantitative phosphoproteomics reveals widespread full phosphorylation site occupancy during mitosis. *Sci Signal* **2010,** 3, (104), ra3.
76. Wagner, P. D.; Vu, N. D., Histidine to aspartate phosphotransferase activity of nm23 proteins: phosphorylation of aldolase C on Asp-319. *Biochem J* **2000,** 346 Pt 3, 623-30.
77. Chi, A.; Huttenhower, C.; Geer, L. Y.; Coon, J. J.; Syka, J. E.; Bai, D. L.; Shabanowitz, J.; Burke, D. J.; Troyanskaya, O. G.; Hunt, D. F., Analysis of phosphorylation sites on proteins from Saccharomyces cerevisiae by electron transfer dissociation (ETD) mass spectrometry. *Proc Natl Acad Sci U S A* **2007,** 104, (7), 2193-8.
78. Rudrabhatla, P.; Jaffe, H.; Pant, H. C., Direct evidence of phosphorylated neuronal intermediate filament proteins in neurofibrillary tangles (NFTs): phosphoproteomics of Alzheimer's NFTs. *FASEB J* 25, (11), 3896-905.
79. Saez-Valero, J.; Fodero, L. R.; Sjogren, M.; Andreasen, N.; Amici, S.; Gallai, V.; Vanderstichele, H.; Vanmechelen, E.; Parnetti, L.; Blennow, K.; Small, D. H., Glycosylation of acetylcholinesterase and butyrylcholinesterase changes as a function of the duration of Alzheimer's disease. *J Neurosci Res* **2003,** 72, (4), 520-6.
80. Silveyra, M. X.; Cuadrado-Corrales, N.; Marcos, A.; Barquero, M. S.; Rabano, A.; Calero, M.; Saez-Valero, J., Altered glycosylation of acetylcholinesterase in Creutzfeldt-Jakob disease. *J Neurochem* **2006,** 96, (1), 97-104.
81. Wei, X.; Li, L., Comparative glycoproteomics: approaches and applications. *Brief Funct Genomic Proteomic* **2009,** 8, (2), 104-13.
82. Tian, Y.; Zhang, H., Glycoproteomics and clinical applications. *Proteomics Clin Appl* **2010,** 4, (2), 124-32.
83. Butterfield, D. A.; Owen, J. B., Lectin-affinity chromatography brain glycoproteomics and Alzheimer disease: insights into protein alterations consistent with the pathology and progression of this dementing disorder. *Proteomics Clin Appl* **2011,** 5, (1-2), 50-6.
84. Wei, X.; Herbst, A.; Ma, D.; Aiken, J.; Li, L., A quantitative proteomic approach to prion disease biomarker research: delving into the glycoproteome. *J Proteome Res* **2010,** 10, (6), 2687-702.
85. Rucevic, M.; Hixson, D.; Josic, D., Mammalian plasma membrane proteins as potential biomarkers and drug targets. *Electrophoresis* **2011,** 32, (13), 1549-64.
86. Gilmore, J. M.; Washburn, M. P., Advances in shotgun proteomics and the analysis of membrane proteomes. *J Proteomics* **2010,** 73, (11), 2078-91.

87. Weekes, M. P.; Antrobus, R.; Lill, J. R.; Duncan, L. M.; Hor, S.; Lehner, P. J., Comparative analysis of techniques to purify plasma membrane proteins. *J Biomol Tech* **2010,** 21, (3), 108-15.
88. Helbig, A. O.; Heck, A. J.; Slijper, M., Exploring the membrane proteome--challenges and analytical strategies. *J Proteomics* **2010,** 73, (5), 868-78.
89. Griffin, N. M.; Schnitzer, J. E., Overcoming key technological challenges in using mass spectrometry for mapping cell surfaces in tissues. *Mol Cell Proteomics* **2011,** 10, (2), R110 000935.
90. Groen, A. J.; Lilley, K. S., Proteomics of total membranes and subcellular membranes. *Expert Rev Proteomics* **2010,** 7, (6), 867-78.
91. Wisniewski, J. R., Tools for phospho- and glycoproteomics of plasma membranes. *Amino Acids* **2011,** 41, (2), 223-33.
92. Wei, X.; Dulberger, C.; Li, L., Characterization of murine brain membrane glycoproteins by detergent assisted lectin affinity chromatography. *Anal Chem* **2010,** 82, (15), 6329-33.
93. Zhang, H.; Guo, T.; Li, X.; Datta, A.; Park, J. E.; Yang, J.; Lim, S. K.; Tam, J. P.; Sze, S. K., Simultaneous characterization of glyco- and phosphoproteomes of mouse brain membrane proteome with electrostatic repulsion hydrophilic interaction chromatography. *Mol Cell Proteomics* **2011,** 9, (4), 635-47.
94. Hui, L.; Cunningham, R.; Zhang, Z.; Cao, W.; Jia, C.; Li, L., Discovery and characterization of the Crustacean hyperglycemic hormone precursor related peptides (CPRP) and orcokinin neuropeptides in the sinus glands of the blue crab Callinectes sapidus using multiple tandem mass spectrometry techniques. *J Proteome Res* **2011,** 10, (9), 4219-29.
95. Ma, M.; Chen, R.; Ge, Y.; He, H.; Marshall, A. G.; Li, L., Combining bottom-up and top-down mass spectrometric strategies for de novo sequencing of the crustacean hyperglycemic hormone from Cancer borealis. *Anal Chem* **2009,** 81, (1), 240-7.
96. Chen, R.; Ma, M.; Hui, L.; Zhang, J.; Li, L., Measurement of neuropeptides in crustacean hemolymph via MALDI mass spectrometry. *J Am Soc Mass Spectrom* **2009,** 20, (4), 708-18.
97. Wei, H.; Nolkrantz, K.; Parkin, M. C.; Chisolm, C. N.; O'Callaghan, J. P.; Kennedy, R. T., Identification and quantification of neuropeptides in brain tissue by capillary liquid chromatography coupled off-line to MALDI-TOF and MALDI-TOF/TOF-MS. *Anal Chem* **2006,** 78, (13), 4342-51.
98. Dowell, J. A.; Heyden, W. V.; Li, L., Rat neuropeptidomics by LC-MS/MS and MALDI-FTMS: Enhanced dissection and extraction techniques coupled with 2D RP-RP HPLC. *J Proteome Res* **2006,** 5, (12), 3368-75.
99. Che, F. Y.; Fricker, L. D., Quantitative peptidomics of mouse pituitary: comparison of different stable isotopic tags. *J Mass Spectrom* **2005,** 40, (2), 238-49.
100. Fricker, L. D., Analysis of mouse brain peptides using mass spectrometry-based peptidomics: implications for novel functions ranging from non-classical neuropeptides to microproteins. *Mol Biosyst* **2010,** 6, (8), 1355-65.
101. Colgrave, M. L.; Xi, L.; Lehnert, S. A.; Flatscher-Bader, T.; Wadensten, H.; Nilsson, A.; Andren, P. E.; Wijffels, G., Neuropeptide profiling of the bovine hypothalamus: thermal stabilization is an effective tool in inhibiting post-mortem degradation. *Proteomics* **2011,** 11, (7), 1264-76.
102. Scholz, B.; Alm, H.; Mattsson, A.; Nilsson, A.; Kultima, K.; Savitski, M. M.; Falth, M.; Skold, K.; Brunstrom, B.; Andren, P. E.; Dencker, L., Neuropeptidomic analysis of the embryonic Japanese quail diencephalon. *BMC Dev Biol* **2010,** 10, 30.

103. Hummon, A. B.; Amare, A.; Sweedler, J. V., Discovering new invertebrate neuropeptides using mass spectrometry. *Mass Spectrom Rev* **2006,** 25, (1), 77-98.
104. Vilim, F. S.; Sasaki, K.; Rybak, J.; Alexeeva, V.; Cropper, E. C.; Jing, J.; Orekhova, I. V.; Brezina, V.; Price, D.; Romanova, E. V.; Rubakhin, S. S.; Hatcher, N.; Sweedler, J. V.; Weiss, K. R., Distinct mechanisms produce functionally complementary actions of neuropeptides that are structurally related but derived from different precursors. *J Neurosci* **2010,** 30, (1), 131-47.
105. Fu, Q.; Li, L., De novo sequencing of neuropeptides using reductive isotopic methylation and investigation of ESI QTOF MS/MS fragmentation pattern of neuropeptides with N-terminal dimethylation. *Anal Chem* **2005,** 77, (23), 7783-95.
106. Chen, R.; Jiang, X.; Conaway, M. C.; Mohtashemi, I.; Hui, L.; Viner, R.; Li, L., Mass spectral analysis of neuropeptide expression and distribution in the nervous system of the lobster Homarus americanus. *J Proteome Res* **2010,** 9, (2), 818-32.
107. Altelaar, A. F.; Mohammed, S.; Brans, M. A.; Adan, R. A.; Heck, A. J., Improved identification of endogenous peptides from murine nervous tissue by multiplexed peptide extraction methods and multiplexed mass spectrometric analysis. *J Proteome Res* **2009,** 8, (2), 870-6.
108. Gelman, J. S.; Sironi, J.; Castro, L. M.; Ferro, E. S.; Fricker, L. D., Peptidomic analysis of human cell lines. *J Proteome Res* **2011,** 10, (4), 1583-92.
109. Li, L.; Sweedler, J. V., Peptides in the brain: mass spectrometry-based measurement approaches and challenges. *Annu Rev Anal Chem (Palo Alto Calif)* **2008,** 1, 451-83.
110. Marouga, R.; David, S.; Hawkins, E., The development of the DIGE system: 2D fluorescence difference gel analysis technology. *Anal Bioanal Chem* **2005,** 382, (3), 669-78.
111. Brechlin, P.; Jahn, O.; Steinacker, P.; Cepek, L.; Kratzin, H.; Lehnert, S.; Jesse, S.; Mollenhauer, B.; Kretzschmar, H. A.; Wiltfang, J.; Otto, M., Cerebrospinal fluid-optimized two-dimensional difference gel electrophoresis (2-D DIGE) facilitates the differential diagnosis of Creutzfeldt-Jakob disease. *Proteomics* **2008,** 8, (20), 4357-66.
112. Ottervald, J.; Franzen, B.; Nilsson, K.; Andersson, L. I.; Khademi, M.; Eriksson, B.; Kjellstrom, S.; Marko-Varga, G.; Vegvari, A.; Harris, R. A.; Laurell, T.; Miliotis, T.; Matusevicius, D.; Salter, H.; Ferm, M.; Olsson, T., Multiple sclerosis: Identification and clinical evaluation of novel CSF biomarkers. *J Proteomics* **2010,** 73, (6), 1117-32.
113. Diez, R.; Herbstreith, M.; Osorio, C.; Alzate, O., 2-D Fluorescence Difference Gel Electrophoresis (DIGE) in Neuroproteomics. **2010**.
114. Lilley, K. S.; Razzaq, A.; Dupree, P., Two-dimensional gel electrophoresis: recent advances in sample preparation, detection and quantitation. *Curr Opin Chem Biol* **2002,** 6, (1), 46-50.
115. Oh-Ishi, M.; Maeda, T., Separation techniques for high-molecular-mass proteins. *J Chromatogr B Analyt Technol Biomed Life Sci* **2002,** 771, (1-2), 49-66.
116. Washburn, M. P.; Wolters, D.; Yates, J. R., 3rd, Large-scale analysis of the yeast proteome by multidimensional protein identification technology. *Nat Biotechnol* **2001,** 19, (3), 242-7.
117. Burke, T. W.; Mant, C. T.; Black, J. A.; Hodges, R. S., Strong cation-exchange high-performance liquid chromatography of peptides. Effect of non-specific hydrophobic interactions and linearization of peptide retention behaviour. *J Chromatogr* **1989,** 476, 377-89.
118. Edelmann, M. J., Strong cation exchange chromatography in analysis of posttranslational modifications: innovations and perspectives. *J Biomed Biotechnol* **2011,** 2011, 936508.

119. Francois, I.; Sandra, K.; Sandra, P., Comprehensive liquid chromatography: fundamental aspects and practical considerations--a review. *Anal Chim Acta* **2009,** 641, (1-2), 14-31.
120. Guiochon, G.; Marchetti, N.; Mriziq, K.; Shalliker, R. A., Implementations of two-dimensional liquid chromatography. *J Chromatogr A* **2008,** 1189, (1-2), 109-68.
121. Song, C.; Ye, M.; Han, G.; Jiang, X.; Wang, F.; Yu, Z.; Chen, R.; Zou, H., Reversed-phase-reversed-phase liquid chromatography approach with high orthogonality for multidimensional separation of phosphopeptides. *Anal Chem* **2010,** 82, (1), 53-6.
122. Alpert, A. J., Hydrophilic-interaction chromatography for the separation of peptides, nucleic acids and other polar compounds. *J Chromatogr* **1990,** 499, 177-96.
123. Gilar, M.; Olivova, P.; Daly, A. E.; Gebler, J. C., Orthogonality of separation in two-dimensional liquid chromatography. *Anal Chem* **2005,** 77, (19), 6426-34.
124. Di Palma, S.; Stange, D.; van de Wetering, M.; Clevers, H.; Heck, A. J.; Mohammed, S., Highly sensitive proteome analysis of FACS-sorted adult colon stem cells. *J Proteome Res* **2011,** 10, (8), 3814-9.
125. Di Palma, S.; Boersema, P. J.; Heck, A. J.; Mohammed, S., Zwitterionic hydrophilic interaction liquid chromatography (ZIC-HILIC and ZIC-cHILIC) provide high resolution separation and increase sensitivity in proteome analysis. *Anal Chem* **2011,** 83, (9), 3440-7.
126. Zarei, M.; Sprenger, A.; Metzger, F.; Gretzmeier, C.; Dengjel, J., Comparison of ERLIC-TiO2, HILIC-TiO2, and SCX-TiO2 for global phosphoproteomics approaches. *J Proteome Res* **2011,** 10, (8), 3474-83.
127. Neue, K.; Mormann, M.; Peter-Katalinic, J.; Pohlentz, G., Elucidation of glycoprotein structures by unspecific proteolysis and direct nanoESI mass spectrometric analysis of ZIC-HILIC-enriched glycopeptides. *J Proteome Res* **2011,** 10, (5), 2248-60.
128. Ow, S. Y.; Salim, M.; Noirel, J.; Evans, C.; Wright, P. C., Minimising iTRAQ ratio compression through understanding LC-MS elution dependence and high-resolution HILIC fractionation. *Proteomics* **2011,** 11, (11), 2341-6.
129. Alpert, A. J., Electrostatic repulsion hydrophilic interaction chromatography for isocratic separation of charged solutes and selective isolation of phosphopeptides. *Anal Chem* **2008,** 80, (1), 62-76.
130. Chien, K. Y.; Liu, H. C.; Goshe, M. B., Development and application of a phosphoproteomic method using electrostatic repulsion-hydrophilic interaction chromatography (ERLIC), IMAC, and LC-MS/MS analysis to study Marek's Disease Virus infection. *J Proteome Res* **2011,** 10, (9), 4041-53.
131. Liu, X.; Plasencia, M.; Ragg, S.; Valentine, S. J.; Clemmer, D. E., Development of high throughput dispersive LC-ion mobility-TOFMS techniques for analysing the human plasma proteome. *Brief Funct Genomic Proteomic* **2004,** 3, (2), 177-86.
132. Valentine, S. J.; Liu, X.; Plasencia, M. D.; Hilderbrand, A. E.; Kurulugama, R. T.; Koeniger, S. L.; Clemmer, D. E., Developing liquid chromatography ion mobility mass spectometry techniques. *Expert Rev Proteomics* **2005,** 2, (4), 553-65.
133. Valentine, S. J.; Plasencia, M. D.; Liu, X.; Krishnan, M.; Naylor, S.; Udseth, H. R.; Smith, R. D.; Clemmer, D. E., Toward plasma proteome profiling with ion mobility-mass spectrometry. *J Proteome Res* **2006,** 5, (11), 2977-84.
134. Valentine, S. J.; Ewing, M. A.; Dilger, J. M.; Glover, M. S.; Geromanos, S.; Hughes, C.; Clemmer, D. E., Using ion mobility data to improve peptide identification: intrinsic amino acid size parameters. *J Proteome Res* **2011,** 10, (5), 2318-29.

135. Ahmed, F. E., The role of capillary electrophoresis-mass spectrometry to proteome analysis and biomarker discovery. *J Chromatogr B Analyt Technol Biomed Life Sci* **2009,** 877, (22), 1963-81.
136. Fonslow, B. R.; Yates, J. R., 3rd, Capillary electrophoresis applied to proteomic analysis. *J Sep Sci* **2009,** 32, (8), 1175-88.
137. Haselberg, R.; de Jong, G. J.; Somsen, G. W., Capillary electrophoresis-mass spectrometry for the analysis of intact proteins. *J Chromatogr A* **2007,** 1159, (1-2), 81-109.
138. Haselberg, R.; de Jong, G. J.; Somsen, G. W., Capillary electrophoresis-mass spectrometry for the analysis of intact proteins 2007-2010. *Electrophoresis* **2011,** 32, (1), 66-82.
139. Huck, C. W.; Bakry, R.; Huber, L. A.; Bonn, G. K., Progress in capillary electrophoresis coupled to matrix-assisted laser desorption/ionization - time of flight mass spectrometry. *Electrophoresis* **2006,** 27, (11), 2063-74.
140. Klampfl, C. W., CE with MS detection: a rapidly developing hyphenated technique. *Electrophoresis* **2009,** 30 Suppl 1, S83-91.
141. Simpson, D. C.; Smith, R. D., Combining capillary electrophoresis with mass spectrometry for applications in proteomics. *Electrophoresis* **2005,** 26, (7-8), 1291-305.
142. Li, Y.; Champion, M. M.; Sun, L.; Champion, P. A.; Wojcik, R.; Dovichi, N. J., Capillary zone electrophoresis-electrospray ionization-tandem mass spectrometry as an alternative proteomics platform to ultraperformance liquid chromatography-electrospray ionization-tandem mass spectrometry for samples of intermediate complexity. *Anal Chem* **2012,** 84, (3), 1617-22.
143. Dai, L.; Li, C.; Shedden, K. A.; Lee, C. J.; Quoc, H.; Simeone, D. M.; Lubman, D. M., Quantitative proteomic profiling studies of pancreatic cancer stem cells. *J Proteome Res* **2010,** 9, (7), 3394-402.
144. Chen, J.; Balgley, B. M.; DeVoe, D. L.; Lee, C. S., Capillary isoelectric focusing-based multidimensional concentration/separation platform for proteome analysis. *Anal Chem* **2003,** 75, (13), 3145-52.
145. Mischak, H.; Delles, C.; Klein, J.; Schanstra, J. P., Urinary proteomics based on capillary electrophoresis-coupled mass spectrometry in kidney disease: discovery and validation of biomarkers, and clinical application. *Adv Chronic Kidney Dis* **2010,** 17, (6), 493-506.
146. Albalat, A.; Mischak, H.; Mullen, W., Urine proteomics in clinical applications: technologies, principal considerations and clinical implementation. *Prilozi* **2011,** 32, (1), 13-44.
147. Zuberovic, A.; Hanrieder, J.; Hellman, U.; Bergquist, J.; Wetterhall, M., Proteome profiling of human cerebrospinal fluid: exploring the potential of capillary electrophoresis with surface modified capillaries for analysis of complex biological samples. *Eur J Mass Spectrom (Chichester, Eng)* **2008,** 14, (4), 249-60.
148. Johannesson, N.; Olsson, L.; Backstrom, D.; Wetterhall, M.; Danielsson, R.; Bergquist, J., Screening for biomarkers in plasma from patients with gangrenous and phlegmonous appendicitis using CE and CEC in combination with MS. *Electrophoresis* **2007,** 28, (9), 1435-43.
149. Guo, T.; Lee, C. S.; Wang, W.; DeVoe, D. L.; Balgley, B. M., Capillary separations enabling tissue proteomics-based biomarker discovery. *Electrophoresis* **2006,** 27, (18), 3523-32.
150. Hwang, S. I.; Thumar, J.; Lundgren, D. H.; Rezaul, K.; Mayya, V.; Wu, L.; Eng, J.; Wright, M. E.; Han, D. K., Direct cancer tissue proteomics: a method to identify candidate cancer biomarkers from formalin-fixed paraffin-embedded archival tissues. *Oncogene* **2007,** 26, (1), 65-76.

151. Desiderio, C.; Rossetti, D. V.; Iavarone, F.; Messana, I.; Castagnola, M., Capillary electrophoresis--mass spectrometry: recent trends in clinical proteomics. *J Pharm Biomed Anal* **2010,** 53, (5), 1161-9.
152. Albalat, A.; Mischak, H.; Mullen, W., Clinical application of urinary proteomics/peptidomics. *Expert Rev Proteomics* **2011,** 8, (5), 615-29.
153. Ye, X.; Luke, B.; Andresson, T.; Blonder, J., 18O stable isotope labeling in MS-based proteomics. *Brief Funct Genomic Proteomic* **2009,** 8, (2), 136-44.
154. Staes, A.; Demol, H.; Van Damme, J.; Martens, L.; Vandekerckhove, J.; Gevaert, K., Global differential non-gel proteomics by quantitative and stable labeling of tryptic peptides with oxygen-18. *J Proteome Res* **2004,** 3, (4), 786-91.
155. Jorge, I.; Navarro, P.; Martinez-Acedo, P.; Nunez, E.; Serrano, H.; Alfranca, A.; Redondo, J. M.; Vazquez, J., Statistical model to analyze quantitative proteomics data obtained by 18O/16O labeling and linear ion trap mass spectrometry: application to the study of vascular endothelial growth factor-induced angiogenesis in endothelial cells. *Mol Cell Proteomics* **2009,** 8, (5), 1130-49.
156. Gygi, S. P.; Rist, B.; Gerber, S. A.; Turecek, F.; Gelb, M. H.; Aebersold, R., Quantitative analysis of complex protein mixtures using isotope-coded affinity tags. *Nat Biotechnol* **1999,** 17, (10), 994-9.
157. Haqqani, A. S.; Kelly, J. F.; Stanimirovic, D. B., Quantitative protein profiling by mass spectrometry using isotope-coded affinity tags. *Methods Mol Biol* **2008,** 439, 225-40.
158. Ross, P. L.; Huang, Y. N.; Marchese, J. N.; Williamson, B.; Parker, K.; Hattan, S.; Khainovski, N.; Pillai, S.; Dey, S.; Daniels, S.; Purkayastha, S.; Juhasz, P.; Martin, S.; Bartlet-Jones, M.; He, F.; Jacobson, A.; Pappin, D. J., Multiplexed protein quantitation in Saccharomyces cerevisiae using amine-reactive isobaric tagging reagents. *Mol Cell Proteomics* **2004,** 3, (12), 1154-69.
159. Thompson, A.; Schafer, J.; Kuhn, K.; Kienle, S.; Schwarz, J.; Schmidt, G.; Neumann, T.; Johnstone, R.; Mohammed, A. K.; Hamon, C., Tandem mass tags: a novel quantification strategy for comparative analysis of complex protein mixtures by MS/MS. *Anal Chem* **2003,** 75, (8), 1895-904.
160. Dayon, L.; Hainard, A.; Licker, V.; Turck, N.; Kuhn, K.; Hochstrasser, D. F.; Burkhard, P. R.; Sanchez, J. C., Relative quantification of proteins in human cerebrospinal fluids by MS/MS using 6-plex isobaric tags. *Anal Chem* **2008,** 80, (8), 2921-31.
161. D'Ascenzo, M.; Choe, L.; Lee, K. H., iTRAQPak: an R based analysis and visualization package for 8-plex isobaric protein expression data. *Brief Funct Genomic Proteomic* **2008,** 7, (2), 127-35.
162. Choe, L.; D'Ascenzo, M.; Relkin, N. R.; Pappin, D.; Ross, P.; Williamson, B.; Guertin, S.; Pribil, P.; Lee, K. H., 8-plex quantitation of changes in cerebrospinal fluid protein expression in subjects undergoing intravenous immunoglobulin treatment for Alzheimer's disease. *Proteomics* **2007,** 7, (20), 3651-60.
163. Xiang, F.; Ye, H.; Chen, R.; Fu, Q.; Li, L., N,N-dimethyl leucines as novel isobaric tandem mass tags for quantitative proteomics and peptidomics. *Anal Chem* **2010,** 82, (7), 2817-25.
164. Ong, S. E.; Blagoev, B.; Kratchmarova, I.; Kristensen, D. B.; Steen, H.; Pandey, A.; Mann, M., Stable isotope labeling by amino acids in cell culture, SILAC, as a simple and accurate approach to expression proteomics. *Mol Cell Proteomics* **2002,** 1, (5), 376-86.

165. Ong, S. E.; Kratchmarova, I.; Mann, M., Properties of 13C-substituted arginine in stable isotope labeling by amino acids in cell culture (SILAC). *J Proteome Res* **2003,** 2, (2), 173-81.
166. Pimienta, G.; Chaerkady, R.; Pandey, A., SILAC for global phosphoproteomic analysis. *Methods Mol Biol* **2009,** 527, 107-16, x.
167. Zhang, G.; Neubert, T. A., Use of stable isotope labeling by amino acids in cell culture (SILAC) for phosphotyrosine protein identification and quantitation. *Methods Mol Biol* **2009,** 527, 79-92, xi.
168. Bondarenko, P. V.; Chelius, D.; Shaler, T. A., Identification and relative quantitation of protein mixtures by enzymatic digestion followed by capillary reversed-phase liquid chromatography-tandem mass spectrometry. *Anal Chem* **2002,** 74, (18), 4741-9.
169. Chelius, D.; Bondarenko, P. V., Quantitative profiling of proteins in complex mixtures using liquid chromatography and mass spectrometry. *J Proteome Res* **2002,** 1, (4), 317-23.
170. Liu, H.; Sadygov, R. G.; Yates, J. R., 3rd, A model for random sampling and estimation of relative protein abundance in shotgun proteomics. *Anal Chem* **2004,** 76, (14), 4193-201.
171. Wang, W.; Zhou, H.; Lin, H.; Roy, S.; Shaler, T. A.; Hill, L. R.; Norton, S.; Kumar, P.; Anderle, M.; Becker, C. H., Quantification of proteins and metabolites by mass spectrometry without isotopic labeling or spiked standards. *Anal Chem* **2003,** 75, (18), 4818-26.
172. Silva, J. C.; Denny, R.; Dorschel, C. A.; Gorenstein, M.; Kass, I. J.; Li, G. Z.; McKenna, T.; Nold, M. J.; Richardson, K.; Young, P.; Geromanos, S., Quantitative proteomic analysis by accurate mass retention time pairs. *Anal Chem* **2005,** 77, (7), 2187-200.
173. Zybailov, B.; Coleman, M. K.; Florens, L.; Washburn, M. P., Correlation of relative abundance ratios derived from peptide ion chromatograms and spectrum counting for quantitative proteomic analysis using stable isotope labeling. *Anal Chem* **2005,** 77, (19), 6218-24.
174. Filiou, M. D.; Martins-de-Souza, D.; Guest, P. C.; Bahn, S.; Turck, C. W., To label or not to label: Applications of quantitative proteomics in neuroscience research. *Proteomics* **2012**.
175. Neilson, K. A.; Ali, N. A.; Muralidharan, S.; Mirzaei, M.; Mariani, M.; Assadourian, G.; Lee, A.; van Sluyter, S. C.; Haynes, P. A., Less label, more free: approaches in label-free quantitative mass spectrometry. *Proteomics* **2011,** 11, (4), 535-53.
176. Zhu, W.; Smith, J. W.; Huang, C. M., Mass spectrometry-based label-free quantitative proteomics. *J Biomed Biotechnol* **2010,** 2010, 840518.
177. Xie, F.; Liu, T.; Qian, W. J.; Petyuk, V. A.; Smith, R. D., Liquid chromatography-mass spectrometry-based quantitative proteomics. *J Biol Chem* **2012,** 286, (29), 25443-9.
178. Shen, Y.; Tolic, N.; Xie, F.; Zhao, R.; Purvine, S. O.; Schepmoes, A. A.; Moore, R. J.; Anderson, G. A.; Smith, R. D., Effectiveness of CID, HCD, and ETD with FT MS/MS for degradomic-peptidomic analysis: comparison of peptide identification methods. *J Proteome Res* **2011,** 10, (9), 3929-43.
179. Zubarev, R. A.; Kelleher, N. L.; McLafferty, F. W., Electron Capture Dissociation of Multiply Charged Protein Cations. A Nonergodic Process. *Journal of the American Chemical Society* **1998,** 120, (13), 3265-3266.
180. Syka, J. E.; Coon, J. J.; Schroeder, M. J.; Shabanowitz, J.; Hunt, D. F., Peptide and protein sequence analysis by electron transfer dissociation mass spectrometry. *Proc Natl Acad Sci U S A* **2004,** 101, (26), 9528-33.
181. Xia, Y.; Gunawardena, H. P.; Erickson, D. E.; McLuckey, S. A., Effects of cation charge-site identity and position on electron-transfer dissociation of polypeptide cations. *J Am Chem Soc* **2007,** 129, (40), 12232-43.

182. Swaney, D. L.; McAlister, G. C.; Coon, J. J., Decision tree-driven tandem mass spectrometry for shotgun proteomics. *Nat Methods* **2008,** 5, (11), 959-64.
183. Zhou, W.; Ross, M. M.; Tessitore, A.; Ornstein, D.; Vanmeter, A.; Liotta, L. A.; Petricoin, E. F., 3rd, An initial characterization of the serum phosphoproteome. *J Proteome Res* **2009,** 8, (12), 5523-31.
184. Liu, H.; Hakansson, K., Electron capture dissociation of tyrosine O-sulfated peptides complexed with divalent metal cations. *Anal Chem* **2006,** 78, (21), 7570-6.
185. Snovida, S. I.; Bodnar, E. D.; Viner, R.; Saba, J.; Perreault, H., A simple cellulose column procedure for selective enrichment of glycopeptides and characterization by nano LC coupled with electron-transfer and high-energy collisional-dissociation tandem mass spectrometry. *Carbohydr Res* **2010,** 345, (6), 792-801.
186. Sobott, F.; Watt, S. J.; Smith, J.; Edelmann, M. J.; Kramer, H. B.; Kessler, B. M., Comparison of CID versus ETD based MS/MS fragmentation for the analysis of protein ubiquitination. *J Am Soc Mass Spectrom* **2009,** 20, (9), 1652-9.
187. Eliuk, S. M.; Maltby, D.; Panning, B.; Burlingame, A. L., High resolution electron transfer dissociation studies of unfractionated intact histones from murine embryonic stem cells using on-line capillary LC separation: determination of abundant histone isoforms and post-translational modifications. *Mol Cell Proteomics* **2010,** 9, (5), 824-37.
188. Hui, L.; Cunningham, R.; Zhang, Z.; Cao, W.; Jia, C.; Li, L., Discovery and characterization of the Crustacean hyperglycemic hormone precursor related peptides (CPRP) and orcokinin neuropeptides in the sinus glands of the blue crab Callinectes sapidus using multiple tandem mass spectrometry techniques. *J Proteome Res* 10, (9), 4219-29.
189. Molina, H.; Matthiesen, R.; Kandasamy, K.; Pandey, A., Comprehensive comparison of collision induced dissociation and electron transfer dissociation. *Anal Chem* **2008,** 80, (13), 4825-35.
190. Olsen, J. V.; Macek, B.; Lange, O.; Makarov, A.; Horning, S.; Mann, M., Higher-energy C-trap dissociation for peptide modification analysis. *Nat Methods* **2007,** 4, (9), 709-12.
191. McAlister, G. C.; Phanstiel, D.; Wenger, C. D.; Lee, M. V.; Coon, J. J., Analysis of tandem mass spectra by FTMS for improved large-scale proteomics with superior protein quantification. *Anal Chem* **2010,** 82, (1), 316-22.
192. Dayon, L.; Pasquarello, C.; Hoogland, C.; Sanchez, J. C.; Scherl, A., Combining low- and high-energy tandem mass spectra for optimized peptide quantification with isobaric tags. *J Proteomics* **2010,** 73, (4), 769-77.
193. Second, T. P.; Blethrow, J. D.; Schwartz, J. C.; Merrihew, G. E.; MacCoss, M. J.; Swaney, D. L.; Russell, J. D.; Coon, J. J.; Zabrouskov, V., Dual-pressure linear ion trap mass spectrometer improving the analysis of complex protein mixtures. *Anal Chem* **2009,** 81, (18), 7757-65.
194. Jedrychowski, M. P.; Huttlin, E. L.; Haas, W.; Sowa, M. E.; Rad, R.; Gygi, S. P., Evaluation of HCD- and CID-type fragmentation within their respective detection platforms for murine phosphoproteomics. *Mol Cell Proteomics* **2011,** 10, (12), M111 009910.
195. Frese, C. K.; Altelaar, A. F.; Hennrich, M. L.; Nolting, D.; Zeller, M.; Griep-Raming, J.; Heck, A. J.; Mohammed, S., Improved peptide identification by targeted fragmentation using CID, HCD and ETD on an LTQ-Orbitrap Velos. *J Proteome Res* **2011,** 10, (5), 2377-88.
196. Chakraborty, A. B.; Berger, S. J.; Gebler, J. C., Use of an integrated MS--multiplexed MS/MS data acquisition strategy for high-coverage peptide mapping studies. *Rapid Commun Mass Spectrom* **2007,** 21, (5), 730-44.

197. Ramos, A. A.; Yang, H.; Rosen, L. E.; Yao, X., Tandem parallel fragmentation of peptides for mass spectrometry. *Anal Chem* **2006,** 78, (18), 6391-7.
198. Barbara, J. E.; Castro-Perez, J. M., High-resolution chromatography/time-of-flight MSE with in silico data mining is an information-rich approach to reactive metabolite screening. *Rapid Commun Mass Spectrom* **2011,** 25, (20), 3029-40.
199. Geromanos, S. J.; Vissers, J. P.; Silva, J. C.; Dorschel, C. A.; Li, G. Z.; Gorenstein, M. V.; Bateman, R. H.; Langridge, J. I., The detection, correlation, and comparison of peptide precursor and product ions from data independent LC-MS with data dependant LC-MS/MS. *Proteomics* **2009,** 9, (6), 1683-95.
200. Koutroukides, T. A.; Guest, P. C.; Leweke, F. M.; Bailey, D. M.; Rahmoune, H.; Bahn, S.; Martins-de-Souza, D., Characterization of the human serum depletome by label-free shotgun proteomics. *J Sep Sci* 34, (13), 1621-6.
201. Martins-de-Souza, D.; Guest, P. C.; Guest, F. L.; Bauder, C.; Rahmoune, H.; Pietsch, S.; Roeber, S.; Kretzschmar, H.; Mann, D.; Baborie, A.; Bahn, S., Characterization of the human primary visual cortex and cerebellum proteomes using shotgun mass spectrometry-data-independent analyses. *Proteomics* 12, (3), 500-4.
202. Scatena, R.; Bottoni, P.; Pontoglio, A.; Giardina, B., Revisiting the Warburg effect in cancer cells with proteomics. The emergence of new approaches to diagnosis, prognosis and therapy. *Proteomics Clin Appl* 4, (2), 143-58.
203. Herberth, M.; Koethe, D.; Cheng, T. M.; Krzyszton, N. D.; Schoeffmann, S.; Guest, P. C.; Rahmoune, H.; Harris, L. W.; Kranaster, L.; Leweke, F. M.; Bahn, S., Impaired glycolytic response in peripheral blood mononuclear cells of first-onset antipsychotic-naive schizophrenia patients. *Mol Psychiatry* 16, (8), 848-59.
204. Krishnamurthy, D.; Levin, Y.; Harris, L. W.; Umrania, Y.; Bahn, S.; Guest, P. C., Analysis of the human pituitary proteome by data independent label-free liquid chromatography tandem mass spectrometry. *Proteomics* 11, (3), 495-500.
205. Perkins, D. N.; Pappin, D. J.; Creasy, D. M.; Cottrell, J. S., Probability-based protein identification by searching sequence databases using mass spectrometry data. *Electrophoresis* **1999,** 20, (18), 3551-67.
206. Eng, J. K.; McCormack, A. L.; Yates Iii, J. R., An approach to correlate tandem mass spectral data of peptides with amino acid sequences in a protein database. *Journal of the American Society for Mass Spectrometry* **1994,** 5, (11), 976-989.
207. Craig, R.; Beavis, R. C., TANDEM: matching proteins with tandem mass spectra. *Bioinformatics* **2004,** 20, (9), 1466-7.
208. Geer, L. Y.; Markey, S. P.; Kowalak, J. A.; Wagner, L.; Xu, M.; Maynard, D. M.; Yang, X.; Shi, W.; Bryant, S. H., Open mass spectrometry search algorithm. *J Proteome Res* **2004,** 3, (5), 958-64.
209. Zhang, J.; Xin, L.; Shan, B.; Chen, W.; Xie, M.; Yuen, D.; Zhang, W.; Zhang, Z.; Lajoie, G. A.; Ma, B., PEAKS DB: De Novo sequencing assisted database search for sensitive and accurate peptide identification. *Mol Cell Proteomics* **2011**.
210. Liu, J.; Erassov, A.; Halina, P.; Canete, M.; Nguyen, D. V.; Chung, C.; Cagney, G.; Ignatchenko, A.; Fong, V.; Emili, A., Sequential interval motif search: unrestricted database surveys of global MS/MS data sets for detection of putative post-translational modifications. *Anal Chem* **2008,** 80, (20), 7846-54.

211. Beausoleil, S. A.; Villen, J.; Gerber, S. A.; Rush, J.; Gygi, S. P., A probability-based approach for high-throughput protein phosphorylation analysis and site localization. *Nat Biotechnol* **2006,** 24, (10), 1285-92.
212. Han, Y.; Ma, B.; Zhang, K., SPIDER: software for protein identification from sequence tags with de novo sequencing error. *J Bioinform Comput Biol* **2005,** 3, (3), 697-716.
213. Singh, S.; Springer, M.; Steen, J.; Kirschner, M. W.; Steen, H., FLEXIQuant: a novel tool for the absolute quantification of proteins, and the simultaneous identification and quantification of potentially modified peptides. *J Proteome Res* **2009,** 8, (5), 2201-10.
214. Searle, B. C., Scaffold: a bioinformatic tool for validating MS/MS-based proteomic studies. *Proteomics* 10, (6), 1265-9.
215. Herbst, A.; McIlwain, S.; Schmidt, J. J.; Aiken, J. M.; Page, C. D.; Li, L., Prion disease diagnosis by proteomic profiling. *J Proteome Res* **2009,** 8, (2), 1030-6.
216. Menschaert, G.; Vandekerckhove, T. T.; Baggerman, G.; Schoofs, L.; Luyten, W.; Van Criekinge, W., Peptidomics coming of age: a review of contributions from a bioinformatics angle. *J Proteome Res* **2010,** 9, (5), 2051-61.
217. Kumar, C.; Mann, M., Bioinformatics analysis of mass spectrometry-based proteomics data sets. *FEBS Lett* **2009,** 583, (11), 1703-12.
218. Craig, R.; Cortens, J. P.; Beavis, R. C., Open source system for analyzing, validating, and storing protein identification data. *J Proteome Res* **2004,** 3, (6), 1234-42.
219. Jones, P.; Cote, R. G.; Cho, S. Y.; Klie, S.; Martens, L.; Quinn, A. F.; Thorneycroft, D.; Hermjakob, H., PRIDE: new developments and new datasets. *Nucleic Acids Res* **2008,** 36, (Database issue), D878-83.
220. Deutsch, E. W.; Lam, H.; Aebersold, R., PeptideAtlas: a resource for target selection for emerging targeted proteomics workflows. *EMBO Rep* **2008,** 9, (5), 429-34.
221. Miliotis, T.; Ali, L.; Palm, J. E.; Lundqvist, A. J.; Ahnoff, M.; Andersson, T. B.; Hilgendorf, C., Development of a highly sensitive method using liquid chromatography-multiple reaction monitoring to quantify membrane P-glycoprotein in biological matrices and relationship to transport function. *Drug Metab Dispos* **2011,** 39, (12), 2440-9.
222. Xiang, Y.; Koomen, J. M., Evaluation of Direct Infusion-Multiple Reaction Monitoring Mass Spectrometry for Quantification of Heat Shock Proteins. *Anal Chem* **2012**.
223. Ossola, R.; Schiess, R.; Picotti, P.; Rinner, O.; Reiter, L.; Aebersold, R., Biomarker validation in blood specimens by selected reaction monitoring mass spectrometry of N-glycosites. *Methods Mol Biol* **2011,** 728, 179-94.
224. Liu, H.; Lam, L.; Dasgupta, P. K., Expanding the linear dynamic range for multiple reaction monitoring in quantitative liquid chromatography-tandem mass spectrometry utilizing natural isotopologue transitions. *Talanta* **2011,** 87, 307-10.
225. Belov, M. E.; Prasad, S.; Prior, D. C.; Danielson, W. F., 3rd; Weitz, K.; Ibrahim, Y. M.; Smith, R. D., Pulsed multiple reaction monitoring approach to enhancing sensitivity of a tandem quadrupole mass spectrometer. *Anal Chem* **2011,** 83, (6), 2162-71.
226. Prentice, R. L.; Paczesny, S.; Aragaki, A.; Amon, L. M.; Chen, L.; Pitteri, S. J.; McIntosh, M.; Wang, P.; Buson Busald, T.; Hsia, J.; Jackson, R. D.; Rossouw, J. E.; Manson, J. E.; Johnson, K.; Eaton, C.; Hanash, S. M., Novel proteins associated with risk for coronary heart disease or stroke among postmenopausal women identified by in-depth plasma proteome profiling. *Genome Med* 2, (7), 48.
227. Gelman, J. S.; Fricker, L. D., Hemopressin and other bioactive peptides from cytosolic proteins: are these non-classical neuropeptides? *AAPS J* **2010,** 12, (3), 279-89.

228. Gelman, J. S.; Sironi, J.; Castro, L. M.; Ferro, E. S.; Fricker, L. D., Hemopressins and other hemoglobin-derived peptides in mouse brain: comparison between brain, blood, and heart peptidome and regulation in Cpefat/fat mice. *J Neurochem* **2010,** 113, (4), 871-80.
229. Li, L.; Garden, R. W.; Sweedler, J. V., Single-cell MALDI: a new tool for direct peptide profiling. *Trends Biotechnol* **2000,** 18, (4), 151-60.
230. Altelaar, A. M.; Heck, A. J., Trends in ultrasensitive proteomics. *Curr Opin Chem Biol*.
231. Bandura, D. R.; Baranov, V. I.; Ornatsky, O. I.; Antonov, A.; Kinach, R.; Lou, X.; Pavlov, S.; Vorobiev, S.; Dick, J. E.; Tanner, S. D., Mass cytometry: technique for real time single cell multitarget immunoassay based on inductively coupled plasma time-of-flight mass spectrometry. *Anal Chem* **2009,** 81, (16), 6813-22.
232. Trimpin, S.; Inutan, E. D.; Herath, T. N.; McEwen, C. N., Laserspray ionization, a new atmospheric pressure MALDI method for producing highly charged gas-phase ions of peptides and proteins directly from solid solutions. *Mol Cell Proteomics* **2010,** 9, (2), 362-7.
233. McEwen, C. N.; Larsen, B. S.; Trimpin, S., Laserspray ionization on a commercial atmospheric pressure-MALDI mass spectrometer ion source: selecting singly or multiply charged ions. *Anal Chem* **2010,** 82, (12), 4998-5001.
234. Wang, B.; Lietz, C. B.; Inutan, E. D.; Leach, S. M.; Trimpin, S., Producing highly charged ions without solvent using laserspray ionization: a total solvent-free analysis approach at atmospheric pressure. *Anal Chem* **2011,** 83, (11), 4076-84.
235. Inutan, E. D.; Richards, A. L.; Wager-Miller, J.; Mackie, K.; McEwen, C. N.; Trimpin, S., Laserspray ionization, a new method for protein analysis directly from tissue at atmospheric pressure with ultrahigh mass resolution and electron transfer dissociation. *Mol Cell Proteomics* **2010,** 10, (2), M110 000760.
236. Wang, H.; Liu, J.; Cooks, R. G.; Ouyang, Z., Paper spray for direct analysis of complex mixtures using mass spectrometry. *Angew Chem Int Ed Engl* 49, (5), 877-80.
237. Zhang, Z.; Xu, W.; Manicke, N. E.; Cooks, R. G.; Ouyang, Z., Silica coated paper substrate for paper-spray analysis of therapeutic drugs in dried blood spots. *Anal Chem* 84, (2), 931-8.
238. Wang, H.; Manicke, N. E.; Yang, Q.; Zheng, L.; Shi, R.; Cooks, R. G.; Ouyang, Z., Direct analysis of biological tissue by paper spray mass spectrometry. *Anal Chem* 83, (4), 1197-201.
239. Liu, J.; Wang, H.; Cooks, R. G.; Ouyang, Z., Leaf spray: direct chemical analysis of plant material and living plants by mass spectrometry. *Anal Chem* 83, (20), 7608-13.
240. Liu, J.; Wang, H.; Manicke, N. E.; Lin, J. M.; Cooks, R. G.; Ouyang, Z., Development, characterization, and application of paper spray ionization. *Anal Chem* 82, (6), 2463-71.
241. Yoo, H. J.; Wang, N.; Zhuang, S.; Song, H.; Hakansson, K., Negative-ion electron capture dissociation: radical-driven fragmentation of charge-increased gaseous peptide anions. *J Am Chem Soc* **2011,** 133, (42), 16790-3.
242. Tian, Q.; Price, N. D.; Hood, L., Systems cancer medicine: towards realization of predictive, preventive, personalized and participatory (P4) medicine. *J Intern Med* 271, (2), 111-21.
243. Hood, L.; Friend, S. H., Predictive, personalized, preventive, participatory (P4) cancer medicine. *Nat Rev Clin Oncol* **2011,** 8, (3), 184-7.
244. Tian, Q.; Price, N. D.; Hood, L., Systems cancer medicine: towards realization of predictive, preventive, personalized and participatory (P4) medicine. *J Intern Med* **2012,** 271, (2), 111-21.

245. Belda-Iniesta, C.; de Castro, J.; Perona, R., Translational proteomics: what can you do for true patients? *J Proteome Res* **2011,** 10, (1), 101-4.
246. Schiess, R.; Wollscheid, B.; Aebersold, R., Targeted proteomic strategy for clinical biomarker discovery. *Mol Oncol* **2009,** 3, (1), 33-44.
247. Hsu, J. L.; Huang, S. Y.; Chow, N. H.; Chen, S. H., Stable-isotope dimethyl labeling for quantitative proteomics. *Anal Chem* **2003,** 75, (24), 6843-52.
248. Schmidt, A.; Kellermann, J.; Lottspeich, F., A novel strategy for quantitative proteomics using isotope-coded protein labels. *Proteomics* **2005,** 5, (1), 4-15.
249. Wang, Y. K.; Ma, Z.; Quinn, D. F.; Fu, E. W., Inverse ^{15}N-metabolic labeling/mass spectrometry for comparative proteomics and rapid identification of protein markers/targets. *Rapid Commun Mass Spectrom* **2002,** 16, (14), 1389-97.

Chapter 3

Differential Expression of Proteins in Naïve and IL-2 Stimulated Primary Human NK Cells Identified by Global Proteomic Analysis

Adapted from: “Differential Expression of Proteins in Naïve and IL-2 Stimulated Primary Human NK Cells Identified by Global Proteomic Analysis**”**. Ma D, Cao W, Kapur A, Scarlett C, Patankar M, Li L. In preparation.

Abstract

Natural killer (NK) cells efficiently cytolyse tumors and virally infected cells. Despite the important role that interleukin (IL)-2 plays in stimulating the proliferation of NK cells and increasing NK cell activity, little is known about the alterations in the global NK cell proteome following IL-2 activation. To characterize the proteome of naïve and IL-2-activated primary NK cells and identify proteins that lead to the discovery of new pathways involved in IL-2 signaling, we performed comparative analysis of naïve and IL-2-activated NK cells isolated from healthy donors by 2D LC ESI-MS/MS followed by label-free quantification. In total, more than 2000 proteins were identified from naïve and IL-2-activated NK cells where 383 proteins were found to be differentially expressed following IL-2 activation. Functional annotation of IL-2 regulated proteins revealed potential targets for future investigation of IL-2 signaling in human primary NK cells. A pathway analysis was performed and revealed several pathways that were not previously known to be involved in IL-2 signaling, including ubiquitin proteasome pathway, integrin signaling pathway, platelet derived growth factor (PDGF) signaling pathway, epidermal growth factor receptor (EGFR) signaling pathway and Wnt signaling pathway. Collectively, the results from this study suggested that the activation of NK cells by IL-2 is a dynamic process through which proteins with various functions were regulated. The identification of IL-2 regulated proteins will be important for the elucidation of mechanism of IL-2 signaling in NK cells and provide new insights into NK cell biology.

Introduction

Natural killer (NK) cells are large granular lymphocytes generated in bone marrow and make up 5–15% of the peripheral blood lymphocytes (PBLs)[1]. NK cells play an important role in innate immune system and defending the host against virus infections and tumor cells. As the major cellular effectors of the innate immune system, NK cells directly kill target cells by employing exocytosis of potent toxins from secretory granules such as granzymes and perforin, or by releasing proinflammatory cytokines such as interferon gamma (INF-γ) and tumor necrosis factor (TNF). The development and cytotoxicity of NK cells are controlled by intracellular signal transduction molecules, most importantly cytokines, and a complex crosstalk between activating and inhibitory surface receptors through which cytokines exert the regulation on NK cell activity[2].

Cytokines such as IL-2, IL-4, IL-6, IL-7, IL-12, and IL-15 are critical regulators of human peripheral blood NK cell. Numerous studies have demonstrated that the development, differentiation, proliferation and function of NK cells are dependent on the systemic and local immunomodulating effects of these cytokines. IL-2 is a glycosylated protein of approximately 15.5 kDa, with an anti-parallel alpha helical core and a small region composed of a β-sheet containing secondary structure[3]. As the first interleukin to be discovered and characterized, IL-2 plays a central role in many aspects of the immune response. IL-2 has been demonstrated to stimulate the proliferation of both T cells and NK cells[4]. In NK cells, IL-2 has the additional effect of augmenting cytotoxic function[5, 6], inducing lymphokine-activated killer (LAK) activity and IFN-γ production. IL-2 mediates its effects through interaction with cell surface receptor complex consisting of IL-2Rα (CD25) and IL-2Rβ (CD122) and γ_c chain (CD132)[7]. IL-2Rβ and γ_c chain associate with two Janus tyrosine-kinases (JAKs), Jak 1 and Jak 3, respectively, two

proteins required for IL-2 signaling[8]. IL-2 signal transduction has been investigated extensively in T cells[9, 10]. In both NK cells and T cells IL-2 induces tyrosine phosphorylation of two members of the Jak family, Jak1 and Jak3 upon binding to its receptors[11]. Phosphorylation of Jak1 and Jak3 leads to the recruitment and activation of signal transducers and activators (STATs), a family of transcription factors that contribute to the diversity of cytokine responses. Following activation, STAT1, STAT3, and STAT5 translocate to the nucleus and activate target genes[12]. Due to the important roles of IL-2 and NK cells in immune system, identifications of other signaling pathways triggered by IL-2 in NK cells have been an area of intensive research. In addition to JAK-STAT pathway, IL-2 has been shown to stimulate protein kinase C (PKC), mitogen-activated protein kinase (MAPK) / extracellular signal-regulated protein kinase (ERK) pathway in leukemic natural killer cell lines (NKL)[13]. Yu *et al*. reported an intact MAPK kinase (MKK)/ERK pathway is activated by IL-2 within a few minutes, which is necessary for NK cells to express at least four known biological responses, including LAK generation, IFN-γ secretion, CD25 and CD69 expression[14]. Moreover, because NK cells possess a large number of activating and inhibitory receptors, the complex crosstalk between them will complicate downstream signaling pathways. Evidence from several studies revealed the activation of additional signaling pathways and transcription factors in IL-2 treated NK cells, although the role of these pathways and proteins remains to be clarified. Zhou *et al*. showed that IL-2 signaling can activate a pathway leading to NF-κB activation in NK cells and ultimately up-regulation of perforin expression[15]. In another study, Ussat *et al*. demonstrated that caspases play a non-apoptotic role in human NK cells regulating the expression of activation markers and the production of IFN-γ and TNF as well as IL-2-induced proliferation[16]. However, compared to the well-described JAK-STAT pathway, less is known about other pathways that are associated with

IL-2 signaling, which limits our understanding of the molecular mechanisms by which IL-2 induces and regulates the immune response in NK cells.

Because IL-2-activated NK cells demonstrate significantly enhanced cytotoxicity and proliferation, there has been numerous effort in developing IL-2 and NK-based immunotherapies for human cancers. To date, FDA has approved the use of IL-2 for the treatment of metastatic melanoma[17] and metastatic renal cell carcinoma (RCC) [18], the most common type of kidney cancer. IL-2-based immunotherapy has also been attempted in clinical trials for the treatment of lymphoma and breast cancer in patients with post-autologous transplantation. It was demonstrated that IL-2 significantly increases the cytotoxicity of NK cells against breast cancer and lymphoma targets[19]. Another study proved that IL-2 stimulated NK cells have an effective cytotoxic activity against multiple myeloma (MM) cell lines and tumor cells from MM patients[20]. Although IL-2 and NK cell-based immunotherapy is an attractive treatment option for certain types of human cancers, the administration of high IL-2 doses to patients results in toxic effects such as fever, chills, nausea, diarrhea, fluid retention, low blood pressure and even death. There is evidence suggesting that the release of proinflammatory cytokines from IL-2-activated NK cells caused some of the IL-2-associated toxicity[21, 22]. However, the mechanism by which IL-2 induces adverse effects is still poorly defined. To improve current strategies for IL-2-based tumor immunotherapy and reduce the risk of IL-2-mediated toxicity in the clinical setting, it is imperative to acquire a clear and comprehensive view of the proteins that are affected by IL-2 signaling.

Despite the importance of understanding NK cell biology especially in the context of immunotherapy, only recently has mass spectrometry (MS)-based proteomics been applied to characterize the NK cell proteome. However, these proteomic studies were mainly focused on

the identification of cell surface proteins from membrane fractions or secretory lysosome of NK cells[23-27] and were all gel-based which limited the detection of low abundance proteins. No study has yet reported using a non-gel-based LC-MS/MS approach to globally characterize NK cell proteome. In this study, we present a comparative analysis of naïve and IL-2-activated NK cells using LC–MS/MS based shotgun proteomics. More than two thousands of proteins were identified from cell lysates of NK cells, which to date represents the largest protein catalog reported. To examine the proteomic change of IL-2-activated NK cells and identify specific proteins or pathways that are crucial for IL-2 signaling, label-free quantification by spectral counting was utilized to determine the relative protein abundance before and after IL-2 stimulation. The result from quantitative analysis revealed a panel of more than 383 proteins in NK cells that were significantly up or down-regulated in response to IL-2 stimulation.

Experimental Methods

Materials

Standard proteins, bovine serum albumin (BSA), bovine cytochrome c (CYC) and horse myoglobin (MYG) were purchased from Sigma-Aldrich (St. Louis, MO). RIPA buffer was purchased from Pierce (Rockford, IL). Urea and ammonium bicarbonate were purchased from Fisher Scientific (Fair Lawn, NJ, USA). Ammonium formate and iodoacetamide (IAM) were purchased from Sigma-Aldrich (St. Louis, MO). Dithiothreitol (DTT) and sequencing grade modified trypsin was purchased from Promega (Madison, WI). The LC-MS grade solvents and Optima grade solvents (ACN and water) were purchased from Fisher Scientific (Fair Lawn, NJ, USA).

Sample collection

Human primary NK cells were isolated from three healthy donors. Informed consent was obtained from all three blood donors recruited and the study was approved by the Institutional Review Board at the University of Wisconsin-Madison. NK cells from the blood samples were isolated by negative selection. The RosetteSep NK cell isolation kit (Stem Cell Technologies) was used and NK cell purification was conducted according to the manufacturer's protocol as described in our previous work[28]. The purified NK cells from each donor were divided equally into two groups. Each group was cultured in medium supplemented with or without IL-2 for 16 hours. NK cells were washed three times with ice-cold PBS and lysed with 200 μL RIPA lysis buffer on ice for 20 min with 20 s of sonication at the beginning. Cellular debris was removed by centrifugation for 30min at 16,100 ×g at 4 °C. Supernatants were collected and protein concentrations were measured using a BCA protein assay kit (Pierce). Protein extract was purified by acetone precipitation. Acetone (chilled to −80 °C) was added gradually (with intermittent vortexing) to the protein extract to a final concentration of 80% (v/v). The solution was then incubated at −20 °C for 60 min and centrifuged at 16,100 ×g for 15 min. The supernatant was decanted, and the pellet was carefully washed twice using cold acetone to ensure the efficient removal of detergent. The residual acetone was evaporated at ambient temperature.

Proteolysis

All protein samples were denatured with 8 M urea in 25 mM ammonium bicarbonate buffer, and reduced by incubating with 50 mM DTT at 37 °C for 1 h. The reduced proteins were alkylated for 1h in darkness with 100 mM iodoacetamide. The alkylation reaction was quenched by adding DTT to a final concentration of 50 mM. The samples were diluted to a final

concentration of 1 M urea. Trypsin was added to the sample at a 30:1 protein to trypsin mass ratio. The sample was incubated at 37 °C overnight.

Off-line first dimension high pH RPLC

38 μg tryptic digests from each sample were injected onto Waters Alliance HPLC (Waters Corp., Milford, MA) with a high pH-stable RP column (Phenomenex Gemini C18, 150 mm × 2.1 mm, 3 μm) at a flow rate of 150 μl/min. The peptides were eluted with a gradient from 5 to 45% solvent B over 45 min (Solvent A: 100 mM ammonium formate, pH 10; Solvent B: acetonitrile (ACN)). Fractions were collected every 2 min. Twenty fractions were collected from the first dimensional RPLC at pH 10, and then every two fractions with equal collection time interval were pooled, one from the early eluted section and the other from the later eluted section as previously described[29]. The pooled ten fractions were dried by Speedvac and reconstituted in 30 μl of 0.1% formic acid. 5μL of each of each fraction was subjected to nanoLC–MS/MS.

LC–ESI ion trap mass spectrometry and MS/MS analysis

Ten pooled fractions collected from high pH RPLC were analyzed using amaZon ion trap mass spectrometer (Bruker Daltonics, Germany) equipped with Waters nanoAcquity UPLC (Waters Corp., Milford, MA). For the chromatographic separation, solvent A consisted of 0.1% formic acid in water and solvent B consisted of 0.1% formic acid in ACN. 5 μl of each sample was injected onto a Waters Symmetry C18 5 μm 180 μm x 20 mm precolumn at a flow rate of 5 μl/min for 5 min at 95% A 5% B, followed by peptide separation performed on Waters BEH130 1.7 μm C18 100 μm x 100 mm analytical column using gradient from 0 to 45% solvent B at 300 nl/min over 90 min. Acquisition of precursor ions and MS/MS spectra was performed using the

parameters as indicated below: Smart parameter setting (SPS) was set to 700m/z, compound stability and trap drive level were set at 100%. Dry gas temperature, 125 °C, dry gas, 4.0 L/min, capillary voltage, −1300 V, end plate offset, −500 V, MS/MS fragmentation amplitude, 1.0 V, and Smart Fragmentation set at 30–300%. Data were generated in data dependent mode with strict active exclusion set after two spectra and released after 1min. MS/MS spectra were obtained via collision induced dissociation (CID) fragmentation for the six most abundant MS ions. For MS generation the ICC target was set to 200,000, maximum accumulation time, 50.00 ms, one spectrometric average, rolling average, 2, acquisition range of 300–1500 m/z, and scan speed (enhanced resolution) of 8100 m/z s^{-1}. For MS/MS generation the ICC target was set to 300,000, maximum accumulation time, 50.00 ms, two spectrometric averages, acquisition range of 100–2000 m/z, and scan speed (Ultrascan) of 32,000 m/z per second.

Database search

MS/MS spectra were converted into mgf. formatted files by DataAnalysis (Ver 4.0, Bruker Daltonics Bremen, Germany). Deviations in parameters from the default Protein Analysis in DataAnalysis were as follows: intensity threshold, 1000, maximum number of compounds, 1E9, and retention time window 0.001 minute. The resulting mgf. files were then searched against a home-built Human SwissProt database (SwissProt_2011_12.fasta, 533657 entries plus 3 standard proteins, BSA, CYC and MYG) with Mascot 2.3.02. The searching parameters and criteria were set as the following: tryptic digestion, maximum 2 missed cleavages, carbamidomethylation of cysteine as the fixed modification, oxidation of methionine as the variable modification, peptide mass tolerance of 1.2 Da, fragment mass tolerance of 0.6 Da, 2+,

3+ and 4+ chosen for charge state. In this study a simultaneous target-decoy search strategy (automatic decoy search) was adopted to facilitate false discovery rate (FDR) estimation. With simultaneous target-decoy search, a MS/MS spectrum is simultaneously searched against a protein sequence from the target database and its scramble version in decoy database. Therefore, FDR can be calculated from decoy hits and target hits. We applied Mascot Percolator to improve peptide and protein identification. Mascot Percolator has been well developed [30] and embedded into Mascot search engine. Mascot Percolator is a well performing machine learning method which constructs a support vector machine by using Mascot search parameters and results to re-rank peptide or protein identification. With Mascot Percolator, some low quality MS/MS spectra were re-searched to produce reliable peptide identification. We check "Percolator" option on Mascot results and control the resulting FDR at ~1%. Set “a bold red peptide required” for protein assembly. Since there were three technical replicates for each sample, only proteins identified in at least two out of three replicates were considered.

Protein quantification

Given the biological variation and technical variation across datasets, only part of identified proteins is qualified for quantification. It is important to select the appropriate amount of quantifiable proteins. Since we prepared three biological samples and each sample has three replicates, we set the following criteria to select quantifiable proteins: 1) a protein is quantifiable if it can be detected in at least two of three technical replicates; and 2) it can be detected in all three biological replicates. The distributive normalized spectral abundance factor (dNSAF) for each quantifiable protein within a chromatographic run is calculated by using the following formula[31]:

$$dNSAF_i = \frac{dSAF_i}{\sum_{i=1}^{N} dSAF_i} \quad (1)$$

$$dSAF_i = \frac{\mu SpC_i + \frac{\mu SpC_i}{\sum_{m=1}^{M} \mu SpC_m} \times sSpC_i}{M_i} \quad (2)$$

where dSAF is distributive spectral abundance factor for a given protein, μSpC is the spectral counts of unique peptides associated with this protein while $sSpC$ is the spectral counts of shared peptides associated with this protein. M is the monoisotopic mass of protein. The definition of "unique" peptide is the peptide whose sequence matched only one protein whereas "shared" peptide means the peptide whose sequence is shared by multiple proteins. The following method was used to impute spectral counts with zero value. Firstly, if a protein had only one zero spectral count out of three technical replicates, we calculated the average value of spectral counts of this protein in all three replicates, and then replace the zero spectral count with the average value. Next, in the case of zero spectral counts in all three replicates, we followed the method as previously described[32] to determine a fraction value within [0,1] to replace the zero spectral counts. An iterative process was used where zero spectral counts were replaced by a fraction of a spectral count between 0 and 1, and the normality of the resulting ln(dNSAF) distribution was evaluated by the Shapiro-Wilk test. It is advisable to use the smallest value in order not to change the total sum significantly. An in-house program written in Java was used to extract peptides from the database results obtained from Mascot Percolator, select quantifiable proteins and then calculate spectral counts and dNSAF values. R program is used to evaluate the normality of ln(dNSAF) distribution by Shapiro-Wilk test. p-value > 0.05 indicates the distribution can be considered as Gaussian distribution.

Sample preparation and protein quantification of standard proteins

NKL cell lysates were obtained from 10 million NKL cells using the same method as described in "Sample collection". Both standard proteins and NKL cell lysates were digested by trypsin using the same protocol as described in "Proteolysis". The amounts of each protein standard spiked into 10 μg of tryptic digests of NKL cell lysates were 4 μg, 1 μg, 0.25 μg, 62.5 ng, 15.625 ng, 3.91 ng of BSA, CYC and MYG, respectively. 300 ng of each sample was injected onto amaZon ion trap mass spectrometer (Bruker Daltonics, Germany) equipped with Waters nanoAcquity UPLC (Waters Corp., Milford, MA). Each sample was run in triplicates. For the chromatographic separation, solvent A consisted of 0.1% formic acid in water and solvent B consisted of 0.1% formic acid in ACN. 5 μl of each sample was injected onto an Waters Symmetry C18 5 μm 180 μm x 20 mm precolumn at a flow rate of 5 μl/min for 5 min at 95% A 5% B, followed by peptide separation performed on Waters BEH130 1.7 μm C18 100 μm x 100 mm analytical column using gradient from 0 to 45% solvent B at 300 nl/min over 120 min. parameters for the acquisition of precursor ions and MS/MS spectra were the same as that of described in "LC–ESI ion trap mass spectrometry and MS/MS analysis". The methods for database search and protein quantification were the same as described above.

Real time PCR

Some of the differentially expressed proteins in naïve and IL2 treated NK cells were validated by real time PCR. The untreated and IL-2 treated NK cells were homogenized in Trizol (Sigma, Cat No T9424) and RNA was extracted according to the manufacturer's instructions. The RNA was reverse transcribed into cDNA using Omniscript RT kit from Qiagen

(Cat. No.205111). Quantitative real-time PCR was performed using the SYBR green chemistry (SsoFast Evagreen Supermix from BioRad, Cat. No. 172-5201) in a CFX96 Real-Time PCR Detection System. The qPCR validated primers used to amplify PTP1B, CD97, PCNA were obtained from SA Biosciences (Real time PCR primers for Human PTP1B, Cat No. PPH00730C; CD97, Cat No PPH07186A ; PCNA, cat No PPH00216B and S27, cat No PPH17248B). The three step cycling conditions used were, 95^0C for 30s, followed by 40 cycles of the denaturation at 95 ^{0}C for 1 s, annealing at 60 ^{0}C for 5 s. The $2^{-\Delta\Delta CT}$ method was used for relative quantitation of gene expression. Data was analyzed using the BioRad CFX manager and GraphPad Prizm.

Results and Discussion

Identification and quantification of proteins in naïve and IL-2-activated NK cells

Our understanding of NK cell biology was mainly the result from studies where individual cell receptors and their ligands were identified. In recent years, MS-based proteomics has been utilized as a global approach to identify proteins present in NK cells. However, due to their experimental design these studies focused attention on a subset of the total proteome rather than the characterization of total protein expression[23-27, 33]. In addition, few studies used primary NK cells for proteomic analysis, instead human NK-like cell lines such as YTS and NKL were used. Although the morphology of NKL and YTS cells closely resemble that of primary NK cells and are used as well established "model cell lines" in NK cell research, NK-like cell lines and primary NK cells differ, substantially in the expression of cell surface receptors and intracellular signal transduction proteins[33]. In this study, we aimed to characterize the total protein expression in human peripheral blood NK cells. We anticipated that the sample complexity of unfractionated cell lysates would be a challenge to identify less abundant proteins, therefore, it was necessary to reduce sample complexity prior to MS analysis to improve overall

protein identifications. We adopted a two dimensional separation approach utilizing high pH RPLC as the first dimension separation. Increasing the number of fractions collected during first dimension liquid chromatography typically results in better separation that allows improved protein identification by downstream LC-MS/MS analysis. However, fraction collection from first dimension separation is limited by overall analysis time; it is important to minimize the numbers of fractions but produce the best output for LC-MS/MS analysis. To address the limitation of fraction collection but at the same time improve the orthogonality of the 2D separation, a new RP-RPLC approach was employed which was reported previously by Song *et al.*[29]. For this approach, 20 fractions were collected in the first dimensional RPLC. Every two fractions with equal collection time interval were pooled, one from the early eluted section and the other from a later elution section (fractions 1 and 11, 2 and 12, and so on). Through this combination only half the number of fractions was submitted to LC-MS/MS analysis, significantly reducing the overall analysis time.

For the present work we applied Mascot Percolator which was embedded into the Mascot search engine to improve peptide and protein identification. We compared the number of peptide spectrum matches (PSMs) identified with Mascot and Mascot Percolator at FDR=0.1% and it was shown that more peptides could be identified by Mascot Percolator (data not shown). In total, 2311 proteins (≥1 unique peptide) were identified from three naïve NK cell samples, while 2413 proteins were identified from their IL-2 stimulated counterparts. Each sample was analyzed in triplicate. Figure 1 shows the Venn Diagrams of the numbers of proteins identified from naïve NK cells or IL-2 activated NK cells. There were 1999 proteins in common that were identified in both cells, whereas 312 proteins and 414 proteins were identified in only naïve or IL-2 activated NK cell, respectively.

To assess differences between protein abundance in naïve NK cells and IL-2-activated NK cells, spectral counting, a label-free protein quantification method was used. To account for shared peptide sequences among protein isoforms and achieve better accuracy, we adopted the distributive normalized spectral abundance factor (dNSAF) strategy previously reported by Zhang *et al.*[31]. However, given that the application of Mascot Percolater in peptide and protein identification may affect the performance of this approach, we first confirmed its effectiveness and reproducibility by spiking known amounts of protein standards into complex mixture of NKL cell lysates. To estimate the dynamic range and determine whether there was a linear correlation between the known amount of protein and their measured dNSAF values, we spiked in the tryptic digests of three protein standards bovine serum albumin (BSA), bovine cytochrome c (CYC) and horse myoglobin (MYG) with 4-fold dilution over 3 orders of magnitude. After protein identification with Mascot Percolator, dNSAF values for all quantifiable proteins were calculated. dNSAF values for BSA, CYC and MYG in different samples were extracted. Figure 2 shows the linear regression between dNSAF values and known protein amounts where Log2-transformed dNSAF values were plotted as a function of log2-transformed protein amounts in micrograms. The results demonstrated acceptable performance as there was a linear correlation coefficient of >0.990 for all three protein standards (Figure 2, a-c). The linear dynamic range for BSA and CYC are three orders of magnitude (1024) while the dynamic range for MYG is two orders of magnitude (256), which is probably due to the poor detection at lower concentration, as the presence of heme stabilizes the structure of MYG and makes it resistant to digestion[34]. Based on this result, we concluded that the application of Mascot Percolater for peptide and protein identification did not affect the accuracy of protein quantification by spectral counting that will be used in the present work. The linearity of our

quantification method is maintained between protein amounts and dNSAF values over a dynamic range of at least three orders of magnitudes.

We analyzed the proteomes from three donors (three biological replicates) where each biological replicate contains three technical replicates because the biological variation and technical variation across datasets have to be taken into consideration prior to protein quantification. To achieve better accuracy we set the following criteria to select quantifiable proteins: 1) a protein is quantifiable if it can be detected in at least two of three technical replicates; and 2) it can be detected in all three biological replicates. Overall, 1375 proteins identified from both naïve NK cells and IL-2 activated NK cells were selected for quantification analysis. The dNSAF value of each protein was calculated and compared between different conditions (naïve vs. IL-2-activated NK cells). Fold change was calculated as the ratio of dNSAF of protein in IL-2-activated NK cells over that of in naïve NK cells. Threshold levels for significantly up- or down-regulated proteins are set to be more than 2-fold or less than 0.5-fold with $p \leq 0.05$ from Student *t*-test. Altogether, 436,421 and 459 proteins exhibited significant abundant differences after IL-2 activation in three donors, respectively. An overlap of 383 proteins was commonly observed across all three donors and demonstrated similar trend of up or down-regulation. A list of 383 IL-2 regulated proteins can be found in Appendix 2.

Functional annotation of IL-2-regulated proteins identified by quantitative analysis

Activation of JAK-STAT pathway and cell proliferation

IL-2 critically regulates the proliferation and cytotoxicity of human NK cells, but relatively little is known about the molecules involved in IL-2 actions. It is well known that IL-2 mediates its effects through the activation of the JAK-STAT pathway in which STAT1, STAT3

and STAT5 are activated. In our analysis, three STAT molecules STAT1, STAT3 and STAT4 were found to be up-regulated upon IL-2 stimulation. While the participation and the role of STAT1 and STAT3 in IL-2 signaling have been well documented, the function of STAT4 in IL-2 signaling is still under investigation. Wang *et al*. reported IL-2 induced STAT4 activation as an alternative to the well-established JAK-STAT pathway in primary NK cells but not in T cells[35], which may explain why IL-2 enhances cytoxicity in NK cells but not in T cells, even though both cells have identical JAK-STAT signaling pathway. Moreover, they investigated the effect of IL-2 on IL-12-activated signaling pathways in NK cells and demonstrated that pretreatment of IL-2 promoted expression of high level of STAT4 through which the response of NK cells to IL-12 was enhanced[36]. Given that the results of current clinical trials for immunotherapy using IL-2 or IL-12 alone were not shown to be quite as successful as expected, STAT4 may prove to be a target for the study of synergistic effect between IL-2 and IL-12 for the development of a more effective strategy. Another important protein involved in JAK-STAT signaling pathway is protein-tyrosine phosphatase 1B (PTP1B), which was also shown to be up-regulated by IL-2 and confirmed by RT-PCR (Figure 3, a). PTP1B is an important phosphatase that can play both negative and positive roles in diverse signaling pathways. Although it has been extensively studied as a negative regulator of insulin and leptin signaling, and more recently as a positive factor in tumorigenesis, the understanding of the role of PTP1B during immune cell signaling is insufficient. PTP1B and T-cell PTP (TC-PTP) form the first nontransmembrane subfamily of PTPs[37]. While previous studies have identified JAK1 and JAK3 as TC-PTP substrates and implicated TC-PTP in the regulation of JAK-STAT signaling activated by IL-2, PTP1B was unable to bind JAK1 and JAK3[38]. However, other studies demonstrated that PTP1B targets the other two JAK family members, JAK2 and tyrosine kinase 2 (TYK2) after IFN stimulation[39].

Also, PTP1B has been implicated in the dephosphorylation of STAT5 in prolactin signaling[40]. Although PTP1B does not appear to be directly associated with the regulation of JAK-STAT activation, it might play an important role in IL-2 signaling through another mechanism.

As expected, many proteins identified to be up or down-regulated are involved in DNA replication, translation initiation/elongation/termination or the regulation of cell cycle since one of the known results of NK cells exposure to IL-2 is stimulation of cell proliferation. Three DNA replication licensing factor MCM2, MCM5 and MCM7 were found to be up-regulated. The MCM proteins are required for DNA replication licensing and consist of a group of ten conserved factors functioning in the replication of the genomes of archae and eukaryotic organisms. Among these, MCM 2–7 proteins are related to each other and form a family of DNA helicases at the initiation step of DNA synthesis. While the other MCM proteins were not detected in our analysis possibly due to their low abundance, the elevated expression of MCM2, MCM5 and MCM7 implicated that increased NK cells proliferation may be attributable to these proteins. Lymphocyte proliferation is often used to mark immune response following immunotherapy. By identifying proteins that improve monitoring of NK cell proliferation to determine the extent of the immune response may prove to be crucial for clinical decision-making during the immunotherapy in order to minimize the risk of toxicity in patients.

Another protein that is associated with the proliferation process of NK cells is proliferating cell nuclear antigen (PCNA) which is synthesized in early G1 and S phases of the cell cycle. Our real-time RT-PCR result confirmed that the level of PCNA mRNA expression was increased by 2-fold in NK cells after 16 hours of stimulation by IL-2 (Figure 3, b). PCNA is a marker to detect early stage T-cell proliferation, as it was found that unstimulated human peripheral blood T-lymphocytes were PCNA negative and their expression was evident only

after stimulation[41]. In the clinical setting, PCNA can be used as a marker to monitor T-cell function that reflects immune condition in patients undergoing immunosuppressive therapy[42, 43]. Monitoring PCNA level in whole blood has proven to be a useful tool to monitor immunosuppressive treatment and warn of over-immunosuppression immediately after transplantation. Such monitoring would be crucial in reducing the risks and providing optimal immunosuppressive therapy for each transplant recipient[42-44]. Recently, Niwa *et al*. has reported an assay where PCNA mRNA level in peripheral blood was measured by real-time RT-PCR for monitoring patient's immune condition after renal transplantation[45]. Although PCNA level in peripheral blood has been implicated as a biomarker to evaluate T-cell proliferation and immunoregulatory status, how this protein can reflect NK cell proliferation capacity has never been reported and knowing this information would provide useful guidance to NK cell-based immunotherapies.

Cluster of differentiation (CD) molecules

In addition to changes in molecules that regulated cell proliferation and the activation of cytotoxicity in NK cells, changes in cluster of differentiation (CD) molecules were also expected, as their functions are often closely tied to the immune system. While CD56, CD48, CD98, CD97, CD225, and CD300a showed increased expression in our analysis, there were decreases in the level of CD11b, CD11d, CD11c and CD43 after IL-2 stimulation.

CD48 is a glycosyl-phosphatidyl-inositol (GPI)-anchored protein expressed on the surface of NK cells and is known as a co-stimulatory factor and a high affinity ligand for natural killer cell receptor 2B4[46, 47]. 2B4/CD48 interactions in NK cells are required for the enhanced proliferation and the development of optimal cytolytic and secretory NK effector functions

during IL-2 activation[48]. To further understand the mechanism of the induction of NK activation by 2B4/CD48, Shiha *et al*. recently investigated both 2B4 and CD48 in IL-2-propagated NK cells[49]. They suggested the clustering of CD48 and colocalization with 2B4 as well as a cis interaction between CD48 and 2B4 in the same cell to form a signaling complex is required for the activation of NK cells. Although understanding of the function of CD48 in modulating immune reaction is limited, the elevated level of CD48 in IL-2 stimulated NK cells may be an important event that indicates the initiation of immune protection against infections.

Human CD97 is a member of the EGF-TM7 family of adhesion class heptahelical receptors and was identified as an early activation marker for human lymphocytes[50]. We observed and validated increased CD97 level in response to IL-2 by real time RT-PCR (Figure 3, c) that was comparable with the results from Kop *et al*.[51]. Interestingly, Kop *et al*. found CD97 levels was not affected by IL-12 and IL-18, which stimulate NK-cell cytokine production and cytotoxicity, respectively, indicating CD97 involves only in NK cell proliferation upon the activation by cytokines.

CD98 is a transmembrane glycoprotein identified as a lymphocyte activation antigen[52, 53]. Because the level of CD98 on cell surface was markedly increased in activated lymphocytes, CD98 has been mainly used as a T cell activation marker[52, 53]. Although the mechanism still remains unknown, CD98 has been implicated as a protein with multiple functions, including regulating integrin signaling, amino acid transport and immune response[54, 55]. Despite the efforts to investigate the function of CD98 in regards to immune response, the role that CD98 plays in lymphocytes activation is not fully understood. CD98 has been demonstrated as a co-stimulatory factor for T-cell activation and function, where co-stimulation required a functional interaction between integrins and CD98[56, 57]. Past studies investigated the role of CD98 in murine T

lymphocytes proliferation following IL-2 activation[58, 59]. However, because of conflicting results from these studies it could not be confirmed that CD98 was regulated by IL-2. So far no studies have investigated the role of CD98 in NK cell activation. Further investigation of CD98 will be of great importance, as the biological processes regulated by CD98, such as integrin signaling and amino acid transport, are critical for lymphocyte function.

CD300a is a cell surface inhibitory receptor that is expressed in all human NK cells and is known to down-regulate the cytotoxicity of NK cells[60]. Different studies have also evaluated the CD300a activity in immune regulation in other immune cells such as plasmacytoid dendritic cells[61], T cells[62] and neutrophils[63]. However, little is known about the functionality and the ligand of CD300a in NK cells so far and it was only until recently that Nakahashi-Oda *et al*. identified phosphatidylserine (PS), which is exposed on the outer leaflet of the plasma membrane of apoptotic cells, as a ligand for CD300a[64]. Alvarez *et al*. reported that inflammatory stimuli such as granulocyte macrophage-colony stimulating factor (GM-CSF) or lipopolysaccharide (LPS) could induce a significant increase in cell surface expression of CD300a in neutrophils and that the signaling through this receptor down-regulated neutrophil function[63]. Nevertheless, the activation and regulation of CD300a by cytokines in NK cells has never been reported. Activation of NK cell results from a balance of activating and inhibitory cell surface receptors that transmit opposing signals to regulate the amplitude of immune response. Inhibition is as important as activation for immune cells, as disruption or loss of inhibitory signaling is often associated with autoreactivity and unchecked inflammatory responses. However, our knowledge of signal transduction of inhibitory receptors and their downstream effectors in NK cells is limited. Further investigation is required to understand how CD300a is regulated by IL-2 and the physiological role of CD300a in NK cells.

Unlike all the CD molecules discussed above, the lack of evidence for the expression, regulation and function of CD225 in NK cells provide little clue to explain the up-regulation of this protein upon IL-2 activation. CD225 is also known as interferon (IFN)-induced transmembrane protein 1 (IFITM1) which is a member of the IFN-inducible transmembrane protein family[65]. It is known that the transcription of CD225 is induced by IFN-γ[66], and that CD225 can mediate IFN-γ-induced inhibition of cell proliferation and inhibit ERK activation[67]. CD225 has also been implicated in the control of cell growth, as it can arrest cell cycle progression in the G1 phase in a p53-dependent manner[67]. The role of CD225 in NK cell activation has never been reported. However, as an important factor for growth control, it is likely that CD225 mediates the negative regulation and plays an anti-proliferative role during NK cell activation.

Three of the down-regulated proteins, CD11b, CD11c and CD11d, are integrin α subunits and form noncovalently linked dimers with the β2 integrin CD18 to generate functional β2 integrin family CD11/CD18[68]. β2 integrin family are known to be essential for the functions of leukocytes in innate immune system, including involvement in several immune processes such as phagocytosis, cell-mediated cytotoxicity, chemotaxis, and regulating leukocyte adhesion, trafficking and migration[69-71]. Although adhesion molecules have been associated with the stimulation of cell proliferation and LAK activity in NK cells long time ago[72], the exact role of adhesion molecules in IL-2 signaling still remains unclear. Interestingly, both CD11b and CD43 which is another down-regulated protein identified in present work, were described as maturation markers on NK cells[73]. The expression of CD11b and CD43 were shown to be developmentally regulated in developing NK cells, and generally have lower expression levels in immature NK cells than in mature NK cells[73, 74]. However, why the expression levels of CD11b and CD43

were down-regulated in NK cells exposed to IL-2 as shown in this study is not clear, and further investigation is required to understand the physiological role of these proteins and how they are regulated by IL-2 signaling.

Gene ontology and pathway analysis

To obtain more information about the molecular function of IL-2 regulated proteins and to identify pathways possibly involved in IL-2 activation in NK cells, we performed gene ontology and pathway analysis using the PATHER database (http://www.pantherdb.org/). Overall, 383 proteins that were found differentially expressed across all three donors could be classified into 25 categories of which the top four are nucleic acid binding proteins (17%), hydrolase (11.3%), enzyme modulator (10.4%), and transferase (10.2%) (Figure 4, a). This is in agreement with the fact that the activation of NK cells in response to cytokines requires protein regulators to bind to DNA and activate new protein synthesis for cell proliferation and enhanced cytotoxicity. An analysis of the molecular function of these proteins revealed that most of these proteins are involved in catalytic activities (41%) and binding (34%) (Figure 4, b). Furthermore, these proteins were found to be involved in various biological processes, of which the top three categories are: metabolic process (30.4%), cell process (15.9%) and transport (11.4%) (Figure 4, c). Taken together, the data from gene ontology analysis suggested that most of these proteins are involved in the most critical cellular events and their function is important for NK cell activation by IL-2.

In search for novel pathways that might be involved in IL-2 signaling in NK cells, a pathway analysis was also performed in PATHER database and a total of 90 pathways were found to be related to the IL-2 regulated proteins based on this study. In addition to the previously known pathways, such as JAK-STAT pathway, MAPK/ERK and NF-κB pathway,

other pathways that are very likely to be associated with IL-2 signaling include: ubiquitin proteasome pathway, integrin signaling pathway, PDGF signaling pathway, EGFR signaling pathway and Wnt signaling pathway. Table 1 provides the names of IL-2 regulated proteins identified in our analysis that are known to be the components of these pathways. Although the roles of these pathways in promoting or regulating the function of NK cells have been investigated in the past, so far none of them have been directly linked to the activation of NK cells by IL-2, and therefore could be the new targets for future studies. Given the pleiotropic effects of IL-2 and diverse functions of IL-2-activated NK cells, there should be many possible downstream effectors that may be necessary to drive IL-2-induced effects.

Conclusions

In summary, we have developed a method for the proteomic analysis in human primary NK cells. We successfully employed 2D LC to reduce the sample complexity prior to MS analysis. To improve protein identification, Mascot percolator was employed, with 2311 and 2413 proteins being identified from naïve and IL-2-activated NK cells, respectively. Label-free quantitative analysis via spectral counting revealed a list of 383 proteins that were up or down-regulated in IL-2 signaling. Functional annotation of IL-2 regulated proteins in present work revealed several proteins with important functions related to IL-2 signaling that could potentially serve as the targets for future investigation of IL-2 signaling in human primary NK cells. A pathway analysis was also performed and revealed several novel pathways not previously known to be involved in IL-2 signaling. The quantitative proteomic analysis in present work provided a comprehensive view of proteins that may be associated with IL-2 signaling. Further functional

analysis of proteins of interests will improve our understanding of signaling transduction and biological processed involved in NK cell activation by IL-2.

References

1. Trinchieri, G., Biology of natural killer cells. *Adv Immunol* **1989,** 47, 187-376.
2. Moretta, A.; Bottino, C.; Vitale, M.; Pende, D.; Cantoni, C.; Mingari, M. C.; Biassoni, R.; Moretta, L., Activating receptors and coreceptors involved in human natural killer cell-mediated cytolysis. *Annu Rev Immunol* **2001,** 19, 197-223.
3. Brandhuber, B. J.; Boone, T.; Kenney, W. C.; McKay, D. B., Three-dimensional structure of interleukin-2. *Science* **1987,** 238, (4834), 1707-9.
4. Smith, K. A., Interleukin-2: inception, impact, and implications. *Science* **1988,** 240, (4856), 1169-76.
5. Caligiuri, M. A.; Zmuidzinas, A.; Manley, T. J.; Levine, H.; Smith, K. A.; Ritz, J., Functional consequences of interleukin 2 receptor expression on resting human lymphocytes. Identification of a novel natural killer cell subset with high affinity receptors. *J Exp Med* **1990,** 171, (5), 1509-26.
6. Bonnema, J. D.; Rivlin, K. A.; Ting, A. T.; Schoon, R. A.; Abraham, R. T.; Leibson, P. J., Cytokine-enhanced NK cell-mediated cytotoxicity. Positive modulatory effects of IL-2 and IL-12 on stimulus-dependent granule exocytosis. *J Immunol* **1994,** 152, (5), 2098-104.
7. Karnitz, L. M.; Abraham, R. T., Interleukin-2 receptor signaling mechanisms. *Adv Immunol* **1996,** 61, 147-99.
8. Russell, S. M.; Johnston, J. A.; Noguchi, M.; Kawamura, M.; Bacon, C. M.; Friedmann, M.; Berg, M.; McVicar, D. W.; Witthuhn, B. A.; Silvennoinen, O.; et al., Interaction of IL-2R beta and gamma c chains with Jak1 and Jak3: implications for XSCID and XCID. *Science* **1994,** 266, (5187), 1042-5.
9. Ellery, J. M.; Nicholls, P. J., Alternate signalling pathways from the interleukin-2 receptor. *Cytokine Growth Factor Rev* **2002,** 13, (1), 27-40.
10. Nelson, B. H.; Willerford, D. M., Biology of the interleukin-2 receptor. *Adv Immunol* **1998,** 70, 1-81.
11. Johnston, J. A.; Kawamura, M.; Kirken, R. A.; Chen, Y. Q.; Blake, T. B.; Shibuya, K.; Ortaldo, J. R.; McVicar, D. W.; O'Shea, J. J., Phosphorylation and activation of the Jak-3 Janus kinase in response to interleukin-2. *Nature* **1994,** 370, (6485), 151-3.
12. Frank, D. A.; Robertson, M. J.; Bonni, A.; Ritz, J.; Greenberg, M. E., Interleukin 2 signaling involves the phosphorylation of Stat proteins. *Proc Natl Acad Sci U S A* **1995,** 92, (17), 7779-83.
13. Garcia-Lora, A.; Martinez, M.; Pedrinaci, S.; Garrido, F., Different regulation of PKC isoenzymes and MAPK by PSK and IL-2 in the proliferative and cytotoxic activities of the NKL human natural killer cell line. *Cancer Immunol Immunother* **2003,** 52, (1), 59-64.
14. Yu, T. K.; Caudell, E. G.; Smid, C.; Grimm, E. A., IL-2 activation of NK cells: involvement of MKK1/2/ERK but not p38 kinase pathway. *J Immunol* **2000,** 164, (12), 6244-51.
15. Zhou, J.; Zhang, J.; Lichtenheld, M. G.; Meadows, G. G., A role for NF-kappa B activation in perforin expression of NK cells upon IL-2 receptor signaling. *J Immunol* **2002,** 169, (3), 1319-25.
16. Ussat, S.; Scherer, G.; Fazio, J.; Beetz, S.; Kabelitz, D.; Adam-Klages, S., Human NK cells require caspases for activation-induced proliferation and cytokine release but not for cytotoxicity. *Scand J Immunol* **2010,** 72, (5), 388-95.
17. Smith, F. O.; Downey, S. G.; Klapper, J. A.; Yang, J. C.; Sherry, R. M.; Royal, R. E.; Kammula, U. S.; Hughes, M. S.; Restifo, N. P.; Levy, C. L.; White, D. E.; Steinberg, S. M.;

Rosenberg, S. A., Treatment of metastatic melanoma using interleukin-2 alone or in conjunction with vaccines. *Clin Cancer Res* **2008,** 14, (17), 5610-8.
18. Klapper, J. A.; Downey, S. G.; Smith, F. O.; Yang, J. C.; Hughes, M. S.; Kammula, U. S.; Sherry, R. M.; Royal, R. E.; Steinberg, S. M.; Rosenberg, S., High-dose interleukin-2 for the treatment of metastatic renal cell carcinoma : a retrospective analysis of response and survival in patients treated in the surgery branch at the National Cancer Institute between 1986 and 2006. *Cancer* **2008,** 113, (2), 293-301.
19. Burns, L. J.; Weisdorf, D. J.; DeFor, T. E.; Vesole, D. H.; Repka, T. L.; Blazar, B. R.; Burger, S. R.; Panoskaltsis-Mortari, A.; Keever-Taylor, C. A.; Zhang, M. J.; Miller, J. S., IL-2-based immunotherapy after autologous transplantation for lymphoma and breast cancer induces immune activation and cytokine release: a phase I/II trial. *Bone Marrow Transplant* **2003,** 32, (2), 177-86.
20. Gottlieb, D. J.; Prentice, H. G.; Mehta, A. B.; Galazka, A. R.; Heslop, H. E.; Hoffbrand, A. V.; Brenner, M. K., Malignant plasma cells are sensitive to LAK cell lysis: pre-clinical and clinical studies of interleukin 2 in the treatment of multiple myeloma. *Br J Haematol* **1990,** 75, (4), 499-505.
21. Assier, E.; Jullien, V.; Lefort, J.; Moreau, J. L.; Di Santo, J. P.; Vargaftig, B. B.; Lapa e Silva, J. R.; Theze, J., NK cells and polymorphonuclear neutrophils are both critical for IL-2-induced pulmonary vascular leak syndrome. *J Immunol* **2004,** 172, (12), 7661-8.
22. Peace, D. J.; Cheever, M. A., Toxicity and therapeutic efficacy of high-dose interleukin 2. In vivo infusion of antibody to NK-1.1 attenuates toxicity without compromising efficacy against murine leukemia. *J Exp Med* **1989,** 169, (1), 161-73.
23. Lund, T. C.; Anderson, L. B.; McCullar, V.; Higgins, L.; Yun, G. H.; Grzywacz, B.; Verneris, M. R.; Miller, J. S., iTRAQ is a useful method to screen for membrane-bound proteins differentially expressed in human natural killer cell types. *J Proteome Res* **2007,** 6, (2), 644-53.
24. Man, P.; Novak, P.; Cebecauer, M.; Horvath, O.; Fiserova, A.; Havlicek, V.; Bezouska, K., Mass spectrometric analysis of the glycosphingolipid-enriched microdomains of rat natural killer cells. *Proteomics* **2005,** 5, (1), 113-22.
25. Hanna, J.; Fitchett, J.; Rowe, T.; Daniels, M.; Heller, M.; Gonen-Gross, T.; Manaster, E.; Cho, S. Y.; LaBarre, M. J.; Mandelboim, O., Proteomic analysis of human natural killer cells: insights on new potential NK immune functions. *Mol Immunol* **2005,** 42, (4), 425-31.
26. Hanna, J.; Gonen-Gross, T.; Fitchett, J.; Rowe, T.; Daniels, M.; Arnon, T. I.; Gazit, R.; Joseph, A.; Schjetne, K. W.; Steinle, A.; Porgador, A.; Mevorach, D.; Goldman-Wohl, D.; Yagel, S.; LaBarre, M. J.; Buckner, J. H.; Mandelboim, O., Novel APC-like properties of human NK cells directly regulate T cell activation. *J Clin Invest* **2004,** 114, (11), 1612-23.
27. Casey, T. M.; Meade, J. L.; Hewitt, E. W., Organelle proteomics: identification of the exocytic machinery associated with the natural killer cell secretory lysosome. *Mol Cell Proteomics* **2007,** 6, (5), 767-80.
28. Gubbels, J. A.; Felder, M.; Horibata, S.; Belisle, J. A.; Kapur, A.; Holden, H.; Petrie, S.; Migneault, M.; Rancourt, C.; Connor, J. P.; Patankar, M. S., MUC16 provides immune protection by inhibiting synapse formation between NK and ovarian tumor cells. *Mol Cancer* **2010,** 9, 11.
29. Song, C.; Ye, M.; Han, G.; Jiang, X.; Wang, F.; Yu, Z.; Chen, R.; Zou, H., Reversed-phase-reversed-phase liquid chromatography approach with high orthogonality for multidimensional separation of phosphopeptides. *Anal Chem* **2010,** 82, (1), 53-6.

30. Brosch, M.; Yu, L.; Hubbard, T.; Choudhary, J., Accurate and sensitive peptide identification with Mascot Percolator. *J Proteome Res* **2009,** 8, (6), 3176-81.
31. Zhang, Y.; Wen, Z.; Washburn, M. P.; Florens, L., Refinements to label free proteome quantitation: how to deal with peptides shared by multiple proteins. *Anal Chem* **2010,** 82, (6), 2272-81.
32. Zybailov, B.; Mosley, A. L.; Sardiu, M. E.; Coleman, M. K.; Florens, L.; Washburn, M. P., Statistical analysis of membrane proteome expression changes in Saccharomyces cerevisiae. *J Proteome Res* **2006,** 5, (9), 2339-47.
33. Schmidt, H.; Gelhaus, C.; Nebendahl, M.; Lettau, M.; Watzl, C.; Kabelitz, D.; Leippe, M.; Janssen, O., 2-D DIGE analyses of enriched secretory lysosomes reveal heterogeneous profiles of functionally relevant proteins in leukemic and activated human NK cells. *Proteomics* **2008,** 8, (14), 2911-25.
34. Strader, M. B.; Tabb, D. L.; Hervey, W. J.; Pan, C.; Hurst, G. B., Efficient and specific trypsin digestion of microgram to nanogram quantities of proteins in organic-aqueous solvent systems. *Anal Chem* **2006,** 78, (1), 125-34.
35. Wang, K. S.; Ritz, J.; Frank, D. A., IL-2 induces STAT4 activation in primary NK cells and NK cell lines, but not in T cells. *J Immunol* **1999,** 162, (1), 299-304.
36. Wang, K. S.; Frank, D. A.; Ritz, J., Interleukin-2 enhances the response of natural killer cells to interleukin-12 through up-regulation of the interleukin-12 receptor and STAT4. *Blood* **2000,** 95, (10), 3183-90.
37. Andersen, J. N.; Mortensen, O. H.; Peters, G. H.; Drake, P. G.; Iversen, L. F.; Olsen, O. H.; Jansen, P. G.; Andersen, H. S.; Tonks, N. K.; Moller, N. P., Structural and evolutionary relationships among protein tyrosine phosphatase domains. *Mol Cell Biol* **2001,** 21, (21), 7117-36.
38. Simoncic, P. D.; Lee-Loy, A.; Barber, D. L.; Tremblay, M. L.; McGlade, C. J., The T cell protein tyrosine phosphatase is a negative regulator of janus family kinases 1 and 3. *Curr Biol* **2002,** 12, (6), 446-53.
39. Myers, M. P.; Andersen, J. N.; Cheng, A.; Tremblay, M. L.; Horvath, C. M.; Parisien, J. P.; Salmeen, A.; Barford, D.; Tonks, N. K., TYK2 and JAK2 are substrates of protein-tyrosine phosphatase 1B. *J Biol Chem* **2001,** 276, (51), 47771-4.
40. Aoki, N.; Matsuda, T., A cytosolic protein-tyrosine phosphatase PTP1B specifically dephosphorylates and deactivates prolactin-activated STAT5a and STAT5b. *J Biol Chem* **2000,** 275, (50), 39718-26.
41. Kurki, P.; Lotz, M.; Ogata, K.; Tan, E. M., Proliferating cell nuclear antigen (PCNA)/cyclin in activated human T lymphocytes. *J Immunol* **1987,** 138, (12), 4114-20.
42. Bohler, T.; Nolting, J.; Kamar, N.; Gurragchaa, P.; Reisener, K.; Glander, P.; Neumayer, H. H.; Budde, K.; Klupp, J., Validation of immunological biomarkers for the pharmacodynamic monitoring of immunosuppressive drugs in humans. *Ther Drug Monit* **2007,** 29, (1), 77-86.
43. Barten, M. J.; Tarnok, A.; Garbade, J.; Bittner, H. B.; Dhein, S.; Mohr, F. W.; Gummert, J. F., Pharmacodynamics of T-cell function for monitoring immunosuppression. *Cell Prolif* **2007,** 40, (1), 50-63.
44. Millan, O.; Benitez, C.; Guillen, D.; Lopez, A.; Rimola, A.; Sanchez-Fueyo, A.; Brunet, M., Biomarkers of immunoregulatory status in stable liver transplant recipients undergoing weaning of immunosuppressive therapy. *Clin Immunol* **2010,** 137, (3), 337-46.
45. Niwa, M.; Miwa, Y.; Kuzuya, T.; Iwasaki, K.; Haneda, M.; Ueki, T.; Katayama, A.; Hiramitsu, T.; Goto, N.; Nagasaka, T.; Watarai, Y.; Uchida, K.; Nakao, A.; Kobayashi, T.,

Stimulation index for PCNA mRNA in peripheral blood as immune function monitoring after renal transplantation. *Transplantation* **2009,** 87, (9), 1411-4.
46. Boles, K. S.; Stepp, S. E.; Bennett, M.; Kumar, V.; Mathew, P. A., 2B4 (CD244) and CS1: novel members of the CD2 subset of the immunoglobulin superfamily molecules expressed on natural killer cells and other leukocytes. *Immunol Rev* **2001,** 181, 234-49.
47. Vaidya, S. V.; Stepp, S. E.; McNerney, M. E.; Lee, J. K.; Bennett, M.; Lee, K. M.; Stewart, C. L.; Kumar, V.; Mathew, P. A., Targeted disruption of the 2B4 gene in mice reveals an in vivo role of 2B4 (CD244) in the rejection of B16 melanoma cells. *J Immunol* **2005,** 174, (2), 800-7.
48. Kim, E. O.; Kim, T. J.; Kim, N.; Kim, S. T.; Kumar, V.; Lee, K. M., Homotypic cell to cell cross-talk among human natural killer cells reveals differential and overlapping roles of 2B4 and CD2. *J Biol Chem* **2010,** 285, (53), 41755-64.
49. Sinha, S. K.; Gao, N.; Guo, Y.; Yuan, D., Mechanism of induction of NK activation by 2B4 (CD244) via its cognate ligand. *J Immunol* **2010,** 185, (9), 5205-10.
50. Gray, J. X.; Haino, M.; Roth, M. J.; Maguire, J. E.; Jensen, P. N.; Yarme, A.; Stetler-Stevenson, M. A.; Siebenlist, U.; Kelly, K., CD97 is a processed, seven-transmembrane, heterodimeric receptor associated with inflammation. *J Immunol* **1996,** 157, (12), 5438-47.
51. Kop, E. N.; Matmati, M.; Pouwels, W.; Leclercq, G.; Tak, P. P.; Hamann, J., Differential expression of CD97 on human lymphocyte subsets and limited effect of CD97 antibodies on allogeneic T-cell stimulation. *Immunol Lett* **2009,** 123, (2), 160-8.
52. Haynes, B. F.; Hemler, M. E.; Mann, D. L.; Eisenbarth, G. S.; Shelhamer, J.; Mostowski, H. S.; Thomas, C. A.; Strominger, J. L.; Fauci, A. S., Characterization of a monoclonal antibody (4F2) that binds to human monocytes and to a subset of activated lymphocytes. *J Immunol* **1981,** 126, (4), 1409-14.
53. Moretta, A.; Mingari, M. C.; Haynes, B. F.; Sekaly, R. P.; Moretta, L.; Fauci, A. S., Phenotypic characterization of human cytolytic T lymphocytes in mixed lymphocyte culture. *J Exp Med* **1981,** 153, (1), 213-8.
54. Yan, Y.; Vasudevan, S.; Nguyen, H. T.; Merlin, D., Intestinal epithelial CD98: an oligomeric and multifunctional protein. *Biochim Biophys Acta* **2008,** 1780, (10), 1087-92.
55. Deves, R.; Boyd, C. A., Surface antigen CD98(4F2): not a single membrane protein, but a family of proteins with multiple functions. *J Membr Biol* **2000,** 173, (3), 165-77.
56. Warren, A. P.; Patel, K.; Miyamoto, Y.; Wygant, J. N.; Woodside, D. G.; McIntyre, B. W., Convergence between CD98 and integrin-mediated T-lymphocyte co-stimulation. *Immunology* **2000,** 99, (1), 62-8.
57. Miyamoto, Y. J.; Mitchell, J. S.; McIntyre, B. W., Physical association and functional interaction between beta1 integrin and CD98 on human T lymphocytes. *Mol Immunol* **2003,** 39, (12), 739-51.
58. Diaz, L. A., Jr.; Friedman, A. W.; He, X.; Kuick, R. D.; Hanash, S. M.; Fox, D. A., Monocyte-dependent regulation of T lymphocyte activation through CD98. *Int Immunol* **1997,** 9, (9), 1221-31.
59. Komada, H.; Imai, A.; Hattori, E.; Ito, M.; Tsumura, H.; Onoda, T.; Kuramochi, M.; Tani, M.; Yamamoto, K.; Yamane, M.; Kawano, M.; Nishio, M.; Yuasa, K.; O'Brien, M.; Yamamoto, H.; Uematsu, J.; Tsurudome, M.; Ito, Y., Possible activation of murine T lymphocyte through CD98 is independent of interleukin 2/interleukin 2 receptor system. *Biomed Res* **2006,** 27, (2), 61-7.

60. Cantoni, C.; Bottino, C.; Augugliaro, R.; Morelli, L.; Marcenaro, E.; Castriconi, R.; Vitale, M.; Pende, D.; Sivori, S.; Millo, R.; Biassoni, R.; Moretta, L.; Moretta, A., Molecular and functional characterization of IRp60, a member of the immunoglobulin superfamily that functions as an inhibitory receptor in human NK cells. *Eur J Immunol* **1999,** 29, (10), 3148-59.
61. Ju, X.; Zenke, M.; Hart, D. N.; Clark, G. J., CD300a/c regulate type I interferon and TNF-alpha secretion by human plasmacytoid dendritic cells stimulated with TLR7 and TLR9 ligands. *Blood* **2008,** 112, (4), 1184-94.
62. Clark, G. J.; Rao, M.; Ju, X.; Hart, D. N., Novel human CD4+ T lymphocyte subpopulations defined by CD300a/c molecule expression. *J Leukoc Biol* **2007,** 82, (5), 1126-35.
63. Alvarez, Y.; Tang, X.; Coligan, J. E.; Borrego, F., The CD300a (IRp60) inhibitory receptor is rapidly up-regulated on human neutrophils in response to inflammatory stimuli and modulates CD32a (FcgammaRIIa) mediated signaling. *Mol Immunol* **2008,** 45, (1), 253-8.
64. Nakahashi-Oda, C.; Tahara-Hanaoka, S.; Honda, S.; Shibuya, K.; Shibuya, A., Identification of phosphatidylserine as a ligand for the CD300a immunoreceptor. *Biochem Biophys Res Commun* **2012,** 417, (1), 646-50.
65. Deblandre, G. A.; Marinx, O. P.; Evans, S. S.; Majjaj, S.; Leo, O.; Caput, D.; Huez, G. A.; Wathelet, M. G., Expression cloning of an interferon-inducible 17-kDa membrane protein implicated in the control of cell growth. *J Biol Chem* **1995,** 270, (40), 23860-6.
66. Friedman, R. L.; Manly, S. P.; McMahon, M.; Kerr, I. M.; Stark, G. R., Transcriptional and posttranscriptional regulation of interferon-induced gene expression in human cells. *Cell* **1984,** 38, (3), 745-55.
67. Yang, G.; Xu, Y.; Chen, X.; Hu, G., IFITM1 plays an essential role in the antiproliferative action of interferon-gamma. *Oncogene* **2007,** 26, (4), 594-603.
68. Luo, B. H.; Springer, T. A., Integrin structures and conformational signaling. *Curr Opin Cell Biol* **2006,** 18, (5), 579-86.
69. Abram, C. L.; Lowell, C. A., The ins and outs of leukocyte integrin signaling. *Annu Rev Immunol* **2009,** 27, 339-62.
70. Kinashi, T., Intracellular signalling controlling integrin activation in lymphocytes. *Nat Rev Immunol* **2005,** 5, (7), 546-59.
71. Evans, R.; Patzak, I.; Svensson, L.; De Filippo, K.; Jones, K.; McDowall, A.; Hogg, N., Integrins in immunity. *J Cell Sci* **2009,** 122, (Pt 2), 215-25.
72. Gray, J. D.; Horwitz, D. A., Lymphocytes expressing type 3 complement receptors proliferate in response to interleukin 2 and are the precursors of lymphokine-activated killer cells. *J Clin Invest* **1988,** 81, (4), 1247-54.
73. Di Santo, J. P., Natural killer cell developmental pathways: a question of balance. *Annu Rev Immunol* **2006,** 24, 257-86.
74. Kim, S.; Iizuka, K.; Kang, H. S.; Dokun, A.; French, A. R.; Greco, S.; Yokoyama, W. M., In vivo developmental stages in murine natural killer cell maturation. *Nat Immunol* **2002,** 3, (6), 523-8.

Figure Captions:

Figure 1. Venn diagram depicting total number of proteins identified in naïve or IL-2-activated NK cells. Human primary NK cells were isolated from three healthy donors were cultured in medium supplemented with or without IL-2 for 16 hours. Total proteins were extracted and digested by trypsin follow by 2D LC-MS/MS analysis. 2311 proteins were identified from naïve NK cell samples, while 2413 proteins were identified in IL-2-activated NK cells. 1999 proteins were commonly identified in both conditions.

Figure 2. Linear regression between dNSAF values and known amount of protein standards BSA (a), cytochrome C (b) and myoglobin (c). Log2-transformed dNSAF values were plotted as a function of log2-transformed protein amounts in micrograms.

Figure 3. Real-time RT-PCR analysis of mRNA level of PTP1B (a), PCNA (b) and CD97 (c) in naïve NK cells and NK cells activated by IL-2 for 16 hours.

Figure 4. Gene ontology analysis of up- and down-regulated proteins. (a) Protein functional classification. 383 proteins that were found differentially expressed across all three donors could be classified into 25 categories, of which the top four are nucleic acid binding proteins (17%), hydrolase (11.3%), enzyme modulator (10.4%), and transferase (10.2%). (b) Molecular function. More than 70% of IL-2 regulated proteins have molecular function related to catalytic activities (41%) and binding (34%). (c) Biological process. IL-2 regulated proteins were found to be involved in 16 biological processes, of which the top three categories are: metabolic process

(30.4%), cell process (15.9%) and transport (11.4%) Gene ontology analysis was performed in PATHER database (http://www.pantherdb.org/).

Table 1. Novel pathways that may be involved in IL-2 signaling in human primary NK cells and names of IL-2 regulated proteins that are known to be the components of these pathways.

Ubiquitin proteasome pathway (11)
26S proteasome non-ATPase regulatory subunit 1 (PSMD1)
26S proteasome non-ATPase regulatory subunit 3 (PSMD3)
26S proteasome non-ATPase regulatory subunit 4 (PSMD4)
26S proteasome non-ATPase regulatory subunit 7 (PSMD7)
26S proteasome non-ATPase regulatory subunit 11 (PSMD11)
26S proteasome non-ATPase regulatory subunit 12 (PSMD12)
NEDD8-activating enzyme E1 catalytic subunit (UBA3)
26S protease regulatory subunit 4 (PRS4)
Ubiquitin-conjugating enzyme E2 L3 (UB2L3)
Ubiquitin carboxyl-terminal hydrolase isozyme L5 (UBP5)
SUMO-activating enzyme subunit 1 (SAE1)
Integrin signaling pathway (9)
Integrin beta-7 (ITB7)
Dual specificity mitogen-activated protein kinase kinase 1 (MP2K1)
Integrin alpha-X (ITAX)
Ras-related C3 botulinum toxin substrate 3 (RAC3)
ADP-ribosylation factor 3 (ARF3)
Rho-related GTP-binding protein RhoB (RHOB)
Actin, gamma-enteric smooth muscle (ACTH)
Proto-oncogene tyrosine-protein kinase Fyn (FYN)
Integrin alpha-D (ITAD)
PDGF signaling pathway (8)
Dual specificity mitogen-activated protein kinase kinase 1 (MP2K1)
Signal transducer and activator of transcription 1-alpha/beta (STAT1)
Signal transducer and activator of transcription 3 (STAT3)
Signal transducer and activator of transcription 4 (STAT4)
Ras-related protein Rab-11B (RB11B)
Rho GTPase-activating protein 4 (RHG04)
Rho-related GTP-binding protein RhoB (RHOB)
Ribosomal protein S6 kinase alpha-3 (KS6A3)
EGF receptor signaling pathway (7)
Dual specificity mitogen-activated protein kinase kinase 1 (MP2K1)
Signal transducer and activator of transcription 1-alpha/beta (STAT1)
Signal transducer and activator of transcription 3 (STAT3)
Signal transducer and activator of transcription 4 (STAT4)
Ras-related C3 botulinum toxin substrate 3 (RAC3)
Serine/threonine-protein phosphatase 2A catalytic subunit beta isoform (PP2AB)
Mitogen-activated protein kinase 14 (MK14)
Wnt signaling pathway (6)
Beta-arrestin-1 (ARRB1)
Serine/threonine-protein phosphatase 2A catalytic subunit beta isoform (PP2AB)
Histone deacetylase 1(HDAC1)
C-terminal-binding protein 2 (CTBP2)
Nuclear factor of activated T-cells, cytoplasmic 2 (NFAC2)
Actin, gamma-enteric smooth muscle (ACTH)

Figure 1.

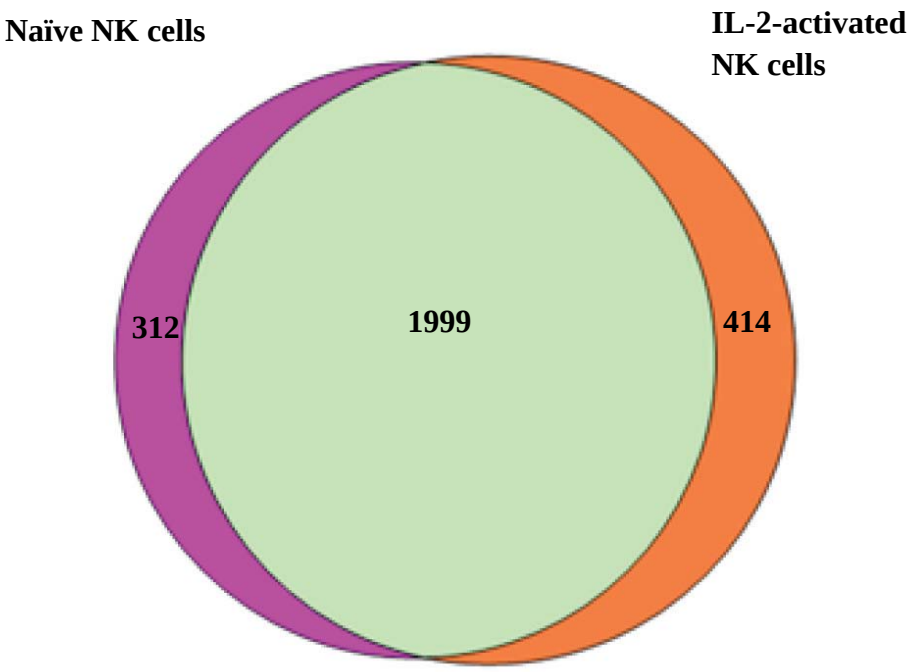

Figure 2.

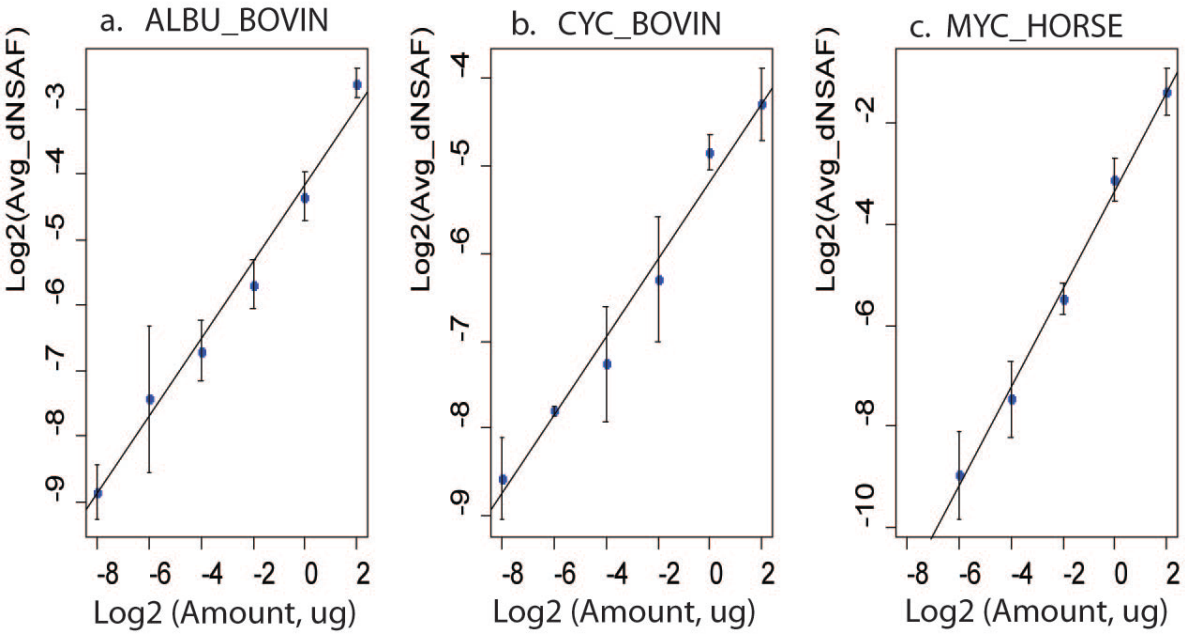
a. ALBU_BOVIN
Log2(Avg_dNSAF)
-9
-8
-7
-6
-5
-4
-3
-8 -6 -4 -2 0 2
Log2 (Amount, ug)
b. CYC_BOVIN
Log2(Avg_dNSAF)
-9
-8
-7
-6
-5
-4
-8 -6 -4 -2 0 2
Log2 (Amount, ug)
c. MYC_HORSE
Log2(Avg_dNSAF)
-10
-8
-6
-4
-2
-8 -6 -4 -2 0 2
Log2 (Amount, ug)

Figure 3.

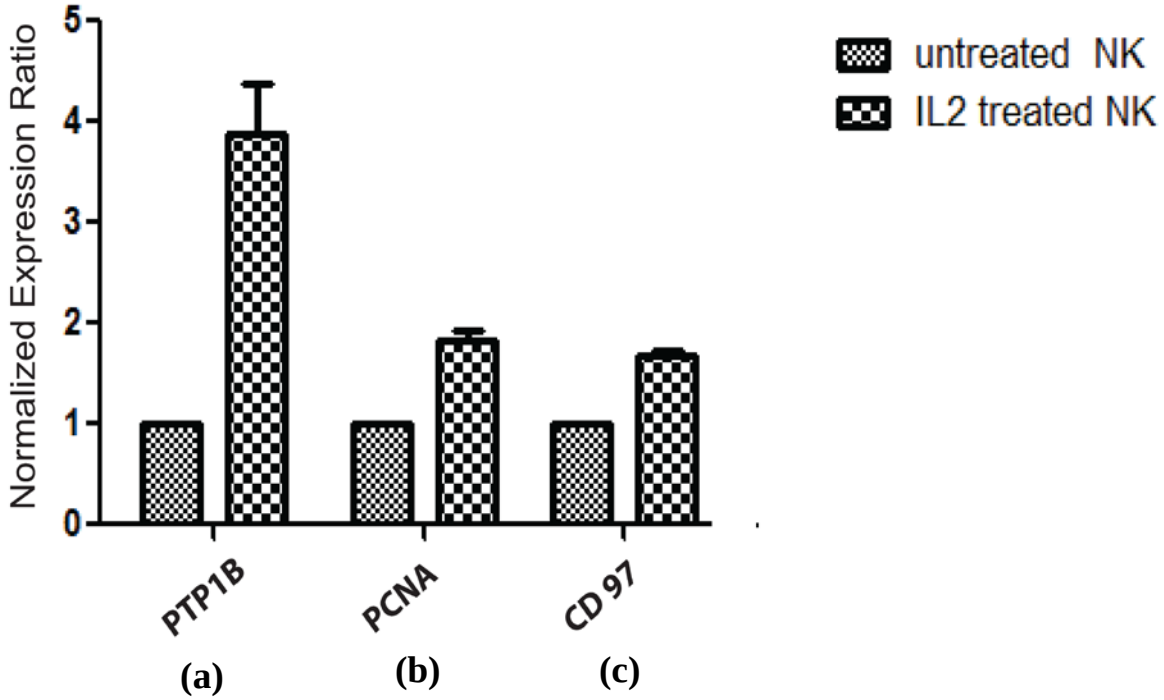
Normalized Expression Ratio
0
1
2
3
4
5
PTP1B
PCNA
CD 97
(a)
(b)
(c)
untreated NK
IL2 treated NK

Figure 4.

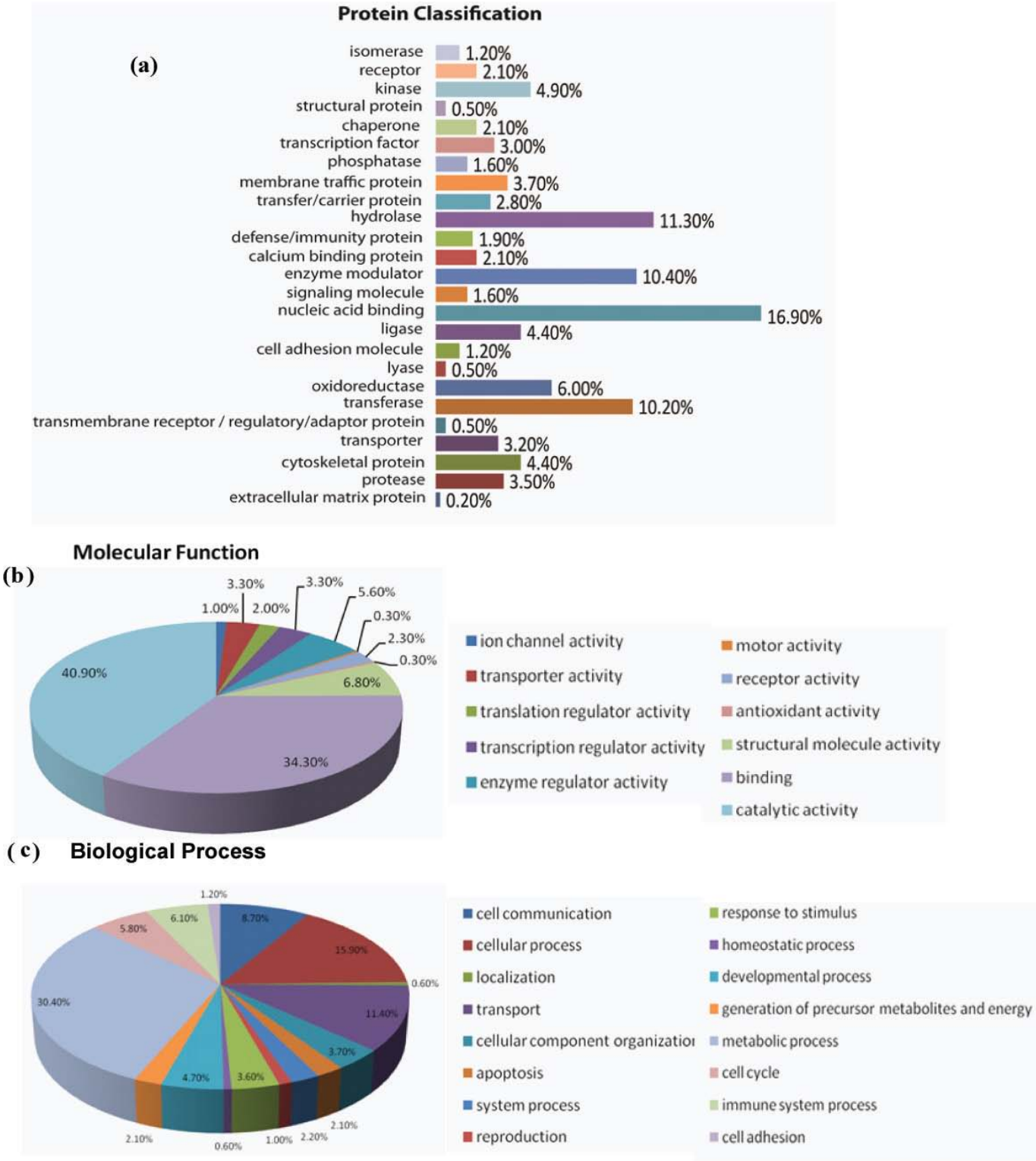
Protein Classification
(a)
isomerase 1.20%
receptor 2.10%
kinase 4.90%
structural protein 0.50%
chaperone 2.10%
transcription factor 3.00%
phosphatase 1.60%
membrane traffic protein 3.70%
transfer/carrier protein 2.80%
hydrolase 11.30%
defense/immunity protein 1.90%
calcium binding protein 2.10%
enzyme modulator 10.40%
signaling molecule 1.60%
nucleic acid binding 16.90%
ligase 4.40%
cell adhesion molecule 1.20%
lyase 0.50%
oxidoreductase 6.00%
transferase 10.20%
transmembrane receptor / regulatory/adaptor protein 0.50%
transporter 3.20%
cytoskeletal protein 4.40%
protease 3.50%
extracellular matrix protein 0.20%
Molecular Function
(b)
3.30%
3.30%
5.60%
1.00%
2.00%
0.30%
2.30%
0.30%
40.90%
6.80%
34.30%
ion channel activity
motor activity
transporter activity
receptor activity
translation regulator activity
antioxidant activity
transcription regulator activity
structural molecule activity
enzyme regulator activity
binding
catalytic activity
(c) Biological Process
1.20%
6.10%
8.70%
5.80%
15.90%
0.60%
30.40%
11.40%
3.70%
4.70%
3.60%
2.10%
2.10%
0.60%
1.00%
2.20%
cell communication
response to stimulus
cellular process
homeostatic process
localization
developmental process
transport
generation of precursor metabolites and energy
cellular component organizatio
metabolic process
apoptosis
cell cycle
system process
immune system process
reproduction
cell adhesion

Chapter 4

Comparative Secretome Analysis of Vascular Smooth Muscle Cells in Response to Smad3-Dependent TGF-β Signaling

Adapted from: "Comparative Secretome Analysis of Vascular Smooth Muscle Cells in Response to Smad3-Dependent TGF-β Signaling". Ma D, Yang C, Shi X and Li L. In preparation.

Abstract

Vascular smooth muscle cells (VSMCs) play a crucial role in cardiovascular disorders and have been used as a model system to study the pathogenesis of atherosclerosis. Transforming growth factor β (TGF-β) and its modulator, SMAD family member 3 (Smad3) play important roles in VSMC differentiation and function and are found to be critically involved in atherosclerotic process. To characterize the proteins secreted from cultured VSMCs and assess temporal changes in the secretome in response to TGF-β/Smad3 signaling, we performed LC ESI-MS/MS analysis followed by label-free quantification to identify proteins secreted into VSMC-conditioned medium before and after cells were treated with TGF-β. The use of one-dimensional LC-MS/MS resulted in identifications of 264 proteins from conditioned media. To distinguish secreted proteins from the contaminations of intracellular proteins from cell death, the protein list was subjected to analysis by SignalP and SecretomeP to yield a refined list of 169 secreted proteins. The quantitative analysis by spectral counting revealed 31 secreted proteins that were significantly up or down-regulated in response to TGF-β. The characterization of the secretome of VSMCs from this study provides new insights in vascular biology. Moreover, the TGF-β induced factors identified from the comparative analysis may provide novel targets for the investigations of the role of TGF-β in atherosclerotic process.

Introduction

According to the statistics from the World Health Organization (WHO) and past research, atherosclerosis and atherosclerosis-associated cardiovascular diseases including myocardial infarction and stroke are the leading causes of death in developed countries including the United States of America where it is estimated that vascular diseases are to be the leading cause of global morbidity and mortality by 2020-2030[1-3] . High levels of plasma lipids, in particular low-density lipoprotein (LDL) cholesterol in blood is widely considered to increase the risk to develop cardiovascular diseases[4]. Although the emergence of atherogenesis is associated with accumulation of lipids within the arterial walls, the development of atherosclerosis is best described as a consequence of chronic inflammation consisting of a series of highly specific cellular and molecular responses with the involvement of both immune cells and vascular smooth muscle cells[5, 6].

Currently, a common clinical procedure to treat coronary and peripheral atherosclerosis is angioplasty due to its high success rate and minimally invasive nature. However, the efficacy of surgical procedure is often undermined by restenosis which occurs within 3–6 months post-angioplasty mainly due to intimal hyperplasia which mimics some aspects of the atherosclerotic process[7]. The proliferation of vascular smooth muscle cells (VSMCs) plays a key role in the development of intimal hyperplasia[8]. Intimal hyperplasia is a complex process associated with abnormal migration and proliferation of vascular smooth muscle cells (VSMCs). In response to injury, VSMCs change their quiescent-contractile physiological phenotype and acquire an activated state endowed with proliferative and migratory properties, once subjected to external stimuli such as cytokines and growth factors[9]. As a consequence of their activation, VSMCs migrate to the subintimal space, proliferate, and secrete abundant amounts of extracellular matrix

(ECM), which forms the bulk of the intimal hyperplastic lesion contributing to restenosis. Transforming growth factor-β (TGF-β) is believed to be a critical factor contributing to intimal hyperplasia as it was shown to play an important role in VSMC differentiation and function[10, 11]. Recently, several studies reported that TGF-β enhances VSMC proliferation through Smad3. The up-regulation and activation of Smad3 at the time of arterial injury is mainly responsible for the stimulatory effect of TGF-β on VSMC proliferation and development of intimal plaque[12-14]. Suwanabol *et al*. reported that Smad3 acts as an intermediate between TGF-β and signaling pathways including ERK/MAPK[12] and PI3K/Akt[13] through which TGF-β stimulates VSMC proliferation. Although these findings provided evidence of the mechanism by which TGF-β enhances intimal hyperplasia, little is known about the Smad3-dependent TGF-β signaling in VSMCs. To this end, a global approach to proteomic profiling of VSMCs treated with TGF-β may serve to identify TGF-β/Smad3 induced factors that reveal previously unknown pathways and mechanisms that mediate intimal hyperplasia. Such knowledge provides potential novel targets that may be used to prevent restenosis.

Both profiling of intracellular proteome and extracellular secretome of primary culture of human arterial smooth muscle cells (SMCs) from patients undergoing coronary artery bypass surgery has been previously reported[15, 16]. The secretome typically includes the proteins of ECM as well as additional proteins shed from the cell surface[17]. The secreted proteins play important roles in both physiological and pathological processes such as cell-cell signaling, communication, and migration[18], and reflect the state of the cells at various stages of disease progression. In secretome analysis, the proteins secreted by cells into conditioned media *in vitro* are studied to better understand the mechanisms *in vivo*. Although *in vitro* conditions may be different from the *in vivo* environment, the analysis of secretome in cultured cells provides a

relatively easier and quicker manner to investigate possible biological pathways involved in these complicated cellular processes.

Previous studies demonstrated that VSMCs from injured rat aortas display elevated matrix production associated with activity of TGF-β and proposed that one of the mechanisms through which TGF-β enhances intimal hyperplasia is the production of ECM proteins including several collagens[14, 19, 20]. To elucidate the complex extracellular signaling in VSMCs in response to TGF-β that may be associated with pathogenesis of intimal hyperplasia, a comprehensive proteomic profiling of secreted proteins from VSMCs will serve an essential starting point for further investigation. Previous mass spectrometry (MS)-based secretome profiling in SMCs used 2-D gel electrophoresis coupled with MALDI-TOF for protein identification which limited the total protein identifications as well as the detection of lower abundance proteins[15, 16]. In the present work, we employed shotgun proteomics with LC-MS/MS for secretome profiling in VSMCs and our result yielded a substantially larger list of putative secreted proteins. Further quantitative analysis by spectral counting revealed 31 secreted proteins that were significantly up or down-regulated in response to TGF-β. Our analysis provides a basis for vascular biology investigations on VSMC protein changes that may lead to a better understanding of the mechanisms and factors that regulate the differentiation of VSMCs in response to TGF-β.

Experimental Methods

Materials

Urea and ammonium bicarbonate were purchased from Fisher Scientific (Fair Lawn, NJ, USA). Ammonium formate and iodoacetamide (IAM) were purchased from Sigma-Aldrich (St. Louis, MO). Dithiothreitol (DTT) and sequencing grade modified trypsin was purchased from

Promega (Madison, WI). The LC-MS grade solvents and Optima grade solvents (ACN and water) were purchased from Fisher Scientific (Fair Lawn, NJ, USA). Recombinant TGF-β was purchased from R&D Systems (Minneapolis, MN). Dulbecco's modified Eagle's medium (DMEM) and cell culture reagents were from Invitrogen (Carlsbad, CA).

Smooth Muscle Cell Culture

Rat aortic vascular SMCs were isolated from the thoracoabdominal aorta of male Sprague-Dawley rats based on a protocol described by Clowes *et al*.[21] and maintained in DMEM containing 10% FBS at 37°C with 5% CO2. Adenoviral (Ad) vectors expressing Smad3 (AdSmad3) and green fluorescent protein (GFP) (AdGFP) were constructed as previously described [22]. AdGFP was used as a control. 5 x 10^5 VSMCs were infected with adenovirus in DMEM containing 2% FBS for 4 h at 37° C followed by recovery in 10% FBS overnight. Cells were then cultured in serum free DMEM for 12 h. After wash once with serum free media, 5 ng/ml TGF-β /or control (4 µl 0.2 N HCl in 4 ml media) was added to culture dishes (counted as time 0). After 6 hours, cell culture media was collected and concentrated with 10KDa MW cut off column (Millipore, Billerica, MA). The concentration of secreted proteins was determined by BCA assay.

Proteolysis

All protein samples were denatured with 8 M urea in 25 mM ammonium bicarbonate buffer, and reduced by incubating with 50 mM DTT at 37 °C for 1 h. The reduced proteins were alkylated for 1 h in darkness with 100 mM iodoacetamide. The alkylation reaction was quenched by adding DTT to a final concentration of 50 mM. The samples were diluted to a final

concentration of 1 M urea. Trypsin was added to the sample at a 30:1 protein to trypsin mass ratio. The sample was incubated at 37 °C overnight. Digests were desalted by ZipTip® Pipette Tips (Millipore, Billerica, MA).

LC–ESI Ion Trap Mass Spectrometry and MS/MS Analysis

400 ng tryptic digests from control or TGF-β stimulated VMSCs conditioned media were analyzed using amaZon ion trap mass spectrometer (Bruker Daltonics, Germany) equipped with Waters nanoAcquity UPLC (Waters Corp., Milford, MA). For the chromatographic separation, solvent A consisted of 0.1% formic acid in water and solvent B consisted of 0.1% formic acid in ACN. 5µl of each sample was injected onto an Waters Symmetry C18 5µm 180µm x 20mm precolumn at a flow rate of 5 µl/min for 5 min at 95% A 5% B, followed by peptide separation performed on Waters BEH130 1.7 µm C18 100 µm x 100 mm analytical column using gradient from 0 to 45% solvent B at 300 nl/min over 120 min. Acquisition of precursor ions and MS/MS spectra was performed using the parameters as indicated below: Smart parameter setting (SPS) was set to 700m/z, compound stability and trap drive level were set at 100%. Dry gas temperature, 125 °C, dry gas, 4.0 L/min, capillary voltage, −1300 V, end plate offset, −500 V, MS/MS fragmentation amplitude, 1.0 V, and Smart Fragmentation set at 30–300%. Data were generated in data dependent mode with strict active exclusion set after two spectra and released after 1min. MS/MS spectra were obtained via collision induced dissociation (CID) fragmentation for the six most abundant MS ions. For MS generation the ICC target was set to 200,000, maximum accumulation time, 50.00ms, one spectrometric average, rolling average, 2, acquisition range of 300–1500 m/z, and scan speed (enhanced resolution) of 8100 m/z s^{-1}. For MS/MS generation the ICC target was set to 300,000, maximum accumulation time, 50.00 ms,

two spectrometric averages, acquisition range of 100–2000 m/z, and scan speed (Ultrascan) of 32,000 m/z per second.

Database Search

MS data were processed with DataAnalysis (Version 4.0, Bruker Daltonics Bremen, Germany). Deviations in parameters from the default Protein Analysis in DataAnalysis were as follows: intensity threshold 1000, maximum number of compounds $1E^9$, and retention time window 0.001 minutes. These parameter changes were required for spectral counting to prevent loss of spectra. Identification of peptides were performed using Mascot[23] (Version 2.4, Matrix Science, London, U.K.). Database searching was performed against a forward and reversed concatenated SwissProt *Rattus rattus* database. Mascot search parameters were as follows: Allowed missed cleavages, 2; enzyme, trypsin; fixed modification, carboxymethylation (C); variable modifications, oxidation (M); peptide tolerance, ±1.2 Da; MS/MS tolerance, ±0.5 Da; instrument type, ESI-Trap. Data was then transformed into .DAT file formats and transferred to ProteoIQ (NuSep, Bogart, GA). False positive analyses were calculated using ProteoIQ and set at 1%.

Result and Discussion

VSMCs with Smad3 Overexpression

The array of effects of TGF-β on cultured VSMCs may be related to differential signaling through numerous downstream pathways. Abundant evidence from previous studies has shown that TGF-β has both stimulatory effects on VSMC fibronectin synthesis and inhibitory effects on

VSMC proliferation and migration[11, 19]. Several recent studies reported that the up-regulation and activation of Smad3 at the time of arterial injury is mainly responsible for the stimulatory effect of TGF-β on VSMC proliferation and development of intimal plaque[12-14]. Since TGF-β enhances SMC proliferation only in the presence of elevated levels of Smad3, we infected cultured VSMCs with adenovirus-expressing Smad3 (AdSmad3) or control (AdGFP) followed by stimulation with or without TGF-β for 6 h. The overexpression of Smad3 enhanced the effect of Smad3-dependent TGF-β signaling, thus simplify the complex and contradictory effects of TGF-β VSMC function.

Given the biological uniformity of the cell cultures as opposed to individual organisms, secretome samples from three replicates of equal amounts of VSMC/AdGFP or VSMC/AdSmad3 cultured in supplement with or without TGF-β were pooled. To our knowledge, there was no evidence showing cell culture-to-cell culture variability from previous studies where immunological and biochemical approaches were utilized to characterize and quantify proteins in VSMCs[12-14]. Although the pooling strategy was not ideal for statistical purpose, it significantly reduces the time and complexity for MS and data analysis without compromising the accuracy of quantitative analysis.

Protein Identification and Data Analysis.

In total, 213 proteins were identified from the conditioned media of control VSMC/AdGFP samples, while 190 proteins were identified from that of TGF-β treated VSMC/AdSmad3 samples. Figure 1 shows the Venn Diagrams of the numbers of proteins identified from the conditioned media from VSMC/AdGFP cultures or VSMC/AdSmad3 cultures, with 139 proteins identified in both cells cultures where each sample was analyzed in

triplicate. The reproducibility of each replicate was demonstrated by the similarity of the base peak chromatogram from the LC-MS/MS analysis of each technical replicate (Figure 2). Figure 3 shows a representative tandem MS/MS spectrum of a tryptic peptide (IQAIELEDLLR) from biglycan. Given that protein identification in secretome analysis is often interfered by the presence of intracellular proteins in culture media mainly due to cell death. To obtain a high quality dataset, our protein list was refined by SignalP/SecretomeP which yielded 169 proteins that are known to be secreted or predicted to be secreted proteins. Table 1 included these proteins which were predicted to have signal peptide by SignalP or had a significant SecretomeP score (0.5 or higher).

Three technical replicates of LC-MS/MS analysis of either VSMC/AdGFP or VSMC/AdSmad3 samples were combined together using ProteoIQ. A spectral counting approach was employed in ProteoIQ for relative quantification where peptide spectral counts were added up for each protein and subjected to dNSAF analysis using ProteoIQ internal algorithms. Details for this method can be found elsewhere[24, 25]. Briefly, peptide spectral counts are summed per protein (SpC) based on unique peptides and a weighted distribution of any shared peptides with homologous proteins. T-tests were used to identify significant changes in protein expression. In total, 185 proteins identified with high confidence were selected for quantification by spectral counting, and 51 proteins showed more than 1.5-fold increase or decrease, 31 of which were known or predicted to be secreted proteins by SignalP/SecretomeP.

Functional Annotation of TGF-β Induced Secreted Proteins

In present work, 15 secreted proteins identified in VSMC-conditioned media were found to be up-regulated following TGF-β stimulation (Table 2). All TGF-β induced proteins were

searched against the Swiss-Prot/TrEMBL annotated database using the online ExPASy interface (http://www.expasy.ch/) to confirm that they are extracellular proteins. Functional annotation analysis using public bioinformatics resources and literature search revealed that most TGF-β induced proteins identified in present work play important roles in cell proliferation, migration and differentiation. Based on the evidence from previous studies, some of the proteins may prove to be critical factors that are involved in the development of atherosclerotic process in response to TGF-β.

Insulin-like growth factor binding protein 7 (IGFBP-7) is a 30 kDa secretory glycoprotein which belongs to insulin-like growth factor binding protein (IGFBP) superfamily[26]. Previous *in vitro* analysis indicated that the expression of IGFBP-7 in human fibroblasts was enhanced by TGF-β and that IGFBP-7 significantly stimulated the proliferation and migration of fibroblasts[27]. However, no evidence so far has directly linked IGFBP-7 to TGF-β signaling in VSMCs. Our results showed that TGF-β stimulates the expression of IGFBP-7 in VSMCs thus further investigation of the role of IGFBP-7 in TGF-β stimulated VSMCs may lead to better understanding of TGF-β/Smad3 signaling pathways.

Two of the TGF-β induced proteins**,** protein disulfide-isomerase A3 (PDI-A3) and protein disulfide-isomerase A6 (PDI-A6), belong to the protein disulfide isomerase family, which encompasses several highly divergent proteins that participate in maturation of secretory proteins in the endoplasmic reticulum[28]. Functioning as chaperones, PDI-family proteins are involved in the proper folding and in the formation and reshuffling of the disulfide bridges of the proteins synthesized in the rough ER. However, proteins of the PDI-family have also been found on the cell surface or as secreted proteins. Results from previous studies confirmed the presence of chaperones such as PDI-A3 and HSP-60 on cell surface suggesting that their phosphorylation

might be responsible for reorientation of receptor complexes as well as key molecules in the process of cell activation[29, 30]. Furthermore, it has been shown that the disulfide exchange function of PDI-A3 is required for cell mediated adhesion by integrins[31]. In a recent study, the phosphorylation of PDI-A3 was shown to be up-regulated in VSMCs activated by recombinant human platelet derived growth factor-BB (PDGF-BB), indicating PDI-A3 is a factor downstream of the receptor signaling cascade[32]. Given the similar effect that TGF-β may have in VSMCs, it is highly likely PDI family proteins are key factors involved in TGF-β dependent VSMC activation.

Ceruloplasmin is a 132-kDa plasma glycoprotein that contains seven copper atoms per molecule and in healthy adults accounts for up to 95% of the total circulating copper[33]. A correlation between serum ceruloplasmin and cardiovascular disease has been demonstrated by previous studies where elevated serum ceruloplasmin level has been observed in patients with atherosclerosis and other cardiovascular diseases[33-35]. Biochemical studies have shown that ceruloplasmin is a potent catalyst of LDL oxidation in vitro and it was suggested that serum ceruloplasmin may be an important risk factor predicting myocardial infarction and cardiovascular disease[36, 37]. However, very little is known about the signaling pathway(s) that regulate ceruloplasmin transcription and expression in VSMCs. Pro-inflammatory cytokines including interleukin (IL)-1, IL-6, tumor necrosis factor (TNF)-α and interferon (IFN)-γ were known to stimulate ceruloplasmin production in hepatic cells[38, 39], but so far there is no evidence that indicates the production and secretion of ceruloplasmin is associated with TGF-β. Given the important roles of ceruloplasmin in LDL oxidation in vascular cells, the present work suggests induction of ceruloplasmin in VSMCs by TGF-β, therefore, it is interesting to speculate that

VSMC-derived ceruloplasmin may be responsible for the potentiation of atherosclerotic process by TGF-β.

Two extracelluar proteoglycans, vesican and biglycan, were up-regulated in response to TGF-β. Both versican and biglycan are believed to play roles in the formation of atherosclerosis [40, 41]. Previous studies showed intimal proteoglycans were up-regulated at sites of intimal hyperplasia suggesting that they have direct roles in the regulation of vascular cell growth and the development of atherosclerosis by binding and retaining apolipoprotein-B containing lipoproteins in the vessel wall [40, 42-44]. It is known that several cytokines including TGF-β can regulate versican synthesis, and the result in our present analysis is in agreement with that of previous study where the expression of vesicant was found to be stimulated by TGF-β [45].

Conclusions

The secretome of VSMC was characterized by MS-based shotgun proteomics. In total, 169 putative VSMC secreted proteins were identified in the conditioned media of VSMC culture and TGF-β stimulated VSMC culture by a combination of LC-MS/MS techniques and bioinformatics analysis. A label-free quantification analysis via spectral counting revealed a list of 31 secreted proteins in that are up or down-regulated following Smad3-dependent TGF-β stimulation. Functional annotation of TGF-β/Smad3 induced proteins revealed several proteins with important functions related to TGF-β/Smad3 signaling that could potentially serve as the targets for future investigation of the mechanism through which TGF-β enhances intimal hyperplasia in VSMCs. Altogether, our investigation sheds light on the intricate role of TGF-β signaling in the atherosclerotic process.

References

1. Mathers, C. D.; Loncar, D., Projections of global mortality and burden of disease from 2002 to 2030. *PLoS Med* **2006,** 3, (11), e442.
2. Murray, C. J.; Lopez, A. D., Alternative projections of mortality and disability by cause 1990-2020: Global Burden of Disease Study. *Lancet* **1997,** 349, (9064), 1498-504.
3. WHO publishes definitive atlas on global heart disease and stroke epidemic. *Indian J Med Sci* **2004,** 58, (9), 405-6.
4. Greenland, P.; Knoll, M. D.; Stamler, J.; Neaton, J. D.; Dyer, A. R.; Garside, D. B.; Wilson, P. W., Major risk factors as antecedents of fatal and nonfatal coronary heart disease events. *JAMA* **2003,** 290, (7), 891-7.
5. Perrins, C. J.; Bobryshev, Y. V., Current advances in understanding of immunopathology of atherosclerosis. *Virchows Arch* **2011,** 458, (2), 117-23.
6. Ross, R.; Glomset, J. A., Atherosclerosis and the arterial smooth muscle cell: Proliferation of smooth muscle is a key event in the genesis of the lesions of atherosclerosis. *Science* **1973,** 180, (4093), 1332-9.
7. Davies, M. G.; Hagen, P. O., Pathobiology of intimal hyperplasia. *Br J Surg* **1994,** 81, (9), 1254-69.
8. Rzucidlo, E. M.; Martin, K. A.; Powell, R. J., Regulation of vascular smooth muscle cell differentiation. *J Vasc Surg* **2007,** 45 Suppl A, A25-32.
9. Newby, A. C.; Zaltsman, A. B., Molecular mechanisms in intimal hyperplasia. *J Pathol* **2000,** 190, (3), 300-9.
10. McCaffrey, T. A.; Consigli, S.; Du, B.; Falcone, D. J.; Sanborn, T. A.; Spokojny, A. M.; Bush, H. L., Jr., Decreased type II/type I TGF-beta receptor ratio in cells derived from human atherosclerotic lesions. Conversion from an antiproliferative to profibrotic response to TGF-beta1. *J Clin Invest* **1995,** 96, (6), 2667-75.
11. Mii, S.; Ware, J. A.; Kent, K. C., Transforming growth factor-beta inhibits human vascular smooth muscle cell growth and migration. *Surgery* **1993,** 114, (2), 464-70.
12. Suwanabol, P. A.; Seedial, S. M.; Shi, X.; Zhang, F.; Yamanouchi, D.; Roenneburg, D.; Liu, B.; Kent, K. C., Transforming growth factor-beta increases vascular smooth muscle cell proliferation through the Smad3 and extracellular signal-regulated kinase mitogen-activated protein kinases pathways. *J Vasc Surg* **2012,** 56, (2), 446-54.
13. Suwanabol, P. A.; Seedial, S. M.; Zhang, F.; Shi, X.; Si, Y.; Liu, B.; Kent, K. C., TGF-beta and Smad3 modulate PI3K/Akt signaling pathway in vascular smooth muscle cells. *Am J Physiol Heart Circ Physiol* **2012,** 302, (11), H2211-9.
14. Tsai, S.; Hollenbeck, S. T.; Ryer, E. J.; Edlin, R.; Yamanouchi, D.; Kundi, R.; Wang, C.; Liu, B.; Kent, K. C., TGF-beta through Smad3 signaling stimulates vascular smooth muscle cell proliferation and neointimal formation. *Am J Physiol Heart Circ Physiol* **2009,** 297, (2), H540-9.
15. Dupont, A.; Pinet, F., The proteome and secretome of human arterial smooth muscle cell. *Methods Mol Biol* **2007,** 357, 225-33.
16. Dupont, A.; Corseaux, D.; Dekeyzer, O.; Drobecq, H.; Guihot, A. L.; Susen, S.; Vincentelli, A.; Amouyel, P.; Jude, B.; Pinet, F., The proteome and secretome of human arterial smooth muscle cells. *Proteomics* **2005,** 5, (2), 585-96.
17. Makridakis, M.; Vlahou, A., Secretome proteomics for discovery of cancer biomarkers. *J Proteomics* **2010,** 73, (12), 2291-305.
18. Doroudgar, S.; Glembotski, C. C., The cardiokine story unfolds: ischemic stress-induced protein secretion in the heart. *Trends Mol Med* **2011,** 17, (4), 207-14.
19. Rasmussen, L. M.; Wolf, Y. G.; Ruoslahti, E., Vascular smooth muscle cells from injured rat aortas display elevated matrix production associated with transforming growth factor-beta activity. *Am J Pathol* **1995,** 147, (4), 1041-8.

20. Nabel, E. G.; Shum, L.; Pompili, V. J.; Yang, Z. Y.; San, H.; Shu, H. B.; Liptay, S.; Gold, L.; Gordon, D.; Derynck, R.; et al., Direct transfer of transforming growth factor beta 1 gene into arteries stimulates fibrocellular hyperplasia. *Proc Natl Acad Sci U S A* **1993,** 90, (22), 10759-63.
21. Clowes, M. M.; Lynch, C. M.; Miller, A. D.; Miller, D. G.; Osborne, W. R.; Clowes, A. W., Long-term biological response of injured rat carotid artery seeded with smooth muscle cells expressing retrovirally introduced human genes. *J Clin Invest* **1994,** 93, (2), 644-51.
22. Zhang, F.; Tsai, S.; Kato, K.; Yamanouchi, D.; Wang, C.; Rafii, S.; Liu, B.; Kent, K. C., Transforming growth factor-beta promotes recruitment of bone marrow cells and bone marrow-derived mesenchymal stem cells through stimulation of MCP-1 production in vascular smooth muscle cells. *J Biol Chem* **2009,** 284, (26), 17564-74.
23. Perkins, D. N.; Pappin, D. J.; Creasy, D. M.; Cottrell, J. S., Probability-based protein identification by searching sequence databases using mass spectrometry data. *Electrophoresis* **1999,** 20, (18), 3551-67.
24. Zybailov, B.; Mosley, A. L.; Sardiu, M. E.; Coleman, M. K.; Florens, L.; Washburn, M. P., Statistical analysis of membrane proteome expression changes in Saccharomyces cerevisiae. *J Proteome Res* **2006,** 5, (9), 2339-47.
25. Zhang, Y.; Wen, Z.; Washburn, M. P.; Florens, L., Refinements to label free proteome quantitation: how to deal with peptides shared by multiple proteins. *Anal Chem* **2010,** 82, (6), 2272-81.
26. Oh, Y.; Nagalla, S. R.; Yamanaka, Y.; Kim, H. S.; Wilson, E.; Rosenfeld, R. G., Synthesis and characterization of insulin-like growth factor-binding protein (IGFBP)-7. Recombinant human mac25 protein specifically binds IGF-I and -II. *J Biol Chem* **1996,** 271, (48), 30322-5.
27. Komiya, E.; Furuya, M.; Watanabe, N.; Miyagi, Y.; Higashi, S.; Miyazaki, K., Elevated expression of angiomodulin (AGM/IGFBP-rP1) in tumor stroma and its roles in fibroblast activation. *Cancer Sci* **2012,** 103, (4), 691-9.
28. Ferrari, D. M.; Soling, H. D., The protein disulphide-isomerase family: unravelling a string of folds. *Biochem J* **1999,** 339 (Pt 1), 1-10.
29. Turano, C.; Coppari, S.; Altieri, F.; Ferraro, A., Proteins of the PDI family: unpredicted non-ER locations and functions. *J Cell Physiol* **2002,** 193, (2), 154-63.
30. Goplen, D.; Wang, J.; Enger, P. O.; Tysnes, B. B.; Terzis, A. J.; Laerum, O. D.; Bjerkvig, R., Protein disulfide isomerase expression is related to the invasive properties of malignant glioma. *Cancer Res* **2006,** 66, (20), 9895-902.
31. Lahav, J.; Wijnen, E. M.; Hess, O.; Hamaia, S. W.; Griffiths, D.; Makris, M.; Knight, C. G.; Essex, D. W.; Farndale, R. W., Enzymatically catalyzed disulfide exchange is required for platelet adhesion to collagen via integrin alpha2beta1. *Blood* **2003,** 102, (6), 2085-92.
32. Lande, C.; Boccardi, C.; Citti, L.; Mercatanti, A.; Rizzo, M.; Rocchiccioli, S.; Tedeschi, L.; Trivella, M. G.; Cecchettini, A., Ribozyme-mediated gene knock down strategy to dissect the consequences of PDGF stimulation in vascular smooth muscle cells. *BMC Res Notes* **2012,** 5, 268.
33. Fox, P. L.; Mukhopadhyay, C.; Ehrenwald, E., Structure, oxidant activity, and cardiovascular mechanisms of human ceruloplasmin. *Life Sci* **1995,** 56, (21), 1749-58.
34. Adelstein, S. J.; Coombs, T. L.; Vallee, B. L., Metalloenzymes and myocardial infarction. I. The relation between serum copper and ceruloplasmin and its catalytic activity. *N Engl J Med* **1956,** 255, (3), 105-9.
35. Salonen, J. T.; Salonen, R.; Korpela, H.; Suntioinen, S.; Tuomilehto, J., Serum copper and the risk of acute myocardial infarction: a prospective population study in men in eastern Finland. *Am J Epidemiol* **1991,** 134, (3), 268-76.
36. Mukhopadhyay, C. K.; Ehrenwald, E.; Fox, P. L., Ceruloplasmin enhances smooth muscle cell- and endothelial cell-mediated low density lipoprotein oxidation by a superoxide-dependent mechanism. *J Biol Chem* **1996,** 271, (25), 14773-8.
37. Manttari, M.; Manninen, V.; Huttunen, J. K.; Palosuo, T.; Ehnholm, C.; Heinonen, O. P.; Frick, M. H., Serum ferritin and ceruloplasmin as coronary risk factors. *Eur Heart J* **1994,** 15, (12), 1599-603.

38. Ramadori, G.; Van Damme, J.; Rieder, H.; Meyer zum Buschenfelde, K. H., Interleukin 6, the third mediator of acute-phase reaction, modulates hepatic protein synthesis in human and mouse. Comparison with interleukin 1 beta and tumor necrosis factor-alpha. *Eur J Immunol* **1988,** 18, (8), 1259-64.
39. Mazumder, B.; Mukhopadhyay, C. K.; Prok, A.; Cathcart, M. K.; Fox, P. L., Induction of ceruloplasmin synthesis by IFN-gamma in human monocytic cells. *J Immunol* **1997,** 159, (4), 1938-44.
40. Wight, T. N.; Merrilees, M. J., Proteoglycans in atherosclerosis and restenosis: key roles for versican. *Circ Res* **2004,** 94, (9), 1158-67.
41. O'Brien, K. D.; Olin, K. L.; Alpers, C. E.; Chiu, W.; Ferguson, M.; Hudkins, K.; Wight, T. N.; Chait, A., Comparison of apolipoprotein and proteoglycan deposits in human coronary atherosclerotic plaques: colocalization of biglycan with apolipoproteins. *Circulation* **1998,** 98, (6), 519-27.
42. Williams, K. J., Arterial wall chondroitin sulfate proteoglycans: diverse molecules with distinct roles in lipoprotein retention and atherogenesis. *Curr Opin Lipidol* **2001,** 12, (5), 477-87.
43. Camejo, G.; Hurt-Camejo, E.; Wiklund, O.; Bondjers, G., Association of apo B lipoproteins with arterial proteoglycans: pathological significance and molecular basis. *Atherosclerosis* **1998,** 139, (2), 205-22.
44. Williams, K. J.; Tabas, I., The response-to-retention hypothesis of early atherogenesis. *Arterioscler Thromb Vasc Biol* **1995,** 15, (5), 551-61.
45. Schonherr, E.; Jarvelainen, H. T.; Sandell, L. J.; Wight, T. N., Effects of platelet-derived growth factor and transforming growth factor-beta 1 on the synthesis of a large versican-like chondroitin sulfate proteoglycan by arterial smooth muscle cells. *J Biol Chem* **1991,** 266, (26), 17640-7.

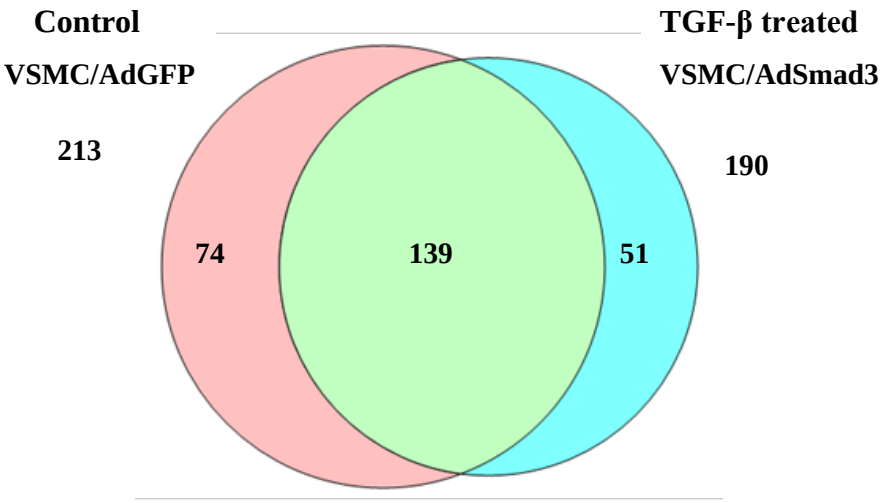

Figure 1. Venn diagram of the numbers of proteins identified by LC-MS/MS from VSMC/AdGFP (control) conditioned media or TGF-β stimulated VSMC/AdSmad3 conditioned media. 139 proteins were identified in the conditioned media of both cell cultures.

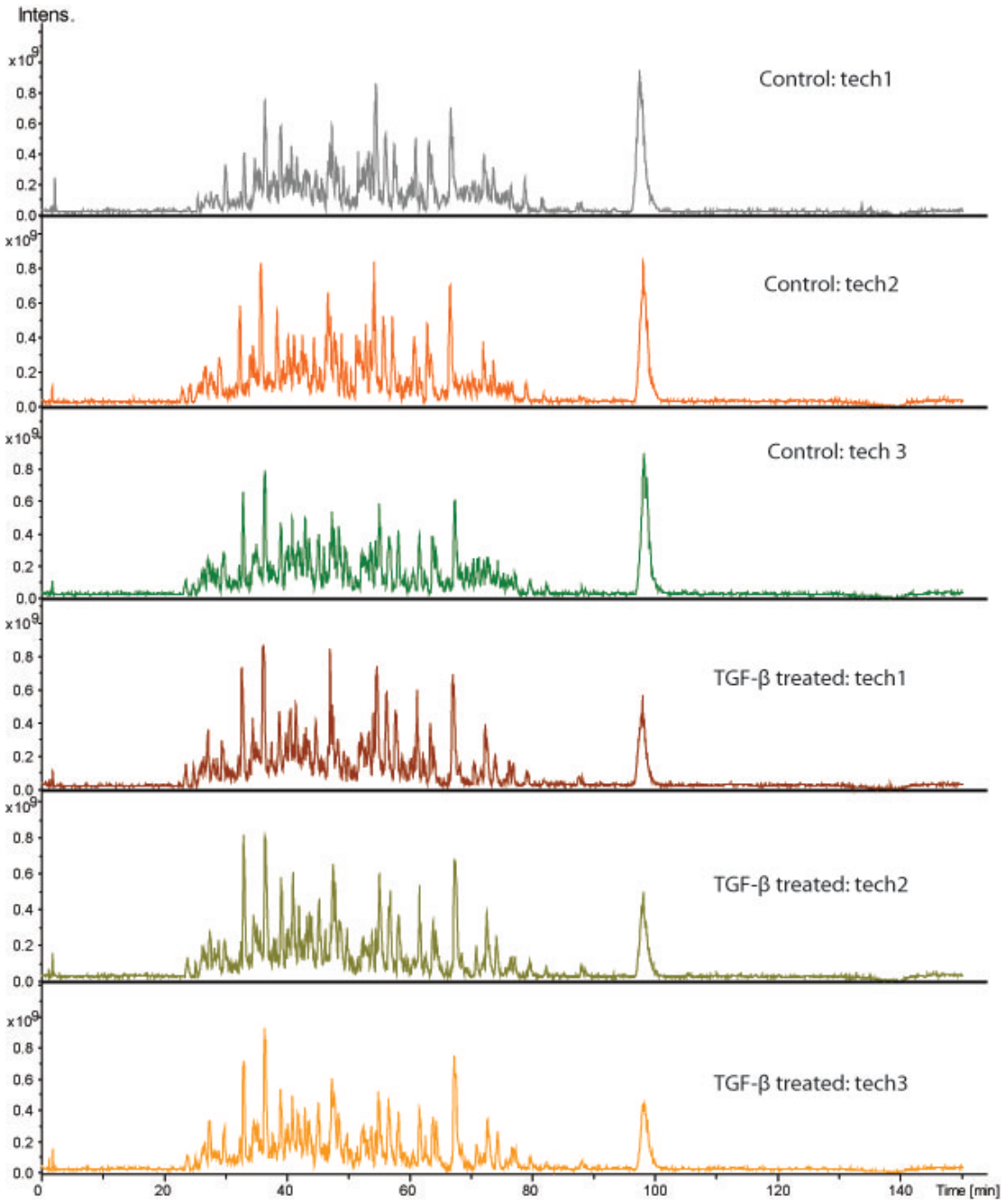

Figure 2. Base peak chromatograms from three technical replicates of LC-MS/MS of tryptic digests of proteins in VSMC conditioned media.

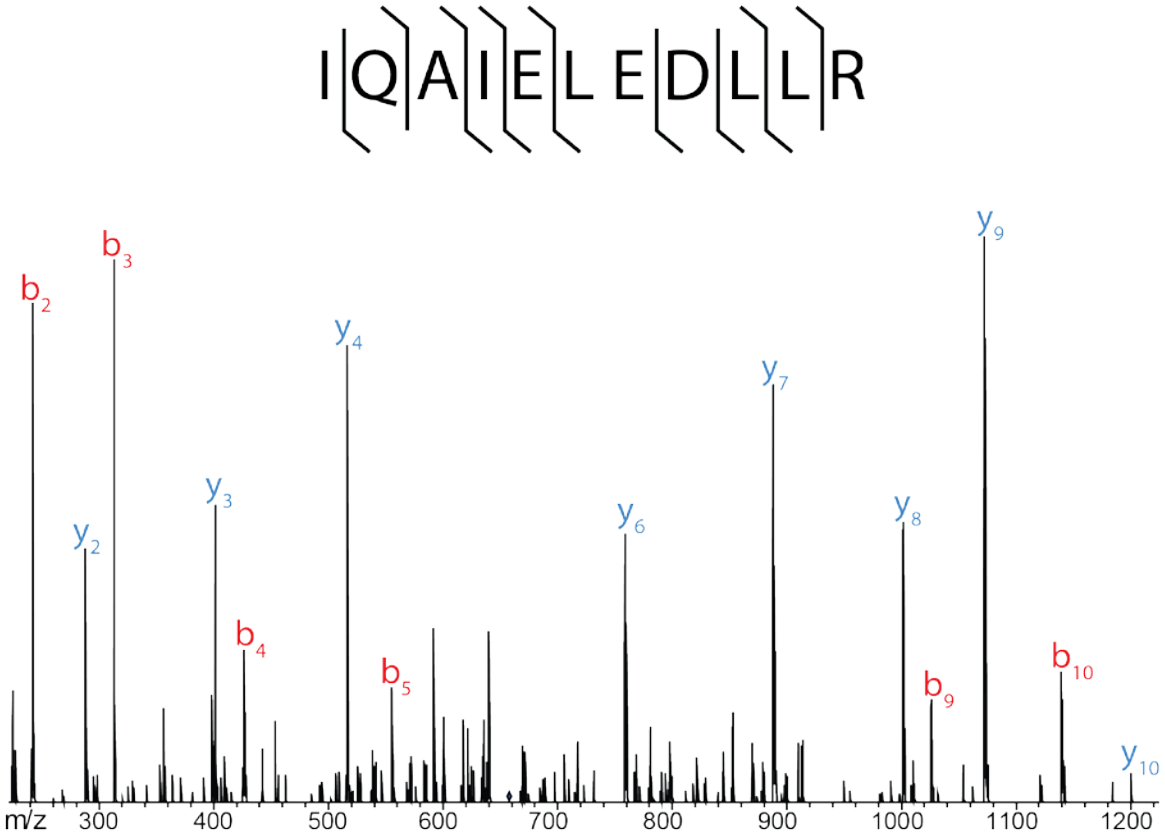

Protein Name: Biglycan OS=Rattus norvegicus

Accession: P47853

Parent m/z: 656.8, 2+

Figure 3. A representative tandem MS/MS profile of the tryptic peptide IQAIELEDLLR from biglycan. MS/MS spectrum is from TGF-β treated sample with an elution at 68.1 minutes.

Table 1. Secreted proteins identified by LC-MS/MS and SecretomeP/SignalP*

Sequence ID	Protein Names	SecP	signal peptide
F1LWQ3	Follistatin-related protein 1 (Fragment)	0.479	y
P25113	Phosphoglycerate mutase 1	0.408	y
D3ZY72	Nucleophosmin	0.649	y
O35814	Stress-induced-phosphoprotein 1	0.44	y
B6DYQ7	Glutathione S-transferase pi	0.406	y
B5DF91	ELAV (Embryonic lethal, abnormal vision, Drosophila)-like 1 (Hu antigen R)	0.409	y
P50503	Hsc70-interacting protein	0.759	y
A1A5L2	Pgm1 protein (Fragment)	0.404	y
Q64599	Hemiferrin	0.733	y
G3V6A4	Heterogeneous nuclear ribonucleoprotein D, isoform CRA_b	0.402	y
P00787	Cathepsin B	0.811	y
D3ZXX2	Protein Flna	0.447	y
Q6P7Q4	Lactoylglutathione lyase	0.388	y
P45592	Cofilin-1	0.628	y
O35264	Platelet-activating factor acetylhydrolase IB subunit beta	0.458	y
O35760	Isopentenyl-diphosphate Delta-isomerase 1	0.386	y
P14841	Cystatin-C	0.938	y
D3ZFC3	Versican core protein	0.477	y
Q6TXF3	LRRGT00046	0.382	y
F1LRG5	Galectin-1	0.376	y
P27605	Hypoxanthine-guanine phosphoribosyltransferase	0.555	y
D4A2L0	Protein Myl6b	0.417	y
P60711	Actin, cytoplasmic 1	0.498	y
P97552	Laminin gamma1 (Fragment)	0.473	y
P31000	Vimentin	0.601	y
G3V900	Fructose-bisphosphate aldolase	0.498	y
D4A5R7	Histidine triad nucleotide-binding protein 1	0.463	y
Q6DGG0	Peptidyl-prolyl cis-trans isomerase D	0.363	y
F1LST1	Anastellin	0.359	y
F1LTJ5	Uncharacterized protein (Fragment)	0.431	y
Q6IN42	Grn protein	0.614	y
Q5XI73	Rho GDP-dissociation inhibitor 1	0.427	y
P16636	Protein-lysine 6-oxidase	0.586	y
Q5PPG2	Legumain	0.734	y
B5DFD8	Protein Sh3bgrl	0.322	y
Q9R063	Peroxiredoxin-5, mitochondrial	0.557	y
P31044	Phosphatidylethanolamine-binding protein 1	0.528	y
P04785	Protein disulfide-isomerase	0.738	y
Q6AYS3	Protective protein for beta-galactosidase	0.809	y

Sequence ID	Protein Names	SecP	signal peptide
D3ZJM9	Glutathione S-transferase omega-1	0.493	y
Q6P6V0	Glucose-6-phosphate isomerase	0.494	y
D3ZS68	Protein Pcbp1	0.549	y
P62804	Histone H4	0.408	y
B2RYX0	Naca protein	0.301	y
P61983	14-3-3 protein gamma	0.29	y
B2GUZ5	F-actin-capping protein subunit alpha-1	0.48	y
Q5RJM3	Insulin-like growth factor binding protein 7	0.622	y
F1M6C2	Elongation factor 1-alpha (Fragment)	0.257	y
D3ZR51	Chloride intracellular channel protein 1	0.414	y
Q499P2	Leukotriene A-4 hydrolase	0.487	y
E9PTI5	Uncharacterized protein	0.177	y
P80254	D-dopachrome decarboxylase	0.456	y
D4ADF5	Protein Pdcd5	0.605	y
G3V8C3	Uncharacterized protein	0.6	y
F1LP73	Uncharacterized protein	0.17	y
P35704	Peroxiredoxin-2	0.562	y
D3ZC88	Elongation factor 1-alpha	0.155	y
A2RUV9	Adipocyte enhancer-binding protein 1	0.149	y
B0BMV1	Set protein	0.115	y
Q6P7S0	Pyruvate kinase	0.422	y
P41562	Isocitrate dehydrogenase [NADP] cytoplasmic	0.573	y
F1M0B2	Protein LOC683295 (Fragment)	0.113	y
P42123	L-lactate dehydrogenase B chain	0.568	y
D3ZSL2	Protein LOC685045	0.896	y
F1LP34	Acidic leucine-rich nuclear phosphoprotein 32 family member B (Fragment)	0.107	y
O88767	Protein DJ-1	0.537	y
D4A315	Protein LOC680058	0.543	y
D3ZGP8	Cathepsin D 34 kDa heavy chain	0.702	y
Q62812	Myosin-9	0.091	y
F1M335	Uncharacterized protein (Fragment)	0.434	y
D3ZPA9	Protein Ctsa	0.729	y
P02454	Collagen alpha-1(I) chain	0.155	y
P02466	Collagen alpha-1(I) chain	0.259	y
P13941	Collagen alpha-1(III) chain	0.259	y
P11883	Aldehyde dehydrogenase, dimeric NADP-preferring	0.537	-
O70598	Collagen alpha 2 type V (Fragment)	0.5	
P63029	Translationally-controlled tumor protein	0.527	-
F8WFP3	Glyceraldehyde-3-phosphate dehydrogenase	0.875	-

Sequence ID	Protein Names	SecP	signal peptide
D4A3L9	Uncharacterized protein	0.843	-
Q63413	Spliceosome RNA helicase Ddx39b	0.513	-
Q63280	Keratin K5 (Fragment)	0.832	-
F1LPC7	Hepatoma-derived growth factor	0.753	-
P18331	Inhibin beta A chain	0.812	-
D3ZG25	Uncharacterized protein	0.632	-
P85971	6-phosphogluconolactonase	0.732	-
D3ZUH7	Uncharacterized protein	0.72	-
Q6LDS4	Superoxide dismutase [Cu-Zn]	0.704	-
F1M5E1	Uncharacterized protein (Fragment)	0.655	-
B3DM95	Parathymosin	0.679	-
F1M2K3	Uncharacterized protein (Fragment)	0.846	-
Q9QX80	CArG-binding factor A	0.574	-
F1M2L5	L-lactate dehydrogenase (Fragment)	0.616	-
P00507	Aspartate aminotransferase, mitochondrial	0.509	-
B5DEN4	L-lactate dehydrogenase	0.575	-
O08628	Procollagen C-endopeptidase enhancer 1	0.548	-
F1LYQ0	Protein RGD1563581 (Fragment)	0.583	-
Q80U96	Exportin-1	0.615	-
Q66HD0	Endoplasmin	0.525	-
F1M2K7	Enolase (Fragment)	0.677	-
A1Z0K8	Beta-actin (Fragment)	0.569	-
P10760	Adenosylhomocysteinase	0.512	-
G3V613	Prolyl endopeptidase	0.552	-
Q63716	Peroxiredoxin-1	0.598	-
Q9R0J8	Legumain	0.718	-
Q810F4	Protein FAM3C	0.821	-
P62963	Profilin-1	0.56	-
B2RZ27	Protein Sh3bgrl3	0.758	-
Q6P6T6	Cathepsin D	0.762	-
Q9ERD1	Clusterin (Fragment)	0.617	-
F1M390	Uncharacterized protein (Fragment)	0.564	-
P52296	Importin subunit beta-1	0.597	-
P08699	Galectin-3	0.78	-
D3ZW08	Adenylosuccinate lyase (Predicted)	0.556	-
P70482	Lamin C2 (Fragment)	0.586	-
Q7M0F1	Glutathione transferase 3 (Fragments)	0.766	-
P06761	78 kDa glucose-regulated protein	0.752	-
Q6P686	Osteoclast-stimulating factor 1	0.608	-
P47853	Biglycan	0.798	-
Q5BJ93	Enolase 1, (Alpha)	0.533	-
Q63081	Protein disulfide-isomerase A6	0.682	-

Sequence ID	Protein Names	SecP	signal peptide
Q9QZK5	Serine protease HTRA1	0.736	-
P07152	Stromelysin-2	0.525	-
P03957	Stromelysin-1	0.645	-
F1LTT5	Protein Ube2l3 (Fragment)	0.702	-
D3ZEN5	Peroxiredoxin-5, mitochondrial	0.541	-
G3V7K3	Ceruloplasmin	0.659	-
P02770	Serum albumin	0.506	-
D4A3K4	Protein RGD1560815	0.553	-
F2Z3Q8	Importin subunit beta-1	0.592	-
D3Z8D3	Similar to Myocyte-specific enhancer factor 2B, isoform CRA_b	0.875	-
P30121	Metalloproteinase inhibitor 2	0.866	-
E2RUH2	Protein LOC100360501	0.594	-
P04961	Proliferating cell nuclear antigen	0.562	-
P01026	Complement C3	0.569	-
F1LV61	Uncharacterized protein (Fragment)	0.559	-
P61972	Nuclear transport factor 2	0.625	-
E9PTW5	Protein Pltp	0.714	-
F1LP27	Eukaryotic initiation factor 4A-II	0.712	-
P11232	Thioredoxin	0.698	-
D3ZTH3	Uncharacterized protein	0.625	-
Q6LDG5	Hypoxanthine-guanine phosporibosyltransferase (Fragment)	0.797	-
Q6P9U0	Protein Serpinb6a	0.514	-
Q6P743	Adenosylhomocysteinase	0.514	-
F1LND7	Farnesyl pyrophosphate synthase	0.638	-
P30904	Macrophage migration inhibitory factor	0.706	-
P63259	Actin, cytoplasmic 2	0.505	-
D3ZG05	40S ribosomal protein S12	0.579	-
P07154	Cathepsin L1	0.65	-
P00762	Anionic trypsin-1	0.892	-
P04797	Glyceraldehyde-3-phosphate dehydrogenase	0.535	-
D3ZGY4	Glyceraldehyde-3-phosphate dehydrogenase	0.513	-
D4A8N3	Protein RGD1563956	0.663	-
Q5XFX0	Transgelin-2	0.833	-
Q9R1T3	Cathepsin Z	0.798	-
Q9WVH8	Fibulin-5	0.814	-
Q6B345	Protein S100-A11	0.848	-
D3ZHM0	Protein Actr3b	0.772	-
Q63453	Prothymosin-alpha (Fragment)	0.669	-
O35763	Moesin	0.577	-
Q920A6	Retinoid-inducible serine carboxypeptidase	0.814	-
F1LRL8	Protein Arpc3 (Fragment)	0.778	-
Q6P7A4	Prosaposin	0.71	-

Sequence ID	Protein Names	SecP	signal peptide
D3ZFY8	Protein Tmem189	0.799	-
P24368	Peptidyl-prolyl cis-trans isomerase B	0.859	-
F1LP60	Uncharacterized protein (Fragment)	0.567	-
P16975	SPARC	0.938	-
Q07936	Annexin A2	0.763	-
P13635	Ceruloplasmin	0.659	-
D3ZVA3	Protein Olr84	0.53	-

*Note: protein name is the Unipro name for the identified protein. Sequence ID is the Unipro accession number for the identified protein. A number in the SecP column indicates the numerical score returned by SecretomeP (greater than 0.5 indicates high probability of secretion). “y” in the signal peptide column indicates a predicted signal peptide from SignalP analysis.

Table 2. The list of significantly up- and down-regulated secreted proteins in VSMCs in response to Smad3-dependent TGF-β signaling.

Sequence ID	Protein Name	Total Peptides	$\log_{1.5}^{(\text{TGF-}\beta\text{ treated/control})}$
B2RZA9	Protein Ube2l3	3	3.404
P11598	Protein disulfide-isomerase A3	4	2.930
P48675	Desmin	3	2.886
Q63081	Protein disulfide-isomerase A6	2	2.539
D3ZY72	Nucleophosmin	3	2.523
Q5RJM3	Insulin-like growth factor binding protein 7	4	1.949
P13635	Ceruloplasmin	3	1.774
F1LSF2	Protein Smoc1	2	1.640
E9PSP1	Protein Pltp	1	1.636
P24368	Peptidyl-prolyl cis-trans isomerase B	4	1.465
Q920A6	Retinoid-inducible serine carboxypeptidase	2	1.221
A2RUV9	Adipocyte enhancer-binding protein 1	4	1.145
Q9ERB4	Versican core protein (Fragments)	4	1.048
P47853	Biglycan	13	1.043
P00762	Anionic trypsin-1	1	1.037
B2RZ27	Protein Sh3bgrl3	1	-1.032
Q9JLZ1	Glutaredoxin-3	3	-1.033
P00787	Cathepsin B	3	-1.052
Q64599	Hemiferrin	3	-1.093
D3ZS68	Protein Pcbp1	2	-1.164
Q5PPG2	Legumain	3	-1.179
D3ZAF5	Periostin, osteoblast specific factor (Predicted), isoform CRA	3	-1.329
P31044	Phosphatidylethanolamine-binding protein 1	3	-1.360
P11883	Aldehyde dehydrogenase, dimeric NADP-preferring	2	-1.456
D4ADF5	Protein Pdcd5	3	-1.697
P18331	Inhibin beta A chain	3	-1.735
B6DYQ2	Glutathione S-transferase mu 2	3	-1.837
P01026	Complement C3	5	-1.888
B0BMT0	RCG47746, isoform CRA	4	-2.161
D4A3L9	Uncharacterized protein	2	-2.744
F1MAA7	Protein Lamc1	2	-3.616

*Note: protein name is the Uniprot name for the identified protein. Sequence ID is the Uniprot accession number for the identified protein. A number in total peptide column indicates how

many peptides identified for each protein. Proteins with $\log_{1.5}^{(\text{TGF-}\beta \text{ treated/control})} > 1$ were up-regulated, while those with $\log_{1.5}^{(\text{TGF-}\beta \text{ treated/control})} < -1$ were down-regulated.

Chapter 5

Searching for Reliable Pre-mortem Protein Biomarkers for Prion Diseases – Progress and Challenges to Date

Adapted from: “Searching for Reliable Pre-mortem Protein Biomarkers for Prion Diseases – Progress and Challenges to Date”. Ma D, Li L. *Expert Rev Proteomics*, **9** (3): 267-280 (2012)

Summary

Prion diseases are a unique family of fatal neurodegenerative diseases caused by abnormal folding of normal cellular prion proteins in the brain. Due to the high risk of prion disease transmission and the lack of effective treatment to cure or delay the disease progression, prion diseases pose a serious threat to public health. To control and prevent prion diseases, an early diagnosis is urgently needed. Proteomic analysis has emerged as a powerful technology to decipher biological and pathophysiological processes and identify protein biomarkers indicative of disease. In this article, we review the use of the latest proteomic technologies for the identification of promising prion disease biomarkers, the challenges that exist in biomarker development pipeline and the new directions of utilizing proteomics for future biomarker discovery in the context of prion disease diagnostics.

Keywords: prion diseases; biomarker; mass spectrometry; proteomics; glycoprotein

Prion diseases and prion protein

Prion diseases, or transmissible spongiform encephalopathies (TSEs) are a unique family of fatal neurodegenerative diseases that affect both animals and humans. Depending on the animal host, prion diseases include scrapie which has been detected for more than 200 years that affects the nervous system of sheep and goats, the much more recently recognized bovine spongiform encephalopathy (BSE or “mad cow disease”) among cattle, and chronic wasting disease (CWD) in deer. Human prion diseases include the following four types: Kuru, which was the first known human TSE found among the Fore people in the highlands of New Guinea that resulted from the practice of ritualistic cannibalism[1], Gerstmann-Sträussler-Scheinker

syndrome (GSS), fatal familial insomnia (FFI), and Creutzfeldt-Jakob disease (CJD). CJD has also been classified into four distinct forms, including classic or sporadic (sCJD), genetic (gCJD), variant (vCJD) and iatrogenic CJD (iCJD).

The infectious agent in prion diseases is prion protein capable of introducing the conversion of normal host cellular prion protein (PrP^{C}) into abnormal protease-resistant isoform (PrP^{Sc}) which has higher proportion of β-sheet structures in place of the normal α-helix structures[2, 3]. PrP^{C} is a 33-35 kDa protein of 253 amino acids encoded by a single copy gene *PRNP*[4, 5]. Molecular genetic studies of prion disease revealed point mutations, insertions, and deletions in *PRNP* and the resulting amino acids change could be the genetic factors that cause PrP^{C} more likely to change spontaneously into the abnormal PrP^{Sc} form in genetic prion diseases such as GSS disease, FFI, and genetically associated CJD[6, 7]. Previous studies have identified more than 30 mutations in *PRNP*, and it is shown that a common coding polymorphism at codon 129 of *PRNP* between methionine and valine has a critical role in susceptibility of prion diseases[8-10]. In contrast, acquired forms of prion disease are transmitted by ingestion of or exposure to, contaminated biological material via food or during medical procedures. Prion diseases are usually rapidly progressive and always fatal. When the normal prion protein converts to the infectious form, the incubation period of prion diseases could vary from months to decades during which time no symptoms exhibited. Following the onset of symptoms, however, disease progresses rapidly, leading to brain damage and death ultimately. Currently, no effective measures of treatment exist for prion diseases. Some chemical compounds that exhibit antiprion properties were used in clinical trials to treat CJD patients. However, these compounds were only effective if administered at the early stage of the disease[11]. Furthermore, issues such as

low bioavailability, blood-brain permeability, and high toxicity compounded the difficulty to develop effective drugs against prion diseases[12].

After an outbreak of BSE that occurred among cattle in many European countries in 1990s, prion diseases attracted attention not only because of the enormous economic losses caused by the slaughtering cattle and animals linked to positive BSE cattle, but also scientific evidence that showed BSE had been transmitted to humans through consuming the BSE-contaminated food products[13, 14]. Moreover, transmission from humans to humans (iatrogenic transmission) can occur via contaminated surgical equipment, the use of human growth hormone derived from cadaveric pituitaries, and transplantation of corneas and dura mater from infected patients, as well as through blood or blood product[15, 16]. It was reported that human-adapted prions are more readily transmitted from human to human via blood transfusion than through ingestion of BSE prions from contaminated meat products[17].

PrP^{Sc} as biomarker for prion diseases diagnosis

Given that there is no cure for prion diseases, it is imperative to develop effective diagnostic assays for routine screening in large population to prevent a potential spread of the disease from animal to human or human to human. Currently, all commercial diagnostic tests for TSEs are carried out by the direct detection of PrP^{Sc} of cellular prion protein in brain tissue. Conventionally, histological and immunohistological methods have served as reference for clinical diagnosis by detection of characteristic vacuolar or spongiform changes in specific areas of the brain[18]. The recent BSE epidemic has led to the development of antibody-based commercial diagnostic assays for BSE, scrapie and CWD. Antibody-based assays utilize a Western Blot/ELISA approach to provide more rapid and large scale analysis which is now a

routine TSE diagnostic assay for use in animals[19-21]. Recently, the capability of mass spectrometry (MS)-based method for more sensitive detection and quantification of PrP^{Sc} has been exploited. Carter's group reported a MS-based multiple reaction monitoring (MRM) method that can be used to both confirm and quantitate PrP 27-30 derived trypsin fragments in several different species [22-24]. The limit of detection for this method (20-30 amol) is considerably lower than any of the previously described detection methods.

Although sensitive and specific, all current commercial diagnostic kits are supplied only for animal TSE diseases and can only be applied to post-mortem diagnosis for discrimination and confirmation of the presence of PrP^{Sc}. Ugnon-Café *et al*. reported that two commercial assays that were developed based on ELISA and Western blot, can be used to detect PrP^{Sc} in cerebral and lymphoid tissues of TSE patients[25] . It was shown that both tests were specific and quite sensitive in detection of PrP^{Sc} in post-mortem brains of affected patients but not in the controls. Furthermore, two pre-mortem tonsils from three patients with vCJD were detected correctly, suggesting that these assays could be used for human TSE diagnosis, and that detection of PrP^{Sc} in the tonsil could be used as pre-mortem diagnosis for CJD. Due to the fact that the concentration of PrP^{Sc} in peripheral tissue is substantially lower than that of in neural tissues, the sensitivity of conventional immunoassays is not high enough for the detection of PrP^{Sc} in easily accessible body fluids for preclinical diagnosis. However, when coupled with an enrichment step of PrP^{Sc} from biological samples, the sensitivity of immunodetection could be significantly increased. Edgeworth *et al*. developed a quantitative blood-based assay for vCJD diagnosis where they used solid-state binding matrix to capture and concentrate PrP^{Sc} from whole blood of vCJD patients and couple this method to direct immunodetection of surface-bound material[26, 27]. A masked panel of 190 whole blood samples from normal controls and patients with vCJD, sCJD

and other neurological diseases were analyzed by this assay, and it showed a sensitivity of 71.4% and a specificity of 100%. Although the sensitivity of this assay is yet to be improved, the findings from this study demonstrated the feasibility of preclinical diagnosis of vCJD by blood assay. Recently, protein misfolding cyclic amplification (PMCA) technology which was developed in 2001 by Claudio Soto's group[28] has been applied to the detection of PrP^{Sc} with enhanced sensitivity[29]. PMCA is based on the ability of small amount of PrP^{Sc} to convert excess amount of normal PrP^{C} to a proteinase K resistant form to the level which can be detected by conventional immunoassays, thus "amplifying" the original infectious seed. Amplification can be increased by breaking down the growing chain of PrPSc to smaller units which in turn act as seeds for further replication. PMCA enabled the development of ultra-sensitive tests for prions and prion diseases. It has been reported PMCA was applied to the pre-mortem detection of CWD infection in the peripheral tissues of cervids[30]. However, the use of PrP^{Sc} as a preclinical biomarker for surveillance will be challenging due to the fact that the amount of PrP^{Sc} is extremely low in easily accessible tissue or body fluids. To circumvent these problems and develop an effective pre-mortem diagnostic method, an alternate strategy is to identify proteins (other than PrP^{Sc}) that are indicative of disease and allow early detection of prion infection, also known as surrogate biomarkers, in easily accessible body fluid. This review focuses on recent efforts to identify potential diagnostic biomarkers by proteomic technologies, the current challenges and possible new directions for biomarker discovery and validation in the future.

Application of proteomics to the discovery and verification of biomarkers for prion diseases

Proteomics approaches for biomarker discovery

The biomarker development pipeline is generally composed of three stages: biomarker discovery, verification and clinical validation (Fig. 1). The process begins with biomarker discovery where unbiased analyses are carried out to compare the differences between normal and prion infected samples to identify proteins differentially expressed in prion infected samples as potential biomarker candidates. In the past decade, advances in mass spectrometry (MS) has made MS-based proteomics a promising tool for protein profiling and biomarker discovery in various types of samples such as cell cultures, tissues, and biological fluids. With the latest technology in chromatographic separations and state-of -the–art MS instrumentation, hundreds of proteins can be identified in a single run. However, the biggest challenges for using proteomics for prion disease biomarker discovery are the complexity of the sample and the presence of high-abundance proteins in body fluids such as the cerebrospinal fluid (CSF) and blood. To overcome these difficulties, several separation techniques can be applied to facilitate the protein identification by mass spectrometry. Based on different separation strategies, three commonly used techniques for biomarker discovery include: two-dimensional gel electrophoresis MS (2D-GE MS) and its variation two-dimensional differential gel electrophoresis MS (2D-DIGE MS), surface-enhanced laser desorption ionizing time of flight MS (SELDI-TOF MS), and shotgun proteomic analysis by liquid chromatography tandem mass spectrometry (LC-MS/MS).

2D-GE MS is the most widely used method in studies of proteomic profiling of prion infected samples where thousands of proteins can be separated on a single gel according to pI and molecular weight. Individual protein spots that show difference in abundance between different samples can then be excised from the gel, digested into peptides and analyzed by matrix-assisted laser desorption/ionization time of flight MS (MALDI-TOF MS) or LC-MS/MS

for protein identification. Built on 2D-GE, 2D-DIGE adds a quantitative dimension to this technique by enabling multiple protein extracts to be separated on the same 2D gel, thus providing a promising approach to comparative analysis of proteomes in complex samples. In 2D-DIGE, up to three different protein extracts, control, infected samples and an internal standard can be labeled with fluorescent dyes, for example Cy3, Cy5 and Cy2 respectively prior to two-dimensional electrophoresis. Compared to traditional 2D-GE, 2D-DIGE overcomes the inter-gel variation problem[31]. Studies using 2D-GE MS or 2D-DIGE MS to profile proteins in CSF have led to the identifications of currently accepted biomarker for sCJD 14-3-3 protein and other potential biomarkers for prion diseases (Table 1).

SELDI-TOF MS is a variation of (MALDI-TOF MS) that selectively captures proteins of interests on a surface modified with chemical functionality prior to co-crystallization with an energy absorbing matrix followed by ionization with a laser for TOF MS analysis. It is another useful method for protein profiling where proteins spotted on a "protein chip" will interact with the chromatographic surface based on absorption, electrostatic interaction, and affinity. The proteins of interests selectively bind to the surface, while the others are removed by washing. This method allows rapid concentration and detection of proteins with good sensitivity below a molecular weight of 20 kDa[32, 33] and therefore complements gel-based approaches. Although SELDI-TOF MS suffers from low resolution, low mass accuracy and lack of tandem MS capabilities, all of which make direct protein identification difficult, the ability of this technique to compare spectra from large number of samples in a relatively short time with little sample preparation is advantageous for low resolution TOF instruments without tandem MS capability. SELDI-TOF MS analysis recognizes differentially expressed proteins and provides the

foundation for the isolation of proteins of interests for further identification by high resolution MS and tandem MS analysis.

In contrast to 2D-GE and SELDI-TOF MS where intact proteins are separated, liquid based shotgun proteomic separation techniques have become increasingly popular in proteomic research because they are reproducible, highly automated, and have a greater likelihood of detecting low abundance proteins. In this case protein mixture is digested, and resulting peptides are separated by LC prior to tandem MS detection, which allows for the identification of different proteins by peptide sequencing. However, due to the complexity of the digested protein samples from biological fluids such as CSF and plasma, one dimensional separation is often insufficient, and thus an orthogonal separation of complex samples is needed prior to LC-MS/MS. More commonly used strategies include Multidimensional Protein Identification Technology (MudPIT)[34] and gel-based liquid chromatography (GeLC)[35, 36]. Another advantage of liquid based shotgun proteomics is the suitability for isotope labeling for protein quantification. Examples of quantification methodology include the use of chemical reactions to introduce isotopic tags at specific functional groups on peptides or proteins, such as ICAT (isotope-coded affinity tags), in which cysteine residues are specifically derivatized with a reagent containing either zero or eight deuterium atoms as well as a biotin group for affinity purification of cysteine-containing peptides[37, 38] and iTRAQ (isobaric tags for relative and absolute quantitation) [39] which labels primary amines at the N-termini and lysine side chains of peptides and enables up to eight samples to be labeled and relatively quantified in a single experiment[40]. Isotope labeling has been demonstrated to be a powerful tool for protein quantitative analysis in CSF and blood samples [41, 42].

All methodologies of proteomics mentioned above have played critical roles in biomarker discovery, and with advances and innovations in current techniques they will be even more powerful than before in terms of accuracy, sensitivity, or analytical throughput. However, each proteomic approach alone has its advantages and disadvantages, and cannot cover the entire proteome. Therefore, a comprehensive study of prion disease biomarkers will rely on the results obtained from various strategies and different instruments. Table 1 provides a list of potential biomarkers for prion diseases identified by different proteomic technologies.

Searching for prion disease related biomarkers in the cerebrospinal fluid (CSF)

Being in close anatomical contact with brain interstitial fluid, CSF has been studied most for diagnostic biomarker identification for neurological diseases due to its obvious association with the central nervous system (CNS). Biochemical changes in CSF caused by disease can be reflected by altered expression or post-translational modification of certain proteins. Various brain-derived proteins have been shown to be differentially expressed in CJD, of which commonly tested CSF proteins as CJD biomarkers include 14-3-3 protein, total tau (T-tau), S100B, and neuron-specific enolase (NSE)[43-46]. To date, only the detection of 14-3-3 protein is included in the diagnostic criteria approved by World Health Organization(WHO) for the pre-mortem diagnosis of clinically suspected cases of sCJD[47]. However, the diagnostic accuracy of this test is still up for debate for large-scale screening purposes because of its high false positive rate where elevated 14-3-3 protein levels were also reported in other conditions associated with acute neuronal damage[48, 49]. Although the high false positive rate caused by conditions such as inflammatory, ischemic and neoplastic disorders could be ruled out by routine CSF test and brain imaging, the differential diagnosis between CJD and other neurodegenerative diseases can be

challenging, and the implication of a combination of multiple biomarkers is often necessary[46]. To improve the sensitivity and specificity of CSF 14-3-3 protein analysis, it is desirable to identify other new biomarkers that are specific to sCJD and can be used in conjunction with 14-3-3 protein to support diagnosis. So far, different proteomic approaches have been used for comparative CSF proteome analysis including 2D-GE[50], 2D-DIGE[51], SELDI-TOF MS[50, 52], MALDI-TOF MS[53]and MALDI-FTMS[54]. These methods have resulted in significant progress to identify sensitive and specific biomarkers for CJD. Qualtieri *et al*. has summarized the existing proteins proposed as surrogate biomarkers for sCJD diagnosis in their review[55]. These proteins showed significant differential expression in CSF samples from CJD patients, but further investigation of each protein is required to examine the specificity and sensitivity for early diagnosis of sCJD in a larger cohort. One of the proposed biomarkers Heart-Type Fatty Acid Binding Protein (H-FABP) was initially investigated in a small group of CJD affected patients (*n* = 8) by 2D-GE MS and immunoassay approach[56]. The amount of H-FABP appeared to be significantly increased in both CSF and plasma of CJD patients in this study, but application of H-FABP as a diagnostic tool was not certain due to the limited number of CJD patients and patients with other causes of rapid progressive dementia included in the investigation. In a recent study, H-FABP level in CSF samples from CJD patients (n=124) was investigated by Rapicheck® kit assay which is a qualitative one-step immunochromatography system and ELISA assay. Results from both assays demonstrated satisfying sensitivity and specificity comparable to 14-3-3 protein and T-tau protein assay, suggesting the applicability of H-FABP as diagnostic biomarker in conjunction with 14-3-3 protein and T-tau may improve diagnostic accuracy [57].

As the level of 14-3-3 protein and T-tau is also elevated in several other dementias besides CJD which is the main reason to cause high false positive rate, the search for proteins that are exclusively or directly involved in the pathological process of the disease will likely result in the identification of CJD specific biomarkers. One such potential protein that might play a pathophysiological role in CJD is extracellular signal regulating kinase ERK1/2, as MAP kinases are activated during the pathogenesis in prion diseases[58]. Steinacker *et al*. measured ERK1/2 level in the CSF samples of patients with CJD, other dementias or neurological disorders by an electrochemiluminescence assay and Western immunoblot, and identified significantly elevated mean levels of total ERK1/2 and phosphorylated ERK1/2 in the CJD patients. The increase of ERK1/2 was also observed in a CJD case that was negative for 14-3-3 protein or had low levels of tau protein, suggesting that ERK1/2 can be used as an alternative CSF biomarker for CJD[59]. In another study, the level of CSF transferrin was examined in the pre-mortem CSF collected between 2006-2008 from 99 patients with autopy-confirmed cases of sCJD (CJD+) and 75 cases of dementia of non-CJD origin (CJD-) by rigorous statistical analysis. It was determined that level of transferrin is significantly lower in the CSF of CJD+ case compared to that of CJD- patients. The decrease in transferrin distinguished sCJD from dementia from non-CJD origin with an accuracy of 80%, and when combined with T-tau, the diagnostic accuracy increased to 86%[60]. This combination enables more accurate diagnosis than the current method of sCJD diagnosis where levels of 14-3-3 protein and T-tau are detected.

Identifying biomarkers in blood or urine for easy and fast pre-mortem screening assays

Blood is a good alternative biological material to search for biomarkers that can be used for routine pre-mortem diagnostic test because its collection is non-invasive, low-cost, safe and

simple. Although blood is not in direct contact with brain, the exchange between CSF and blood allows some brain-derived proteins to leak to blood, and such exchange could be enhanced in cases of neurodegenerative diseases where the blood-brain barrier was damaged[61]. Recently, the evidence that transmission of vCJD in humans can occur through blood infusion have raised concerns on prion contamination in human blood or blood products[16, 62]. Therefore, an effective diagnosis of TSEs during the early phase by a reliable and sensitive test performed in blood is desired. Unfortunately, very few proteomic analyses for biomarkers of prion disease in blood have been reported partially due to the scarcity of samples from CJD patients and prion infected animal models. The biggest challenge that impedes the biomarker discovery in blood, however, is the large dynamic range of proteins that has been reported to exceed 10^{10} and the high abundances of twelve proteins that comprise approximately 95% of the serum proteome that mask the detection of lower abundance proteins [63]. As a result, the successful detection of low-abundance proteins that are likely to be disease indicative biomarkers rely heavily on an effective pre-fractionation or enrichment strategy to remove highly abundant proteins from the serum/plasma prior to proteomic analysis. The most common strategy to reduce dynamic range is immunodepletion in which several major high abundance proteins in human or mouse plasma are removed by commercially available multi-affinity columns [64]. Alternatively, the complexity of blood sample can be reduced by using affinity separations to enrich a subproteome of interests, e.g., phosphoproteome, glycoproteome, low molecular weight subproteome, etc. Our group utilized lectin affinity chromatography to enrich glycoproteins in healthy and prion infected mouse plasma followed by shotgun proteomic analysis by MudPIT. Using this strategy we identified 708 proteins in mouse plasma from three time points of disease progression [65].

SELDI-TOF MS has been proposed as a powerful approach for blood biomarker discovery as this technology focuses on a particular subset of the proteome for each of the capture conditions, and additional prefractionation or enrichment steps help reduce sample dynamic range prior to SELDI-TOF MS, which further improves sensitivity[66, 67]. A recent study by Batxelli-Molina *et al*. analyzed a large number of serum samples from control sheep and animals with early phase (EP) or late phase (LP) scrapie to detect biomarkers characteristic of the EP and LP of scrapie by SELDI-TOF MS analysis[68]. To reduce sample complexity, serum samples were prefractionated by anion exchange chromatography according to their charge characteristics that resulted in six fractions eluted at different pH values. SELDI-TOF MS analysis of the profiles of proteins included in the 2-20 kDa range in all fractions obtained from serum samples of sheep with (EP or LP) scrapie and healthy controls led to the detection of 15 peaks found to significantly differentiate EP or LP animals from control animals. The authors suggested that a combination of four differentially expressed peaks in either EP or LP scrapie could be used as biomarkers for scrapie at different stages. Moreover, the mass of three of the fifteen peaks with differential expression in sheep could be detected in hamster infected with scrapie and used as EP or LP biomarkers of disease in the hamster model. One peak that was detected in both sheep and hamster was identified as a fragment of the transthyretin monomer. In previous studies, transthyretin has been shown as a potential CSF biomarker with altered levels in sCJD patients[51].

Urine is another easily accessible body fluid that contains a complex mixture of proteins and peptides that can serve as a good reservoir for biomarker discovery because protein content of urine is relatively low and protein composition appears to be less complex compared to serum. Moreover, several studies have confirmed that PrP^{Sc} is excreted into the urine and PrP^{Sc} could be

detected in the urine of hamsters infected with scrapie[69-72]. Using proteomic approaches, two groups identified prion protein in urine-derived gonadotropins[73, 74], raising the concern about the presence of infectious prion protein in urinary-derived injectable fertility products. Therefore, the development of a sensitive and robust diagnostic test for prion disease in urine is also highly desirable. Simon *et al*. utilized 2D-DIGE MS to examine the urine of infected cattle over the course of the disease and found immunoglobulin γ-2 chain C region and clusterin were significantly increased in abundance[75]. Increased abundance of immunoglobulins have also been reported in the urine of scrapie-infected hamsters and sheep[72, 76]. The elevated level of clusterin has been reported previously in astrocytes as well as a significant accumulation in CSF and blood plasma[77]. Simon *et al*. demonstrated that only certain isoforms of clusterin exhibited differential abundance in urine samples collected from control and infected cattle[75]. The specificity of these particular isoforms was further investigated by using clusterin *β* subunit-specific antibodies to confirm that it was *β*-subunits of clusterin that exhibited differential abundance in response to BSE infection. Moreover, further examination revealed that the differentially expressed protein isoforms are *β*-subunits of the glycoprotein clusterin that possessed N-linked glycans[78] (also discussed in next section).

One issue concerning the reliability and accuracy of urine-based biomarkers is that whether protein biomarkers identified from homogenous population where the infected subjects and control subjects are matched based on their breeds, genders and ages can be applied to heterogeneous population, as the urine proteome will be affected by these factors. To address this issue, Plews *et al*. utilized 2D-DIGE to profile the urine proteome of both a known set and an associated blinded unknown set that contained control and BSE infected cattle of different breeds, genders and ages[79]. Based on the gel images obtained from the known set, nine selected

spot features were used to create a classifier that distinguish the infected from the uninfected samples. When applied to the 19 samples in an independent unknown data set, such classifier was able to discriminate between control and infected samples with 74% accuracy. However, five samples that were collected relatively early in the disease course were misclassified, which indicates that the disease status of the animals was influential in affecting differential abundance of individual proteins in urine. To further analyze the influence of breed, age and gender on the protein profiles in urine, a merged sample set was created where all control or infected animals from both known and unknown sets were included. All three factors are demonstrated to significantly affect the urinary proteome. However, despite the presence of confounding factors, a new classifier comprised of proteins best able to discriminate between the samples based on different factors was generated by the RDA (regularized discriminant analysis) algorithms.

Delving into the glycoproteome

As previously mentioned, direct profiling of CSF or blood proteome by conventional MS-based approaches to search for prion disease biomarkers is challenging because of the complexity of the proteome and the presence of very high-abundance proteins. An effective strategy is to focus on a subproteome that is more relevant to disease development and progression. Post-translational modifications (PTMs) play a key role to modulate the activity and function of most proteins in biological systems. Important PTMs such as phosphorylation, glycosylation and ubiquitination also regulate the functions, cellular targeting and degradation of proteins in the central nervous system (CNS)[80-82]. Thus, in addition to the change of protein concentrations, the aberrant PTM patterns of various proteins could be associated with the onset and progression of several neurodegenerative diseases. In recent years, MS-based proteomics

has been widely employed to both discover novel modifications and study the differential PTMs of proteins in a disease state [83, 84]. Among various PTMs, glycosylation represents the most common and complicated forms. Types of protein glycosylation are categorized as either N-linked, where glycans are attached to asparagine residues in a consensus sequence N-X-S/T (X can be any amino acid except proline) via an N-acetylglucosamine (N-GlcNAc) residue, or the O-glycosylation, where the glycans are attached to serine or threonine. Glycosylation plays a fundamental role in numerous biological processes, and aberrant alterations in protein glycosylation are associated with neurodegenerative disease states, such as CJD and Alzheimer's disease (AD)[85, 86]. It was found that PrP^{Sc} has decreased level of bisecting GlcNAc and increased levels of tri- and tetraantennary glycans compared to PrP^{C}, suggesting a decrease in the activity of an enzyme called N-acetylglucosaminyltransferase III[87]. This possible perturbation to the glycosylation machinery of the cells might cause changes in other glycosylation events and lead to glycoprotein profile changes. Liu *et al*. showed that aberrant glycosylation may modulate the tau protein at a substrate level, stabilizing its phosphorylated isoforms from brains in AD patients[81]. In another study, Reelin, a glycoprotein that is essential for the correct cytosolic organization of the CNS, is up-regulated in the brain and CSF in several neurodegenerative diseases, including frontotemporal dementia, progressive supranuclear palsy, Parkinson's disease (PD), as well as AD[88]. As mentioned earlier, Lamoureux *et al*. found the level of protein β-subunits of clusterin was elevated in urine of BSE-infected cow[78]. Presence of multiple isoforms of clusterin led to the further glycosylation analysis. Briefly, samples of BSE-infected urine were treated with enzyme PNGaseF to release N-linked glycan chains. Western blotting analysis of PNGaseF treated and mock-treated control and infected urine samples revealed that the differentially expressed protein is highly glycosylated clusterin. Given that aberrant

glycosylation and glycoproteins play critical role in neurodegenerative disorders, in-depth glycoproteomic analyses of body fluids from patients would provide great potential for the discovery of new diagnostic markers. The glycoproteomic approaches have been applied to biomarker discovery in CSF of AD patients. A previous study used 2D-GE to identify several potential glycoprotein biomarkers, including apolipoprotein E, clusterin and α-1-β-glycoprotein in the CSF from AD patients[89]. In a similar study, Sihlbom *et al*. utilized albumin depletion prior to 2D gel electrophoresis to enhance glycoprotein concentration in the CSF of AD patients and healthy control individuals for image analysis and determined the structure of N-linked glycans of apolipoprotein J by FT-ICR MS[90]. However, the analysis of glycoproteome in tissues or body fluids is challenging due to the low abundance of glycosylated forms of proteins compared to non-glycosylated proteins. Therefore, the analysis of glycoprotein by MS-based proteomics requires effective approaches to enrich glycoproteins.

Two most common methods to enrich glycoproteins are lectin affinity chromatography and hydrazide chemistry. In hydrazide chemistry method, N-glycans of glycoproteins are conjugated to a solid support with hydrazide chemistry after periodate-mediated oxidation of the carbohydrate. Peptide moieties of the covalently captured glycopeptides are then released with PNGase F treatment to allow the peptide and glycosylation site to be identified[91]. On the other hand, lectins are a class of proteins isolated from plants, fungi, bacteria and animals that recognize carbohydrates on the surface of proteins. Lectins can specifically capture distinct oligosaccharide epitopes, thus not only allowing the isolation and enrichment of glycoproteins and glycopeptides, but also enables discrimination of glycan structures among different proteins and different glycoforms of the same protein. Lectins are usually immobilized onto appropriate matrices like agarose or magnetic beads in a number of chromatographic formats, including

tubes, columns and microfluidic channels[92, 93]. Two lectins Concanavalin A (ConA) and Wheat Germ Agglutinin (WGA) are commonly used in lectin affinity chromatography due to their broad selectivity. Con A has a high affinity to high-mannose type N-glycans[94, 95], whereas WGA is selective for N-GlcNAc and sialic acids[96]. Because individual lectins can specifically enrich only a subset of glycoproteins, multi-lectin column are applied to maximize the coverage of glycoproteomes in biological fluids[97-99]. By utilizing a multi-lectin column that contained both Con A and WGA to enrich N-linked glycoproteins in mouse plasma, followed by multidimensional liquid chromatography to separate tryptic peptides prior to MS analysis, our group identified a low-abundance protein serum amyloid P-component (SAP) in control and prion-infected mouse plasma collected at 108, 158, and 198 days post inoculation (dpi)[65]. Relative quantitative analysis by isotopic formaldehyde labeling revealed that the level of SAP was significantly elevated in infected 108 dpi samples, which was also validated by Western blotting using SAP antibody. Interestingly, the Western blot experiments showed two bands of SAP at 26 and 30 kDa, respectively. The intensity of the 26 kDa band remains relatively constant regardless of the physiological status, whereas the level of 30 kDa band was significantly elevated from the infected sample at 108 dpi (Figure 2A). SAP is a 224-residue secreted glycoprotein with a single N-glycosylation site at position 52[100, 101]. PNGase F digestion analysis of the sample in which N-glycans were cleaved prior to Western blotting confirmed that the 30 kDa band is the glycosylated form of SAP (Figure 2B) and the elevation of SAP observed in infected samples at 108 dpi in MS analysis can be fully attributed to the increase of glycosylated SAP following the enrichment by lectin affinity chromatography, whereas the level of nonglycosylated isoform remained relatively stable. SAP is previously reported to be associated *in vivo* with all types of amyloid deposits, and has been found to co-

localize with neurofibrillary pathology in various neurodegenerative diseases including AD, CJD, PD, and diffuse Lewy body disorders[102-104]. The result from this study suggested that glycosylated form of SAP could be used as a potential preclinical biomarker for prion diseases and the glycosylation SAP plays an important role in the progression of prion disease.

Verification of biomarkers by targeted proteomics

After potential biomarkers are discovered by means of MS-based proteomic analysis, validations that require a large number of clinical samples and have much higher threshold for accuracy have to be performed to examine their sensitivity and specificity before they can be developed into clinical assays. However, due to the enormous expense and effort spent in the validation phase and the risk that very few candidates will be qualified; a verification stage is usually needed with the goal of selecting those biomarkers that can potentially pass a final validation from the list of candidates generated in biomarker discovery phase. At present, although the number of potential biomarkers for prion diseases has been increasing, the verification of these proteins has become the major bottleneck in the biomarker development pipeline, allowing few proposed biomarkers to enter clinical validation. One of the main reasons that hindered the process of verification phase is the lack of technologies that can verify most of candidates identified in proteomics analysis across a large population of clinical samples. Currently, antibody based methods such as Western blotting and ELISA are the most widely used method for biomarker verification. These methods rely on specific antibodies for the protein of interests and cannot be applied to all biomarker candidates because commercial assays or antibodies are only available for a limited number of proteins, and the development of new assays will be an expensive and time-consuming process. Also, it is important that multiple

biomarker candidates be validated in the same assay not only for the concern of time and cost, but also for the reason that a panel of biomarkers rather than a single protein will be implemented in diagnostic screening for higher specificity and accuracy. Furthermore, biomarker validation by ELISA or Western blotting is limited by cross reactivity of different antibodies and the difficulty of having a uniform assay condition that are suitable for all antibodies in multiplexed assays.

Recently, quantitative assays based on multiple-reaction monitoring (MRM) MS using a triple quadrupole mass spectrometer in combination with stable isotope labeled internal standards have been employed in biomarker verification as an alternative to ELISA[105, 106]. In this approach, the targeted parent ion is selected in the first quadrupole (Q1) and enters the second quadrupole (Q2) where it undergoes collision-induced dissociation. One or more fragment ions are then selected according to the predefined transitions and the ensuing signal provides the spectral counts for quantification. MRM-MS has shown good sensitivity, reproducibility and linear dynamic range for direct quantification of proteins in serum samples[107]. The high throughput and multiplexing capability of this approach for biomarker verification in complex samples was also demonstrated by the quantification of 45 endogenous proteins of moderate to high abundance in plasma without fractionation of enrichment in single LC-MS run[108]. For the verification of low abundance biomarkers, a recent approach using Stable Isotope-Labeled Standards with Capture on Anti-Peptide Antibodies (SISCAPA) was applied to enrich for targeted peptides prior to MRM-MS, thereby significantly improve the sensitivity. In SISCAPA, the peptides of interest are enriched from digested plasma samples that are spiked with known amounts of their stable isotope labeled internal standard counterparts by utilizing immobilized

antibodies generated against specific peptides. The peptides are released from the antibody and then quantified using MRM-MS [109].

Currently, the verification of protein biomarkers for prion diseases are still conducted using antibody-based platforms, and only a small number of proteins have been selected for verification based on the consideration of the availability and the cost of antibodies, which created a big gap between discovery and validation phase in the biomarker development pipeline. The application of MRM-MS assay for the verification of more potential biomarkers identified from large-scale comparative proteomics experiments holds promise to accelerate the development process and generate more candidates for clinical validation. However, an accurate and reproducible MRM-MS assay requires a careful method optimization including sample preparation, LC condition and MS parameters that is specific to each potential biomarker, which presents new challenges in biomarker verification studies.

New scope in the discovery of prion disease biomarkers

As mentioned earlier, the biomarker discovery in blood has made little progress largely due to the sample complexity. Moreover, biomarkers identified in blood are often times not specific to a disease state as many of them are expressed and released from multiple organs. Other diseases or environmental perturbations can also cause the changes in protein level. Instead of mining protein biomarkers showing differential expression simply based on the comparison of control and prion infected sample, other efforts have been made to identify prion disease specific biomarkers by means of proteomics. Herein, we will highlight two different strategies: identifying interacting partners of prion proteins and using systems biology approach to understand the pathological processes in prion diseases.

Identification of interacting partners of prion protein

As previously mentioned, prion diseases are caused by protein misfolding. How this event leads to pathology is not fully understood, but increasing evidence suggested that the infectivity of PrP^{Sc} to native PrP^{C} requires other interacting proteins in the cell. Therefore, there has been a growing interest in identifying different partners with which PrP^{C} might be associated. Although the major goal of the present studies is to provide new insights into the physiological functions and pathological role of PrP^{C}, the characterization of the binding partners of PrP^{C} might provide diagnostic information and lead to the discovery of protein biomarkers, with the idea that any of those interacting proteins could be released into CSF or blood with an altered level in association with prion infection. A study showed that the 14-3-3 protein, a biomarker for sCJD, is an interacting partner of PrP^{c} in association with heat shock protein 60 (HSP60) [110]. Heat shock proteins (HSPs) are a group of proteins of similar function that increase their expression in response to cellular stress. All HSPs, to some extent, serve as molecular chaperones, proteins involved in the correct folding and biogenesis of cellular proteins and prevention of misfolding and aggregation of aggregation-prone proteins [111]. Several analyses of the expression patterns of genes and proteins during prion infection implicated an elevated level of HSP family members in different prion disease models[112-115]. At present, the investigation of protein expression profiles of HSPs during prion infection are undertaken using brain tissue after the sacrifice of animals. The development of pre-mortem biomarker, however, requires further studies of HSPs in easily accessible body fluid such as blood and CSF. Due to the advantage of high sensitivity and unambiguous identification of proteins over other techniques, mass spectrometry has been employed for protein complex analysis. In a recent study, Zafar *et al*.

utilized a proteomic approach to identify the interacting partners of human PrP^C which was expressed with a STrEP-tag at its C-terminus in prion protein-deficient murine hippocampus (HpL3-4) neuronal cells. The PrP^C along with its interacting proteins were affinity purified using STrEPT actin-chromatography and then separated on 1D SDS-PAGE. After in-gel digestion followed by Q-TOF MS/MS analysis, 43 proteins were identified to interact with PrP^C, 34 out of which were identified as novel PrP^C ligands[116].

From "omics" to systems biology

Advances in sample separation techniques and state-of-the-art mass spectrometers have enabled a large number of differentially expressed proteins to be identified in proteomic analysis. However, how to select a subset of differentially expressed proteins among large dataset as potential biomarkers for further verification and functional analysis can be challenging. Therefore, a meaningful interpretation of proteins with altered expression levels is indispensable for deeper insights into the roles they play in the complex cellular systems. In the last decade, systems biology has emerged as a field in biology aiming at systems level understanding of biological processes and seeking to investigate the role of biomolecules by studying their functions as well as their temporal and spatial interactions. In addition to MS-based proteomics, systems biology also integrates and analyzes the data generated by other techniques such as microarray and protein chips in a consistent way to explain the function of biomarker candidates in a cellular context and to discover regulatory networks and signaling pathways in a disease state. Using whole-brain mRNA expression data from various mouse strain–prion strain combinations, Hwang *et al*. identified 333 differentially expressed genes (DEGs) with shared temporal patterns of differential expression in the five core mouse-prion combinations[117].

Shared DEGs were mapped into functional pathways and networks involving prion accumulation, glial cell activation, synapse degeneration and nerve cell death that were significantly perturbed by PrP^{Sc} during disease progression. The gene expression dataset generated in this study was also used to test the utility of principal network analysis (PNA) that can automatically capture major dynamic activation patterns over multiple conditions and generate their associated principal sub-networks. PNA resulted in the identification of 20 activation patterns, and differential expression patterns of top 20 DEGs with the smallest *P*-values were well-correlated with the top four activation patterns [118]. A systems biology approach can assist in transferring experimental data like expression profiles or differences in protein abundances into a systems context, which will be helpful for narrowing down and evaluating candidates for biomarkers. The candidates that are predicted to be secreted proteins might exhibit an altered level in body fluids as a reflection of the disease, and such proteins will have great potential to be used as blood biomarkers. In conjunction with MS-based proteomic analysis in the future, it becomes possible to identify diagnostic biomarkers for prion diseases that are associated with prion pathology.

Expert commentary

Given the infectious and incurable nature of prion diseases, early diagnosis is highly desirable. Although current antibody based assays allow specific and sensitive detection of biomarker PrP^{Sc} in brain tissue, they cannot be applied to pre-mortem screening in readily accessible biological fluids due to the low concentration of misfolded PrP^{Sc}. MS-based proteomics has emerged as a powerful tool to identify surrogate protein biomarkers that are associated with prion diseases in complex biological samples such as plasma/serum, CSF, and

urine. In combination with prefractionation and affinity enrichment strategies, quantitative MS analysis allows more low abundance proteins to be detected.

As the list of potential biomarkers for prion disease is growing, the validatory studies on these proteins are not being carried out at the same pace. Reasons for this include the inherent problems of prion diseases such as the small number of clinical cases and the long incubation period. Also, ELISA based verification is limited by the availability of the antibodies, and is not suitable for multiplexed assays. Therefore, the development of MRM-MS based verification platform seems to be a promising alternative. As some of the pathways in neuropathogenesis of prion diseases also exist in other neurodegenerative as well as other infectious disease, the specificity of individual potential biomarkers needs to be examined carefully in the verification phase. It would be prudent to use a combination of multiple biomarkers rather than one single biomarker in order to reach higher sensitivity and specificity.

Five-year view

At current stage, discovery of biomarkers for early detection of prion diseases has been mostly confined to general profiling of proteome in easily accessible biological fluids. As the important role of glycosylation in neurodegenerative diseases has been revealed, the application of MS-based glycoproteomics holds promise in the identification of new glycoprotein biomarkers. Moreover, approaches to distinguishing prion disease related glycosylated form of a potential biomarker from the non-glycosylated form or other isoforms will promote the development of diagnostic assays that detect only glycosylated form of a protein, thus increasing the specificity and lowering false positive rate. Structural elucidation of aberrant glycosylation by MS analysis will also provide new insights into the cellular and molecular pathology of prion

diseases, and lead to the identification of enzymes involved in neuropathogenesis that can be used as diagnostic markers or treatment targets.

The application of systems biology approach based on dataset from genomic or proteomic analysis will permit discovery of pathophysiological pathways underlying interconnected patterns from seemingly irrelevant misregulated proteins, and thereby sort out the ones with higher probability of being genuine biomarkers for prion diseases.

Key issues

- Prion diseases are a family of rare fatal neurodegenerative disease caused by abnormal folding of normal cellular prion proteins (PrP^{C}) to result in the formation of pathological prion protein (PrP^{Sc}) in the brain.
- So far the pre-mortem diagnosis of prion diseases remains challenges due to the low amount of PrP^{Sc} in easily accessible body fluids. 14-3-3 protein was accepted by WHO as a surrogate biomarker for the pre-mortem diagnosis of sCJD. However, 14-3-3 protein cannot be used for large scale screening test because it is not a specific marker for CJD.MS-based proteomics has emerged as a power tool to identify non-prion protein biomarkers that are associated with prion diseases in complex biological samples such as plasma/serum, CSF, and urine. These MS-based strategies in combination with sample prefractionation or affinity enrichment steps enhance the detection of low abundance proteins.
- Current potential biomarkers for prion diseases need to be verified for their sensitivity and specificity. The use of a panel of multiple biomarkers rather than one single biomarker may lead to increased sensitivity and specificity.

- Targeted proteomics by multiple-reaction monitoring (MRM) MS is a promising strategy to accelerate biomarker verification process as an alternative to ELISA assays.
- Glycosylation plays important roles in the development and progression of neurodegenerative diseases. The analysis of glycoproteome and attached glycans will result in the identification of glycoprotein biomarkers that are more intimately related to prion diseases.

Acknowledgement:

This work was supported in part by the Graduate School and Wisconsin Alumni Research Foundation at the University of Wisconsin-Madison. L. Li acknowledges an H.I. Romnes Faculty Research Fellowship.

References

Papers of special note have been highlighted as:

1. Gajdusek, D. C., Unconventional viruses and the origin and disappearance of kuru. *Science* **1977,** 197, (4307), 943-60.
2. Pan, K. M.; Baldwin, M.; Nguyen, J.; Gasset, M.; Serban, A.; Groth, D.; Mehlhorn, I.; Huang, Z.; Fletterick, R. J.; Cohen, F. E.; et al., Conversion of alpha-helices into beta-sheets features in the formation of the scrapie prion proteins. *Proc Natl Acad Sci U S A* **1993,** 90, (23), 10962-6.
3. Aguzzi, A.; Polymenidou, M., Mammalian prion biology: one century of evolving concepts. *Cell* **2004,** 116, (2), 313-27.
4. Chesebro, B.; Race, R.; Wehrly, K.; Nishio, J.; Bloom, M.; Lechner, D.; Bergstrom, S.; Robbins, K.; Mayer, L.; Keith, J. M.; et al., Identification of scrapie prion protein-specific mRNA in scrapie-infected and uninfected brain. *Nature* **1985,** 315, (6017), 331-3.
5. Oesch, B.; Westaway, D.; Walchli, M.; McKinley, M. P.; Kent, S. B.; Aebersold, R.; Barry, R. A.; Tempst, P.; Teplow, D. B.; Hood, L. E.; et al., A cellular gene encodes scrapie PrP 27-30 protein. *Cell* **1985,** 40, (4), 735-46.
6. Hsiao, K.; Baker, H. F.; Crow, T. J.; Poulter, M.; Owen, F.; Terwilliger, J. D.; Westaway, D.; Ott, J.; Prusiner, S. B., Linkage of a prion protein missense variant to Gerstmann-Straussler syndrome. *Nature* **1989,** 338, (6213), 342-5.
7. Goldfarb, L. G.; Brown, P.; Little, B. W.; Cervenakova, L.; Kenney, K.; Gibbs, C. J., Jr.; Gajdusek, D. C., A new (two-repeat) octapeptide coding insert mutation in Creutzfeldt-Jakob disease. *Neurology* **1993,** 43, (11), 2392-4.
8. Mead, S., Prion disease genetics. *Eur J Hum Genet* **2006,** 14, (3), 273-81.
9. Kovacs, G. G.; Trabattoni, G.; Hainfellner, J. A.; Ironside, J. W.; Knight, R. S.; Budka, H., Mutations of the prion protein gene phenotypic spectrum. *J Neurol* **2002,** 249, (11), 1567-82.
10. Collinge, J., Molecular neurology of prion disease. *J Neurol Neurosurg Psychiatry* **2005,** 76, (7), 906-19.
11. Kawasaki, Y.; Kawagoe, K.; Chen, C. J.; Teruya, K.; Sakasegawa, Y.; Doh-ura, K., Orally administered amyloidophilic compound is effective in prolonging the incubation periods of animals cerebrally infected with prion diseases in a prion strain-dependent manner. *J Virol* **2007,** 81, (23), 12889-98.
12. Webb, S.; Lekishvili, T.; Loeschner, C.; Sellarajah, S.; Prelli, F.; Wisniewski, T.; Gilbert, I. H.; Brown, D. R., Mechanistic insights into the cure of prion disease by novel antiprion compounds. *J Virol* **2007,** 81, (19), 10729-41.
13. Hill, A. F.; Desbruslais, M.; Joiner, S.; Sidle, K. C.; Gowland, I.; Collinge, J.; Doey, L. J.; Lantos, P., The same prion strain causes vCJD and BSE. *Nature* **1997,** 389, (6650), 448-50, 526.
14. Will, R. G.; Ironside, J. W.; Zeidler, M.; Cousens, S. N.; Estibeiro, K.; Alperovitch, A.; Poser, S.; Pocchiari, M.; Hofman, A.; Smith, P. G., A new variant of Creutzfeldt-Jakob disease in the UK. *Lancet* **1996,** 347, (9006), 921-5.
15. Brown, P.; Brandel, J. P.; Preece, M.; Sato, T., Iatrogenic Creutzfeldt-Jakob disease: the waning of an era. *Neurology* **2006,** 67, (3), 389-93.
16. Llewelyn, C. A.; Hewitt, P. E.; Knight, R. S.; Amar, K.; Cousens, S.; Mackenzie, J.; Will, R. G., Possible transmission of variant Creutzfeldt-Jakob disease by blood transfusion. *Lancet* **2004,** 363, (9407), 417-21.
17. Bishop, M. T.; Hart, P.; Aitchison, L.; Baybutt, H. N.; Plinston, C.; Thomson, V.; Tuzi, N. L.; Head, M. W.; Ironside, J. W.; Will, R. G.; Manson, J. C., Predicting susceptibility and incubation time of human-to-human transmission of vCJD. *Lancet Neurol* **2006,** 5, (5), 393-8.
18. Fraser, H., The pathology of a natural and experimental scrapie. *Front Biol* **1976,** 44, 267-305.

19. Oesch, B.; Doherr, M.; Heim, D.; Fischer, K.; Egli, S.; Bolliger, S.; Biffiger, K.; Schaller, O.; Vandevelde, M.; Moser, M., Application of Prionics Western blotting procedure to screen for BSE in cattle regularly slaughtered at Swiss abattoirs. *Arch Virol Suppl* **2000**, (16), 189-95.
20. Schaller, O.; Fatzer, R.; Stack, M.; Clark, J.; Cooley, W.; Biffiger, K.; Egli, S.; Doherr, M.; Vandevelde, M.; Heim, D.; Oesch, B.; Moser, M., Validation of a western immunoblotting procedure for bovine PrP(Sc) detection and its use as a rapid surveillance method for the diagnosis of bovine spongiform encephalopathy (BSE). *Acta Neuropathol* **1999,** 98, (5), 437-43.
21. Grassi, J.; Creminon, C.; Frobert, Y.; Fretier, P.; Turbica, I.; Rezaei, H.; Hunsmann, G.; Comoy, E.; Deslys, J. P., Specific determination of the proteinase K-resistant form of the prion protein using two-site immunometric assays. Application to the post-mortem diagnosis of BSE. *Arch Virol Suppl* **2000**, (16), 197-205.
22. Onisko, B.; Dynin, I.; Requena, J. R.; Silva, C. J.; Erickson, M.; Carter, J. M., Mass spectrometric detection of attomole amounts of the prion protein by nanoLC/MS/MS. *J Am Soc Mass Spectrom* **2007,** 18, (6), 1070-9.
23. Onisko, B. C.; Silva, C. J.; Dynin, I.; Erickson, M.; Vensel, W. H.; Hnasko, R.; Requena, J. R.; Carter, J. M., Sensitive, preclinical detection of prions in brain by nanospray liquid chromatography/tandem mass spectrometry. *Rapid Commun Mass Spectrom* **2007,** 21, (24), 4023-6.
24. Silva, C. J.; Onisko, B. C.; Dynin, I.; Erickson, M. L.; Requena, J. R.; Carter, J. M., Utility of Mass Spectrometry in the Diagnosis of Prion Diseases. *Anal Chem* **2011,** 83, 1609–1615.
25. Ugnon-Cafe, S.; Dorey, A.; Bilheude, J. M.; Streichenberger, N.; Viennet, G.; Meyronet, D.; Maues de Paula, A.; Perret-Liaudet, A.; Quadrio, I., Rapid screening and confirmatory methods for biochemical diagnosis of human prion disease. *J Virol Methods* **2011,** 175, (2), 216-23.
26. Edgeworth, J. A.; Farmer, M.; Sicilia, A.; Tavares, P.; Beck, J.; Campbell, T.; Lowe, J.; Mead, S.; Rudge, P.; Collinge, J.; Jackson, G. S., Detection of prion infection in variant Creutzfeldt-Jakob disease: a blood-based assay. *Lancet* **2011,** 377, (9764), 487-93.
27. Edgeworth, J. A.; Jackson, G. S.; Clarke, A. R.; Weissmann, C.; Collinge, J., Highly sensitive, quantitative cell-based assay for prions adsorbed to solid surfaces. *Proc Natl Acad Sci U S A* **2009,** 106, (9), 3479-83.
28. Saborio, G. P.; Permanne, B.; Soto, C., Sensitive detection of pathological prion protein by cyclic amplification of protein misfolding. *Nature* **2001,** 411, (6839), 810-3.
29. Orru, C. D.; Caughey, B., Prion seeded conversion and amplification assays. *Top Curr Chem* **2011,** 305, 121-33.
30. Haley, N. J.; Mathiason, C.; Carver, S.; Telling, G. C.; Zabel, M. C.; Hoover, E. A., Sensitivity of protein misfolding cyclic amplification vs. immunohistochemistry in antemortem detection of CWD infection. *J Gen Virol* **2012**.
31. Marouga, R.; David, S.; Hawkins, E., The development of the DIGE system: 2D fluorescence difference gel analysis technology. *Anal Bioanal Chem* **2005,** 382, (3), 669-78.
32. Bischoff, R.; Luider, T. M., Methodological advances in the discovery of protein and peptide disease markers. *J Chromatogr B Analyt Technol Biomed Life Sci* **2004,** 803, (1), 27-40.
33. Tang, N.; Tornatore, P.; Weinberger, S. R., Current developments in SELDI affinity technology. *Mass Spectrom Rev* **2004,** 23, (1), 34-44.
34. Wolters, D. A.; Washburn, M. P.; Yates, J. R., 3rd, An automated multidimensional protein identification technology for shotgun proteomics. *Anal Chem* **2001,** 73, (23), 5683-90.
35. Wilm, M.; Shevchenko, A.; Houthaeve, T.; Breit, S.; Schweigerer, L.; Fotsis, T.; Mann, M., Femtomole sequencing of proteins from polyacrylamide gels by nano-electrospray mass spectrometry. *Nature* **1996,** 379, (6564), 466-9.
36. Schirle, M.; Heurtier, M. A.; Kuster, B., Profiling core proteomes of human cell lines by one-dimensional PAGE and liquid chromatography-tandem mass spectrometry. *Mol Cell Proteomics* **2003,** 2, (12), 1297-305.
37. Gygi, S. P.; Rist, B.; Gerber, S. A.; Turecek, F.; Gelb, M. H.; Aebersold, R., Quantitative analysis of complex protein mixtures using isotope-coded affinity tags. *Nat Biotechnol* **1999,** 17, (10), 994-9.

38. Haqqani, A. S.; Kelly, J. F.; Stanimirovic, D. B., Quantitative protein profiling by mass spectrometry using isotope-coded affinity tags. *Methods Mol Biol* **2008,** 439, 225-40.
39. Aggarwal, K.; Choe, L. H.; Lee, K. H., Shotgun proteomics using the iTRAQ isobaric tags. *Brief Funct Genomic Proteomic* **2006,** 5, (2), 112-20.
40. D'Ascenzo, M.; Choe, L.; Lee, K. H., iTRAQPak: an R based analysis and visualization package for 8-plex isobaric protein expression data. *Brief Funct Genomic Proteomic* **2008,** 7, (2), 127-35.
41. Dayon, L.; Hainard, A.; Licker, V.; Turck, N.; Kuhn, K.; Hochstrasser, D. F.; Burkhard, P. R.; Sanchez, J. C., Relative quantification of proteins in human cerebrospinal fluids by MS/MS using 6-plex isobaric tags. *Anal Chem* **2008,** 80, (8), 2921-31.
42. Pendyala, G.; Trauger, S. A.; Siuzdak, G.; Fox, H. S., Quantitative plasma proteomic profiling identifies the vitamin E binding protein afamin as a potential pathogenic factor in SIV induced CNS disease. *J Proteome Res* **2010,** 9, (1), 352-8.
43. Hsich, G.; Kenney, K.; Gibbs, C. J.; Lee, K. H.; Harrington, M. G., The 14-3-3 brain protein in cerebrospinal fluid as a marker for transmissible spongiform encephalopathies. *N Engl J Med* **1996,** 335, (13), 924-30.
44. Jesse, S.; Steinacker, P.; Cepek, L.; von Arnim, C. A.; Tumani, H.; Lehnert, S.; Kretzschmar, H. A.; Baier, M.; Otto, M., Glial fibrillary acidic protein and protein S-100B: different concentration pattern of glial proteins in cerebrospinal fluid of patients with Alzheimer's disease and Creutzfeldt-Jakob disease. *J Alzheimers Dis* **2009,** 17, (3), 541-51.
45. Otto, M.; Wiltfang, J.; Cepek, L.; Neumann, M.; Mollenhauer, B.; Steinacker, P.; Ciesielczyk, B.; Schulz-Schaeffer, W.; Kretzschmar, H. A.; Poser, S., Tau protein and 14-3-3 protein in the differential diagnosis of Creutzfeldt-Jakob disease. *Neurology* **2002,** 58, (2), 192-7.
46. Sanchez-Juan, P.; Green, A.; Ladogana, A.; Cuadrado-Corrales, N.; Saanchez-Valle, R.; Mitrovaa, E.; Stoeck, K.; Sklaviadis, T.; Kulczycki, J.; Hess, K.; Bodemer, M.; Slivarichova, D.; Saiz, A.; Calero, M.; Ingrosso, L.; Knight, R.; Janssens, A. C.; van Duijn, C. M.; Zerr, I., CSF tests in the differential diagnosis of Creutzfeldt-Jakob disease. *Neurology* **2006,** 67, (4), 637-43.
47. World Health Organization: Global surveillance, diagnosis and therapy of human transmissible spongiform encephalopathies: report from a WHO consultation. **1998,** World Health Organization, Geneva, Switzerland, 9-11 February 1998, 1-26.
48. Saiz, A.; Graus, F.; Dalmau, J.; Pifarre, A.; Marin, C.; Tolosa, E., Detection of 14-3-3 brain protein in the cerebrospinal fluid of patients with paraneoplastic neurological disorders. *Ann Neurol* **1999,** 46, (5), 774-7.
49. Bartosik-Psujek, H.; Archelos, J. J., Tau protein and 14-3-3 are elevated in the cerebrospinal fluid of patients with multiple sclerosis and correlate with intrathecal synthesis of IgG. *J Neurol* **2004,** 251, (4), 414-20.
50. Piubelli, C.; Fiorini, M.; Zanusso, G.; Milli, A.; Fasoli, E.; Monaco, S.; Righetti, P. G., Searching for markers of Creutzfeldt-Jakob disease in cerebrospinal fluid by two-dimensional mapping. *Proteomics* **2006,** 6 Suppl 1, S256-61.
51. Brechlin, P.; Jahn, O.; Steinacker, P.; Cepek, L.; Kratzin, H.; Lehnert, S.; Jesse, S.; Mollenhauer, B.; Kretzschmar, H. A.; Wiltfang, J.; Otto, M., Cerebrospinal fluid-optimized two-dimensional difference gel electrophoresis (2-D DIGE) facilitates the differential diagnosis of Creutzfeldt-Jakob disease. *Proteomics* **2008,** 8, (20), 4357-66.
52. Sanchez, J. C.; Guillaume, E.; Lescuyer, P.; Allard, L.; Carrette, O.; Scherl, A.; Burgess, J.; Corthals, G. L.; Burkhard, P. R.; Hochstrasser, D. F., Cystatin C as a potential cerebrospinal fluid marker for the diagnosis of Creutzfeldt-Jakob disease. *Proteomics* **2004,** 4, (8), 2229-33.
53. Qualtieri, A., Urso, E., Le Pera, M., Bossio, S., Bernaudo, F., Ferraro, T., Crescibene, L., Aguglia, U. and Quattrone, A., Thymosin β4 is differentially expressed in the cerebrospinal fluid of Creutzfeldt-Jakob disease patients: a MALDI-TOF MS protein profiling study. *Proteomics Clin. Appl.* **2009,** 3, 574–583.
54. Herbst, A.; McIlwain, S.; Schmidt, J. J.; Aiken, J. M.; Page, C. D.; Li, L., Prion disease diagnosis by proteomic profiling. *J Proteome Res* **2009,** 8, (2), 1030-6.

55. Qualtieri, A.; Urso, E.; Le Pera, M.; Sprovieri, T.; Bossio, S.; Gambardella, A.; Quattrone, A., Proteomic profiling of cerebrospinal fluid in Creutzfeldt-Jakob disease. *Expert Rev Proteomics* **2010,** 7, (6), 907-17.
56. Guillaume, E.; Zimmermann, C.; Burkhard, P. R.; Hochstrasser, D. F.; Sanchez, J. C., A potential cerebrospinal fluid and plasmatic marker for the diagnosis of Creutzfeldt-Jakob disease. *Proteomics* **2003,** 3, (8), 1495-9.
57. Matsui, Y.; Satoh, K.; Mutsukura, K.; Watanabe, T.; Nishida, N.; Matsuda, H.; Sugino, M.; Shirabe, S.; Eguchi, K.; Kataoka, Y., Development of an ultra-rapid diagnostic method based on heart-type fatty acid binding protein levels in the CSF of CJD patients. *Cell Mol Neurobiol* **2010,** 30, (7), 991-9.
58. Lee, H. P.; Jun, Y. C.; Choi, J. K.; Kim, J. I.; Carp, R. I.; Kim, Y. S., Activation of mitogen-activated protein kinases in hamster brains infected with 263K scrapie agent. *J Neurochem* **2005,** 95, (2), 584-93.
59. Steinacker, P.; Klafki, H.; Lehnert, S.; Jesse, S.; Arnim, C. A.; Tumani, H.; Pabst, A.; Kretzschmar, H. A.; Wiltfang, J.; Otto, M., ERK2 is increased in cerebrospinal fluid of Creutzfeldt-Jakob disease patients. *J Alzheimers Dis* 22, (1), 119-28.
60. Singh, A.; Beveridge, A. J.; Singh, N., Decreased CSF transferrin in sCJD: a potential pre-mortem diagnostic test for prion disorders. *PLoS One* 6, (3), e16804.
61. Reiber, H., Proteins in cerebrospinal fluid and blood: barriers, CSF flow rate and source-related dynamics. *Restor Neurol Neurosci* **2003,** 21, (3-4), 79-96.
62. Hunter, N.; Foster, J.; Chong, A.; McCutcheon, S.; Parnham, D.; Eaton, S.; MacKenzie, C.; Houston, F., Transmission of prion diseases by blood transfusion. *J Gen Virol* **2002,** 83, (Pt 11), 2897-905.
63. Anderson, N. L.; Anderson, N. G., The human plasma proteome: history, character, and diagnostic prospects. *Mol Cell Proteomics* **2002,** 1, (11), 845-67.
64. Bjorhall, K.; Miliotis, T.; Davidsson, P., Comparison of different depletion strategies for improved resolution in proteomic analysis of human serum samples. *Proteomics* **2005,** 5, (1), 307-17.
65. Wei, X.; Herbst, A.; Ma, D.; Aiken, J.; Li, L., A quantitative proteomic approach to prion disease biomarker research: delving into the glycoproteome. *J Proteome Res* **2011,** 10, (6), 2687-702.
66. Roche, S.; Tiers, L.; Provansal, M.; Piva, M. T.; Lehmann, S., Interest of major serum protein removal for Surface-Enhanced Laser Desorption/Ionization - Time Of Flight (SELDI-TOF) proteomic blood profiling. *Proteome Sci* **2006,** 4, 20.
67. Sihlbom, C.; Kanmert, I.; Bahr, H.; Davidsson, P., Evaluation of the combination of bead technology with SELDI-TOF-MS and 2-D DIGE for detection of plasma proteins. *J Proteome Res* **2008,** 7, (9), 4191-8.
68. Batxelli-Molina, I.; Salvetat, N.; Andreoletti, O.; Guerrier, L.; Vicat, G.; Molina, F.; Mourton-Gilles, C., Ovine serum biomarkers of early and late phase scrapie. *BMC Vet Res* **2010,** 6, 49.
69. Kariv-Inbal, Z.; Ben-Hur, T.; Grigoriadis, N. C.; Engelstein, R.; Gabizon, R., Urine from scrapie-infected hamsters comprises low levels of prion infectivity. *Neurodegener Dis* **2006,** 3, (3), 123-8.
70. Gregori, L.; Kovacs, G. G.; Alexeeva, I.; Budka, H.; Rohwer, R. G., Excretion of transmissible spongiform encephalopathy infectivity in urine. *Emerg Infect Dis* **2008,** 14, (9), 1406-12.
71. Murayama, Y.; Yoshioka, M.; Okada, H.; Takata, M.; Yokoyama, T.; Mohri, S., Urinary excretion and blood level of prions in scrapie-infected hamsters. *J Gen Virol* **2007,** 88, (Pt 10), 2890-8.
72. Rubenstein, R.; Chang, B.; Gray, P.; Piltch, M.; Bulgin, M. S.; Sorensen-Melson, S.; Miller, M. W., Prion Disease Detection, PMCA Kinetics, and IgG in Urine from Sheep Naturally/Experimentally Infected with Scrapie and Deer with Preclinical/Clinical Chronic Wasting Disease. *J Virol* 85, (17), 9031-8.
73. Kuwabara, Y.; Mine, K.; Katayama, A.; Inagawa, T.; Akira, S.; Takeshita, T., Proteomic analyses of recombinant human follicle-stimulating hormone and urinary-derived gonadotropin preparations. *J Reprod Med* **2009,** 54, (8), 459-66.
74. Van Dorsselaer, A.; Carapito, C.; Delalande, F.; Schaeffer-Reiss, C.; Thierse, D.; Diemer, H.; McNair, D. S.; Krewski, D.; Cashman, N. R., Detection of prion protein in urine-derived injectable fertility products by a targeted proteomic approach. *PLoS One* 6, (3), e17815.

75. Simon, S. L.; Lamoureux, L.; Plews, M.; Stobart, M.; LeMaistre, J.; Ziegler, U.; Graham, C.; Czub, S.; Groschup, M.; Knox, J. D., The identification of disease-induced biomarkers in the urine of BSE infected cattle. *Proteome Sci* **2008,** 6, 23.
76. Serban, A.; Legname, G.; Hansen, K.; Kovaleva, N.; Prusiner, S. B., Immunoglobulins in urine of hamsters with scrapie. *J Biol Chem* **2004,** 279, (47), 48817-20.
77. Sasaki, K.; Doh-ura, K.; Ironside, J. W.; Iwaki, T., Increased clusterin (apolipoprotein J) expression in human and mouse brains infected with transmissible spongiform encephalopathies. *Acta Neuropathol* **2002,** 103, (3), 199-208.
78. Lamoureux, L.; Simon, S. L.; Plews, M.; Stobart, M.; Groschup, M.; Czub, S.; Graham, C.; Knox, J. D., Analysis of clusterin glycoforms in the urine of BSE-infected Fleckvieh-Simmental cows. *J Toxicol Environ Health A* **2011,** 74, (2-4), 138-45.
79. Plews, M.; Lamoureux, L.; Simon, S. L.; Graham, C.; Ruddat, V.; Czub, S.; Knox, J. D., Factors affecting the accuracy of urine-based biomarkers of BSE. *Proteome science* **2011,** 9, (1), 6.
80. Wang, J.; Tung, Y. C.; Wang, Y.; Li, X. T.; Iqbal, K.; Grundke-Iqbal, I., Hyperphosphorylation and accumulation of neurofilament proteins in Alzheimer disease brain and in okadaic acid-treated SY5Y cells. *FEBS Lett* **2001,** 507, (1), 81-7.
81. Liu, F.; Iqbal, K.; Grundke-Iqbal, I.; Hart, G. W.; Gong, C. X., O-GlcNAcylation regulates phosphorylation of tau: a mechanism involved in Alzheimer's disease. *Proc Natl Acad Sci U S A* **2004,** 101, (29), 10804-9.
82. Keller, J. N.; Hanni, K. B.; Markesbery, W. R., Impaired proteasome function in Alzheimer's disease. *J Neurochem* **2000,** 75, (1), 436-9.
83. Wei, X.; Li, L., Comparative glycoproteomics: approaches and applications. *Brief Funct Genomic Proteomic* **2009,** 8, (2), 104-13.
84. Wei, X.; Li, L., Mass spectrometry-based proteomics and peptidomics for biomarker discovery in neurodegenerative diseases. *Int J Clin Exp Pathol* **2009,** 2, (2), 132-48.
85. Saez-Valero, J.; Fodero, L. R.; Sjogren, M.; Andreasen, N.; Amici, S.; Gallai, V.; Vanderstichele, H.; Vanmechelen, E.; Parnetti, L.; Blennow, K.; Small, D. H., Glycosylation of acetylcholinesterase and butyrylcholinesterase changes as a function of the duration of Alzheimer's disease. *J Neurosci Res* **2003,** 72, (4), 520-6.
86. Silveyra, M. X.; Cuadrado-Corrales, N.; Marcos, A.; Barquero, M. S.; Rabano, A.; Calero, M.; Saez-Valero, J., Altered glycosylation of acetylcholinesterase in Creutzfeldt-Jakob disease. *J Neurochem* **2006,** 96, (1), 97-104.
87. Rudd, P. M.; Endo, T.; Colominas, C.; Groth, D.; Wheeler, S. F.; Harvey, D. J.; Wormald, M. R.; Serban, H.; Prusiner, S. B.; Kobata, A.; Dwek, R. A., Glycosylation differences between the normal and pathogenic prion protein isoforms. *Proc Natl Acad Sci U S A* **1999,** 96, (23), 13044-9.
88. Botella-Lopez, A.; Burgaya, F.; Gavin, R.; Garcia-Ayllon, M. S.; Gomez-Tortosa, E.; Pena-Casanova, J.; Urena, J. M.; Del Rio, J. A.; Blesa, R.; Soriano, E.; Saez-Valero, J., Reelin expression and glycosylation patterns are altered in Alzheimer's disease. *Proc Natl Acad Sci U S A* **2006,** 103, (14), 5573-8.
89. Puchades, M.; Hansson, S. F.; Nilsson, C. L.; Andreasen, N.; Blennow, K.; Davidsson, P., Proteomic studies of potential cerebrospinal fluid protein markers for Alzheimer's disease. *Brain Res Mol Brain Res* **2003,** 118, (1-2), 140-6.
90. Sihlbom, C.; Davidsson, P.; Nilsson, C. L., Prefractionation of cerebrospinal fluid to enhance glycoprotein concentration prior to structural determination with FT-ICR mass spectrometry. *J Proteome Res* **2005,** 4, (6), 2294-301.
91. Zhang, H.; Li, X. J.; Martin, D. B.; Aebersold, R., Identification and quantification of N-linked glycoproteins using hydrazide chemistry, stable isotope labeling and mass spectrometry. *Nat Biotechnol* **2003,** 21, (6), 660-6.
92. Mao, X.; Luo, Y.; Dai, Z.; Wang, K.; Du, Y.; Lin, B., Integrated lectin affinity microfluidic chip for glycoform separation. *Anal Chem* **2004,** 76, (23), 6941-7.

93. Xiong, L.; Andrews, D.; Regnier, F., Comparative proteomics of glycoproteins based on lectin selection and isotope coding. *J Proteome Res* **2003,** 2, (6), 618-25.
94. Goldstein, I. J.; Hollerman, C. E.; Smith, E. E., Protein-Carbohydrate Interaction. Ii. Inhibition Studies on the Interaction of Concanavalin a with Polysaccharides. *Biochemistry* **1965,** 4, 876-83.
95. Kamra, A.; Gupta, M. N., Crosslinked concanavalin A-O-(diethylaminoethyl)-cellulose--an affinity medium for concanavalin A-interacting glycoproteins. *Anal Biochem* **1987,** 164, (2), 405-10.
96. Nagata, Y.; Burger, M. M., Wheat germ agglutinin. Molecular characteristics and specificity for sugar binding. *J Biol Chem* **1974,** 249, (10), 3116-22.
97. Wang, Y.; Wu, S. L.; Hancock, W. S., Approaches to the study of N-linked glycoproteins in human plasma using lectin affinity chromatography and nano-HPLC coupled to electrospray linear ion trap--Fourier transform mass spectrometry. *Glycobiology* **2006,** 16, (6), 514-23.
98. Yang, Z.; Hancock, W. S., Approach to the comprehensive analysis of glycoproteins isolated from human serum using a multi-lectin affinity column. *J Chromatogr A* **2004,** 1053, (1-2), 79-88.
99. Yang, Z.; Hancock, W. S.; Chew, T. R.; Bonilla, L., A study of glycoproteins in human serum and plasma reference standards (HUPO) using multilectin affinity chromatography coupled with RPLC-MS/MS. *Proteomics* **2005,** 5, (13), 3353-66.
100. Bernhard, O. K.; Kapp, E. A.; Simpson, R. J., Enhanced analysis of the mouse plasma proteome using cysteine-containing tryptic glycopeptides. *J Proteome Res* **2007,** 6, (3), 987-95.
101. Mole, J. E.; Beaulieu, B. L.; Geheran, C. A.; Carnazza, J. A.; Anderson, J. K., Isolation and analysis of murine serum amyloid P component cDNA clones. *J Immunol* **1988,** 141, (10), 3642-6.
102. Kalaria, R. N.; Golde, T. E.; Cohen, M. L.; Younkin, S. G., Serum amyloid P in Alzheimer's disease. Implications for dysfunction of the blood-brain barrier. *Ann N Y Acad Sci* **1991,** 640, 145-8.
103. Akiyama, H.; Yamada, T.; Kawamata, T.; McGeer, P. L., Association of amyloid P component with complement proteins in neurologically diseased brain tissue. *Brain Res* **1991,** 548, (1-2), 349-52.
104. Coria, F.; Castano, E.; Prelli, F.; Larrondo-Lillo, M.; van Duinen, S.; Shelanski, M. L.; Frangione, B., Isolation and characterization of amyloid P component from Alzheimer's disease and other types of cerebral amyloidosis. *Lab Invest* **1988,** 58, (4), 454-8.
105. Addona, T. A.; Abbatiello, S. E.; Schilling, B.; Skates, S. J.; Mani, D. R.; Bunk, D. M.; Spiegelman, C. H.; Zimmerman, L. J.; Ham, A. J.; Keshishian, H.; Hall, S. C.; Allen, S.; Blackman, R. K.; Borchers, C. H.; Buck, C.; Cardasis, H. L.; Cusack, M. P.; Dodder, N. G.; Gibson, B. W.; Held, J. M.; Hiltke, T.; Jackson, A.; Johansen, E. B.; Kinsinger, C. R.; Li, J.; Mesri, M.; Neubert, T. A.; Niles, R. K.; Pulsipher, T. C.; Ransohoff, D.; Rodriguez, H.; Rudnick, P. A.; Smith, D.; Tabb, D. L.; Tegeler, T. J.; Variyath, A. M.; Vega-Montoto, L. J.; Wahlander, A.; Waldemarson, S.; Wang, M.; Whiteaker, J. R.; Zhao, L.; Anderson, N. L.; Fisher, S. J.; Liebler, D. C.; Paulovich, A. G.; Regnier, F. E.; Tempst, P.; Carr, S. A., Multi-site assessment of the precision and reproducibility of multiple reaction monitoring-based measurements of proteins in plasma. *Nat Biotechnol* **2009,** 27, (7), 633-41.
106. Kim, K.; Kim, S. J.; Yu, H. G.; Yu, J.; Park, K. S.; Jang, I. J.; Kim, Y., Verification of biomarkers for diabetic retinopathy by multiple reaction monitoring. *J Proteome Res* **2010,** 9, (2), 689-99.
107. Kuhn, E.; Wu, J.; Karl, J.; Liao, H.; Zolg, W.; Guild, B., Quantification of C-reactive protein in the serum of patients with rheumatoid arthritis using multiple reaction monitoring mass spectrometry and 13C-labeled peptide standards. *Proteomics* **2004,** 4, (4), 1175-86.
108. Kuzyk, M. A.; Smith, D.; Yang, J.; Cross, T. J.; Jackson, A. M.; Hardie, D. B.; Anderson, N. L.; Borchers, C. H., Multiple reaction monitoring-based, multiplexed, absolute quantitation of 45 proteins in human plasma. *Mol Cell Proteomics* **2009,** 8, (8), 1860-77.
109. Anderson, N. L.; Anderson, N. G.; Haines, L. R.; Hardie, D. B.; Olafson, R. W.; Pearson, T. W., Mass spectrometric quantitation of peptides and proteins using Stable Isotope Standards and Capture by Anti-Peptide Antibodies (SISCAPA). *J Proteome Res* **2004,** 3, (2), 235-44.
110. Satoh, J.; Onoue, H.; Arima, K.; Yamamura, T., The 14-3-3 protein forms a molecular complex with heat shock protein Hsp60 and cellular prion protein. *J Neuropathol Exp Neurol* **2005,** 64, (10), 858-68.

111. Hayes, S. A.; Dice, J. F., Roles of molecular chaperones in protein degradation. *J Cell Biol* **1996,** 132, (3), 255-8.
112. Booth, S.; Bowman, C.; Baumgartner, R.; Dolenko, B.; Sorensen, G.; Robertson, C.; Coulthart, M.; Phillipson, C.; Somorjai, R., Molecular classification of scrapie strains in mice using gene expression profiling. *Biochem Biophys Res Commun* **2004,** 325, (4), 1339-45.
113. Diedrich, J. F.; Carp, R. I.; Haase, A. T., Increased expression of heat shock protein, transferrin, and beta 2-microglobulin in astrocytes during scrapie. *Microb Pathog* **1993,** 15, (1), 1-6.
114. Kenward, N.; Hope, J.; Landon, M.; Mayer, R. J., Expression of polyubiquitin and heat-shock protein 70 genes increases in the later stages of disease progression in scrapie-infected mouse brain. *J Neurochem* **1994,** 62, (5), 1870-7.
115. Tatzelt, J.; Voellmy, R.; Welch, W. J., Abnormalities in stress proteins in prion diseases. *Cell Mol Neurobiol* **1998,** 18, (6), 721-9.
116. Zafar, S.; von Ahsen, N.; Oellerich, M.; Zerr, I.; Schulz-Schaeffer, W. J.; Armstrong, V. W.; Asif, A. R., Proteomics approach to identify the interacting partners of cellular prion protein and characterization of Rab7a interaction in neuronal cells. *J Proteome Res* **2011,** 10, (7), 3123-35.
117. Hwang, D.; Lee, I. Y.; Yoo, H.; Gehlenborg, N.; Cho, J. H.; Petritis, B.; Baxter, D.; Pitstick, R.; Young, R.; Spicer, D.; Price, N. D.; Hohmann, J. G.; Dearmond, S. J.; Carlson, G. A.; Hood, L. E., A systems approach to prion disease. *Mol Syst Biol* **2009,** 5, 252.
118. Kim, Y.; Kim, T. K.; Yoo, J.; You, S.; Lee, I.; Carlson, G.; Hood, L.; Choi, S.; Hwang, D., Principal network analysis: identification of subnetworks representing major dynamics using gene expression data. *Bioinformatics* **2011,** 27, (3), 391-8.
119. Harrington, M. G.; Merril, C. R.; Asher, D. M.; Gajdusek, D. C., Abnormal proteins in the cerebrospinal fluid of patients with Creutzfeldt-Jakob disease. *N Engl J Med* **1986,** 315, (5), 279-83.
120. Choe, L. H.; Green, A.; Knight, R. S.; Thompson, E. J.; Lee, K. H., Apolipoprotein E and other cerebrospinal fluid proteins differentiate ante mortem variant Creutzfeldt-Jakob disease from ante mortem sporadic Creutzfeldt-Jakob disease. *Electrophoresis* **2002,** 23, (14), 2242-6.
121. Steinacker, P.; Rist, W.; Swiatek-de-Lange, M.; Lehnert, S.; Jesse, S.; Pabst, A.; Tumani, H.; von Arnim, C. A.; Mitrova, E.; Kretzschmar, H. A.; Lenter, M.; Wiltfang, J.; Otto, M., Ubiquitin as potential cerebrospinal fluid marker of Creutzfeldt-Jakob disease. *Proteomics* 10, (1), 81-9.

Table 1: Potential biomarkers of prion diseases identified by MS-based proteomics

Protein	Source of sample	Identification method	Prion disease	Ref.
14-3-3 protein	CSF	2D-GE	CJD	[119]
α1-antichymotripsin	CSF	2D-GE	CJD	[50]
Apolipoprotein A1	CSF	2D-GE	CJD	[50]
Apolipoprotein A4	CSF	2D-GE	CJD	[50]
Apolipoprotein J	CSF	2D-GE	CJD	[50]
Apoliprotein E	CSF	2D-GE	CJD	[120]
Complement factor B/3a	CSF	2D-GE	CJD	[50]
Cystatin C	CSF	2D-GE; SELDI-TOF	CJD	[50, 52]
Fatty acid-binding protein	CSF, plasma	2D-GE	CJD	[56]
Fibrin-β	CSF	2D-GE	CJD	[50]
Fibrinogen γ chain	CSF	2D-GE	CJD	[50]
Gelsolin	CSF	2D-GE; 2D-DIGE	CJD	[50, 51]
Hp2-α haptoglobin	CSF	2D-GE	CJD	[50]
Lactate dehydrogenase B chain	CSF	2D-DIGE	CJD	[51]
Neuron-specific enolase	CSF	2D-DIGE	CJD	[51]
Prostaglandin D2 synthase	CSF	2D-DE	CJD	[50]
Transferrin	CSF	2D-DE	CJD	[50]
Transthyretin	CSF, serum	2D-DIGE, SELDI-TOF	CJD, scrapie	[51, 68]
Thymosin-β 4	CSF	MALDI-TOF	CJD	[53]
Ubiquitin	CSF	2D-GE ; MALDI-TOF; SELDI-TOF	CJD	[50, 53, 121]
Serum amyloid P-component	Plasma	2D LC-MS/MS	Scrapie	[65]
Clusterin E/M	Urine	2D-DIGE	BSE	[75, 78]
Ig γ-2 chain C region	Urine	2D-DIGE	BSE	[75]
Cystatin	Urine	2D-DIGE	BSE	[75]
Cathelicidin antimicrobial peptide	Urine	2D-DIGE	BSE	[75]
Uroguanylin	Urine	2-DIGE	BSE	[75]

Figure Legends

Figure 1. A summary of general workflows of biomarker development pipeline by proteomic approaches.

Figure 2. Validation of MS-based glycoproteomic approach using Western blotting analysis and enzymatic treatment. (A) Immunoblotting for serum amyloid P-component (SAP) protein. 2 μL of mouse plasma from control uninfected (U) and infected (I) groups on 108, 158, and 198 days postinoculation (dpi) were separated by SDS-PAGE and analyzed by Western blotting with anti-SAP antibody. Two forms of SAP were detected. (B) Glycosylated SAP is up-regulated at 108 dpi in infected mice. One or 2 μL of mouse plasma from both control uninfected (U) and infected (I) groups on 108 dpi were treated by PNGase F or left untreated. The mouse plasma were then separated by SDS-PAGE and analyzed by Western blotting with anti-SAP antibody. After PNGase F treatment, the band with molecular weight of 30 kDa shifted to 26 kDa, confirming that the glycosylated SAP is elevated in the infected group. Adapted with permission from Ref. 58.

Figure 1.

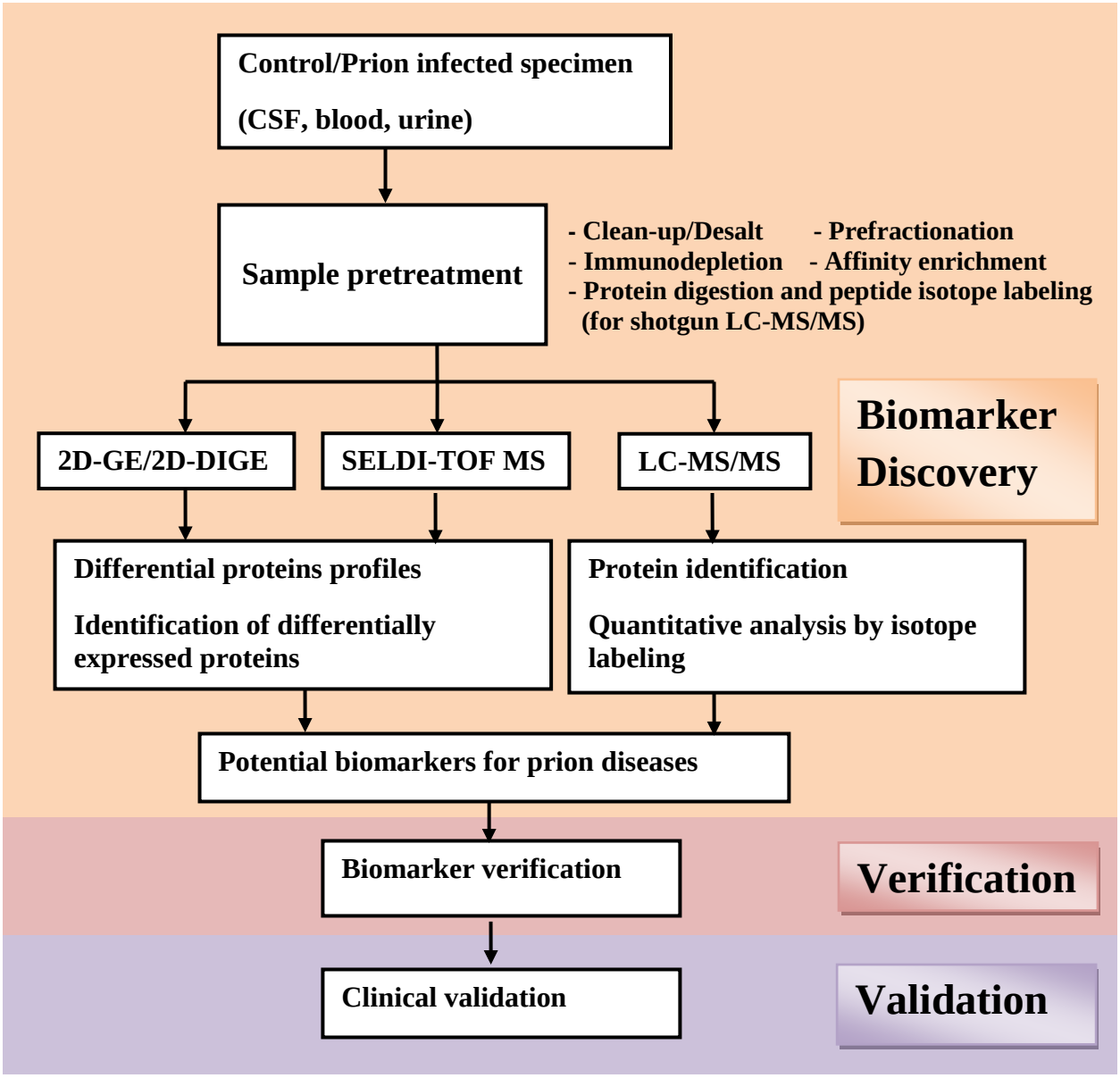
Control/Prion infected specimen
(CSF, blood, urine)
Sample pretreatment
- Clean-up/Desalt - Prefractionation
- Immunodepletion - Affinity enrichment
- Protein digestion and peptide isotope labeling (for shotgun LC-MS/MS)
2D-GE/2D-DIGE
SELDI-TOF MS
LC-MS/MS
Biomarker Discovery
Differential proteins profiles
Identification of differentially expressed proteins
Protein identification
Quantitative analysis by isotope labeling
Potential biomarkers for prion diseases
Biomarker verification
Verification
Clinical validation
Validation

Figure 2(A)

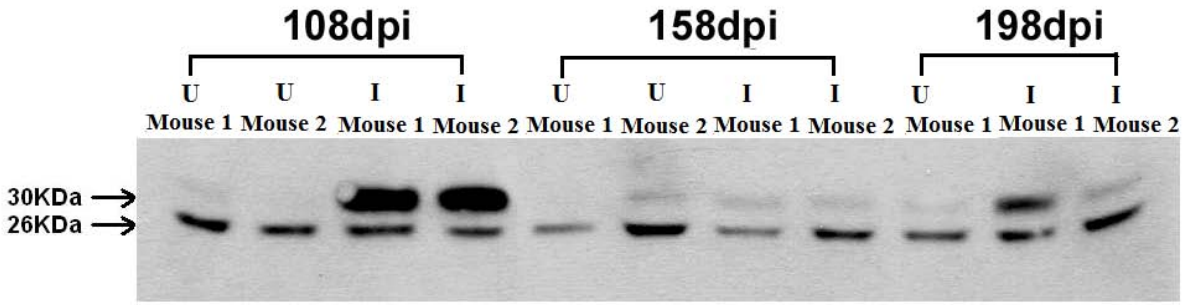

Figure 2(B)

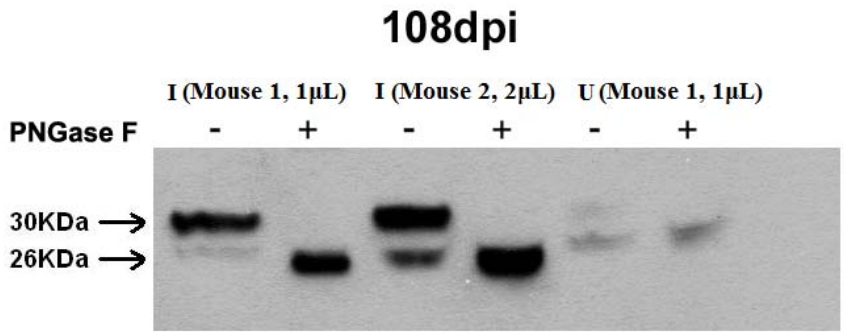

Chapter 6

Identification and Validation of a Potential Protein Biomarker for Prion Diseases by Mass Spectrometry-Based Quantitative Glycoproteomics

Adapted from: “A Quantitative Proteomic Approach to Prion Disease Biomarker Research: Delving into the Glycoproteome”. Wei X, Herbst A, Ma D, Aiken J, Li L. *J Proteome Res,* 10(6), 2687-2702 (2011).

Abstract

Mass spectrometry (MS) – based proteomic approaches have evolved as powerful tools for the discovery of biomarkers. However, the identification of potential protein biomarkers from biofluid samples is challenging because of the limited dynamic range of detection. Currently there is a lack of sensitive and reliable pre-mortem diagnostic test for prion diseases. Here, we describe the use of a combined MS-based approach for biomarker discovery in prion diseases from mouse plasma samples. To overcome the limited dynamic range of detection and sample complexity of plasma samples, we used lectin affinity chromatography and multi-dimensional separations to enrich and isolate glycoproteins at low abundance. Relative quantitation of a panel of proteins was obtained by a combination of isotopic labeling and validated by spectral counting. Overall 708 proteins were identified, 53 of which showed more than 2-fold increase in concentration whereas 58 exhibited more than 2-fold decrease. A few of the potential candidate markers were previously associated with prion or other neurodegenerative diseases.

Introduction

Prion diseases, also known as transmissible spongiform encephalopathies (TSEs), are a unique group of neurodegenerative diseases of the central nervous system, which include bovine spongiform encephalopathy (BSE) in cattle, scrapie in sheep, chronic wasting disease (CWD) in deer. Human forms of the prion diseases include: genetic disease, Gerstmann-Sträussler-Scheinker syndrome and fatal familial insomnia; sporadic disease, Creutzfeldt-Jakob disease (CJD), and infectious disease, variant CJD (vCJD), caused by the consumption of BSE infected cattle, and kuru, linked to the practice of ritualistic cannibalism in Papua New Guinea. Although the species barrier provides significant protection from the interspecies transmission of prion disease, the outbreaks of BSE epidemic and the resulting rise in vCJD illustrates the potential impact of prion disease upon human and economic health.

TSEs are caused by the conversion of a normal cellular prion protein (PrP^{C}) into an abnormal form (PrP^{Sc})[1, 2]. PrP^{C} is a 33-35 kDa protein encoded by a single copy gene[3, 4]. During the course of a scrapie infection, PrP^{C} undergoes a post-translational conformational conversion to disease-specific isoforms (PrP^{Sc}) that have increased resistance to proteinase K digestion. *In vitro* cell culture studies have suggested that PrP^{C} is the precursor to infectious isoform[1]. Disease specific PrP^{Sc} isoforms are present in various types of tissues but predominantly in the brain tissue and spinal cord at terminal stages of disease. Clinical symptoms of affected animals generally include pruritus, ataxia, and ultimately, death following an extended asymptomatic incubation period of months to decades during which infectious agent can replicate to very high titers (>1 × 10^{8} infectious units per gram) [1, 2]. Histopathological features of TSEs are characterized by spongiform degeneration, reactive astrocytosis, and the accumulation of aggregated prion proteins in the central nervous system.

Currently validated diagnostic tests for prion diseases are all post-mortem. Confirmation of the disease is carried out by the observation of characteristic vacuolar or spongiform changes in specific areas of the brain by histopathological examination of fixed brain sections using light microscopy. The "gold standard" in prion diagnostic testing is immunohistochemistry utilizing anti-prion protein antibodies on the obex region of the brain[5]. Despite the good specificity and sensitivity of these tests, animals infected with prion disease can only be diagnosed late in the pre-clinical period when sufficient abnormal PrP^{Sc} has accumulated in brain tissue. Pre-mortem tests that allow early detection of infection would reduce the risk of infected animals entering the marketplace, prevent unnecessary slaughtering of healthy animals, enable accurate prediction of TSE epidemic, and improve our understanding of the disease, thereby facilitating the development of effective treatments.

Development of non-prion protein biomarkers for TSEs has resulted in the identifications of surrogate markers in patients presenting clinical signs of CJD. Elevated levels of central nervous system-specific proteins such as 14-3-3, tau, apolipoprotein E, cystatin C, and neuron-specific enolase have been observed in the cerebrospinal fluid (CSF) or brains of patients[6-12]. The identification of biomarkers from more readily available sample sources such as blood plasma, however, remains challenging, due to the inherent complexity and vast dynamic range of proteins in the samples.

In the post-genomic era, there has been a growing interest in applying MS-based proteomics technology to research on biomarker discovery and clinical diagnostics of diseases such as cancers and neurodegenerative disorders from blood plasma. The current bottleneck of discovering biomarker in biofluid using MS is its limited dynamic range of detection compared to a much wider range of protein concentrations in the samples[13]. Efforts have been made to

simplify blood plasma samples by using affinity separations to enrich a sub-proteome with a common structural feature. For example, lectin affinity chromatography has been used to enrich the glycoproteins, which constitute one of the major subproteomes of blood[14-16]. Functionally, the oligosaccharide moieties of various glycoproteins act as selectivity determinants, playing a fundamental role in many biological processes such as immune response and cellular regulation because cell-to-cell interactions involve sugar-sugar or sugar-protein specific recognition[17]. Embryonic development and cellular activation in vertebrates are typically accompanied by changes in cellular glycosylation profiles. Thus, it is not surprising that glycosylation changes are also a universal feature of malignant transformation and tumor progression. For this reason, glycoproteomics and glycomics approaches have found increasing applications in cancer biomarker research[18]. In fact, many clinically relevant cancer biomarkers are glycoproteins, including Her2/neu (breast cancer), prostate-specific antigen (PSA, prostate cancer) and CA 125 (ovarian cancer)[19]. In addition to cancer, several studies have suggested that aberrant glycosylation changes occur in neurodegenerative disorders. Liu *et al* have shown that aberrant glycosylation may modulate the tau protein at a substrate level, stabilizing its phosphorylated isoforms from brains in Alzheimer's disease (AD) patients[20]. Reelin, a glycoprotein that is essential for the correct cytosolic organization of the central nervous system, is up-regulated in the brain and CSF in several neurodegenerative diseases, including frontotemporal dementia, progressive supranuclear palsy, Parkinson's disease (PD) as well as AD[21]. Furthermore, it is found that compared to PrP^{C}, a glycoprotein with two conserved glycosylation sites, PrP^{Sc} has decreased level of bisecting GlcNAc and increased level of tri- and tetraantennary glycans, which indicated a decrease in the activity of an enzyme called *N*-acetylglucosaminyltransferase III[22]. This possible perturbation to the glycosylation machinery of the cells that express prion

proteins might cause changes in other glycosylation events, and lead to glycoprotein profile changes. Therefore, in-depth information extracted from the glycoproteome is useful for understanding the pathogenesis and facilitating diagnosis of prion diseases.

This study shows the utility of glycoprotein enrichment in biomarker discovery for prion disease, enabling the isolation, identification and relative quantification of glycoproteins from blood samples using lectin affinity enrichment, multidimensional separation and tandem mass spectrometry. More than seven hundred proteins were characterized with their relative abundances quantified in mouse plasma. Many of the identified proteins are known to be present at very low abundance, which demonstrates the utility of the approach for revealing low-abundance disease biomarkers. Isotopic labeling and spectral counting quantitation techniques showed strong correlation with each other. A panel of proteins exhibited significant changes in relative abundances at various time points of inoculation, suggesting that the enrichment of glycoprotein sub-proteomes prior to MS analysis may allow for the identification of prion disease biomarkers.

Materials and Methods

Sample preparation

C57/Bl6 mice were inoculated intraperitoneally with 50 µl of 10% brain homogenate derived from mice clinically affected with RML prions or control unaffected mice. At 108, 158 and 198 days post inoculation (dpi), animals were anaesthetized with isoflorane and blood was collected by cardiac puncture into EDTA treated vacutainer tubes. The whole blood was centrifuged at 1000 x g for 5 minutes. Plasma was decanted and immediately frozen in liquid nitrogen for future use.

Materials

Tris hydrochloride, N-acetyl-D-glucosamine, methyl-α-D-mannopyranoside, methyl-α-D-glucopyranoside, manganese chloride tetrahydrate, formaldehyde, deuterated formaldehyde and sodium cyanoborohydride were purchased from Sigma-Aldrich (St. Louis, MO). Sodium chloride, calcium chloride, sodium acetate, urea were obtained from Fisher Scientific (Pittsburgh, PA). Agarose bound Concanavalin A (Con A, 6 mg lectin/ml gel) and Wheat Germ Agglutinin (WGA, 7 mg lectin/ml gel) were purchased from Vector Laboratories (Burlingame, CA). Dithiothreitol (DTT) and sequencing grade modified trypsin were purchased from Promega (Madison, WI). Iodoacetamide was obtained from MP Biomedicals (Solon, OH).

Lectin affinity chromatography

Lectin affinity columns were prepared by adding 400µl each of Con A and WGA slurry to empty Micro Bio-Spin columns (Bio-Rad Laboratories, Hercules, CA). Plasma samples from 7 infected and 7 control mice were separately pooled. 40µl pooled mouse plasma from each group was diluted 10 times with the binding buffer (20 mM Tris, 0.15 M NaCl, 1 mM Ca^{2+}, 1 mM Mn^{2+}, pH 7.4) and loaded onto the lectin affinity column. After shaking for 6 hours the un-retained proteins were discarded and the lectin beads were washed with 2.5 ml binding buffer. The captured glycoproteins were eluted with 2 ml elution buffer (10 mM Tris, 0.075 M NaCl, 0.25 M N-acetyl-D-glucosamine, 0.17 M methyl-α-D-mannopyranoside, and 0.17 M methyl-α-D-glucopyranoside). The eluted fraction was concentrated by a 10kD Centricon Ultracel YM-10 filter (Millipore, Billerica, MA).

Gel electrophoresis

Protein samples were separated with a NuPAGE 10% Bis-Tris Gel and the NuPAGE MOPS SDS buffer (Invitrogen, Carlsbad, CA) at 200 V for 50 min. The manufacturer's instructions were followed. The gel was then stained with SimplyBlue SafeStain (Invitrogen) for 1 hr, and washed with water overnight to increase the band intensity.

Proteolysis

Concentrated samples were denatured with 6 M urea in 0.2 M sodium acetate buffer, pH 8 and reduced by incubating with 10 mM DTT at 37^{o}C for 1 hr. The reduced proteins were alkylated for 1 hr in darkness with 40 mM iodoacetamide. The alkylation reaction was quenched by adding DTT to a final concentration of 50 mM. The samples were diluted to a final concentration of 1 M urea. Trypsin was added at a 50:1 protein to trypsin mass ratio, and the samples were incubated at 37 ^{o}C overnight.

Isotopic labeling

Sodium cyanoborohydride was added to the protein digest to the final concentration of 50mM. Samples were labeled with 0.2 mM formaldehyde or 0.2 mM deuterated-formaldehyde. The mixed peptides were vortexed, incubated at 37 ^{o}C for 1 hr. 2 M NH_4OH was added to quench the reaction and the mixture was immediately dried in Speedvac. The samples were reconstituted in H_2O.

High-pH RP LC

Equal amounts of light and heavy-labeled samples were combined and injected onto a

Rainin HPLC with a high pH-stable RP column (Phenomenex Gemini C18, 150 x 2.1 mm, 3 micron) at a flow rate of 150µl/min. The peptides were eluted with a 40min gradient 5-45% buffer B (Buffer A: 100 mM ammonium formate, pH 10; Buffer B: acetonitrile (ACN)). Fractions were collected every 3 min for 60 min. Collected fractions were dried by Speedvac and reconstituted in 20 µl of 0.1% formic acid. 2 µl of each of the 12 fractions containing peptides were subjected to LC-MS/MS.

LC-MS/MS

A nanoLC system (Eksigent, Dublin, CA) was used to deliver the sample to a trap column and the solvent gradient (Mobile phase A: 0.1% formic acid in H_2O; Mobile phase B: 0.1% formic acid in ACN). Samples were flushed with mobile phase A at 5 µl/min for 3 min and loaded onto a self-packed column (Prosphere HP C18, 100 x 0.15 mm, 3µ). The peptides were eluted via a 5%-40% B gradient in 90min into a nanoelectrospray ionization (nESI) LTQ linear ion trap mass spectrometer (Thermo Electron Corp, San Jose, CA). The LTQ mass spectrometer was operated in a data-dependent mode in which an initial MS scan recorded the mass range of *m/z* 500-2000, and then the six most abundant ions were automatically selected for collision-activated dissociation (CAD). The spray voltage was 3.0 kV. The normalized collision energy was set at 35% for MS/MS.

Imunoblotting

Mouse plasma was boiled in NuPAGE® LDS 4X Sample Buffer (Invitrogen, Carlsbad, CA) and NuPAGE® Reducing Agent (Invitrogen, Carlsbad, CA) for 5 minutes. The proteins in mouse plasma were separated by NuPAGE® Novex 4-12% Bis-Tris Gel (Invitrogen, Carlsbad,

CA), transferred onto nitrocellulose (GE Healthcare, UK) or Immobilon P (Millipore, Billerica, MA) membranes and probed with antibodies against murine serum amyloid protein (SAP) [23-25] or apolipoprotein E (ApoE) (ab40882 or ab20874 respectively, Abcam, Cambridge, MA) Goat anti-rabbit IgG-HRP secondary antibodies were used with luminescent detection (sc-2004, Santa Cruz Biotechnology, Santa Cruz, CA or 170-6515, Bio-Rad Hercules, CA), ECL Plus (GE Healthcare, UK). An equal amount of sample was loaded onto each lane, and equal loading and transfer to nitrocellulose was confirmed by Ponceau S or Coomassie blue staining.

Deglycosylation of SAP

1μl of mouse plasma diluted in 8 μl water was denatured by 1μl of 10X Glycoprotein Denaturing Buffer (New England Biolabs, Ipswich, MA) at 100 °C for 10 minutes. After proteins were denatured, 2 μl of 10XG7 Reaction Buffer (New England Biolabs, Ipswich, MA), 2 μl of 10% NP40, and 1 μl of PNGase F (New England Biolabs, Ipswich, MA) were added. The volume of the reaction system was brought up to 20 μl by adding water. The reaction mixture was incubated at 37 °C for 1 hour.

Data analysis

Raw LTQ data were converted to dta files by Bioworks Browser 3.3 software (Thermo Electron Corp), and searched against the Uniprot/Swiss-Prot *Mus musculus* (mouse) protein database using SEQUEST algorithm. The following parameters were applied during the database search: 2 Dalton precursor mass error tolerance, 1 Dalton fragment mass error tolerance, static modifications of carbamidomethylation for all cysteine residues (+57 Da), dimethylation for the formaldehyde labeled sample (+28 Da) or deuterated-formaldehyde labeled (+32 Da) lysine and

the N-terminus. One missed cleavage site of trypsin was allowed. The following filtering criteria were applied for the protein identification: Xcorr ≥ 1.8 (+1 charge), 2.5 (+2 charge) and 3.5 (+3 charge); $\Delta Cn \geq 0.1$; SEQUEST search Protein Probability < 0.001. Protein identifications were validated by the Trans-Proteomics Pipeline (TPP, Institute for System Biology). The proteins were filtered with a probability of 80% or higher, so that the false positive rates were about 3% for all time points. The relative abundance of each protein was calculated by the XPRESS software embedded in the TPP platform by reconstructing the light and heavy elution profiles of the precursor ions and determining the elution areas of each peak[26]. Open Mass Spectrometry Search Algorithm (OMSSA) developed at the National Center for Biotechnology Information [27] was used to merge the dta files and search the peak list against the Swissprot *Mus musculus* (mouse) protein database. E-value of 0.005 was used to filter the peptides/proteins with higher confidence for relative quantitation by spectral counting. The search results were sorted and the spectral counts of each identified protein were summed by an Excel macro function written in house. Gene ontology analysis of the identified proteins was conducted by the Onto-Express program developed by the Intelligent Systems and Bioinformatics Laboratory[28].

Results and Discussion

Proteomic analysis of plasma is very challenging due to the extreme dynamic range and complexity of proteins in this biofluid. By employing glycoprotein enrichment via lectin affinity chromatography and 2D RP-RPLC prior to tandem MS, we reduces sample complexity, dynamic range and improved separation of peptides. We identified 708 proteins from three time points of disease progression with a false discovery rate of 3% as determined by the ProteinProphet program. Each time point was analyzed in two replicate experiments. The complete list of

identified proteins is shown in the Supplemental Information (Table S1). Figure 1A shows the Venn Diagrams of the numbers of proteins identified from all experiments. 171 proteins were commonly identified in all three time points, whereas 102 proteins were identified in two of the three time points. Among all the proteins identified, more than 80% of the proteins were identified by two or more unique peptides, indicating a comprehensive coverage of the glycoproteome in the blood plasma. 139 proteins (19.6%) were identified with single unique peptides (Figure 1B). We have chosen to include proteins identified with a single unique peptide, because they represent putative biomarkers with a low abundance in the blood proteome, a likely source of surrogate markers of disease. However, extra caution is needed for the validation of these proteins as potential candidate biomarkers.

Glycoprotein enrichment by lectin affinity chromatography

Direct analysis of complex proteomes such as blood plasma by conventional MS-based procedures is challenging because of the presence of very high-abundance proteins. For example, serum albumin is the single most abundant protein in blood, occupying 50% of the protein mass. Albumin's tryptic peptides are over represented in the identified peptide list because the high abundance and large number of albumin tryptic peptides induce signal suppression of peptides from other proteins [29]. Since albumin, along with several other abundant protein species in plasma, are nonglycosylated, they can be readily removed by negative adsorption on lectins, which have affinity to the glycans on glycoproteins [30]. In this study, we utilized this "glyco-catch method," by combining two lectins with broad selectivity on a single column, maximizing the coverage of the glycoproteome. Con A has a high affinity to high-mannose type N-glycans, whereas WGA is selective for N-acetyl-glucosamine (GlcNAc). The effectiveness of the removal

of albumin and other abundant proteins via lectin affinity chromatography was confirmed by gel electrophoresis (data not shown). The lanes of the original plasma sample and the unbound fraction are dominated by just a few bands of proteins. The most dominant band is albumin, which is so abundant that other proteins close to it are obscured. Following glycoprotein enrichment, the elution fraction contains previously bound proteins showed a significant increase in the number of bands. These proteins spanned a wide molecular weight range, especially in the regions previously obscured by albumin. The effectiveness of glycoprotein enrichment can be further demonstrated by the database search results. With lectin selection, albumin no longer appears on the top of the list, although a moderate number of albumin peptides could still be detected, probably due to the non-specific and secondary binding events. We have further tested the combined use of immunodepletion, which removes the seven most abundant proteins in mouse plasma, before lectin affinity enrichment (Data not shown). Although this strategy works well for human blood samples, adding another dimension of depletion does not seem to be very beneficial for mouse blood samples, as the glycoproteins that dominate the MS/MS events such as α-2-macroglobulin and complement C3 precursor, are not removed using commercial mouse blood immunodepletion kits. In addition, by performing immunodepletion one risks losing important low abundance proteins that interact with the seven most abundant proteins.

Many of the 708 proteins identified are known glycoproteins present at low abundance in blood. For example, Figure 2A shows a representative example of MS/MS detection and identification of a tryptic peptide from the epidermal growth factor receptor (EGFR), a protein with a reported plasma abundance as low as 400 ng/ml [31]. EGFR is a known transmembrane glycoprotein with 3 known glycosylation sites and 7 potential glycosylation sites. Figure 2B shows a tryptic peptide from angiotensin-converting enzyme (ACE), another glycoprotein that is

reported to be present in human plasma at about 453.7±159.8 ng/ml [32]. Both EGFR and ACE were identified with multiple distinct peptides. It is commonly observed that most false protein identifications tend to be the ones identified by a single peptide and many proteomic studies routinely discard single peptide identifications to reduce the false discovery rate. Since many glycoproteins exist at very low concentrations and glycopeptides are usually too large to be in the effective detection range of MS, it is likely that glycoproteins would only be identified by a single peptide. The removal of these protein identifications significantly increases the false-negative rate and reduces the overall sensitivity of the analysis. Therefore, single peptide hits were retained in our study as long as they met the probability cutoff from the ProteinProphet. For example, CD44, an integral cell membrane glycoprotein with reported human serum concentration as low as 81ng/ml and known correlation with invasion and metastasis in certain types of human carcinoma[33], was detected with a single unique peptide in our study (Figure 2C). This single peptide was reproducibly identified in both light- and heavy-formaldehyde labeled samples.

Although studies demonstrating the transmission of prion diseases by blood transfusion have suggested that prion proteins are present in the blood of afflicted animals and people [34], they were not detected in our study, most likely due to their extremely low abundance. Efforts are being made to develop more sensitive antibody-based methods to detect disease-associated prion aggregate in the blood as an alternative to the traditional postmortem test in the brain [35]. Because prion protein is glycosylated [36], our glycoprotein enrichment protocol has the potential to detect it if increased sensitivity could be achieved by the use of optimized separation and MS detection.

High-pH RPLC

Multidimensional separations have been employed in proteomics studies to reduce the complexity of the samples[37]. Instead of using the popular strong cation exchange chromatography (SCX) as the first dimension, we used RPLC in both dimensions of separation under dramatically different pH conditions. Our lab has successfully adopted this scheme to enhance rat neuropeptide detection[38]. The first and second dimensions exhibit great orthogonality in peptide separations due to charge changes in acidic and basic amino acid side chains under different pH conditions. Under high pH condition, the basic amino acids are neutral while the acidic ones are in negative charge state. In contrast, at low pH condition, the acidic amino acids remain neutral and the basic amino acids turn positively charged. Using RP as the first dimension bears several advantages: (i) high resolution permits collections of fractions with minimal overlap; (ii) higher recovery of peptides compared to SCX; (iii) the use of salt is minimal [39]. The effectiveness of peptide separation by this method is demonstrated in Figure 3. Although there is a slight migration of elution time profiles, as the peptides eluting earlier in the first RPLC dimension tend to elute earlier in the second dimension as well, the widespread of peaks in all 12 fractions in the second dimension provides great resolution to enhance the proteomic detection. The co-elution of light- and heavy-labeled peptide pairs has also been achieved by this 2D RP-RP method.

Assessment of reproducibility of relative quantitation

The isotopic labeling technique we used in this study is based on the reductive dimethylation of peptide primary amine groups (lysine or N-terminus) with formaldehyde and deuterated formaldehyde in the presence of reducing agent such as cyanoborohydride[40]. A mass

difference of 4 Da is produced for each labeling pair. The reaction is fast, easy to perform, and has been shown to be quantitative and free of detectable by-products[40]. At the peptide level, as expected, the distribution of all the isotopic-labeled peptide ratios exhibits a Gaussian profile, with the mean ratio of all the quantified tryptic peptides close to 1 (0.96), with a small standard deviation (SD) of 0.14, suggesting that the majority of the blood plasma glycoproteins remained unchanged despite different pathophysiological conditions. The ProteinProphet program integrates the quantitative information calculated from the spectra and the mean values of the ratios plus standard deviations are calculated for each protein expression value when multiple peptide measurements are available. Even though a large variation of relative quantitative ratios was observed at the peptide level, run-to-run variation between the replicate experiments at the protein level was well-controlled because the contribution from multiple peptides to the quantitation significantly lowers the effect of individual variation. Likewise proteins identified by a single peptide peak need to be interpreted with caution as their quantitation is highly variable.

Figure 4 A-C illustrates the distribution of the heavy-to-light ratios in log2 scale for individual time points at the protein level. Threshold levels for significantly up- or down-regulated proteins are set to be 2-fold (+/-1 in log2 scale). The log2 ratio values of 86-91% of the proteins identified from individual time points fall between -1 and +1. Figure 4 D-F displays the distribution of SD for the protein ratios detected at each time point. Overall, the mean SD of protein ratios is 0.26. The 171 proteins commonly identified at all time points displayed even lower variance, as these are among the most abundant proteins producing multiple unique peptides with high intensities. Overall, 90.5% of all the quantified proteins had a SD less than 0.5, a reasonably good measure of quantitative reproducibility in quantitative proteomic experiments

for plasma biomarker discovery, taking into account of the underlying variation due to the multiple experimental steps[41]. A caveat to keep in mind when generating a panel of biomarker candidates from the proteins with large ratio changes is that those proteins tend to have relatively higher SD. Therefore one should conservatively interpret those displaying a higher SD and manually verify the quality and validity of the quantitative data.

In order to assess the validity of our quantitation study by isotopic labeling, we employed spectral counting to cross-check the protein ratios on the dataset collected at 158dpi. Spectral counting is based on the hypothesis that the MS/MS sampling rate of a particular protein, i.e. the number of tryptic peptides from a protein selected for collision induced dissociation (CID) in a large data set, is directly related to the abundance of the parent protein. Zybailov *et al*. recently compared quantitative MudPIT (multidimensional protein identification technology) results using spectral counting and stable isotope peak intensity to calculate protein expression ratios and demonstrated strong positive correlation between the two approaches[42]. Consistent with the work of Zybailov *et al*., the quantitation results we observed from spectral counting positively correlated with those from extracted ion chromatograms of isotopically labeled peptide pairs. For example, in our study haptoglobin precursor was elevated more than 3-fold in the light form (SC_{Light} : SC_{Heavy} = 3.2), as determined by the spectral counting approach. A representative tryptic peptide LKYVMLPVADQDK was shown to have a XIC_{Light} : XIC_{Heavy} = 3.8 ratio from the extracted ion chromatograms of isotopic labeled pairs. Similarly, for hemoglobin (Hb) alpha chain, it is calculated that SC_{Light} : SC_{Heavy} = 3.8 , which strongly correlates with the isotopic labeling result that XIC_{Light} : XIC_{Heavy} = 3.8 for the tryptic peptide TYFPHFDVSHGSAQVK. Interestingly, both haptoglobin and Hb are acute response proteins and it is well-known that the complex of haptoglobin and Hb is elevated in sera in response to inflammation[43]. Note that Hb

protein is not glycosylated and it is likely that it has survived the lectin selection process by the formation of a complex with the glycoprotein haptoglobin. The calculation of the extracted ion chromatograms were performed by the PepQuan function of Bioworks software. Calculations of haptoglobin and hemoglobin by the XPRESS based algorithm, however, identified a 2.4 and 1.9 fold up-regulation respectively in the 158dpi samples, indicating that the XPRESS algorithm generates more conservative quantitation results than could be obtained directly from extracted ion chromatograms. This conservation makes those proteins exceeding the 2-fold threshold more likely to have dramatic changes in the diseased conditions. Overall, the two quantitation techniques, quantifying extracted chromatograms and spectral counting, positively correlate with each other and provide complementary means to cross validate quantitative results. Although spectral counting is convenient, free from isotope labeling procedures and is reported to provide a greater dynamic range of quantitation compared with stable isotopic labeling strategies, the results can be unreliable for proteins at low abundance since only a small number of peptide identifications are used for quantitation. On a number of occasions we have observed that the results obtained from isotopic labeling outperformed those from spectral counting for proteins with low counts. For peptides identified with both isotopic forms, extracted ion chromatograms gave better accuracy in measuring the relative quantity. Since potential biomarkers are likely to be proteins with low abundance and quantitation accuracy and reproducibility are key factors, we utilized the isotope labeling approach for quantitation.

The consistency of glycoprotein enrichment across different samples, which is important for accurate quantitation of potential biomarkers, has been demonstrated in our previous work by spiking chicken ovalbumin into mouse plasma as an internal standard[44]. All the tryptic peptides identified from the spiked ovalbumin were averaged to give a 1.1:1 ratio for isotopically-labeled

pairs, a 10% error for such a multi-step procedure.

Among the 708 total proteins identified at all three time points, 53 proteins (7.5%) were increased more than two-fold in one or more time points, whereas 58 proteins (8.2%) had more than a 2-fold decrease. The lists of these two groups are illustrated in Table S3. It is not surprising that the majority of proteins exhibiting large fold changes are not shared amongst the three time points, as many differentially-regulated proteins are at very low abundances, which are not detected in great reproducibility due to the inherent limits of this methodology originating from the multi-step sample processing, the dynamic range of detection and the random precursor selection in the MS/MS analysis.

Biological Significance

Gene ontology analysis of proteins listed in Table S3 revealed that more than 75% of the proteins with significant changes are involved in binding, which was in agreement with the percentage of all identified proteins that are related to binding (78.5%) (Figure 5). More than 30% from both groups have catalytic activities. About three quarters of the up-regulated proteins are involved in cellular processes, whereas the percentage of down-regulated proteins in this category is significantly lower. It is interesting to note that the proteins responsible for positive regulation of biological process are enriched in the up-regulated pool, whereas those responsible for negative regulation of biological process are enriched in the down-regulated pool. This suggests that certain biological processes are either enhanced or less inhibited with the onset of prion disease.

One up-regulated protein in prion infected samples that also positively regulates biological process is apolipoprotein E (ApoE). In this study, ApoE has been shown to be up-

regulated constantly throughout all the three time points, with changes of 3.3, 8.3 and 2.7-fold, respectively. Although murine ApoE is not a known glycoprotein, the well-known hydrophobic binding property of Con A in addition to its lectin-glycan interaction[45] may lead to the reproducible isolation of ApoE. Another possible mechanism of ApoE isolation is the formation of protein complex, similar to that of the aforementioned hemoglobin-haptoglobin complex.

ApoE is the major component of the very low density lipoproteins (VLDL), whose function is to remove excess cholesterol from the blood and transport it to the liver for processing. In the nervous system, non-neuronal cell types such as astroglia and microglia are the primary producers of ApoE, while neurons preferentially express the receptors for this protein. The role of ApoE in the nervous system is thought to be involved in nerve growth, regeneration and neuronal repair[46]. ApoE is associated with age-related risk for Alzheimer's disease (AD) and plays critical roles in Aβ homeostasis. Research has suggested that ApoE acts both within microglia and in the extracellular space to affect the clearance of Aβ through promoting its proteolysis. Importantly, the ApoE4 isoform exhibits an impaired ability to promote Aβ proteolysis, resulting in increased vulnerability to AD in individuals with that gene variation[47]. Several studies have reported the involvement of ApoE with TSE progression. Elevated ApoE concentrations have been reported in the brains of scrapie infected mice and has been detected in some prion protein aggregates[48]. Choe *et al*. have shown increased concentration of ApoE in the CSF of patients with vCJD as compared to sporadic CJD (sCJD)[49]. Despite the long-established relationship between ApoE and prion diseases, the sample sources of previous studies have been limited to brain and CSF, which are not as accessible compared to blood. The earliest time point of elevated ApoE concentration can be used as a useful diagnosis that has not been previously established. To the best of our knowledge, our study is the first report on the elevated

concentration of ApoE from blood plasma at different time points during prion disease onset and progression.

As discussed, the 171 proteins commonly found in all time points mainly represent those present at relatively higher abundance and thus may have a lower chance to be used as potential biomarkers of lower abundance. Therefore, it is of equal importance to look for significant changes in other parts of the Venn diagram. Among the significantly changed proteins that were only detected in two of the three time points, serum amyloid P-component (SAP) has drawn our attention. SAP was characterized 7 unique peptides at 108 days and 4 peptides at 158 post inoculation (Table S1 & Table S3). Representative spectra for two peptides, VGEYSLYIGQSK and SQSLFSYSVK from 108 and 158dpi are shown in Figure 6. Overall, SAP was significantly elevated in the mass spectra of infected 108dpi samples by 3.4 fold (Table S3), but not in 158dpi samples (Table S1). SAP is a 204-residue secreted glycoprotein present at low abundance (30-45 μg/ml in plasma) with a single N-glycosylation site at position 51. SAP is associated *in vivo* with all types of amyloid deposits, and it is now believed that the tissue accumulation of SAP in various types of amyloids is due to its particular affinity for the amyloid molecules[50]. SAP has also been found to co-localize with neurofibrillary pathology in various neurodegenerative diseases including AD, Creutzfedt-Jacob disease (CJD), PD, and diffuse Lewy body disorders[51-53]. It is suggested that SAP may contribute to the failure of clearance of amyloid deposits *in vivo*, causing tissue damage and disease, which has made it a new therapeutic target to both systemic amyloidosis and diseases associated with local amyloid deposits including AD[54].

To validate our observation in quantitative MS experiments, Western blotting was performed using a well-established anti-SAP antibody[23-25] with plasma samples from all three time points (Figure 7A). Interestingly, the Western blot experiments showed two bands at 26 kDa

and 30 kDa, respectively. The intensity of the 26 kDa band remains relatively constant regardless of the physiological status, whereas the level of the heavy band was significantly elevated from the infected sample at 108dpi. Previously, using mink, Husby and coworkers identified for the first time the non-glycosylated SAP from a mammalian species[55]. Therefore we speculated that the two bands corresponded to the mono- and un-glycosylated forms, respectively. This was confirmed by deglycosylating the proteins using PNGase F digestion, which cleaves N-glycans. The molecular weight of the heavy band changed to its light counterpart after cleavage (Figure 7B), further supporting the band assignment. We conclude that the observed 3.4 fold elevation of SAP in the MS analysis was solely due to the increase in glycosylated SAP from infected samples at 108dpi, whereas the level of non-glycosylated isoform remained relatively stable. The glycosylated SAP returned to its normal level with the progression of the disease. The faint heavy bands at 198dpi attributed to the failure of MS detection of SAP at that time point. The reproduction of the glycoproteomic result for SAP using immunoblotting and PNGase F treatment strongly validates the lectin fractionation and subsequent MS-based quantitative proteomic approach. While the underlying mechanism leading to the elevation of the glycosylated form and its particular trend at different time points is unclear at this point, this study provides a basis for further investigation on SAP as a potential biomarker and its pathological role in the progression of prion disease.

Our finding that a number of proteins exhibited altered expression either qualitatively or quantitatively in the plasma samples collected from inoculated animals suggests a molecular link of these proteins with disease onset and progression. This MS-based global analysis of glycoproteins in plasma samples provides a new opportunity for quantitative examination of proteins from diseased samples and investigation of the pathological mechanisms underlying

their changes in abundance.

Conclusions

In summary, we have successfully developed an analytical platform that can readily detect and quantify glycoproteins in complex biofluid samples to facilitate the biomarker discovery for prion diseases. By applying this platform 708 proteins were identified and relatively quantified. Spectral counting and isotopic labeling quantitation positively correlated with each other and was useful to cross-validate quantitation. A protein list was generated, which can serve as a reference for future prion disease biomarker investigation. Western blot validation was performed on Serum Amyloid Protein, suggesting its potential use as a biomarker for prion disease. Further quantitative validations of the proteins exhibiting significant changes, either using MS-based multiple reaction monitoring (MRM), or antibody based measurements, are likely to reveal more information on the correlation of these proteins to prion disease state. This comparative glycoproteomic methodology offers significant promise in the search for low-abundance, glycosylated disease biomarkers.

In the future, immuno-depletion of the most abundant proteins prior to lectin selection will be further explored. Different lectin combinations with various selectivities towards glycan structures can enrich for different profiles of the serum glycoproteome and provides more information on the changes of the glycoproteome with prion disease. Once a panel of proteins can be detected with reproducible changes by mass spectrometry, other methods such as antibody-based assays will be required for validation before the candidates could be useful in diagnostic assays.

Acknowledgement

We thank University of Wisconsin Human Proteomics Program for access to the LTQ instrument. This work was supported in part by National Institutes of Health through grant AI0272588 and the Wisconsin Alumni Research Foundation at the University of Wisconsin-Madison. L.L. acknowledges an Alfred P. Sloan Research Fellowship. We thank Dr. Timothy Heath for writing the Excel macro function for spectral counting.

References

1. Borchelt, D. R.; Scott, M.; Taraboulos, A.; Stahl, N.; Prusiner, S. B., Scrapie and Cellular Prion Proteins Differ in Their Kinetics of Synthesis and Topology in Cultured-Cells. *Journal of Cell Biology* **1990,** 110, (3), 743-752.
2. Caughey, B.; Race, R. E.; Ernst, D.; Buchmeier, M. J.; Chesebro, B., Prion Protein-Biosynthesis in Scrapie-Infected and Uninfected Neuro-Blastoma Cells. *Journal of Virology* **1989,** 63, (1), 175-181.
3. Chesebro, B.; Race, R.; Wehrly, K.; Nishio, J.; Bloom, M.; Lechner, D.; Bergstrom, S.; Robbins, K.; Mayer, L.; Keith, J. M., *Nature* **1985,** 315, 331.
4. Oesch, B.; Westaway, D.; Walchli, M.; McKinley, M. P.; Kent, S. B.; Aebersold, R.; Barry, R. A.; Tempst, P.; Teplow, D. B.; Hood, L. E., *Cell* **1985,** 40, 735.
5. Schaller, O., Fatzer, R., Stack, M., Clark, J., Cooley, W., Biffiger, K., Egli, S., Doherr, M., Vandevelde, M., Heim, D., Oesch, B., and Moser, M., Validation of a western immunoblotting procedure for bovine PrP(Sc) detection and its use as a rapid surveillance method for the diagnosis of bovine spongiform encephalopathy (BSE). *Acta Neuropathologica* **1999,** 98, 7.
6. Burkhard, P. R.; Sanchez, J. C.; Landis, T.; Hochstrasser, D. F., *Neurology* **2001,** 56, 1528.
7. Choe, L. H.; Green, A.; Knight, R. S.; Thompson, E. J.; Lee, K. H., *Electrophoresis.* **2002,** 23, 2242.
8. Otto, M.; Wiltfang, J.; Cepek, L.; Neumann, M.; Mollenhauer, B.; Steinacker, P.; Ciesielczyk, B.; Schulz-Schaeffer, W.; Kretzschmar, H. A.; Poser, S., *Neurology* **2002,** 58, 192.
9. Parveen, I.; Moorby, J.; Allison, G.; Jackman, R., *Vet. Res.* **2005,** 36, 665.
10. Sanchez, J. C.; Guillaume, E.; Lescuyer, P.; Allard, L.; Carrette, O.; Scherl, A.; Burgess, J.; Corthals, G. L.; Burkhard, P. R.; Hochstrasser, D. F., *Proteomics.* **2004,** 4, 2229.
11. Van Everbroeck, B.; Boons, J.; Cras, P., *Clin. Neurol. Neurosurg.* **2005,** 107, 355.
12. Zerr, I.; Bodemer, M.; Otto, M.; Poser, S.; Windl, O.; Kretzschmar, H. A.; Gefeller, O.; Weber, T., *Lancet* **1996,** 348, 846.
13. Rifai, N.; Gillette, M. A.; Carr, S. A., Protein biomarker discovery and validation: the long and uncertain path to clinical utility. *Nat Biotech* **2006,** 24, (8), 971-983.
14. Madera, M.; Mechref, Y.; Klouckova, I.; Novotny, M. V., High-sensitivity profiling of glycoproteins from human blood serum through multiple-lectin affinity chromatography and liquid chromatography/tandem mass spectrometry. *Journal of Chromatography B* **2007,** 845, (1), 121-137.
15. Yang, Z.; Harris, L. E.; Palmer-Toy, D. E.; Hancock, W. S., Multilectin Affinity Chromatography for Characterization of Multiple Glycoprotein Biomarker Candidates in Serum from Breast Cancer Patients. *Clin Chem* **2006,** 52, (10), 1897-1905.
16. Qiu, R.; Regnier, F. E., Use of Multidimensional Lectin Affinity Chromatography in Differential Glycoproteomics. *Anal. Chem.* **2005,** 77, (9), 2802-2809.
17. Bertozzi, C. R.; Kiessling, L. L., Chemical Glycobiology. *Science* **2001,** 291, (5512), 2357-2364.
18. Wei, X.; Li, L., Comparative glycoproteomics: approaches and applications. *Brief Funct Genomic Proteomic* **2009,** 8, (2), 104-113.
19. Diamandis, E. P., Mass Spectrometry as a Diagnostic and a Cancer Biomarker Discovery Tool: Opportunities and Potential Limitations. *Mol Cell Proteomics* **2004,** 3, (4), 367-378.
20. Liu, F.; Iqbal, K.; Grundke-Iqbal, I.; Hart, G. W.; Gong, C.-X., O-GlcNAcylation regulates phosphorylation of tau: A mechanism involved in Alzheimer's disease. *Proceedings of the National Academy of Sciences* **2004,** 101, (29), 10804-10809.
21. Botella-Lopez, A.; Burgaya, F.; Gavin, R.; Garcia-Ayllon, M. S.; Gomez-Tortosa, E.; Pena-Casanova, J.; Urena, J. M.; Del Rio, J. A.; Blesa, R.; Soriano, E.; Saez-Valero, J., Reelin expression and glycosylation patterns are altered in Alzheimer's disease. *Proceedings of the National Academy of Sciences of the United States of America* **2006,** 103, (14), 5573-5578.
22. Rudd, P. M.; Endo, T.; Colominas, C.; Groth, D.; Wheeler, S. F.; Harvey, D. J.; Wormald, M. R.; Serban, H.; Prusiner, S. B.; Kobata, A.; Dwek, R. A., Glycosylation differences between the normal and pathogenic prion protein isoforms. *Proceedings of the National Academy of Sciences of the United States of America* **1999,** 96, (23), 13044-13049.
23. Hutchinson, W. L.; Noble, G. E.; Hawkins, P. N.; Pepys, M. B., The pentraxins, C-reactive protein and serum amyloid P component, are cleared and catabolized by hepatocytes in vivo. *J Clin Invest* **1994,** 94, (4), 1390-6.
24. Mold, C.; Baca, R.; Du Clos, T. W., Serum amyloid P component and C-reactive protein opsonize apoptotic cells for phagocytosis through Fcgamma receptors. *J Autoimmun* **2002,** 19, (3), 147-54.

25. Togashi, S.; Lim, S. K.; Kawano, H.; Ito, S.; Ishihara, T.; Okada, Y.; Nakano, S.; Kinoshita, T.; Horie, K.; Episkopou, V.; Gottesman, M. E.; Costantini, F.; Shimada, K.; Maeda, S., Serum amyloid P component enhances induction of murine amyloidosis. *Lab Invest* **1997,** 77, (5), 525-31.
26. Han, D. K.; Eng, J.; Zhou, H.; Aebersold, R., Quantitative profiling of differentiation-induced microsomal proteins using isotope-coded affinity tags and mass spectrometry. *Nat Biotech* **2001,** 19, (10), 946-951.
27. Geer, L. Y.; Markey, S. P.; Kowalak, J. A.; Wagner, L.; Xu, M.; Maynard, D. M.; Yang, X.; Shi, W.; Bryant, S. H., Open Mass Spectrometry Search Algorithm. *J. Proteome Res.* **2004,** 3, (5), 958-964.
28. Khatri, P.; Draghici, S.; Ostermeier, G. C.; Krawetz, S. A., Profiling Gene Expression Using Onto-Express. *Genomics* **2002,** 79, (2), 266-270.
29. Ramstrom, M.; Hagman, C.; Mitchell, J. K.; Derrick, P. J.; Hakansson, P.; Bergquist, J., Depletion of high-abundant proteins in body fluids prior to liquid chromatography fourier transform ion cyclotron resonance mass spectrometry. *Journal of Proteome Research* **2005,** 4, (2), 410-416.
30. Brzeski, H.; Katenhusen, R. A.; Sullivan, A. G.; Russell, S.; George, A.; Somiari, R. I.; Shriver, C., Albumin depletion method for improved plasma glycoprotein analysis by two-dimensional difference gel electrophoresis. *Biotechniques* **2003,** 35, (6), 1128-32.
31. Baron, A. T.; Lafky, J. M.; Boardman, C. H.; Balasubramaniam, S.; Suman, V. J.; Podratz, K. C.; Maihle, N. J., Serum sErbB1 and epidermal growth factor levels as tumor biomarkers in women with stage III or IV epithelial ovarian cancer. *Cancer Epidemiology Biomarkers & Prevention* **1999,** 8, (2), 129-137.
32. Edmund, A. W.; Brice, M. B.; Friedlander, W.; Bateman, E. D.; Kirsch, R. E., Serum Angiotensin-Converting Enzyme Activity, Concentration, and Specific Activity in Granulomatous Interstitial Lung Disease, Tuberculosis, and COPD. *Chest* **1995,** 107, (3), 706-710.
33. Hiroaki, S.; Shunichi, T.; Kuniyuki, K.; Masahide, I.; Michio, M.; Nobuaki, K., Serum concentration of CD44 variant 6 and its relation to prognosis in patients with gastric carcinoma. *Cancer* **1998,** 83, (6), 1094-1101.
34. Hunter, N.; Foster, J.; Chong, A.; McCutcheon, S.; Parnham, D.; Eaton, S.; MacKenzie, C.; Houston, F., Transmission of prion diseases by blood transfusion. *Journal of General Virology* **2002,** 83, 2897-2905.
35. Chang, B. G.; Cheng, X.; Yin, S. M.; Pan, T.; Zhang, H. T.; Wong, P. K.; Kang, S. C.; Xiao, F.; Yan, H. M.; Li, C. Y.; Wolfe, L. L.; Miller, M. W.; Wisniewski, T.; Greene, M. I.; Sy, M. S., Test for detection of disease-associated prion aggregate in the blood of infected but asymptomatic animals. *Clinical and Vaccine Immunology* **2007,** 14, (1), 36-43.
36. Rudd, P. M.; Merry, A. H.; Wormald, M. R.; Dwek, R. A., Glycosylation and prion protein. *Current Opinion in Structural Biology* **2002,** 12, (5), 578-586.
37. Fournier, M. L.; Gilmore, J. M.; Martin-Brown, S. A.; Washburn, M. P., Multidimensional separations-based shotgun proteomics. *Chemical Reviews* **2007,** 107, (8), 3654-3686.
38. Dowell, J. A.; VanderHeyden, W.; Li, L., Rat Neuropeptidomics by LC-MS/MS and MALDI-FTMS: Enhanced Dissection and Extraction Techniques Coupled with 2D RP-RP HPLC. *J. Proteome Res.* **2006,** 5, (12), 3368-3375.
39. Gilar, M.; Olivova, P.; Daly, A. E.; Gebler, J. C., Two-dimensional separation of peptides using RP-RP-HPLC system with different pH in first and second separation dimensions. *Journal of Separation Science* **2005,** 28, (14), 1694-1703.
40. Hsu, J. L.; Huang, S. Y.; Chow, N. H.; Chen, S. H., Stable-Isotope Dimethyl Labeling for Quantitative Proteomics. *Anal. Chem.* **2003,** 75, (24), 6843-6852.
41. Song, X.; Bandow, J.; Sherman, J.; Baker, J. D.; Brown, P. W.; McDowell, M. T.; Molloy, M. P., iTRAQ Experimental Design for Plasma Biomarker Discovery. *Journal of Proteome Research* **2008,** 7, (7), 2952-2958.
42. Zybailov, B.; Coleman, M. K.; Florens, L.; Washburn, M. P., Correlation of Relative Abundance Ratios Derived from Peptide Ion Chromatograms and Spectrum Counting for Quantitative Proteomic Analysis Using Stable Isotope Labeling. *Anal. Chem.* **2005,** 77, (19), 6218-6224.
43. Watanabe, J.; Grijalva, V.; Hama, S.; Barbour, K.; Berger, F. G.; Navab, M.; Fogelman, A. M.; Reddy, S. T., Hemoglobin and Its Scavenger Protein Haptoglobin Associate with ApoA-1-containing Particles and Influence the Inflammatory Properties and Function of High Density Lipoprotein. *Journal of Biological Chemistry* **2009,** 284, (27), 18292-18301.
44. Wei, X.; Herbst, A.; Schmidt, J.; Aikent, J.; Li, L. J., Facilitating Discovery of Prion Disease Biomarkers by Quantitative Glycoproteomics. *Lc Gc North America* **2009,** 27, (2), 154-162.
45. Edelman, G. M.; Wang, J. L., Binding and functional properties of concanavalin A and its derivatives. III. Interactions with indoleacetic acid and other hydrophobic ligands. *Journal of Biological Chemistry* **1978,** 253, (9), 3016-3022.
46. Holtzman, D. M.; Pitas, R. E.; Kilbridge, J.; Nathan, B.; Mahley, R. W.; Bu, G.; Schwartz, A. L., Low

density lipoprotein receptor-related protein mediates apolipoprotein E-dependent neurite outgrowth in a central nervous system-derived neuronal cell line. *Proceedings of the National Academy of Sciences of the United States of America* **1995,** 92, (21), 9480-9484.

47. Jiang, Q.; Lee, C. Y. D.; Mandrekar, S.; Wilkinson, B.; Cramer, P.; Zelcer, N.; Mann, K.; Lamb, B.; Willson, T. M.; Collins, J. L.; Richardson, J. C.; Smith, J. D.; Comery, T. A.; Riddell, D.; Holtzman, D. M.; Tontonoz, P.; Landreth, G. E., ApoE Promotes the Proteolytic Degradation of Aβ. *Neuron* **2008,** 58, (5), 681-693.

48. Diedrich, J. F.; Minnigan, H.; Carp, R. I.; Whitaker, J. N.; Race, R.; Frey, W.; Haase, A. T., Neuropathological Changes in Scrapie and Alzheimers-Disease Are Associated with Increased Expression of Apolipoprotein-E and Cathepsin-D in Astrocytes. *Journal of Virology* **1991,** 65, (9), 4759-4768.

49. Leila, H. C.; Alison, G.; Richard, S. G. K.; Edward, J. T.; Kelvin, H. L., Apolipoprotein E and other cerebrospinal fluid proteins differentiate ante mortem variant Creutzfeldt-Jakob disease from ante mortem sporadic Creutzfeldt-Jakob disease. *Electrophoresis* **2002,** 23, (14), 2242-2246.

50. Pepys, M. B.; Booth, D. R.; Hutchinson, W. L.; Gallimore, J. R.; Collins, P. M.; Hohenester, E., Amyloid P component. A critical review. *Amyloid-Journal of Protein Folding Disorders* **1997,** 4, (4), 274-295.

51. Kalaria, R. N.; Golde, T. E.; Cohen, M. L.; Younkin, S. G., Serum Amyloid-P in Alzheimers-Disease - Implications for Dysfunction of the Blood-Brain-Barrier. *Annals of the New York Academy of Sciences* **1991,** 640, 145-148.

52. Akiyama, H.; Yamada, T.; Kawamata, T.; McGeer, P. L., Association of Amyloid-P Component with Complement Proteins in Neurologically Diseased Brain-Tissue. *Brain Research* **1991,** 548, (1-2), 349-352.

53. Coria, F.; Castano, E.; Prelli, F.; Larrondolillo, M.; Vanduinen, S.; Shelanski, M. L.; Frangione, B., Isolation and Characterization of Amyloid P-Component from Alzheimers-Disease and Other Types of Cerebral Amyloidosis. *Laboratory Investigation* **1988,** 58, (4), 454-458.

54. Pepys, M. B.; Herbert, J.; Hutchinson, W. L.; Tennent, G. A.; Lachmann, H. J.; Gallimore, J. R.; Lovat, L. B.; Bartfai, T.; Alanine, A.; Hertel, C.; Hoffmann, T.; Jakob-Roetne, R.; Norcross, R. D.; Kemp, J. A.; Yamamura, K.; Suzuki, M.; Taylor, G. W.; Murray, S.; Thompson, D.; Purvis, A.; Kolstoe, S.; Wood, S. P.; Hawkins, P. N., Targeted pharmacological depletion of serum amyloid P component for treatment of human amyloidosis. *Nature* **2002,** 417, (6886), 254-259.

55. Omtvedt, L. A.; Wien, T. N.; Myran, T.; Sletten, K.; Husby, G., Serum amyloid P component in mink, a non-glycosylated protein with affinity for phosphorylethanolamine and phosphorylcholine. *Amyloid-Journal of Protein Folding Disorders* **2004,** 11, (2), 101-108.

Figure Captions:

Figure 1. Number of proteins identified from all time points. (A) Venn diagram of the number of proteins identified at each time point after inoculation with 171 commonly identified in all three points; (B) Distribution of proteins identified by different numbers of unique peptides. More than 80% of total proteins were identified with multiple unique peptides.

Figure 2. Tandem mass spectra of tryptic peptides from representative low-abundance glycoproteins identified in the global glycoproteomic analysis of serum samples. (A) Tryptic peptide CNILEGEPR from epidermal growth factor receptor; (B) Tryptic peptide SLYESDNLEQDLEK from angiotensin-converting enzyme; (C) The single tryptic peptide YGFIEGNVVIPR identified from CD44.

Figure 3. Chromatograms of the 2nd dimension of HPLC separation. Each of the 12 fractions was obtained from 3 min collection of the 1st dimension of high-pH reversed phase HPLC separation. Great orthogonality was achieved between the two dimensions.

Figure 4. The log2 ratios between infected (Heavy) and control samples (Light) at each time points (A: 108dpi; B: 158dpi; C: 198dpi) and the distribution of the standard deviations for each ratio (D: 108dpi; E: 158dpi; F: 198dpi). The standard deviations are calculated from the ratios of the peptides contributing to each individual protein.

Figure 5. Molecular function (MF) and biological process (BP) comparisons of the up- and down-regulated proteins. Gene ontology analysis was performed by Onto-Express

(http://vortex.cs.wayne.edu/ontoexpress).

Figure 6. Identification of serum amyloid P-component (SAP) as a putative biomarker in prion disease. (A) and (B): Representative tryptic peptides from SAP. (C): Extracted ion chromatograms of SAP peptides indicate elevated concentration in the infected samples.

Figure 7. Validation of MS-based glycoproteomic approach using Western blotting analysis and enzymatic treatment. (A) Immunoblotting for Serum Amyloid Protein (SAP). 2μl mouse plasma from control uninfected (U) and infected (I) groups on 108, 158 and 198 days post-inoculation (dpi) were separated by SDS-PAGE and analyzed by Western blotting with anti-SAP antibody. Two forms of SAP were detected. (B) Glycosylated SAP is up-regulated at 108 dpi in infected mice. 1μl or 2μl mouse plasma from both control uninfected (U) and infected (I) group on 108dpi were treated by PNGase F or left untreated. The mouse plasma were then separated by SDS-PAGE and analyzed by Western blotting with anti-SAP antibody. After PNGase F treatment, the band with molecular weight of 30KDa shifted to 26KDa, confirming that the glycosylated SAP is elevated in the infected group.

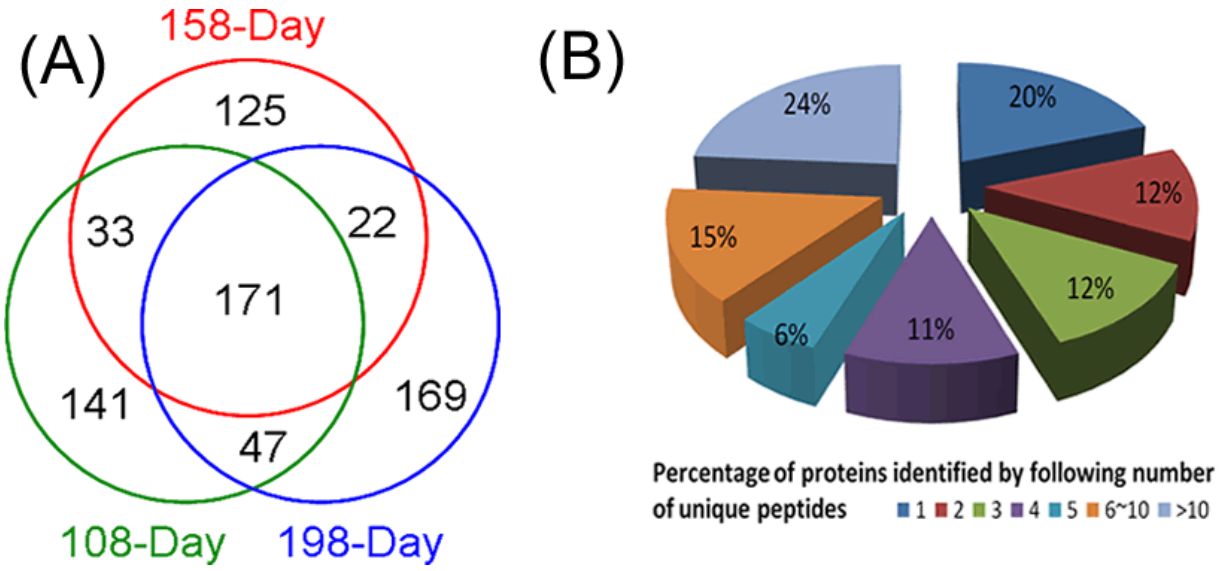
(A)
158-Day
125
33
22
171
141
169
47
108-Day
198-Day
(B)
24%
20%
12%
15%
12%
6%
11%
Percentage of proteins identified by following number of unique peptides
1 2 3 4 5 6~10 >10

Figure 1.

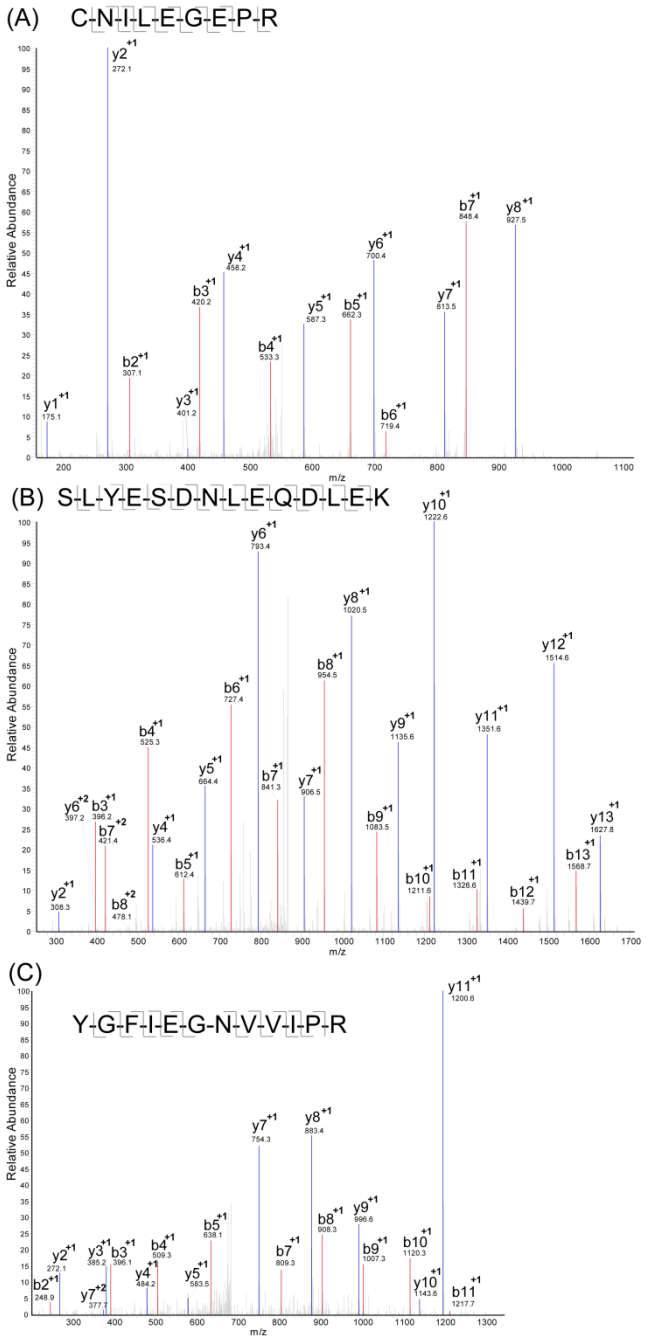
(A) C-N-I-L-E-G-E-P-R
(B) S-L-Y-E-S-D-N-L-E-Q-D-L-E-K
(C) Y-G-F-I-E-G-N-V-V-I-P-R
Relative Abundance
m/z

Figure 2.

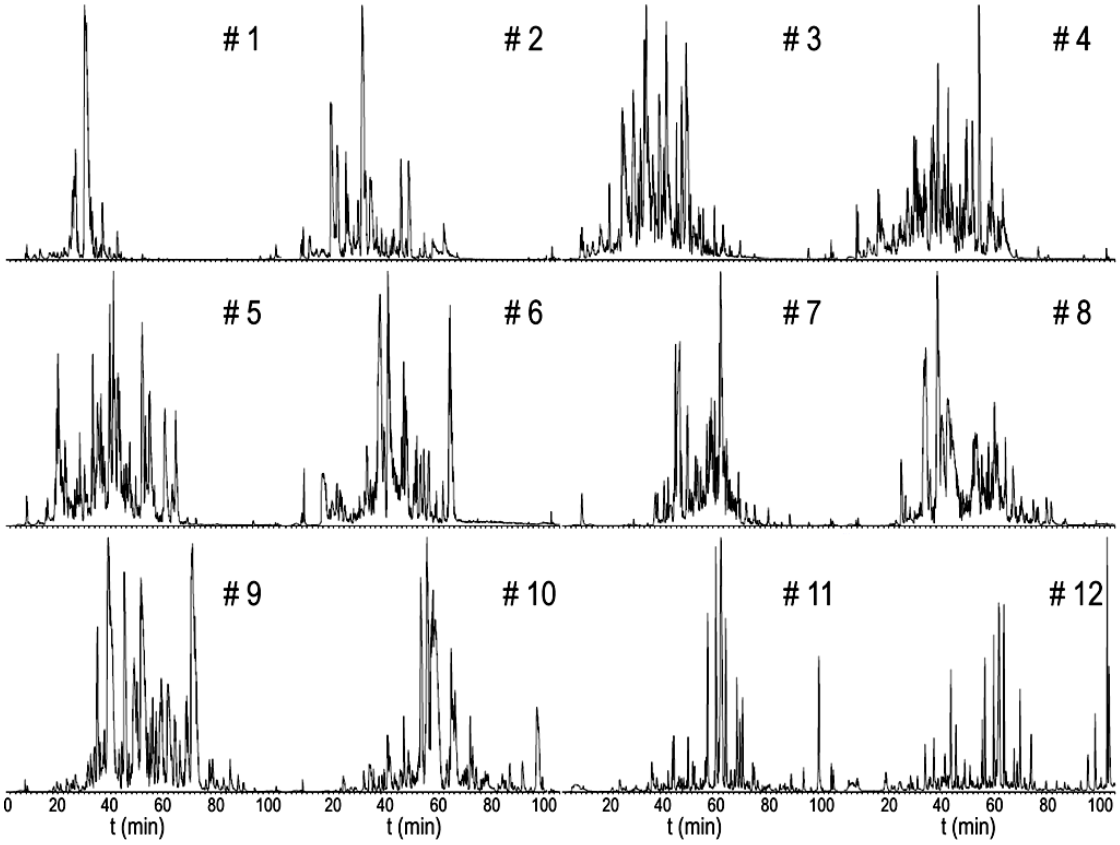

Figure 3.

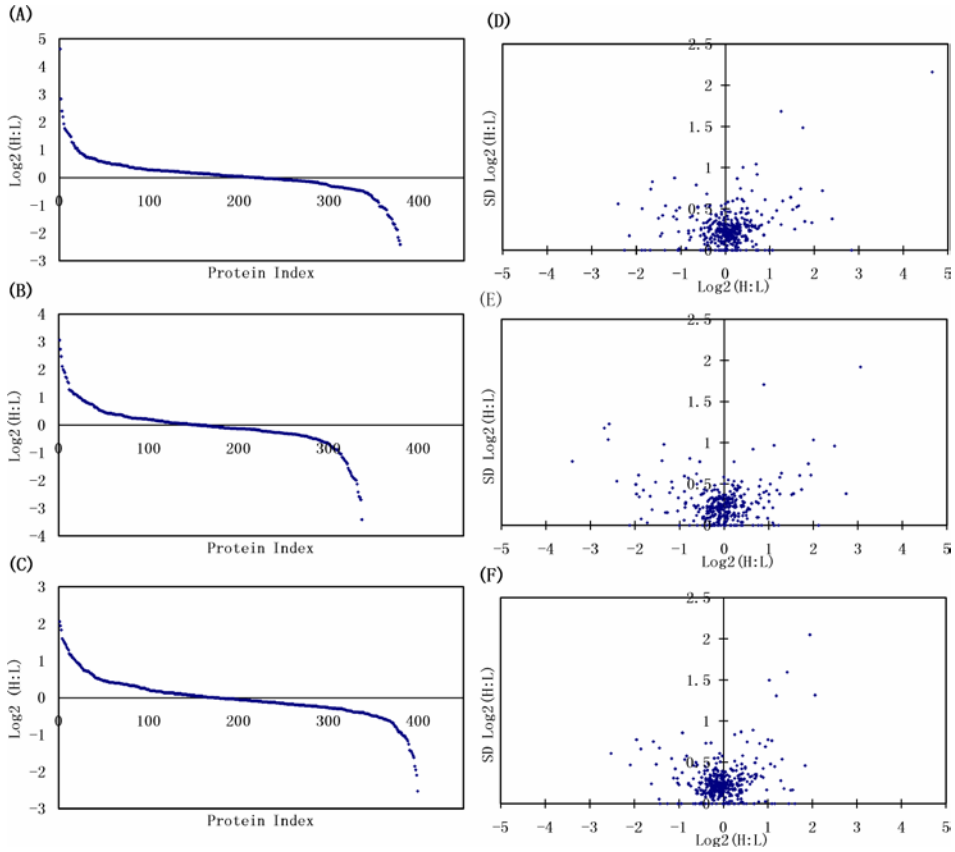
(A)
Log2 (H:L)
Protein Index
(B)
Log2 (H:L)
Protein Index
(C)
Log2 (H:L)
Protein Index
(D)
SD Log2 (H:L)
Log2 (H:L)
(E)
SD Log2 (H:L)
Log2 (H:L)
(F)
SD Log2 (H:L)
Log2 (H:L)

Figure 4.

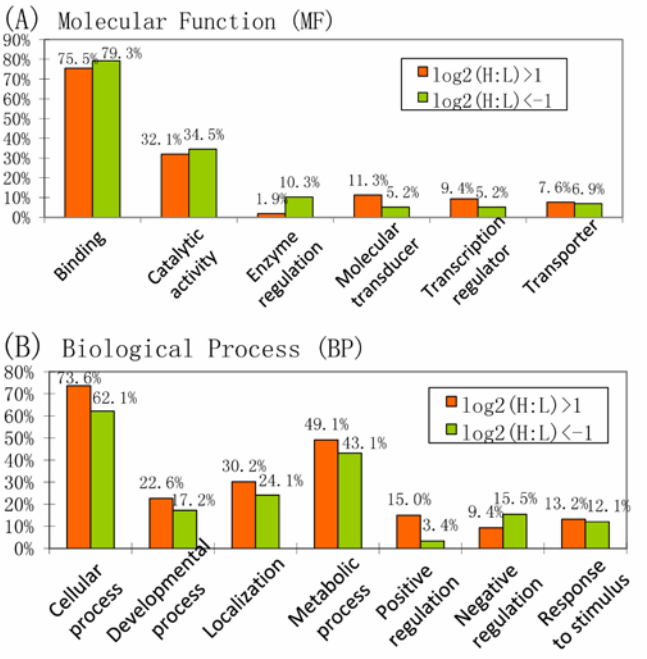
(A) Molecular Function (MF)
log2(H:L)>1
log2(H:L)<-1
75.5%
79.3%
32.1%
34.5%
1.9%
10.3%
11.3%
5.2%
9.4%
5.2%
7.6%
6.9%
Binding
Catalytic activity
Enzyme regulation
Molecular transducer
Transcription regulator
Transporter
(B) Biological Process (BP)
log2(H:L)>1
log2(H:L)<-1
73.6%
62.1%
22.6%
17.2%
30.2%
24.1%
49.1%
43.1%
15.0%
3.4%
9.4%
15.5%
13.2%
12.1%
Cellular process
Developmental process
Localization
Metabolic process
Positive regulation
Negative regulation
Response to stimulus

Figure 5.

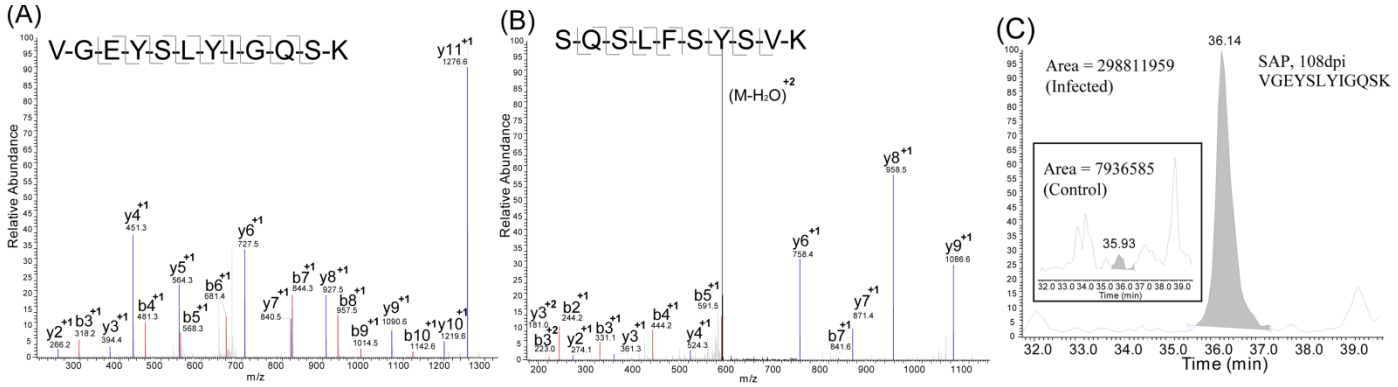
(A)
V-G-E-Y-S-L-Y-I-G-Q-S-K
Relative Abundance
m/z
(B)
S-Q-S-L-F-S-Y-S-V-K
(M-H2O)+2
Relative Abundance
m/z
(C)
36.14
Area = 298811959
(Infected)
SAP, 108dpi
VGEYSLYIGQSK
Area = 7936585
(Control)
35.93
Time (min)

Figure 6.

(A)

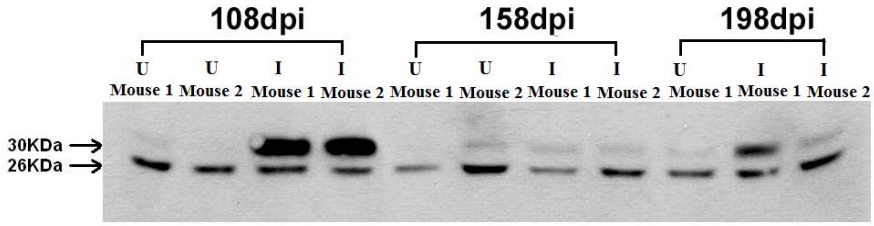
108dpi
158dpi
198dpi
U U I I U U I I U I I
Mouse 1 Mouse 2 Mouse 1 Mouse 2 Mouse 1 Mouse 2 Mouse 1 Mouse 2 Mouse 1 Mouse 1 Mouse 2
30KDa
26KDa

(B)

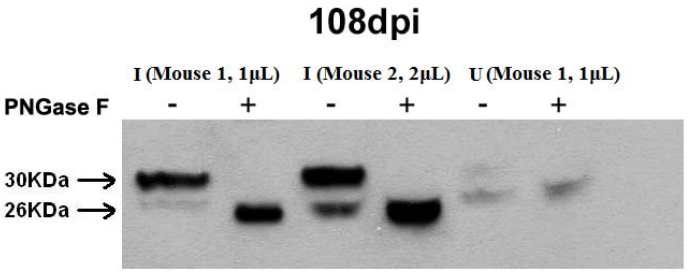
108dpi
I (Mouse 1, 1µL) I (Mouse 2, 2µL) U (Mouse 1, 1µL)
PNGase F - + - + - +
30KDa
26KDa

Figure 7.

SUPPORTING INFORMATION (available upon request)

Supplementary Table 1. The list of proteins identified at each time point (108, 158, and 198 dpi) showing the sequence coverage, unique peptides, spectral count, expression ratio and standard deviations. N/A indicates that the XPRESS function was unable to use a peptide profile to calculate the expression ratio.

Supplementary Table 2. The list of peptides identified at each time point and each replicate experiments. The lists of identifications include amino acid sequences, theoretical and observed precursor masses and confidence of identification.

Supplementary Table 3. The list of significantly up- and down-regulated proteins at each time point. Infected samples were labeled in the heavy form (H) whereas control samples were labeled with light form (L).

Table of Content (TOC)

A Quantitative Proteomic Approach to Prion Disease Biomarker Research: Delving into the Glycoproteome

Synopsis:

Sensitive and reliable pre-mortem diagnostic tests for prion diseases are currently lacking. This article reports the findings from a proteomic search for biomarkers of prion diseases from mouse plasma samples. An analytical platform integrating lectin affinity chromatography, multi-dimensional separations, isotopic labeling and mass spectrometry was implemented to detect and relatively quantify glycoproteins with low abundance. A list of the potential candidate markers has been generated.

Figure:

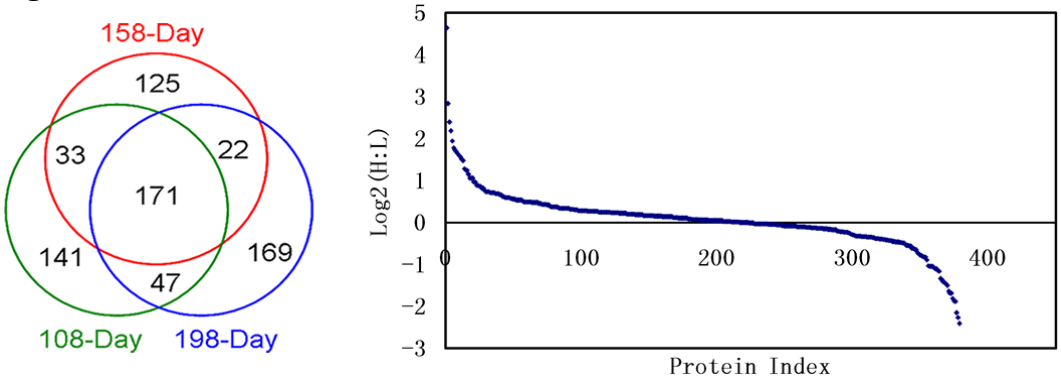

Chapter 7

Conclusions and Future Directions

7.1 Summary

The central theme for the research projects presented in this thesis involves the use of chromatographic separation and mass spectrometry for the large scale proteomic profiling in complex biological samples in search of key protein factors or biomarkers that are associated with diseases. Typically, each project consists of a method development phase where methods for MS analysis of different types of biological samples were tested and optimized, and an application phase where various statistics and bioinformatics tools were utilized to interpret dataset generated by MS analysis in order to address biological problems. Although the projects presented in my thesis were conducted in only a few types of biological materials including cell lysates, cell culture media and plasma, the general workflows and optimized methods for sample preparation and separation can be applied to the analysis of other complex biological samples. The results and methods from present work will provide valuable references for future MS-based proteomic analysis in our lab.

For the project that aimed at identifying IL-2 regulated proteins in human primary NK cells (Chapter 2), I developed a workflow that can be readily used for the proteomic analysis of cell lysates from limited amount of cell samples (10^6-10^7 cells). 2D LC was successfully employed to reduce the sample complexity prior to MS analysis, and a novel fraction collection strategy was optimized and used to reduce instrument analysis time. To improve protein identification, Mascot percolator was employed, and 2311 and 2413 proteins were identified from naïve or IL-2-activated NK cells, respectively. Label-free quantitative analysis via spectral counting revealed a list of 383 proteins that were up or down-regulated in IL-2 signaling. The function of IL-2 regulated proteins were reviewed by gene ontology analysis and literature search where some proteins that are closely involved in JAK-STAT pathway signaling, cell

proliferation and immune response were selected as potential targets for future investigation of IL-2 signaling in human primary NK cells. A pathway analysis was performed and revealed several novel pathways not previously known to be involved in IL-2 signaling. The quantitative proteomic analysis in this study provided a comprehensive view of proteins that are associated with IL-2 signaling, which will serve as a starting point of further investigations of key proteins, signaling transduction pathways and biological processed involved in NK cell activation by IL-2.

The aim of the study in Chapter 3 was to characterize the secretome of VSMC and identify secreted proteins that may be involved in Smad3-dependent TGF-β signaling through analyzing proteins concentrated from conditioned media of VSMC cultures by LC ESI-MS/MS. Given that the cell supernatant is usually less complex than cell lysates or biofluids, a 1D LC-MS/MS was employed for protein identifications. If necessary, the results from this study will serve as a reference for an improvement of protein identification by 2D LC separation. Overall, the use of one-dimensional LC-MS/MS resulted in identifications of 264 proteins from conditioned media of VSMCs cultures treated before or after TGF-β. The dataset was then subjected to SignalP and SecretomeP to filter out contaminations of intracellular proteins from cell death. As a result, a refined list of 169 secreted proteins was generated. Quantitative analysis by spectral counting revealed 31 secreted proteins that were significantly up- or down-regulated in response to TGF-β. The characterization of the secretome of VSMCs from this study will provide new insights into the research in vascular biology. Moreover, the TGF-β induced factors identified from comparative analysis may provide novel targets for the investigations of the role of TGF-β in atherosclerotic process. As a part of an ongoing project, the results presented in this thesis lay the foundation for further studies of the VSMC secretome with other quantitative approaches (will be discussed later in this chapter).

For the prion disease biomarker discovery project discussed in Chapter 4, an analytical workflow that readily detects and quantifies glycoproteins in complex biofluid samples was developed and tested. The workflow integrates lectin affinity chromatography, multidimensional separations, isotopic labeling and mass spectrometry, which results in significantly reduced sample complexity. In this study, 708 plasma proteins were identified and quantified. A list of 111 proteins with more than two-fold increase or decrease in prion infected samples was generated, which may serve as a reference for future prion disease biomarker investigation. In addition, the up-regulation of one of the potential candidate markers serum amyloid component-P (SAP) in prion infected mouse plasma was validated by Western blot. The deglycosylation analysis of this SAP also revealed that only the level of glycosylated SAP was up-regulated in response to prion infection. The finding from this study provides a novel target for further investigation on SAP as a potential pre-mortem biomarker for prion disease. The platform of MS based global glycoproteomics in plasma developed in this study proved to be an effective and sensitive tool that can be utilized in future biomarker discovery in complex biological samples.

7.2 Future Directions

Proteomic profiling in human primary NK cells

The workflow developed for proteomic profiling in human primary NK cells and the results presented in this thesis research lay a foundation for future proteomic analysis in NK cells or other types of immune cells. To identify as many proteins as possible, a protein extraction by RIPA buffer was adopted for this study. Although RIPA buffer is one of the most effective buffers used to lyse cultured mammalian cells which enables protein extraction from different

subcellular components including cytoplasmic, membrane and nuclear proteins, we only identified a small portion of membrane proteins possibly due to their highly hydrophobic and low abundance nature. Given that many of the membrane proteins are cell surface receptors and the activities of NK cells are mediated by the contact between these molecules and their ligands, it is essential to define the membrane composition in the proteomic profiling in NK cells or other immune cells.

Previous proteomic studies of NK cells reported the identification of cell surface proteins from membrane fractions of NK cells[1-3], and provided valuable experience on sample preparation and the enrichment of membrane proteins. Recently, our lab developed detergent assisted lectin affinity chromatography (DALAC) to increase the recovery of plasma membrane glycoproteins[4]. In DALAC, low concentration of detergent was added during lectin affinity chromatography. It was shown that DALAC can minimize the nonspecific binding and facilitate the elution of hydrophobic membrane glycoproteins. For the next step of this project DALAC can be utilized for specific enrichment of membrane glycoproteins. Following DALAC, quantitative proteomics approaches via label-free spectral counting or isobaric labeling may be employed to study the changes of those proteins under different biological or physiological states.

Secretome analysis in VSMC culture in response to Smad3-dependent TGF-β signaling

The quantitative approach employed for VSMC secreteome analysis was spectral counting rather than the metabolic labeling strategy SILAC (stable isotope labeling by amino acids in cell culture) which is typically used for the proteomic analysis in cell culture. Although metabolic labeling can eliminate the error introduced during sample preparation or from incomplete labeling which is usually the drawback for *in vitro* derivatization labeling techniques,

the high cost of SILAC labeling reagents limited its use. Compared to SILAC, label-free quantification via spectral counting is more affordable and can be directly applied to any number of protein samples from any source. However, the spectral counting based quantification often suffers from low accuracy and it also requires longer instrument time.

Recently, a new variant of label-free quantification, known as absolute quantification by LC/MS^E, was introduced for quadrupole time-of-flight (Q-TOF) mass spectrometers[5]. The detailed working principle and methodology of LC/MS^E was reviewed in Chapter 2. Briefly, alternating scans of low collision energy and elevated collision energy during LC/MS analysis are used to obtain both protein quantification and protein identification data in a single experiment. The low energy scan generates precursor ions with data including mass and intensity for quantification, while the elevated collision energy mode generates peptide fragments that can be associated with their precursor ions for database searching and subsequent protein identification. Under LC/MS^E mode, absolute quantification for proteins present in the sample can be achieved by adding a protein standard at a given concentration. In a previous study it was demonstrated that the average signal intensity measured by LC/MS^E of the three most intense tryptic peptides for any given protein is constant at a given concentration, regardless of protein size[6]. In addition to absolute quantification, another advantage of LC/MS^E is that MS^E utilizes parallel, multiplex fragmentation where all peptide precursors are simultaneously fragmented throughout the chromatographic separation process regardless of intensity. This allows lower abundance peptides to be detected compared to data-dependent LC-MS/MS analysis where only more abundant peaks can be selected for fragmentation.

The Waters Synapt G2 HDMS Q-Tof mass spectrometer our lab recently purchased is capable of performing LC/MS^E. It would be interesting to compare the results of our protein

identification and quantification of the VSMC secretome conducted on an amaZon ETD ion trap (Bruker Daltonics, Germany) to the data captured by data-independent LC/MS^E for protein identification followed by absolute quantification. VSMC secretome serves as perfect samples for method development for absolute quantification by LC/MS^E due to its relatively lower complexity. The comparison between LC/MS^E and conventional data-dependent LC/MS/MS analysis using two different mass spectrometers will provide guidance on the selection of instruments and analysis methods for future proteomic studies.

Prion disease biomarker discovery

The profiling and quantitative analysis of plasma glycoproteome in mouse infected by prion disease led to the discovery of a potential biomarker SAP that may be used for early identification of prion disease. The result from MS analysis was validated by Western blot. However, in the biomarker discovery pipeline, this is only the first step towards the goal of successful development of a diagnostic biomarker with high sensitivity and accuracy for clinical purpose. Currently, antibody based methods such as Western blotting and ELISA are the most widely used method for biomarker verification. However, the application of antibody based methods is sometimes limited by the high cost and limited availability of specific antibodies. Furthermore, antibody based methods are not suitable when a panel of biomarkers rather than a single protein is necessary for higher specificity and accuracy during diagnostic screening. As an alternative, the quantitative analysis based on multiple-reaction monitoring (MRM) MS could be utilized for biomarker validation. The capability of MRM-MS assay for high-throughput screening and quantifying multiple biomarkers present in one sample will accelerate the process of biomarker development.

For future studies several protein candidates that were significantly up- or down-regulated following prion infection based on the MS analysis will be selected for method development of MRM-MS. Recently, our lab successfully developed a workflow for absolute quantification of prion protein (90-231) by LC-MRM[7]. The method developed for this work provides a good foundation for the application of LC-MRM assays in the validation of potential prion disease biomarkers.

Expansion of the scope of this project could be to further investigate the glycan structure of SAP. Given that only glycosylated SAP was associated with the progression of prion diseases, it is highly likely aberrant glycosylation plays important roles in the development of prion diseases, therefore, enzymes involved in this process serve as ideal targets for the investigation of molecular mechanisms causing prion diseases. The elucidation of glycan structures attached to SAP provides important clues to understand the complex enzymatic process of glycosylation. Towards this goal, glycosidase could be utilized to simplify the analysis of the glycan components due to their specificities for different glycan structure. For example, different from PNGase F which removes the intact oligosaccharide, Endoglycosidase H (Endo H) cleaves asparagine-linked hybrid or high mannose oligosaccharides, but not complex oligosaccharides (Fig. 1)[8]. It cleaves between the two N-acetylglucosamine residues in the diacetylchitobiose core of the oligosaccharide, generating a truncated sugar molecule with one N-acetylglucosamine residue remaining on the asparagine. The results from deglycosylation analysis will provide useful information for MS-based glycomics study in future.

References

1. Hanna, J.; Fitchett, J.; Rowe, T.; Daniels, M.; Heller, M.; Gonen-Gross, T.; Manaster, E.; Cho, S. Y.; LaBarre, M. J.; Mandelboim, O., Proteomic analysis of human natural killer cells: insights on new potential NK immune functions. *Mol Immunol* **2005,** 42, (4), 425-31.
2. Hanna, J.; Gonen-Gross, T.; Fitchett, J.; Rowe, T.; Daniels, M.; Arnon, T. I.; Gazit, R.; Joseph, A.; Schjetne, K. W.; Steinle, A.; Porgador, A.; Mevorach, D.; Goldman-Wohl, D.; Yagel, S.; LaBarre, M. J.; Buckner, J. H.; Mandelboim, O., Novel APC-like properties of human NK cells directly regulate T cell activation. *J Clin Invest* **2004,** 114, (11), 1612-23.
3. Lund, T. C.; Anderson, L. B.; McCullar, V.; Higgins, L.; Yun, G. H.; Grzywacz, B.; Verneris, M. R.; Miller, J. S., iTRAQ is a useful method to screen for membrane-bound proteins differentially expressed in human natural killer cell types. *J Proteome Res* **2007,** 6, (2), 644-53.
4. Wei, X.; Dulberger, C.; Li, L., Characterization of murine brain membrane glycoproteins by detergent assisted lectin affinity chromatography. *Anal Chem* **2010,** 82, (15), 6329-33.
5. Chakraborty, A. B.; Berger, S. J.; Gebler, J. C., Use of an integrated MS--multiplexed MS/MS data acquisition strategy for high-coverage peptide mapping studies. *Rapid Commun Mass Spectrom* **2007,** 21, (5), 730-44.
6. Silva, J. C.; Denny, R.; Dorschel, C.; Gorenstein, M. V.; Li, G. Z.; Richardson, K.; Wall, D.; Geromanos, S. J., Simultaneous qualitative and quantitative analysis of the Escherichia coli proteome: a sweet tale. *Mol Cell Proteomics* **2006,** 5, (4), 589-607.
7. Sturm, R.; Sheynkman, G.; Booth, C.; Smith, L. M.; Pedersen, J. A.; Li, L., Absolute quantification of prion protein (90-231) using stable isotope-labeled chymotryptic peptide standards in a LC-MRM AQUA workflow. *J Am Soc Mass Spectrom* **2012,** 23, (9), 1522-33.
8. Maley, F.; Trimble, R. B.; Tarentino, A. L.; Plummer, T. H., Jr., Characterization of glycoproteins and their associated oligosaccharides through the use of endoglycosidases. *Anal Biochem* **1989,** 180, (2), 195-204.

Figure. 1. Illustration of PNGase F and Endoglycosidase H specificities

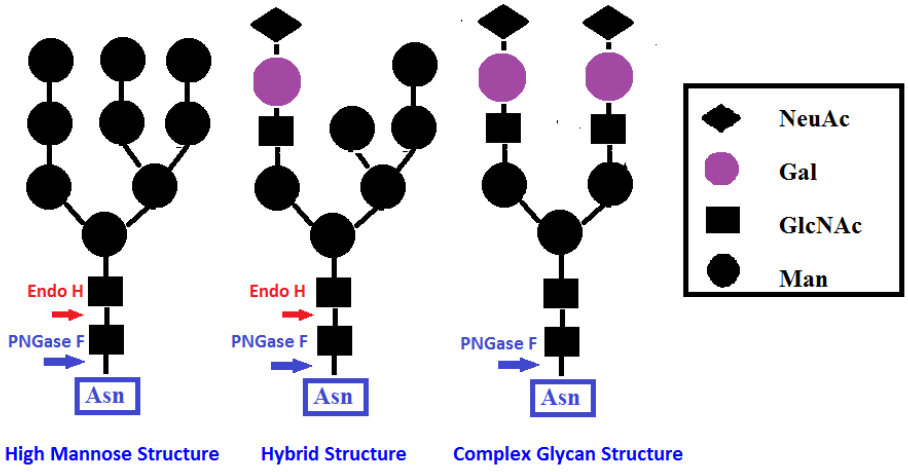

Appendix 1

Selected Protocols for Comparative Proteomic Profiling and Biomarker Discovery in Complex Biological Samples by Mass Spectrometry.

Protein Extraction from Human Primary NK Cells

Urea-Assisted Tryptic Digestion

High pH RPLC Off-line Separation

SDS-PAGE

Western Blot

Protein Extraction from Human Primary NK Cells

1. Pellet the human primary NK cells by centrifugation at 1000 × *g* for 5 minutes. Discard the supernatant.
2. Wash cells twice in cold PBS. Pellet cells by centrifugation at 1000 × *g* for 5 minutes.

   Note: Sometimes red blood cells are co-isolated with NK cells from peripheral blood. Water lysis can remove most of the red blood cells. Briefly, add 200 µl of deionized water in to cell pellet. Quickly pipette up and down to suspend the pellet and add 1ml of PBS. This can be repeated three times to completely remove red blood cells. Pellet cells by centrifugation at 1000 × *g* for 5 minutes.
3. Add protease to the RIPA Buffer immediately before use.
4. Add 200 µl RIPA Buffer to wet cell pellet (~ 5 x 10^6 cells). Pipette the mixture up and down to suspend the pellet.
5. To increase yields, sonicate the pellet for 10 seconds for three times with 10 seconds pulse each time.
6. Incubate the NK cells in RIPA buffer for 15 minutes on ice. Centrifuge mixture at 16,000 × *g* for 15 minutes to pellet the cell debris.
7. Transfer supernatant to a new tube for further analysis.

Urea-Assisted Tryptic Digestion

All solutions are made in a 50 mM NH_4HCO_3 buffer.

1. Dry sample and reconstitute sample in 20 µL 8.0 M urea.
2. Add 1 µl of 1 M Dithiothreitol (DTT) and mix the sample by gentle vortex.
3. Reduce the mixture for 1 hour at 37° C.
4. Add 20 µl of Iodoacetamide (IAA) alkylate for 20 minutes in the dark.
5. Quench reaction with 4µl of 1 M DTT solution to consume any leftover alkylating agent.
6. Dilute with 120 µl of 50 mM NH_4HCO_3 solution.
7. Add trypsin in appropriate ratio (1:30) to approximate amount of protein by weight. Digest overnight at 37°C.
8. Add 1 µL of formic acid to the sample and gently vortex to inactivate trypsin.
9. Dry sample and perform desalting as needed for experiment.

High pH RPLC Offline Separation

1. High pH-stable RP C18 columns are typically used for high pH RPLC offline separation. Phenomenex Gemini CI8 (150 x 2.1mm, 3 micron) with sample capacity of 20-50 µg was used in this protocol.
2. Equilibrate the column at a flow rate of 150uL/min by buffer A (Buffer A: l00 mM ammonium formate, pH 10).
3. Reconstitute 20-50 µg dried tryptic peptides in 100 mM ammonium formate, pH 10.

4. Inject sample and run a gradient of 5-45% buffer B (acetonitrile (ACN)) over 45 minutes at a flow rate of 150 µl/minute. Monitor the separation by a UV detector set at 280 nm wavelength.

   Note: Heat the column to about 45-60°C to obtain better resolution.

5. Collect fractions every 2min for 60min.

6. Dry the collected fractions by Speedvac, and reconstitute the samples in 30 ul of 0.1% formic acid for further LC-MS/MS analysis.

   Note: Peptides are normally in the fractions #5-24 if the above RP-HPLC condition is used. The fractions can be first screened with UV detect or for apparent peaks. For those fractions whose chromatogram signals are not strong, MALDI-FTMS can be used to have a snapshot of the peptide content in each fraction.

Enrichment Plasma Glycoproteins by Lectin Affinity Chromatography (LAC)

1. Measure the concentration of plasma by BCA assay.

   Note: In order to be accurately measured by BCA assay, plasma needs to be diluted to 0.5-1.5 µg/µl.

2. Prepare the multi-lectin affinity columns by adding 400 ul each of Con A and WGA slurry to empty Micro Bio-Spin columns (Bio-Rad Laboratories, Hercules, CA) or Handee spin cup columns (Pierce, Rockford, IL).

   Note: The settled gel is 50% v/v slurry.

3. Wash the lectin beads 3 times with 400 ul lectin binding buffer (20 mM Tris, 0.15 M NaCl, 1 mM Ca^{2+}, 1 mM Mn^{2+}, pH 7.4).

4. Separately pool the plasma samples from 7 infected and 7 control mice. Dilute 40uL of the plasma sample with 400 uL lectin binding buffer, and add the sample to lectin beads.

   Note: Avoid adding excess amount of plasma. Proteins of high concentration will precipitate out once in contact with lectin beads.

7. Incubate the sample with lectin beads for 6 hr or overnight with gentle rotation at 4 °C. Make sure the end cap is tightly sealed to prevent leakage and sample loss.
8. Centrifuge the sample at 1000 xg for lmin, and collect the flow through fraction. This is the unbound fraction containing most of the non-glycosylated proteins.
9. Wash the beads 5 times with 500 uL of lectin binding buffer to remove the contaminants from non-specific binding. Discard the wash fraction to waste.

   Note: Treat the waste samples with 40% freshly made household bleach for at least one hour before disposing them down the sink.
10. Incubate the lectin beads with 400 uL of multi-lectin elution buffer (10 mM Tris, 75mM NaCl, 0.25M N-acetyl-D-glucosamine, 0.17M methyl-a-Dmannopyranoside, and 0.17 M methyl-a-D-glucopyranoside) for 30 min at 4 °C. Centrifuge the sample at 1000 x g for l min to collect the elution fraction. This is the bound fraction containing the glycoproteins.
11. Repeat the elution process to a total of 5 times, so that the total elution volume is 2 ml. In the last three elution process, the incubation time can be shortened to 5 min.

SDS-PAGE

1. Mix protein samples with proper volume of 4x Sample Buffer (Invitrogen #NP0007), 10x Reducing Agent (Invitrogen #NP0004).

2. Boil the mixture in water for 10 min.

3. Prepare 1x NuPAGE MOPS SDS running buffer (Invitrogen #NP0002) and fill the chamber with SDS running enough to cover the wells of NuPAGE 10% Bis-Tris Gel.

4. Load protein samples and protein markers into the wells of the gel.

5. Run the gel with 200 V constant voltage for 50 min. Expected start current is 100-125 mA and end is 60-80 mA.

6. The gel was then stained with SimplyBlue SafeStain (Invitrogen) for 1 hr, and destained with water overnight to increase the band intensity.

Westen Blot

Western blot can be conducted after running SDS-PAGE.

I. Prewet blotting pads, filter paper and membrane

1. Soak blotting pads in transfer buffer, pressing down to remove trapped air bubbles. Leave soaked pads in buffer until ready to assemble the blotting sandwich.

   Note: If using PVDF, pre-wet the membrane in pure methanol, then equilibrate in transfer buffer by shaking in a shallow tray filled with buffer. Nitrocellulose can be placed directly into transfer buffer to equilibrate (nitrocellulose membrane will dissolve in pure methanol).

II. Removing the gel and making blotting sandwich

1. After electrophoresis, separate each of the 3 bonded sides of the gel cassette by inserting the gel knife into the gap between the cassette's 2 plates. The notched ("well") side of the cassette should face up.

2. Push up and down on the knife handle to separate the plates. Repeat on each side of the cassette until the plates are completely separated.

   Caution: Use caution while inserting the gel knife between the 2 plates to avoid excessive pressure towards the gel.

3. The gel may adhere to either side of plates upon opening the cassette. Carefully remove and discard the plate without the gel. The gel remains on the other plate.

4. Remove wells on the gel with the gel knife.

5. Place a piece of pre-soaked filter paper on top of the gel, and lay just above the "foot" at the bottom of the gel (leaving the "foot" of the gel uncovered). Keep the filter paper saturated with transfer buffer and remove all trapped air bubbles by gentle rolling over the surface using a glass pipette.

6. Turn the plate over so the gel and filter paper are facing downwards over a gloved hand or clean flat surface covered with a piece of Parafilm.

7. Remove gel from the plate using the following methods:

1) If the gel rests on the longer (slotted) plate, use the gel knife to push the foot out of the slot in the plate and the gel will fall off easily.

2) If the gel rests on the shorter (notched) plate, use the gel knife to carefully loosen the bottom of the gel and allow the gel to peel away from the plate.

8. When the gel is on a flat surface, cut the “foot” off the gel with the gel knife.

Note: Once you have removed the gel from the unit and the cassette, perform the transfer immediately.

III. Transferring

1. Wet the surface of the gel with the transfer buffer and place pre-soaked transfer membrane on the gel. Remove air bubbles by rolling a glass pipette over the membrane surface.

2. Place the pre-soaked filter paper on top of the transfer membrane. Remove any trapped air bubbles.

3. Place 2 soaked blotting pads into the cathode (–) core of the blot module. The cathode core is the deeper of the 2 cores and the corresponding electrode plate is a darker shade of gray. Carefully pick up the gel membrane assembly with your gloved hand and place on the pad in the same sequence, such that the gel is closest to the cathode plate (see figure below).

4. Add enough pre-soaked blotting pads to rise 0.5 cm over the rim of the cathode core. Place the anode (+) core on top of the pads. The gel/membrane sandwich should be held securely between the two halves of the blot module ensuring complete contact of all components.

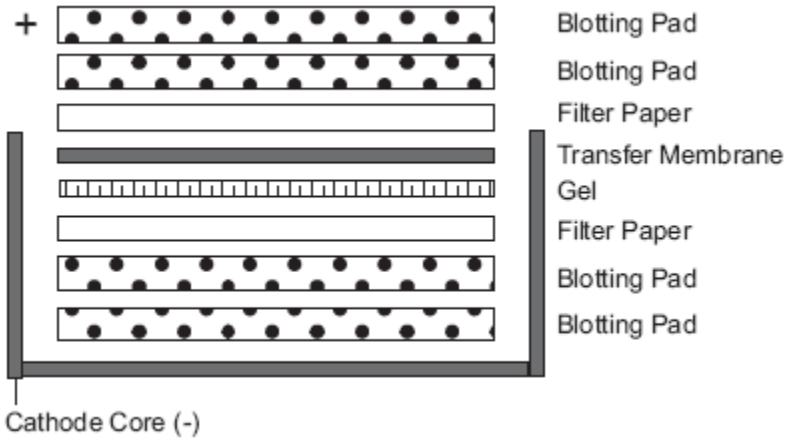

Note: To ensure a snug fit, use an additional pad since pads lose their resiliency after many uses. Replace pads when they begin to lose resiliency and are discolored.

5. Position the gel membrane sandwich and blotting pads in the cathode core of the XCell II™ Blot Module to fit horizontally across the bottom of the unit. There should be a gap of ~ 1 cm at the top of the electrodes when the pads and assembly are in place (see figure above).

6. Hold the blot module together firmly and slide it into the guide rails on the lower buffer chamber. The blot module fits into the unit in only one way, such that the (+) sign is seen in the upper left hand corner of the blot module. The inverted gold post on the right hand side of the blot module fits into the hole next to the upright gold post on the right side of the lower buffer chamber.

7. For XCell *SureLock*™ Mini-Cell, place the gel tension wedge such that the vertical face of the wedge is against the blot module. Push the lever forward to lock it into place.

8. Fill the blot module with transfer buffer until the gel/membrane sandwich is covered in transfer buffer. **Do not fill all the way to the top as this will generate extra conductivity and heat.**

9. Fill the outer buffer chamber with ~ 650 mL deionized water by pouring in the gap between the front of the blot module and front of the lower buffer chamber. The water level should reach approximately 2 cm from the top of the lower buffer chamber. This serves to dissipate heat produced during the run.

10. Place the lid on top of the unit. With the power turned off, plug the red and black leads into the power supply. Transfer is conducted at 30V constant for 1-1.5 hour.

IV. Staining the membrane

1. After the transfer, stain the membrane with 0.1% Ponceau S in 7% trichloroacetic acid (TCA) for 5 minutes and use permanent marker to mark molecular weight markers. Rinse the membrane in deionized water to wash off the stain.

V. Immunoblotting

1. Block membrane 30-60 min in blotto at room temperature.

2. Wash membrane in TBS-T for 5min, repeat three times.

3. Incubate membrane with 1° antibody diluted 1:10,000 (or 1:5000; may need to adjust concentration) in blotto overnight at room temperature with gentle agitation.

4. Wash membrane in TBS-T for 5min, repeat three times.

5. Incubate membrane with 2°-conjugated antibody diluted 1:3000 (company dependant) in blotto for 1 hr at room temperature with gentle agitation.

6. Wash membrane in TBS-T for 5min, repeat three times.

7. Equilibrate ECL Plus reagents (GE Healthcare, UK) to room temperature. Incubate at room temperature for 5min. Scan blot using STORM imager or develop the film in the dark room.

Reagents:

10X Transfer Buffer for wet blotting (1 L)

30.3 g Tris base

144.1 g glycine

Add water to 1 L

1 X Transfer Buffer for wet blotting (1 L)

100 ml 10 X stock

500 ml H_2O

200 ml methanol

Add water to 1 L

10X TBS

24.23 g Trizma HCl

80.06 g NaCl

mix w/ 800 mL H_2O

pH 7.6 w/ HCl

Top to 1 L

TBS-T (0.001%)

For 1 L:

100 mL 10X TBS

1 mL Tween-20

Top to 1 L

Blotto (100 ml)

5g non-fat milk

10ml 10 X TBS-T

Top to 100 ml

Ponceau S (0.1% in 5% acetic aicd)

1g Ponceau S

50 ml acetic acid

Top to 1 L

Appendix 2

List of IL-2 regulated proteins with more than 2-fold increase (Table 1) or 2-fold decrease (Table 2) in human primary NK cells that are identified in all three donors (Chapter 3). "Accession" is UniProtKB accession numbers and "Entry Name" is the uniProtKB/Swiss-Prot entry names for each identified protein.

Table 1. Proteins in human primary NK cells that were up-regulated following IL-2 stimulation.

Accession	Entry Name	Protein Name
P30466	1B18_HUMAN	HLA class I histocompatibility antigen B-18 alpha chain (MHC class I antigen B*18)
O14579	COPE_HUMAN	Coatomer subunit gamma (Gamma-coat protein) (Gamma-COP)
P09769	FGR_HUMAN	Tyrosine-protein kinase Fgr (EC 2.7.10.2) (Proto-oncogene c-Fgr) (p55-Fgr)
P48668	K2C6C_HUMAN	Keratin type II cytoskeletal 6C (Cytokeratin-6C) (CK-6C) (Cytokeratin-6E) (CK-6E) (Keratin K6h) (Keratin-6C) (K6C) (Type-II keratin Kb12)
P49588	SYAC_HUMAN	Alanyl-tRNA synthetase cytoplasmic (EC 6.1.1.7) (Alanine--tRNA ligase) (AlaRS) (Renal carcinoma antigen NY-REN-42)
P55145	MANF_HUMAN	Mesencephalic astrocyte-derived neurotrophic factor (Arginine-rich protein) (Protein ARMET)
Q96F15	GIMA5_HUMAN	GTPase IMAP family member 5 (Immunity-associated nucleotide 4-like 1 protein) (Immunity-associated nucleotide 5 protein) (IAN-5) (hIAN5) (Immunity-associated protein 3)
Q06210	GFPT1_HUMAN	Glucosamine--fructose-6-phosphate aminotransferase [isomerizing] 1 (EC 2.6.1.16) (D-fructose-6-phosphate amidotransferase 1) (Glutamine:fructose 6 phosphate amidotransferase 1) (GFAT 1) (GFAT1) (Hexosephosphate aminotransferase 1)
P12004	PCNA_HUMAN	Proliferating cell nuclear antigen (PCNA) (Cyclin)
Q8NF50	DOCK8_HUMAN	Dedicator of cytokinesis protein 8
P08195	4F2_HUMAN	4F2 cell-surface antigen heavy chain (4F2hc) (4F2 heavy chain antigen) (Lymphocyte activation antigen 4F2 large subunit) (CD antigen CD98)
P56202	CATW_HUMAN	Cathepsin W (EC 3.4.22.-) (Lymphopain)
Q9UN37	VPS4A_HUMAN	Vacuolar protein sorting-associated protein 4A (Protein SKD2) (VPS4-1) (hVPS4)

Q9Y295	DRG1_HUMAN	Double-stranded RNA-specific adenosine deaminase (DRADA) (EC 3.5.4.-) (136 kDa double-stranded RNA-binding protein) (p136) (Interferon-inducible protein 4) (IFI-4) (K88DSRBP)
P63151	2ABA_HUMAN	Serine/threonine-protein phosphatase 2A 55 kDa regulatory subunit B alpha isoform (PP2A subunit B isoform B55-alpha) (PP2A subunit B isoform PR55-alpha) (PP2A subunit B isoform R2-alpha) (PP2A subunit B isoform alpha)
Q96BY6	DOC10_HUMAN	Dedicator of cytokinesis protein 10 (Zizimin-3)
P13693	TCTP_HUMAN	Translationally-controlled tumor protein (TCTP) (Fortilin) (Histamine-releasing factor) (HRF) (p23)
O00429	DNM1L_HUMAN	Dynamin-1-like protein (EC 3.6.5.5) (Dnm1p/Vps1p-like protein) (DVLP) (Dynamin family member proline-rich carboxyl-terminal domain less) (Dymple) (Dynamin-like protein) (Dynamin-like protein 4) (Dynamin-like protein IV) (HdynIV) (Dynamin-related protein 1)
P21108	PRPS3_HUMAN	Ribose-phosphate pyrophosphokinase 3 (EC 2.7.6.1) (Phosphoribosyl pyrophosphate synthase 1-like 1) (PRPS1-like 1) (Phosphoribosyl pyrophosphate synthase III) (PRS-III)
Q9UPN3	MACF1_HUMAN	Microtubule-actin cross-linking factor 1 isoforms 1/2/3/5 (620 kDa actin-binding protein) (ABP620) (Actin cross-linking family protein 7) (Macrophin-1) (Trabeculin-alpha)
P14678	RSMB_HUMAN	Small nuclear ribonucleoprotein-associated proteins B and B' (snRNP-B) (Sm protein B/B') (Sm-B/B') (SmB/B')
P46781	RS9_HUMAN	40S ribosomal protein S9
Q13283	G3BP1_HUMAN	Ras GTPase-activating protein-binding protein 1 (G3BP-1) (EC 3.6.4.12) (EC 3.6.4.13) (ATP-dependent DNA helicase VIII) (hDH VIII) (GAP SH3 domain-binding protein 1)
P48960	CD97_HUMAN	CD97 antigen (Leukocyte antigen CD97) (CD antigen CD97) [Cleaved into: CD97 antigen subunit alpha; CD97 antigen subunit beta]
Q15758	AAAT_HUMAN	Neutral amino acid transporter B(0) (ATB(0)) (Baboon M7 virus receptor) (RD114/simian type D retrovirus receptor) (Sodium-dependent neutral amino acid transporter type 2) (Solute carrier family 1 member 5)
P09326	CD48_HUMAN	CD48 antigen (B-lymphocyte activation marker BLAST-1) (BCM1 surface antigen) (Leukocyte antigen MEM-102) (TCT.1) (CD antigen CD48)
O00410	IPO5_HUMAN	Importin-5 (Imp5) (Importin subunit beta-3) (Karyopherin beta-3) (Ran-binding protein 5) (RanBP5)
P34897	GLYM_HUMAN	Serine hydroxymethyltransferase mitochondrial (SHMT) (EC 2.1.2.1) (Glycine hydroxymethyltransferase) (Serine methylase)
Q9P107	GMIP_HUMAN	GEM-interacting protein (GMIP)
Q9BXW7	CECR5_HUMAN	Cat eye syndrome critical region protein 5
Q02880	TOP2B_HUMAN	DNA topoisomerase 2-beta (EC 5.99.1.3) (DNA topoisomerase II beta isozyme)
Q7Z4W1	DCXR_HUMAN	L-xylulose reductase (XR) (EC 1.1.1.10) (Carbonyl reductase II) (Dicarbonyl/L-xylulose reductase) (Kidney dicarbonyl reductase) (kiDCR) (Sperm surface protein P34H)
Q9P1U1	ARP3B_HUMAN	Actin-related protein 3B (ARP3-beta) (Actin-like protein 3B) (Actin-related protein ARP4)

Q96CW1	AP2M1_HUMAN	AP-2 complex subunit mu (AP-2 mu chain) (Adapter-related protein complex 2 mu subunit) (Adaptin-mu2) (Adaptor protein complex AP-2 subunit mu) (Clathrin assembly protein complex 2 medium chain) (Clathrin coat assembly protein AP50) (Clathrin coat-associated protein AP50) (HA2 50 kDa subunit) (Plasma membrane adaptor AP-2 50 kDa protein)
P08574	CY1_HUMAN	Cytochrome c1 heme protein mitochondrial (Complex III subunit 4) (Complex III subunit IV) (Cytochrome b-c1 complex subunit 4) (Ubiquinol-cytochrome-c reductase complex cytochrome c1 subunit) (Cytochrome c-1)
Q9BXP5	SRRT_HUMAN	Serrate RNA effector molecule homolog (Arsenite-resistance protein 2)
Q9UBS4	DJB11_HUMAN	DnaJ homolog subfamily B member 11 (APOBEC1-binding protein 2) (ABBP-2) (DnaJ protein homolog 9) (ER-associated DNAJ) (ER-associated Hsp40 co-chaperone) (ER-associated dnaJ protein 3) (ERdj3) (ERj3p) (HEDJ) (Human DnaJ protein 9) (hDj-9) (PWP1-interacting protein 4)
P61289	PSME3_HUMAN	Proteasome activator complex subunit 3 (11S regulator complex subunit gamma) (REG-gamma) (Activator of multicatalytic protease subunit 3) (Ki nuclear autoantigen) (Proteasome activator 28 subunit gamma) (PA28g) (PA28gamma)
Q99459	CDC5L_HUMAN	Cell division cycle 5-like protein (Cdc5-like protein) (Pombe cdc5-related protein)
P62304	RUXE_HUMAN	Small nuclear ribonucleoprotein E (snRNP-E) (Sm protein E) (Sm-E) (SmE)
P51858	HDGF_HUMAN	Hepatoma-derived growth factor (HDGF) (High mobility group protein 1-like 2) (HMG-1L2)
O76003	GLRX3_HUMAN	Glutaredoxin-3 (PKC-interacting cousin of thioredoxin) (PICOT) (PKC-theta-interacting protein) (PKCq-interacting protein) (Thioredoxin-like protein 2)
P41091	IF2G_HUMAN	Eukaryotic translation initiation factor 2 subunit 3 (Eukaryotic translation initiation factor 2 subunit gamma X) (eIF-2-gamma X) (eIF-2gX)
A2A3N6	PIPSL_HUMAN	Putative PIP5K1A and PSMD4-like protein (PIP5K1A-PSMD4)
Q13423	NNTM_HUMAN	NAD(P) transhydrogenase mitochondrial (EC 1.6.1.2) (Nicotinamide nucleotide transhydrogenase) (Pyridine nucleotide transhydrogenase)
Q29RF7	PDS5A_HUMAN	Sister chromatid cohesion protein PDS5 homolog A (Cell proliferation-inducing gene 54 protein) (Sister chromatid cohesion protein 112) (SCC-112)
Q8TBC4	UBA3_HUMAN	NEDD8-activating enzyme E1 catalytic subunit (EC 6.3.2.-) (NEDD8-activating enzyme E1C) (Ubiquitin-activating enzyme E1C) (Ubiquitin-like modifier-activating enzyme 3) (Ubiquitin-activating enzyme 3)
P20591	MX1_HUMAN	Interferon-induced GTP-binding protein Mx1 (Interferon-induced protein p78) (IFI-78K) (Interferon-regulated resistance GTP-binding protein MxA) (Myxoma resistance protein 1) (Myxovirus resistance protein 1) [Cleaved into: Interferon-induced GTP-binding protein Mx1 N-terminally processed]
Q8NFI4	F10A5_HUMAN	Putative protein FAM10A5 (Suppression of tumorigenicity 13 pseudogene 5)
Q8TF09	DLRB2_HUMAN	Dynein light chain roadblock-type 2 (Dynein light chain 2B cytoplasmic) (Roadblock domain-containing protein 2)
P49736	MCM2_HUMAN	DNA replication licensing factor MCM2 (EC 3.6.4.12) (Minichromosome maintenance protein 2 homolog) (Nuclear protein BM28)

P31153	METK2_HUMAN	S-adenosylmethionine synthase isoform type-2 (AdoMet synthase 2) (EC 2.5.1.6) (Methionine adenosyltransferase 2) (MAT 2) (Methionine adenosyltransferase II) (MAT-II)
Q96I99	SUCB2_HUMAN	Succinyl-CoA ligase [GDP-forming] subunit beta mitochondrial (EC 6.2.1.4) (GTP-specific succinyl-CoA synthetase subunit beta) (Succinyl-CoA synthetase beta-G chain) (SCS-betaG)
Q9UEW8	STK39_HUMAN	STE20/SPS1-related proline-alanine-rich protein kinase (Ste-20-related kinase) (EC 2.7.11.1) (DCHT) (Serine/threonine-protein kinase 39)
Q92598	HS105_HUMAN	Heat shock protein 105 kDa (Antigen NY-CO-25) (Heat shock 110 kDa protein)
P39023	RL3_HUMAN	60S ribosomal protein L3 (HIV-1 TAR RNA-binding protein B) (TARBP-B)
P22102	PUR2_HUMAN	Trifunctional purine biosynthetic protein adenosine-3 [Includes: Phosphoribosylamine--glycine ligase (EC 6.3.4.13) (Glycinamide ribonucleotide synthetase) (GARS) (Phosphoribosylglycinamide synthetase); Phosphoribosylformylglycinamidine cyclo-ligase (EC 6.3.3.1) (AIR synthase) (AIRS) (Phosphoribosyl-aminoimidazole synthetase); Phosphoribosylglycinamide formyltransferase (EC 2.1.2.2) (5'-phosphoribosylglycinamide transformylase) (GAR transformylase) (GART)]
P53794	SC5A3_HUMAN	Sodium/myo-inositol cotransporter (Na(+)/myo-inositol cotransporter) (Solute carrier family 5 member 3)
A6NHR9	SMHD1_HUMAN	Structural maintenance of chromosomes flexible hinge domain-containing protein 1
P42224	STAT1_HUMAN	Signal transducer and activator of transcription 1-alpha/beta (Transcription factor ISGF-3 components p91/p84)
Q14669	TRIPC_HUMAN	Probable E3 ubiquitin-protein ligase TRIP12 (EC 6.3.2.-) (Thyroid receptor-interacting protein 12) (TR-interacting protein 12) (TRIP-12)
P40763	STAT3_HUMAN	Signal transducer and activator of transcription 3 (Acute-phase response factor)
Q9NR30	DDX21_HUMAN	Probable ATP-dependent RNA helicase DDX46 (EC 3.6.4.13) (DEAD box protein 46) (PRP5 homolog)
Q99460	PSMD1_HUMAN	26S proteasome non-ATPase regulatory subunit 1 (26S proteasome regulatory subunit RPN2) (26S proteasome regulatory subunit S1) (26S proteasome subunit p112)
Q14683	SMC1A_HUMAN	Structural maintenance of chromosomes protein 1A (SMC protein 1A) (SMC-1-alpha) (SMC-1A) (Sb1.8)
Q92616	GCN1L_HUMAN	Translational activator GCN1 (HsGCN1) (GCN1-like protein 1)
P61204	ARF3_HUMAN	ADP-ribosylation factor 3
Q04637	IF4G1_HUMAN	Eukaryotic translation initiation factor 4 gamma 1 (eIF-4-gamma 1) (eIF-4G 1) (eIF-4G1) (p220)
P60763	RAC3_HUMAN	Ras-related C3 botulinum toxin substrate 3 (p21-Rac3)
Q96JY6	PDLI2_HUMAN	PDZ and LIM domain protein 2 (PDZ-LIM protein mystique)
Q96SI9	STRBP_HUMAN	Spermatid perinuclear RNA-binding protein
P19367	HXK1_HUMAN	Hexokinase-1 (EC 2.7.1.1) (Brain form hexokinase) (Hexokinase type I) (HK I)
P19404	NDUV2_HUMAN	NADH dehydrogenase [ubiquinone] flavoprotein 2 mitochondrial (EC 1.6.5.3) (EC 1.6.99.3) (NADH-ubiquinone oxidoreductase 24 kDa subunit)
Q9Y3F4	STRAP_HUMAN	Serine-threonine kinase receptor-associated protein (MAP activator with WD repeats) (UNR-interacting protein) (WD-40 repeat protein PT-WD)

O15371	EIF3D_HUMAN	Eukaryotic translation initiation factor 3 subunit D (eIF3d) (Eukaryotic translation initiation factor 3 subunit 7) (eIF-3-zeta) (eIF3 p66)
Q9NRW1	RAB6B_HUMAN	Ras-related protein Rab-6B
Q9NUJ1	ABHDA_HUMAN	Abhydrolase domain-containing protein 10 mitochondrial (EC 3.4.-.-)
Q16186	ADRM1_HUMAN	Proteasomal ubiquitin receptor ADRM1 (110 kDa cell membrane glycoprotein) (Gp110) (Adhesion-regulating molecule 1) (ARM-1) (Proteasome regulatory particle non-ATPase 13) (hRpn13) (Rpn13 homolog)
Q9NUB1	ACS2L_HUMAN	Acetyl-coenzyme A synthetase 2-like mitochondrial (EC 6.2.1.1) (Acetate--CoA ligase 2) (Acetyl-CoA synthetase 2) (AceCS2) (Acyl-CoA synthetase short-chain family member 1)
P46060	RAGP1_HUMAN	Ran GTPase-activating protein 1 (RanGAP1)
O15260	SURF4_HUMAN	Surfeit locus protein 4
Q9UNH7	SNX6_HUMAN	Sorting nexin-6 (TRAF4-associated factor 2)
P33992	MCM5_HUMAN	DNA replication licensing factor MCM5 (EC 3.6.4.12) (CDC46 homolog) (P1-CDC46)
Q00059	TFAM_HUMAN	Transcription factor A mitochondrial (mtTFA) (Mitochondrial transcription factor 1) (MtTF1) (Transcription factor 6) (TCF-6) (Transcription factor 6-like 2)
P15927	RFA2_HUMAN	Replication protein A 32 kDa subunit (RP-A p32) (Replication factor A protein 2) (RF-A protein 2) (Replication protein A 34 kDa subunit) (RP-A p34)
P04271	S100B_HUMAN	Protein S100-B (S-100 protein beta chain) (S-100 protein subunit beta) (S100 calcium-binding protein B)
P19971	TYPH_HUMAN	Thymidine phosphorylase (TP) (EC 2.4.2.4) (Gliostatin) (Platelet-derived endothelial cell growth factor) (PD-ECGF) (TdRPase)
O75340	PDCD6_HUMAN	Programmed cell death protein 6 (Apoptosis-linked gene 2 protein) (Probable calcium-binding protein ALG-2)
P63092	GNAS2_HUMAN	Guanine nucleotide-binding protein G(s) subunit alpha isoforms short (Adenylate cyclase-stimulating G alpha protein)
P26358	DNMT1_HUMAN	DNA (cytosine-5)-methyltransferase 1 (Dnmt1) (EC 2.1.1.37) (CXXC-type zinc finger protein 9) (DNA methyltransferase HsaI) (DNA MTase HsaI) (M.HsaI) (MCMT)
P42285	SK2L2_HUMAN	Superkiller viralicidic activity 2-like 2 (EC 3.6.4.13) (ATP-dependent helicase SKIV2L2)
O15117	FYB_HUMAN	FYN-binding protein (Adhesion and degranulation promoting adaptor protein) (ADAP) (FYB-120/130) (p120/p130) (FYN-T-binding protein) (SLAP-130) (SLP-76-associated phosphoprotein)
P61201	CSN2_HUMAN	COP9 signalosome complex subunit 2 (SGN2) (Signalosome subunit 2) (Alien homolog) (JAB1-containing signalosome subunit 2) (Thyroid receptor-interacting protein 15) (TR-interacting protein 15) (TRIP-15)
P42704	LPPRC_HUMAN	Leucine-rich PPR motif-containing protein mitochondrial (130 kDa leucine-rich protein) (LRP 130) (GP130)
Q13596	SNX1_HUMAN	Sorting nexin-1
Q96IU4	ABHEB_HUMAN	Abhydrolase domain-containing protein 14B (EC 3.-.-.-) (CCG1-interacting factor B)
Q9Y2B0	CNPY2_HUMAN	Coatomer subunit beta' (Beta'-coat protein) (Beta'-COP) (p102)
Q96HY6	DDRGK_HUMAN	DDRGK domain-containing protein 1

Q16795	NDUA9_HUMAN	NADH dehydrogenase [ubiquinone] 1 alpha subcomplex subunit 9 mitochondrial (Complex I-39kD) (CI-39kD) (NADH-ubiquinone oxidoreductase 39 kDa subunit)
Q9NR31	SAR1A_HUMAN	GTP-binding protein SAR1a (COPII-associated small GTPase)
Q9BZF1	OSBL8_HUMAN	Oxysterol-binding protein-related protein 8 (ORP-8) (OSBP-related protein 8)
O75152	ZC11A_HUMAN	Zinc finger CCCH domain-containing protein 11A
O95232	LC7L3_HUMAN	Luc7-like protein 3 (Cisplatin resistance-associated-overexpressed protein) (Luc7A) (Okadaic acid-inducible phosphoprotein OA48-18) (cAMP regulatory element-associated protein 1) (CRE-associated protein 1) (CREAP-1)
P33993	MCM7_HUMAN	DNA replication licensing factor MCM7 (EC 3.6.4.12) (CDC47 homolog) (P1.1-MCM3)
Q14765	STAT4_HUMAN	Signal transducer and activator of transcription 4
P19838	NFKB1_HUMAN	Nuclear factor NF-kappa-B p105 subunit (DNA-binding factor KBF1) (EBP-1) (Nuclear factor of kappa light polypeptide gene enhancer in B-cells 1) [Cleaved into: Nuclear factor NF-kappa-B p50 subunit]
O75347	TBCA_HUMAN	Tubulin-specific chaperone A (TCP1-chaperonin cofactor A) (Tubulin-folding cofactor A) (CFA)
P35658	NU214_HUMAN	Nuclear pore complex protein Nup214 (214 kDa nucleoporin) (Nucleoporin Nup214) (Protein CAN)
P51665	PSD7_HUMAN	26S proteasome non-ATPase regulatory subunit 7 (26S proteasome regulatory subunit RPN8) (26S proteasome regulatory subunit S12) (Mov34 protein homolog) (Proteasome subunit p40)
Q93009	UBP7_HUMAN	Ubiquitin carboxyl-terminal hydrolase 7 (EC 3.4.19.12) (Deubiquitinating enzyme 7) (Herpesvirus-associated ubiquitin-specific protease) (Ubiquitin thioesterase 7) (Ubiquitin-specific-processing protease 7)
P62280	RS11_HUMAN	40S ribosomal protein S11
Q14061	COX17_HUMAN	Cytochrome c oxidase copper chaperone
P43307	SSRA_HUMAN	Translocon-associated protein subunit alpha (TRAP-alpha) (Signal sequence receptor subunit alpha) (SSR-alpha)
Q9UPT8	ZC3H4_HUMAN	Zinc finger CCCH domain-containing protein 4
O43681	ASNA_HUMAN	ATPase ASNA1 (EC 3.6.-.-) (Arsenical pump-driving ATPase) (Arsenite-stimulated ATPase) (Transmembrane domain recognition complex 40 kDa ATPase subunit) (hARSA-I) (hASNA-I)
P06241	FYN_HUMAN	Tyrosine-protein kinase Fyn (EC 2.7.10.2) (Proto-oncogene Syn) (Proto-oncogene c-Fyn) (Src-like kinase) (SLK) (p59-Fyn)
Q2VIR3	IF2GL_HUMAN	Eukaryotic translation initiation factor 2 subunit 3-like protein (Eukaryotic translation initiation factor 2 subunit gamma A) (eIF-2-gamma A) (eIF-2gA)
Q7L2H7	EIF3M_HUMAN	Eukaryotic translation initiation factor 3 subunit M (eIF3m) (Fetal lung protein B5) (hFL-B5) (PCI domain-containing protein 1)
P67809	YBOX1_HUMAN	Nuclease-sensitive element-binding protein 1 (CCAAT-binding transcription factor I subunit A) (CBF-A) (DNA-binding protein B) (DBPB) (Enhancer factor I subunit A) (EFI-A) (Y-box transcription factor) (Y-box-binding protein 1) (YB-1)
Q9NQG5	RPR1B_HUMAN	Regulation of nuclear pre-mRNA domain-containing protein 1B (Cell cycle-related and expression-elevated

		protein in tumor)
Q12873	CHD3_HUMAN	Chromodomain-helicase-DNA-binding protein 3 (CHD-3) (EC 3.6.4.12) (ATP-dependent helicase CHD3) (Mi-2 autoantigen 240 kDa protein) (Mi2-alpha) (Zinc finger helicase) (hZFH)
A6NHQ2	FBLL1_HUMAN	rRNA/tRNA 2'-O-methyltransferase fibrillarin-like protein 1 (EC 2.1.1.-)
Q8TAT6	NPL4_HUMAN	Nuclear protein localization protein 4 homolog (Protein NPL4)
Q96EP5	DAZP1_HUMAN	DAZ-associated protein 1 (Deleted in azoospermia-associated protein 1)
Q8TDI0	CHD5_HUMAN	Chromodomain-helicase-DNA-binding protein 5 (CHD-5) (EC 3.6.4.12) (ATP-dependent helicase CHD5)
P30419	NMT1_HUMAN	Glycylpeptide N-tetradecanoyltransferase 1 (EC 2.3.1.97) (Myristoyl-CoA:protein N-myristoyltransferase 1) (NMT 1) (Type I N-myristoyltransferase) (Peptide N-myristoyltransferase 1)
Q12904	AIMP1_HUMAN	Aminoacyl tRNA synthase complex-interacting multifunctional protein 1 (Multisynthase complex auxiliary component p43) [Cleaved into: Endothelial monocyte-activating polypeptide 2 (EMAP-2) (Endothelial monocyte-activating polypeptide II) (EMAP-II) (Small inducible cytokine subfamily E member 1)]
Q04826	1B40_HUMAN	HLA class I histocompatibility antigen B-40 alpha chain (Bw-60) (MHC class I antigen B*40)
Q92900	RENT1_HUMAN	Regulator of nonsense transcripts 1 (EC 3.6.4.-) (ATP-dependent helicase RENT1) (Nonsense mRNA reducing factor 1) (NORF1) (Up-frameshift suppressor 1 homolog) (hUpf1)
P00387	NB5R3_HUMAN	NADH-cytochrome b5 reductase 3 (B5R) (Cytochrome b5 reductase) (EC 1.6.2.2) (Diaphorase-1) [Cleaved into: NADH-cytochrome b5 reductase 3 membrane-bound form; NADH-cytochrome b5 reductase 3 soluble form]
Q9NQC3	RTN4_HUMAN	Reticulon-4 (Foocen) (Neurite outgrowth inhibitor) (Nogo protein) (Neuroendocrine-specific protein) (NSP) (Neuroendocrine-specific protein C homolog) (RTN-x) (Reticulon-5)
O00186	STXB3_HUMAN	Syntaxin-binding protein 3 (Platelet Sec1 protein) (PSP) (Protein unc-18 homolog 3) (Unc18-3) (Protein unc-18 homolog C) (Unc-18C)
P17612	KAPCA_HUMAN	cAMP-dependent protein kinase catalytic subunit alpha (PKA C-alpha) (EC 2.7.11.11)
Q460N5	PAR14_HUMAN	Poly [ADP-ribose] polymerase 14 (PARP-14) (EC 2.4.2.30) (B aggressive lymphoma protein 2)
P22087	FBRL_HUMAN	rRNA 2'-O-methyltransferase fibrillarin (EC 2.1.1.-) (34 kDa nucleolar scleroderma antigen)
O60518	RNBP6_HUMAN	Ran-binding protein 6 (RanBP6)
P52701	MSH6_HUMAN	DNA mismatch repair protein Msh6 (hMSH6) (G/T mismatch-binding protein) (GTBP) (GTMBP) (MutS-alpha 160 kDa subunit) (p160)
Q96PK6	RBM14_HUMAN	RNA-binding protein 14 (Paraspeckle protein 2) (PSP2) (RNA-binding motif protein 14) (RRM-containing coactivator activator/modulator) (Synaptotagmin-interacting protein) (SYT-interacting protein)
O43776	SYNC_HUMAN	Asparaginyl-tRNA synthetase cytoplasmic (EC 6.1.1.22) (Asparagine--tRNA ligase) (AsnRS)
P01860	IGHG3_HUMAN	Ig gamma-3 chain C region (HDC) (Heavy chain disease protein)
P31937	3HIDH_HUMAN	3-hydroxyisobutyrate dehydrogenase mitochondrial (HIBADH) (EC 1.1.1.31)
Q9NXR7	BRE_HUMAN	BRCA1-A complex subunit BRE (BRCA1/BRCA2-containing complex subunit 45) (Brain and reproductive organ-expressed protein)

P61769	B2MG_HUMAN	Beta-2-microglobulin [Cleaved into: Beta-2-microglobulin form pI 5.3]
Q15369	ELOC_HUMAN	Endoplasmin (94 kDa glucose-regulated protein) (GRP-94) (Heat shock protein 90 kDa beta member 1) (Tumor rejection antigen 1) (gp96 homolog)
Q9H4A4	AMPB_HUMAN	Aminopeptidase B (AP-B) (EC 3.4.11.6) (Arginine aminopeptidase) (Arginyl aminopeptidase)
P54707	AT12A_HUMAN	Sodium/potassium-transporting ATPase subunit alpha-2 (Na(+)/K(+) ATPase alpha-2 subunit) (EC 3.6.3.9) (Sodium pump subunit alpha-2)
Q9Y305	ACOT9_HUMAN	Acyl-coenzyme A thioesterase 9 mitochondrial (Acyl-CoA thioesterase 9) (EC 3.1.2.-) (Acyl-CoA thioester hydrolase 9)
P61020	RAB5B_HUMAN	Ras-related protein Rab-5B
P63173	RL38_HUMAN	60S ribosomal protein L38
P08779	K1C16_HUMAN	Keratin type I cytoskeletal 16 (Cytokeratin-16) (CK-16) (Keratin-16) (K16)
P30085	KCY_HUMAN	UMP-CMP kinase (EC 2.7.4.14) (Cytidine monophosphate kinase) (Cytidylate kinase) (Deoxycytidylate kinase) (Uridine monophosphate kinase) (Uridine monophosphate/cytidine monophosphate kinase) (UMP/CMP kinase) (UMP/CMPK)
Q9NTX5	ECHD1_HUMAN	Putative elongation factor 1-alpha-like 3 (EF-1-alpha-like 3) (Eukaryotic elongation factor 1 A-like 3) (eEF1A-like 3) (Eukaryotic translation elongation factor 1 alpha-1 pseudogene 5)
A7KAX9	RHG32_HUMAN	Rho GTPase-activating protein 32 (Brain-specific Rho GTPase-activating protein) (GAB-associated Cdc42/Rac GTPase-activating protein) (GC-GAP) (GTPase regulator interacting with TrkA) (Rho-type GTPase-activating protein 32) (Rho/Cdc42/Rac GTPase-activating protein RICS) (RhoGAP involved in the beta-catenin-N-cadherin and NMDA receptor signaling) (p200RhoGAP) (p250GAP)
O75694	NU155_HUMAN	Nuclear pore complex protein Nup155 (155 kDa nucleoporin) (Nucleoporin Nup155)
P20042	IF2B_HUMAN	Eukaryotic translation initiation factor 2 subunit 2 (Eukaryotic translation initiation factor 2 subunit beta) (eIF-2-beta)
P11182	ODB2_HUMAN	Lipoamide acyltransferase component of branched-chain alpha-keto acid dehydrogenase complex mitochondrial (EC 2.3.1.168) (Branched-chain alpha-keto acid dehydrogenase complex component E2) (BCKAD-E2) (BCKADE2) (Dihydrolipoamide acetyltransferase component of branched-chain alpha-keto acid dehydrogenase complex) (Dihydrolipoamide branched chain transacylase) (Dihydrolipoyllysine-residue (2-methylpropanoyl)transferase)
P40429	RL13A_HUMAN	60S ribosomal protein L13a (23 kDa highly basic protein)
P35914	HMGCL_HUMAN	Hydroxymethylglutaryl-CoA lyase mitochondrial (HL) (HMG-CoA lyase) (EC 4.1.3.4) (3-hydroxy-3-methylglutarate-CoA lyase)
P43034	LIS1_HUMAN	Platelet-activating factor acetylhydrolase IB subunit alpha (Lissencephaly-1 protein) (LIS-1) (PAF acetylhydrolase 45 kDa subunit) (PAF-AH 45 kDa subunit) (PAF-AH alpha) (PAFAH alpha)
P46939	UTRO_HUMAN	Utrophin (Dystrophin-related protein 1) (DRP-1)
Q15427	SF3B4_HUMAN	Splicing factor 3B subunit 4 (Pre-mRNA-splicing factor SF3b 49 kDa subunit) (SF3b50) (Spliceosome-associated

		protein 49) (SAP 49)
Q2M1Z3	RHG31_HUMAN	Rho GTPase-activating protein 31 (Cdc42 GTPase-activating protein)
Q8TCU6	PREX1_HUMAN	Phosphatidylinositol 3 4 5-trisphosphate-dependent Rac exchanger 1 protein (P-Rex1) (PtdIns(3 4 5)-dependent Rac exchanger 1)
Q96HV5	TM41A_HUMAN	Transmembrane protein 41A
P56192	SYMC_HUMAN	Methionyl-tRNA synthetase cytoplasmic (EC 6.1.1.10) (Methionine--tRNA ligase) (MetRS)
P63208	SKP1_HUMAN	S-phase kinase-associated protein 1 (Cyclin-A/CDK2-associated protein p19) (Organ of Corti protein 2) (OCP-2) (Organ of Corti protein II) (OCP-II) (RNA polymerase II elongation factor-like protein) (SIII) (Transcription elongation factor B) (p19A) (p19skp1)
Q13547	HDAC1_HUMAN	Histone deacetylase 1 (HD1) (EC 3.5.1.98)
Q71UM5	RS27L_HUMAN	40S ribosomal protein S27-like
Q8TCT9	HM13_HUMAN	Minor histocompatibility antigen H13 (EC 3.4.23.-) (Intramembrane protease 1) (IMP-1) (IMPAS-1) (hIMP1) (Presenilin-like protein 3) (Signal peptide peptidase)
Q02750	MP2K1_HUMAN	Dual specificity mitogen-activated protein kinase kinase 1 (MAP kinase kinase 1) (MAPKK 1) (MKK1) (EC 2.7.12.2) (ERK activator kinase 1) (MAPK/ERK kinase 1) (MEK 1)
Q15907	RB11B_HUMAN	Ras-related protein Rab-11B (GTP-binding protein YPT3)
O00203	AP3B1_HUMAN	AP-3 complex subunit beta-1 (Adapter-related protein complex 3 subunit beta-1) (Adaptor protein complex AP-3 subunit beta-1) (Beta-3A-adaptin) (Clathrin assembly protein complex 3 beta-1 large chain)
O95861	BPNT1_HUMAN	3'(2') 5'-bisphosphate nucleotidase 1 (EC 3.1.3.7) (Bisphosphate 3'-nucleotidase 1) (PAP-inositol-1 4-phosphatase) (PIP)
Q07021	C1QBP_HUMAN	Complement component 1 Q subcomponent-binding protein mitochondrial (GC1q-R protein) (Glycoprotein gC1qBP) (C1qBP) (Hyaluronan-binding protein 1) (Mitochondrial matrix protein p32) (p33)
O00232	PSD12_HUMAN	26S proteasome non-ATPase regulatory subunit 12 (26S proteasome regulatory subunit RPN5) (26S proteasome regulatory subunit p55)
P10644	KAP0_HUMAN	cAMP-dependent protein kinase type I-alpha regulatory subunit (Tissue-specific extinguisher 1) (TSE1)
P55060	XPO2_HUMAN	Exportin-2 (Exp2) (Cellular apoptosis susceptibility protein) (Chromosome segregation 1-like protein) (Importin-alpha re-exporter)
Q9H9B4	SFXN1_HUMAN	Sideroflexin-1 (Tricarboxylate carrier protein) (TCC)
Q5T1M5	FKB15_HUMAN	FK506-binding protein 15 (FKBP-15) (133 kDa FK506-binding protein) (133 kDa FKBP) (FKBP-133) (WASP and FKBP-like) (WAFL)
P26885	FKBP2_HUMAN	Peptidyl-prolyl cis-trans isomerase FKBP2 (PPIase FKBP2) (EC 5.2.1.8) (13 kDa FK506-binding protein) (13 kDa FKBP) (FKBP-13) (FK506-binding protein 2) (FKBP-2) (Immunophilin FKBP13) (Rotamase)
Q13561	DCTN2_HUMAN	Dynactin subunit 2 (50 kDa dynein-associated polypeptide) (Dynactin complex 50 kDa subunit) (DCTN-50) (p50 dynamitin)

P20292	AL5AP_HUMAN	Arachidonate 5-lipoxygenase-activating protein (FLAP) (MK-886-binding protein)
O14983	AT2A1_HUMAN	Sarcoplasmic/endoplasmic reticulum calcium ATPase 3 (SERCA3) (SR Ca(2+)-ATPase 3) (EC 3.6.3.8) (Calcium pump 3)
P18031	PTN1_HUMAN	Tyrosine-protein phosphatase non-receptor type 1 (EC 3.1.3.48) (Protein-tyrosine phosphatase 1B) (PTP-1B)
P29218	IMPA1_HUMAN	Inositol monophosphatase 1 (IMP 1) (IMPase 1) (EC 3.1.3.25) (Inositol-1(or 4)-monophosphatase 1) (Lithium-sensitive myo-inositol monophosphatase A1)
Q13094	LCP2_HUMAN	Lymphocyte cytosolic protein 2 (SH2 domain-containing leukocyte protein of 76 kDa) (SLP-76 tyrosine phosphoprotein) (SLP76)
Q13442	HAP28_HUMAN	28 kDa heat- and acid-stable phosphoprotein (PDGF-associated protein) (PAP) (PDGFA-associated protein 1) (PAP1)
Q8WVM8	SCFD1_HUMAN	Sec1 family domain-containing protein 1 (SLY1 homolog) (Sly1p) (Syntaxin-binding protein 1-like 2)
Q9UHY1	NRBP_HUMAN	Nuclear receptor-binding protein
O60220	TIM8A_HUMAN	Mitochondrial import inner membrane translocase subunit Tim8 A (Deafness dystonia protein 1) (X-linked deafness dystonia protein)
P61970	NTF2_HUMAN	Nuclear transport factor 2 (NTF-2) (Placental protein 15) (PP15)
O60256	KPRB_HUMAN	Phosphoribosyl pyrophosphate synthase-associated protein 2 (PRPP synthase-associated protein 2) (41 kDa phosphoribosypyrophosphate synthetase-associated protein) (PAP41)
P13591	NCAM1_HUMAN	Neural cell adhesion molecule 1 (N-CAM-1) (NCAM-1) (CD antigen CD56)
P26640	SYVC_HUMAN	Valyl-tRNA synthetase (EC 6.1.1.9) (Protein G7a) (Valine--tRNA ligase) (ValRS)
P13164	IFM1_HUMAN	Interferon-induced transmembrane protein 1 (Interferon-induced protein 17) (Interferon-inducible protein 9-27) (Leu-13 antigen) (CD antigen CD225)
P31483	TIA1_HUMAN	Nucleolysin TIA-1 isoform p40 (RNA-binding protein TIA-1) (T-cell-restricted intracellular antigen-1) (TIA-1) (p40-TIA-1)
Q86U42	PABP2_HUMAN	Polyadenylate-binding protein 2 (PABP-2) (Poly(A)-binding protein 2) (Nuclear poly(A)-binding protein 1) (Poly(A)-binding protein II) (PABII) (Polyadenylate-binding nuclear protein 1)
Q93008	USP9X_HUMAN	Probable ubiquitin carboxyl-terminal hydrolase FAF-X (EC 3.4.19.12) (Deubiquitinating enzyme FAF-X) (Fat facets in mammals) (hFAM) (Fat facets protein-related X-linked) (Ubiquitin thiolesterase FAF-X) (Ubiquitin-specific protease 9 X chromosome) (Ubiquitin-specific-processing protease FAF-X)
Q9NPQ8	RIC8A_HUMAN	Synembryn-A (Protein Ric-8A)
Q9UBV8	PEF1_HUMAN	Peflin (PEF protein with a long N-terminal hydrophobic domain) (Penta-EF hand domain-containing protein 1)
Q92890	UFD1_HUMAN	Ubiquitin fusion degradation protein 1 homolog (UB fusion protein 1)
Q9H2U2	IPYR2_HUMAN	Inorganic pyrophosphatase 2 mitochondrial (EC 3.6.1.1) (Pyrophosphatase SID6-306) (Pyrophosphate phospho-hydrolase 2) (PPase 2)
Q9UBE0	SAE1_HUMAN	SUMO-activating enzyme subunit 1 (Ubiquitin-like 1-activating enzyme E1A)

O00231	PSD11_HUMAN	26S proteasome non-ATPase regulatory subunit 11 (26S proteasome regulatory subunit RPN6) (26S proteasome regulatory subunit S9) (26S proteasome regulatory subunit p44.5)
O43837	IDH3B_HUMAN	Isocitrate dehydrogenase [NAD] subunit beta mitochondrial (EC 1.1.1.41) (Isocitric dehydrogenase subunit beta) (NAD(+)-specific ICDH subunit beta)
P57088	TMM33_HUMAN	Transmembrane protein 33 (Protein DB83)
Q93045	STMN2_HUMAN	Stathmin-2 (Superior cervical ganglion-10 protein) (Protein SCG10)
O60613	SEP15_HUMAN	15 kDa selenoprotein
P62191	PRS4_HUMAN	26S protease regulatory subunit 4 (P26s4) (26S proteasome AAA-ATPase subunit RPT2) (Proteasome 26S subunit ATPase 1)
P14854	CX6B1_HUMAN	Cytochrome c oxidase subunit 6B1 (Cytochrome c oxidase subunit VIb isoform 1) (COX VIb-1)
P20073	ANXA7_HUMAN	Annexin A7 (Annexin VII) (Annexin-7) (Synexin)
Q9NWU2	CT011_HUMAN	Protein C20orf11 (Two hybrid-associated protein 1 with RanBPM) (Twa1)
Q9UGN4	CLM8_HUMAN	CMRF35-like molecule 8 (CLM-8) (CD300 antigen-like family member A) (CMRF-35-H9) (CMRF35-H9) (CMRF35-H) (IRC1/IRC2) (Immunoglobulin superfamily member 12) (IgSF12) (Inhibitory receptor protein 60) (IRp60) (NK inhibitory receptor) (CD antigen CD300a)
P63162	RSMN_HUMAN	Small nuclear ribonucleoprotein-associated protein N (snRNP-N) (Sm protein D) (Sm-D) (Sm protein N) (Sm-N) (SmN) (Tissue-specific-splicing protein)
Q86UP2	KTN1_HUMAN	Kinectin (CG-1 antigen) (Kinesin receptor)
Q9NTI5	PDS5B_HUMAN	Sister chromatid cohesion protein PDS5 homolog B (Androgen-induced proliferation inhibitor) (Androgen-induced prostate proliferative shutoff-associated protein AS3)
O14737	PDCD5_HUMAN	Programmed cell death protein 5 (TF-1 cell apoptosis-related protein 19) (Protein TFAR19)
P55884	EIF3B_HUMAN	Eukaryotic translation initiation factor 3 subunit B (eIF3b) (Eukaryotic translation initiation factor 3 subunit 9) (Prt1 homolog) (hPrt1) (eIF-3-eta) (eIF3 p110) (eIF3 p116)
O94776	MTA2_HUMAN	Metastasis-associated protein MTA2 (Metastasis-associated 1-like 1) (MTA1-L1 protein) (p53 target protein in deacetylase complex)
Q96AG4	LRC59_HUMAN	Leucine-rich repeat-containing protein 59
O14880	MGST3_HUMAN	Microsomal glutathione S-transferase 3 (Microsomal GST-3) (EC 2.5.1.18) (Microsomal GST-III)
P11216	PYGB_HUMAN	Glycogen phosphorylase brain form (EC 2.4.1.1)
P49257	LMAN1_HUMAN	Protein ERGIC-53 (ER-Golgi intermediate compartment 53 kDa protein) (Gp58) (Intracellular mannose-specific lectin MR60) (Lectin mannose-binding 1)
P98179	RBM3_HUMAN	Putative RNA-binding protein 3 (RNA-binding motif protein 3) (RNPL)
Q01085	TIAR_HUMAN	Nucleolysin TIAR (TIA-1-related protein)
Q9Y5K5	UCHL5_HUMAN	Ubiquitin carboxyl-terminal hydrolase isozyme L5 (UCH-L5) (EC 3.4.19.12) (Ubiquitin C-terminal hydrolase UCH37) (Ubiquitin thioesterase L5)

P24752	THIL_HUMAN	Acetyl-CoA acetyltransferase mitochondrial (EC 2.3.1.9) (Acetoacetyl-CoA thiolase) (T2)
P82979	SARNP_HUMAN	SAP domain-containing ribonucleoprotein (Cytokine-induced protein of 29 kDa) (Nuclear protein Hcc-1) (Proliferation-associated cytokine-inducible protein CIP29)
Q03519	TAP2_HUMAN	Antigen peptide transporter 2 (APT2) (ATP-binding cassette sub-family B member 3) (Peptide supply factor 2) (Peptide transporter PSF2) (PSF-2) (Peptide transporter TAP2) (Peptide transporter involved in antigen processing 2) (Really interesting new gene 11 protein)
Q9UQ35	SRRM2_HUMAN	Serine/arginine repetitive matrix protein 2 (300 kDa nuclear matrix antigen) (Serine/arginine-rich splicing factor-related nuclear matrix protein of 300 kDa) (SR-related nuclear matrix protein of 300 kDa) (Ser/Arg-related nuclear matrix protein of 300 kDa) (Splicing coactivator subunit SRm300) (Tax-responsive enhancer element-binding protein 803) (TaxREB803)
Q9NS69	TOM22_HUMAN	Mitochondrial import receptor subunit TOM22 homolog (hTom22) (1C9-2) (Translocase of outer membrane 22 kDa subunit homolog)
P63027	VAMP2_HUMAN	Vesicle-associated membrane protein 2 (VAMP-2) (Synaptobrevin-2)
Q05193	DYN1_HUMAN	Dynamin-1 (EC 3.6.5.5)
Q9H3K6	BOLA2_HUMAN	BolA-like protein 2
Q9NX63	CHCH3_HUMAN	Coiled-coil-helix-coiled-coil-helix domain-containing protein 3 mitochondrial
P56545	CTBP2_HUMAN	C-terminal-binding protein 2 (CtBP2)
Q8IY67	RAVR1_HUMAN	Ribonucleoprotein PTB-binding 1 (Protein raver-1)
O43242	PSMD3_HUMAN	26S proteasome non-ATPase regulatory subunit 3 (26S proteasome regulatory subunit RPN3) (26S proteasome regulatory subunit S3) (Proteasome subunit p58)
O43920	NDUS5_HUMAN	NADH dehydrogenase [ubiquinone] iron-sulfur protein 5 (Complex I-15 kDa) (CI-15 kDa) (NADH-ubiquinone oxidoreductase 15 kDa subunit)
P47897	SYQ_HUMAN	Glutaminyl-tRNA synthetase (EC 6.1.1.18) (Glutamine--tRNA ligase) (GlnRS)
P51688	SPHM_HUMAN	N-sulphoglucosamine sulphohydrolase (EC 3.10.1.1) (Sulfoglucosamine sulfamidase) (Sulphamidase)
Q9NX24	NHP2_HUMAN	H/ACA ribonucleoprotein complex subunit 2 (Nucleolar protein family A member 2) (snoRNP protein NHP2)
O75822	EIF3J_HUMAN	Eukaryotic translation initiation factor 3 subunit J (eIF3j) (Eukaryotic translation initiation factor 3 subunit 1) (eIF-3-alpha) (eIF3 p35)
A6NHG4	DDTL_HUMAN	D-dopachrome decarboxylase-like protein (EC 4.1.1.-) (D-dopachrome tautomerase-like protein)
P55036	PSMD4_HUMAN	26S proteasome non-ATPase regulatory subunit 4 (26S proteasome regulatory subunit RPN10) (26S proteasome regulatory subunit S5A) (Antisecretory factor 1) (AF) (ASF) (Multiubiquitin chain-binding protein)
Q08170	SRSF4_HUMAN	Serine/arginine-rich splicing factor 4 (Pre-mRNA-splicing factor SRP75) (SRP001LB) (Splicing factor arginine/serine-rich 4)
O60361	NDK8_HUMAN	Putative nucleoside diphosphate kinase (NDK) (NDP kinase) (EC 2.7.4.6)
P49407	ARRB1_HUMAN	Beta-arrestin-1 (Arrestin beta-1)

P25788	PSA3_HUMAN	Proteasome subunit alpha type-3 (EC 3.4.25.1) (Macropain subunit C8) (Multicatalytic endopeptidase complex subunit C8) (Proteasome component C8)
Q15181	IPYR_HUMAN	Inorganic pyrophosphatase (EC 3.6.1.1) (Pyrophosphate phospho-hydrolase) (PPase)
Q8IYB3	SRRM1_HUMAN	Serine/arginine repetitive matrix protein 1 (SR-related nuclear matrix protein of 160 kDa) (SRm160) (Ser/Arg-related nuclear matrix protein)
Q8WXX5	DNJC9_HUMAN	DnaJ homolog subfamily C member 9 (DnaJ protein SB73)
P12268	IMDH2_HUMAN	Inosine-5'-monophosphate dehydrogenase 2 (IMP dehydrogenase 2) (IMPD 2) (IMPDH 2) (EC 1.1.1.205) (IMPDH-II)
P48651	PTSS1_HUMAN	Phosphatidylserine synthase 1 (PSS-1) (PtdSer synthase 1) (EC 2.7.8.-) (Serine-exchange enzyme I)
Q12846	STX4_HUMAN	Syntaxin-4 (Renal carcinoma antigen NY-REN-31)
Q9Y6B6	SAR1B_HUMAN	GTP-binding protein SAR1b (GTP-binding protein B) (GTBPB)
P18077	RL35A_HUMAN	60S ribosomal protein L35a (Cell growth-inhibiting gene 33 protein)
P51970	NDUA8_HUMAN	NADH dehydrogenase [ubiquinone] 1 alpha subcomplex subunit 8 (Complex I-19kD) (CI-19kD) (Complex I-PGIV) (CI-PGIV) (NADH-ubiquinone oxidoreductase 19 kDa subunit)
P61009	SPCS3_HUMAN	Signal peptidase complex subunit 3 (EC 3.4.-.-) (Microsomal signal peptidase 22/23 kDa subunit) (SPC22/23) (SPase 22/23 kDa subunit)
P67812	SC11A_HUMAN	Signal peptidase complex catalytic subunit SEC11A (EC 3.4.21.89) (Endopeptidase SP18) (Microsomal signal peptidase 18 kDa subunit) (SPase 18 kDa subunit) (SEC11 homolog A) (SEC11-like protein 1) (SPC18)
Q13242	SRSF9_HUMAN	Serine/arginine-rich splicing factor 9 (Pre-mRNA-splicing factor SRp30C) (Splicing factor arginine/serine-rich 9)
P63267	ACTH_HUMAN	Actin gamma-enteric smooth muscle (Alpha-actin-3) (Gamma-2-actin) (Smooth muscle gamma-actin)
O75937	DNJC8_HUMAN	DnaJ homolog subfamily C member 8 (Splicing protein spf31)
Q6PIW4	FIGL1_HUMAN	Fidgetin-like protein 1 (EC 3.6.4.-)
O60551	NMT2_HUMAN	Glycylpeptide N-tetradecanoyltransferase 2 (EC 2.3.1.97) (Myristoyl-CoA:protein N-myristoyltransferase 2) (NMT 2) (Peptide N-myristoyltransferase 2) (Type II N-myristoyltransferase)
Q31610	1B81_HUMAN	HLA class I histocompatibility antigen B-81 alpha chain (B'DT) (MHC class I antigen B*81)
O14559	RHG33_HUMAN	Rho GTPase-activating protein 33 (Rho-type GTPase-activating protein 33) (Sorting nexin-26) (Tc10/CDC42 GTPase-activating protein)
O60749	SNX2_HUMAN	Sorting nexin-2 (Transformation-related gene 9 protein) (TRG-9)
Q13162	PRDX4_HUMAN	Peroxiredoxin-4 (EC 1.11.1.15) (Antioxidant enzyme AOE372) (AOE37-2) (Peroxiredoxin IV) (Prx-IV) (Thioredoxin peroxidase AO372) (Thioredoxin-dependent peroxide reductase A0372)
P07864	LDHC_HUMAN	L-lactate dehydrogenase C chain (LDH-C) (EC 1.1.1.27) (Cancer/testis antigen 32) (CT32) (LDH testis subunit) (LDH-X)
P62745	RHOB_HUMAN	Rho-related GTP-binding protein RhoB (Rho cDNA clone 6) (h6)

Q8N7X1	RMXL3_HUMAN	RNA-binding motif protein X-linked-like-3
P11908	PRPS2_HUMAN	Ribose-phosphate pyrophosphokinase 2 (EC 2.7.6.1) (PPRibP) (Phosphoribosyl pyrophosphate synthase II) (PRS-II)
P26010	ITB7_HUMAN	Integrin beta-7 (Gut homing receptor beta subunit)
P50452	SPB8_HUMAN	Serpin B8 (Cytoplasmic antiproteinase 2) (CAP-2) (CAP2) (Peptidase inhibitor 8) (PI-8)
Q16576	RBBP7_HUMAN	Histone-binding protein RBBP7 (Histone acetyltransferase type B subunit 2) (Nucleosome-remodeling factor subunit RBAP46) (Retinoblastoma-binding protein 7) (RBBP-7) (Retinoblastoma-binding protein p46)
Q6ZMR3	LDH6A_HUMAN	L-lactate dehydrogenase A-like 6A (EC 1.1.1.27)
Q9NVJ2	ARL8B_HUMAN	ADP-ribosylation factor-like protein 8B (ADP-ribosylation factor-like protein 10C) (Novel small G protein indispensable for equal chromosome segregation 1)
P20718	GRAH_HUMAN	Granzyme H (EC 3.4.21.-) (CCP-X) (Cathepsin G-like 2) (CTSGL2) (Cytotoxic T-lymphocyte proteinase) (Cytotoxic serine protease C) (CSP-C)
Q96JB5	CK5P3_HUMAN	CDK5 regulatory subunit-associated protein 3 (CDK5 activator-binding protein C53) (Protein HSF-27)
Q9Y3D6	FIS1_HUMAN	Mitochondrial fission 1 protein (FIS1 homolog) (hFis1) (Tetratricopeptide repeat protein 11) (TPR repeat protein 11)
P78356	PI42B_HUMAN	Phosphatidylinositol-5-phosphate 4-kinase type-2 beta (EC 2.7.1.149) (1-phosphatidylinositol-5-phosphate 4-kinase 2-beta) (Diphosphoinositide kinase 2-beta) (Phosphatidylinositol-5-phosphate 4-kinase type II beta) (PI(5)P 4-kinase type II beta) (PIP4KII-beta) (PtdIns(5)P-4-kinase isoform 2-beta)
P07947	YES_HUMAN	Tyrosine-protein kinase Yes (EC 2.7.10.2) (Proto-oncogene c-Yes) (p61-Yes)
P08631	HCK_HUMAN	Tyrosine-protein kinase HCK (EC 2.7.10.2) (Hemopoietic cell kinase) (p59-HCK/p60-HCK)
Q13153	PAK1_HUMAN	Serine/threonine-protein kinase PAK 1 (EC 2.7.11.1) (Alpha-PAK) (p21-activated kinase 1) (PAK-1) (p65-PAK)
O95716	RAB3D_HUMAN	Ras-related protein Rab-3D
P16930	FAAA_HUMAN	Fumarylacetoacetase (FAA) (EC 3.7.1.2) (Beta-diketonase) (Fumarylacetoacetate hydrolase)
P30481	1B44_HUMAN	HLA class I histocompatibility antigen B-44 alpha chain (Bw-44) (MHC class I antigen B*44)
P30505	1C08_HUMAN	HLA class I histocompatibility antigen Cw-8 alpha chain (MHC class I antigen Cw*8)
Q9UEY8	ADDG_HUMAN	Gamma-adducin (Adducin-like protein 70)
Q9H223	EHD4_HUMAN	EH domain-containing protein 4 (Hepatocellular carcinoma-associated protein 10/11) (PAST homolog 4)
Q13733	AT1A4_HUMAN	Sodium/potassium-transporting ATPase subunit alpha-4 (Na(+)/K(+) ATPase alpha-4 subunit) (EC 3.6.3.9) (Sodium pump subunit alpha-4)
P48444	COPD_HUMAN	Coatomer subunit delta (Archain) (Delta-coat protein) (Delta-COP)
Q9Y6V7	DDX49_HUMAN	Probable ATP-dependent RNA helicase DDX49 (EC 3.6.4.13) (DEAD box protein 49)
Q6DD88	ATLA3_HUMAN	ATP synthase subunit d mitochondrial (ATPase subunit d)
P48507	GSH0_HUMAN	Glutamate--cysteine ligase regulatory subunit (GCS light chain) (Gamma-ECS regulatory subunit) (Gamma-

		glutamylcysteine synthetase regulatory subunit) (Glutamate--cysteine ligase modifier subunit)
O75964	ATP5L_HUMAN	ATP synthase subunit g mitochondrial (ATPase subunit g)
Q9BTC0	DIDO1_HUMAN	Death-inducer obliterator 1 (DIO-1) (hDido1) (Death-associated transcription factor 1) (DATF-1)
Q9UBF2	COPG2_HUMAN	Coatomer subunit gamma-2 (Gamma-2-coat protein) (Gamma-2-COP)
Q9BS26	ERP44_HUMAN	Endoplasmic reticulum resident protein 44 (ER protein 44) (ERp44) (Thioredoxin domain-containing protein 4)
P33316	DUT_HUMAN	Deoxyuridine 5'-triphosphate nucleotidohydrolase mitochondrial (dUTPase) (EC 3.6.1.23) (dUTP pyrophosphatase)

Table 2. Proteins in human primary NK cells that were down-regulated following IL-2 stimulation.

Accession	Entry Name	Protein Name
P30450	1A26_HUMAN	HLA class I histocompatibility antigen A-26 alpha chain (MHC class I antigen A*26)
P03989	1B27_HUMAN	HLA class I histocompatibility antigen B-27 alpha chain (MHC class I antigen B*27)
P30480	1B42_HUMAN	HLA class I histocompatibility antigen B-42 alpha chain (MHC class I antigen B*42)
P10319	1B58_HUMAN	HLA class I histocompatibility antigen B-58 alpha chain (Bw-58) (MHC class I antigen B*58)
P11171	41_HUMAN	Protein 4.1 (P4.1) (4.1R) (Band 4.1) (EPB4.1)
P01023	A2MG_HUMAN	Alpha-2-macroglobulin (Alpha-2-M) (C3 and PZP-like alpha-2-macroglobulin domain-containing protein 5)
Q7Z5R6	AB1IP_HUMAN	Amyloid beta A4 precursor protein-binding family B member 1-interacting protein (APBB1-interacting protein 1) (Proline-rich EVH1 ligand 1) (PREL-1) (Proline-rich protein 73) (Rap1-GTP-interacting adapter molecule) (RIAM) (Retinoic acid-responsive proline-rich protein 1) (RARP-1)
Q9P2A4	ABI3_HUMAN	ABI gene family member 3 (New molecule including SH3) (Nesh)
O96019	ACL6A_HUMAN	Actin-like protein 6A (53 kDa BRG1-associated factor A) (Actin-related protein Baf53a) (ArpNbeta) (BRG1-associated factor 53A) (BAF53A) (INO80 complex subunit K)
P00813	ADA_HUMAN	Adenosine deaminase (EC 3.5.4.4) (Adenosine aminohydrolase)
Q8NCW5	AIBP_HUMAN	Apolipoprotein A-I-binding protein (AI-BP) (YjeF N-terminal domain-containing protein 1) (YjeF_N1)
P08758	ANXA5_HUMAN	Annexin A5 (Anchorin CII) (Annexin V) (Annexin-5) (Calphobindin I) (CBP-I) (Endonexin II) (Lipocortin V) (Placental anticoagulant protein 4) (PP4) (Placental anticoagulant protein I) (PAP-I) (Thromboplastin inhibitor) (Vascular anticoagulant-alpha) (VAC-alpha)
Q8NHP1	ARK74_HUMAN	Aflatoxin B1 aldehyde reductase member 4 (EC 1.-.-.-) (AFB1 aldehyde reductase 3) (AFB1-AR 3) (Aldoketoreductase 7-like)

P56385	ATP5I_HUMAN	ATP synthase subunit e mitochondrial (ATPase subunit e)
O00499	BIN1_HUMAN	Myc box-dependent-interacting protein 1 (Amphiphysin II) (Amphiphysin-like protein) (Box-dependent myc-interacting protein 1) (Bridging integrator 1)
Q9Y376	CAB39_HUMAN	Calcium-binding protein 39 (MO25alpha) (Protein Mo25)
Q8IX12	CCAR1_HUMAN	Cell division cycle and apoptosis regulator protein 1 (Cell cycle and apoptosis regulatory protein 1) (CARP-1) (Death inducer with SAP domain)
Q9H444	CHM4B_HUMAN	Charged multivesicular body protein 4b (Chromatin-modifying protein 4b) (CHMP4b) (SNF7 homolog associated with Alix 1) (SNF7-2) (hSnf7-2) (Vacuolar protein sorting-associated protein 32-2) (Vps32-2) (hVps32-2)
Q9BUH6	CI142_HUMAN	Uncharacterized protein C9orf142
O95833	CLIC3_HUMAN	Chloride intracellular channel protein 3
Q14019	COTL1_HUMAN	Coactosin-like protein
P50416	CPT1A_HUMAN	Carnitine O-palmitoyltransferase 1 liver isoform (CPT1-L) (EC 2.3.1.21) (Carnitine O-palmitoyltransferase I liver isoform) (CPT I) (CPTI-L) (Carnitine palmitoyltransferase 1A)
Q6JBY9	CPZIP_HUMAN	CapZ-interacting protein (Protein kinase substrate CapZIP) (RCSD domain-containing protein 1)
Q9Y394	DHRS7_HUMAN	Dehydrogenase/reductase SDR family member 7 (EC 1.1.-.-) (Retinal short-chain dehydrogenase/reductase 4) (retSDR4)
P31040	DHSA_HUMAN	Succinate dehydrogenase [ubiquinone] flavoprotein subunit mitochondrial (EC 1.3.5.1) (Flavoprotein subunit of complex II) (Fp)
P63167	DYL1_HUMAN	Dynein light chain 1 cytoplasmic (8 kDa dynein light chain) (DLC8) (Dynein light chain LC8-type 1) (Protein inhibitor of neuronal nitric oxide synthase) (PIN)
Q96FJ2	DYL2_HUMAN	Dynein light chain 2 cytoplasmic (8 kDa dynein light chain b) (DLC8b) (Dynein light chain LC8-type 2)
O15372	EIF3H_HUMAN	Eukaryotic translation initiation factor 3 subunit H (eIF3h) (Eukaryotic translation initiation factor 3 subunit 3) (eIF-3-gamma) (eIF3 p40 subunit)
O95571	ETHE1_HUMAN	Protein ETHE1 mitochondrial (EC 3.-.-.-) (Ethylmalonic encephalopathy protein 1) (Hepatoma subtracted clone one protein)
P35754	GLRX1_HUMAN	Glutaredoxin-1 (Thioltransferase-1) (TTase-1)
Q86SX6	GLRX5_HUMAN	Glutaredoxin-related protein 5 mitochondrial (Monothiol glutaredoxin-5)
P46976	GLYG_HUMAN	Glycogenin-1 (GN-1) (GN1) (EC 2.4.1.186)
Q9HAV7	GRPE1_HUMAN	GrpE protein homolog 1 mitochondrial (HMGE) (Mt-GrpE#1)
Q9BX68	HINT2_HUMAN	Histidine triad nucleotide-binding protein 2 mitochondrial (HINT-2) (EC 3.-.-.-) (HINT-3) (HIT-17kDa) (PKCI-1-related HIT protein)
P05204	HMGN2_HUMAN	Non-histone chromosomal protein HMG-17 (High mobility group nucleosome-binding domain-containing protein 2)
Q58FG0	HS905_HUMAN	Putative heat shock protein HSP 90-alpha A5 (Heat shock protein 90-alpha E) (Heat shock protein 90Ae)

Q13349	ITAD_HUMAN	Integrin alpha-D (ADB2) (CD11 antigen-like family member D) (Leukointegrin alpha D) (CD antigen CD11d)
P20702	ITAX_HUMAN	Integrin alpha-X (CD11 antigen-like family member C) (Leu M5) (Leukocyte adhesion glycoprotein p150 95 alpha chain) (Leukocyte adhesion receptor p150 95) (CD antigen CD11c)
P17858	K6PL_HUMAN	6-phosphofructokinase liver type (EC 2.7.1.11) (Phosphofructo-1-kinase isozyme B) (PFK-B) (Phosphofructokinase 1) (Phosphohexokinase)
P51812	KS6A3_HUMAN	Ribosomal protein S6 kinase alpha-3 (S6K-alpha-3) (EC 2.7.11.1) (90 kDa ribosomal protein S6 kinase 3) (p90-RSK 3) (p90RSK3) (Insulin-stimulated protein kinase 1) (ISPK-1) (MAP kinase-activated protein kinase 1b) (MAPK-activated protein kinase 1b) (MAPKAP kinase 1b) (MAPKAPK-1b) (Ribosomal S6 kinase 2) (RSK-2) (pp90RSK2)
P16150	LEUK_HUMAN	Leukosialin (Galactoglycoprotein) (GALGP) (Leukocyte sialoglycoprotein) (Sialophorin) (CD antigen CD43)
Q8N1G4	LRC47_HUMAN	Leucine-rich repeat-containing protein 47
P61626	LYSC_HUMAN	Lysozyme C (EC 3.2.1.17) (1 4-beta-N-acetylmuramidase C)
Q9H8H3	MET7A_HUMAN	Methyltransferase-like protein 7A (EC 2.1.1.-) (Protein AAM-B)
Q16539	MK14_HUMAN	Mitogen-activated protein kinase 14 (MAP kinase 14) (MAPK 14) (EC 2.7.11.24) (Cytokine suppressive anti-inflammatory drug-binding protein) (CSAID-binding protein) (CSBP) (MAP kinase MXI2) (MAX-interacting protein 2) (Mitogen-activated protein kinase p38 alpha) (MAP kinase p38 alpha) (SAPK2A)
O60502	NCOAT_HUMAN	Bifunctional protein NCOAT (Meningioma-expressed antigen 5) (Nuclear cytoplasmic O-GlcNAcase and acetyltransferase) [Includes: Protein O-GlcNAcase (EC 3.2.1.169) (Glycoside hydrolase O-GlcNAcase) (Hexosaminidase C) (N-acetyl-beta-D-glucosaminidase) (N-acetyl-beta-glucosaminidase) (O-GlcNAcase) (OGA); Histone acetyltransferase (HAT) (EC 2.3.1.48)]
Q13469	NFAC2_HUMAN	Nuclear factor of activated T-cells cytoplasmic 2 (NF-ATc2) (NFATc2) (NFAT pre-existing subunit) (NF-ATp) (T-cell transcription factor NFAT1)
Q8WXI9	P66B_HUMAN	Transcriptional repressor p66-beta (GATA zinc finger domain-containing protein 2B) (p66/p68)
Q9UHG3	PCYOX_HUMAN	Prenylcysteine oxidase 1 (EC 1.8.3.5) (Prenylcysteine lyase)
Q53EL6	PDCD4_HUMAN	Programmed cell death protein 4 (Neoplastic transformation inhibitor protein) (Nuclear antigen H731-like) (Protein 197/15a)
Q7RTV0	PHF5A_HUMAN	PHD finger-like domain-containing protein 5A (PHD finger-like domain protein 5A) (Splicing factor 3B-associated 14 kDa protein) (SF3b14b)
Q9BZL4	PP12C_HUMAN	Protein phosphatase 1 regulatory subunit 12C (Protein phosphatase 1 myosin-binding subunit of 85 kDa) (Protein phosphatase 1 myosin-binding subunit p85)
P62714	PP2AB_HUMAN	Serine/threonine-protein phosphatase 2A catalytic subunit beta isoform (PP2A-beta) (EC 3.1.3.16)
Q9UPN7	PP6R1_HUMAN	Serine/threonine-protein phosphatase 6 regulatory subunit 1 (SAPS domain family member 1)
O43172	PRP4_HUMAN	U4/U6 small nuclear ribonucleoprotein Prp4 (PRP4 homolog) (hPrp4) (U4/U6 snRNP 60 kDa protein) (WD splicing factor Prp4)

P49721	PSB2_HUMAN	Proteasome subunit beta type-2 (EC 3.4.25.1) (Macropain subunit C7-I) (Multicatalytic endopeptidase complex subunit C7-I) (Proteasome component C7-I)
Q00577	PURA_HUMAN	Transcriptional activator protein Pur-alpha (Purine-rich single-stranded DNA-binding protein alpha)
P20742	PZP_HUMAN	Pregnancy zone protein (C3 and PZP-like alpha-2-macroglobulin domain-containing protein 6)
P20339	RAB5A_HUMAN	Ras-related protein Rab-5A
P51159	RB27A_HUMAN	Ras-related protein Rab-27A (Rab-27) (GTP-binding protein Ram)
P18754	RCC1_HUMAN	Regulator of chromosome condensation (Cell cycle regulatory protein) (Chromosome condensation protein 1)
P98171	RHG04_HUMAN	Rho GTPase-activating protein 4 (Rho-GAP hematopoietic protein C1) (Rho-type GTPase-activating protein 4) (p115)
P62273	RS29_HUMAN	40S ribosomal protein S29
P08621	RU17_HUMAN	U1 small nuclear ribonucleoprotein 70 kDa (U1 snRNP 70 kDa) (U1-70K) (snRNP70)
P09234	RU1C_HUMAN	U1 small nuclear ribonucleoprotein C (U1 snRNP C) (U1-C) (U1C)
P23526	SAHH_HUMAN	Adenosylhomocysteinase (AdoHcyase) (EC 3.3.1.1) (S-adenosyl-L-homocysteine hydrolase)
Q15436	SC23A_HUMAN	Protein transport protein Sec23A (SEC23-related protein A)
Q9UQE7	SMC3_HUMAN	Structural maintenance of chromosomes protein 3 (SMC protein 3) (SMC-3) (Basement membrane-associated chondroitin proteoglycan) (Bamacan) (Chondroitin sulfate proteoglycan 6) (Chromosome-associated polypeptide) (hCAP)
Q9H254	SPTN4_HUMAN	Spectrin beta chain brain 3 (Beta-IV spectrin) (Spectrin non-erythroid beta chain 3)
Q9Y5M8	SRPRB_HUMAN	Signal recognition particle receptor subunit beta (SR-beta) (Protein APMCF1)
Q9Y228	T3JAM_HUMAN	TRAF3-interacting JNK-activating modulator (TRAF3-interacting protein 3)
Q13148	TADBP_HUMAN	TAR DNA-binding protein 43 (TDP-43)
Q9BVC6	TM109_HUMAN	Transmembrane protein 109 (Mitsugumin-23) (Mg23)
A8MW06	TMSL3_HUMAN	Thymosin beta-4-like protein 3
P02787	TRFE_HUMAN	Serotransferrin (Transferrin) (Beta-1 metal-binding globulin) (Siderophilin)
Q9NNW7	TRXR2_HUMAN	Thioredoxin reductase 2 mitochondrial (EC 1.8.1.9) (Selenoprotein Z) (SelZ) (TR-beta) (Thioredoxin reductase TR3)
P68036	UB2L3_HUMAN	Ubiquitin-conjugating enzyme E2 L3 (EC 6.3.2.19) (L-UBC) (UbcH7) (Ubiquitin carrier protein L3) (Ubiquitin-conjugating enzyme E2-F1) (Ubiquitin-protein ligase L3)
P54578	UBP14_HUMAN	Ubiquitin carboxyl-terminal hydrolase 14 (EC 3.4.19.12) (Deubiquitinating enzyme 14) (Ubiquitin thiolesterase 14) (Ubiquitin-specific-processing protease 14)
Q70J99	UN13D_HUMAN	Protein unc-13 homolog D (Munc13-4)
Q99536	VAT1_HUMAN	Synaptic vesicle membrane protein VAT-1 homolog (EC 1.-.-.-)
P04004	VTNC_HUMAN	Vitronectin (S-protein) (Serum-spreading factor) (V75) [Cleaved into: Vitronectin V65 subunit; Vitronectin V10

		subunit; Somatomedin-B]
O43516	WIPF1_HUMAN	WAS/WASL-interacting protein family member 1 (Protein PRPL-2) (Wiskott-Aldrich syndrome protein-interacting protein) (WASP-interacting protein)

Appendix 3

List of publications and presentations

Publications:

1. **Ma D**, Cao W, Kapur A, Scarlett C, Patankar M, Li L. Differential Expression of Proteins in Naïve and IL-2 Stimulated Primary Human NK Cells Identified by Global Proteomic Analysis". In preparation.
2. **Ma D**, Yang C, Shi X and Li L. Comparative Secretome Analysis of Vascular Smooth Muscle Cells in Response to Smad3-Dependent TGF-β Signaling. In preparation.
3. **Ma D**, Li L. "Searching for Reliable Pre-mortem Protein Biomarkers for Prion Diseases – Progress and Challenges to Date". *Expert Rev Proteomics*, 9 (3): 267-280 (2012).
4. Cunningham R, **Ma D**, Li L. "Mass spectrometry-based proteomics and peptidomics for systems biology and biomarker discovery". *Frontiers in Biology*. 2012; **7**(4): 313-35.
5. Cao W, **Ma D**, Kapur A, Patankar M, Ma Y, Li L. "RT-SVR+q: A strategy for post-mascot analysis using retention time and q value metric to improve peptide and protein identifications". *J Proteomics*, 75 (2): 480-490 (2011).
6. Wei X, Herbst A, **Ma D**, Aiken J, Li L. "A quantitative proteomic approach to prion disease biomarker research: delving into the glycoproteome". *J Proteome Res*, 10 (6), 2687-2702 (2011).

Presentations:

1. **Ma D**, Cao W, Kapur A, Scarlett C, Patankar M, Li L. "Comparative analysis of the global proteome of naïve and IL-2 stimulated human NK cells". Poster Session, 60th ASMS Conference on Mass Spectrometry. May 2012, Vancouver, BC, Canada.
2. Qiu Y, **Ma D**, Li L. "Comparative analysis of proteomic profile of leukemic and primary human NK cells". Introductory Biology Mentored Research Poster Session. May 2012, University of Wisconsin-Madison.
3. **Ma D**, Kapur A, Felder M, Patankar M, Li L. "Characterization and comparative analysis of proteomic profile of leukemic and primary human NK cells". Poster Session, Wisconsin Human Proteomics Symposium. August 2011, Madison, Wisconsin.
4. Cao W, **Ma D**, Kapur A, Patankar M, Ma Y, Li L. "RT-SVR+q: A strategy for post-mascot analysis using retention time and q value metric to improve peptide and protein identifications". Poster Session, Wisconsin Human Proteomics Symposium. August 2011, Madison, Wisconsin.
5. **Ma D**, Kapur A, Felder M, Patankar M, Li L. "Characterization and comparative analysis of proteomic profile of leukemic and primary human NK cells". Poster Session, 59th ASMS Conference on Mass Spectrometry. June 2011, Denver, Colorado.
6. Wei X, Herbst A, Ma D, Li L, Aiken J. "A comparative glycoproteomics approach to the discovery of biomarkers in prion diseases". Poster Session, 58th ASMS Conference on Mass Spectrometry. May 2010, Salt Lake City, Utah.